THE UNIVERSITY
of EDINBURGH

Investigation into DNAm and brain structural and connectomic covariance: a life course approach

Emily Nicola Wynne Wheater

THE UNIVERSITY *of* EDINBURGH

A thesis submitted for the degree of Doctor of Philosophy

March 2021

Publications:

Caitlin Davies, Olivia K L Hamilton, Monique Hooley, Tuula E Ritakari, Anna J Stevenson, Emily N W Wheater, Translational neuroscience: the state of the nation (a PhD student perspective), *Brain Communications*, Volume 2, Issue 1, 2020, fcaa038, https://doi.org/10.1093/braincomms/fcaa038

Wheater, E., Mair, G., Sudlow, C. *et al.* A validated natural language processing algorithm for brain imaging phenotypes from radiology reports in UK electronic health records. *BMC Med Inform Decis Mak* **19,** 184 (2019). https://doi.org/10.1186/s12911-019-0908-7

Blesa M, Galdi P, Sullivan G, Wheater EN, Stoye DQ, Lamb GJ, Quigley AJ, Thrippleton MJ, Bastin ME and Boardman JP (2020) Peak Width of Skeletonized Water Diffusion MRI in the Neonatal Brain. *Front. Neurol.* 11:235. doi: 10.3389/fneur.2020.00235

Emily N.W. Wheater, D.Q. Stoye, S.R. Cox, J.M. Wardlaw, A.J. Drake, M.E. Bastin, J.P. Boardman (2020) DNA methylation and brain structure and function across the life course: a systematic review Neurosci. Biobehav. Rev., 113, pp. 133-156, 10.1016/j.neubiorev.2020.03.007

Currently under revision:

Emily N.W. Wheater, Susan D. Shenkin, Susana Muñoz Maniega, Maria Valdés Hernández, Joanna M. Wardlaw, Ian J. Deary, Mark E. Bastin, James P. Boardman, Simon R. Cox. Birth weight is associated with brain tissue volumes seven decades later, but not with age-associated changes to brain structure bioRxiv 2020.08.27.270033; doi: 10.1101/2020.08.27.270033 Revisions have been submitted to NeuroImage: Clinical.

In submission:

Emily N.W. Wheater, Paola Galdi, Daniel L. McCartney, Manuel Blesa, Gemma Sullivan, David Q. Stoye, Gillian Lamb, Sarah Sparrow, Lee Murphy, Alan J Quigley, Joanna M Wardlaw, Mark E. Bastin, Riccardo E. Marioni, Simon R. Cox, James P. Boardman. DNA methylation and brain dysmaturation in preterm infants

Presentations

DNA methylation and brain structure and function across the life course: a systematic review. DOHaD Society World Congress Melbourne, Australia October 2019 (Poster)

Birth weight is associated with brain tissue volumes seven decades later, but not with age-associated changes to brain structure. Organisation for Human Brain Mapping Annual Meeting, Virtual June 2020 (Poster)

Association between preterm birth, differential DNA methylation and brain dysmaturation. Society Spring Meeting, Virtual March 2021 (Talk)

Abstract

Early life environmental stress, indexed by perinatal factors such as birth weight and gestational age, is associated with differences in brain structure and connectivity in early life, as well as being associated with a range of neurodevelopmental, psychiatric and cognitive outcomes, from childhood and into adulthood. While studies have investigated how these early life factor influence brain structure in early life, few have investigated this in older age. The molecular underpinnings of these relationships are not well understood. DNA methylation is an epigenetic mechanism that regulates gene expression; it is developmentally dynamic and responsive to environmental factors, making it a promising candidate for providing mechanistic insight into how early life stressors exert their effects. The aims of this thesis are as follows: to better characterise the associations between birth weight and brain structure and connectivity in later-life; to evaluate the evidence that DNAm is implicated in brain structure and function; to investigate the impact of gestational age at birth on the neonatal methylome and its association with brain connectivity.

In the first study, I investigated the associations between variation in normal birth weight and measures of brain structure and connectivity in participants aged 73 years from the Lothian Birth Cohort 1936. Larger birth weight was associated with larger brain volume, and with regional cortical surface area, but not with white matter microstructure. This relationship between birth weight and brain size did not appear to be related to the degree of atrophy that had taken place. Early life growth is likely to be associated with brain tissue reserve, in evidence in later life.

In the second study, I conducted a systematic review to evaluate the evidence linking DNA methylation to brain structure and function across the life-course. Sixty studies, encompassing both health and disease contexts, were identified. Together, these studies indicated that differential DNAm is

associated with brain structure and function for 8 categories of disease across the life course, although uncertainties remain. Modest consistency between DNAm and neuroimaging features precluded the possibility of quantitative synthesis. I identified potential sources of bias in existing literature, enabling the development of guidelines that could reduce methodological heterogeneity in imaging-DNAm studies.

Finally, I identified a DNAm signature of gestational age in neonatal saliva samples and tested its association with brain white matter microstructure. Participants were neonates, born preterm or term, recruited to the Theirworld Edinburgh Birth Cohort. There was widespread differential methylation associated with gestational age at birth, at term equivalent age. Several genes were identified that have previously been implicated in association with gestational age in cord blood, and with disorders known to contribute to the aetiology of preterm birth, such as pre-eclampsia. An epigenome-wide variable of the DNAm signature was associated with white matter microstructure, suggesting that DNAm contributes to white matter dysconnectivity in the neonatal period.

This thesis provides evidence that early life exerts an effect on brain structure into later life, that DNAm and MRI neuroimaging are associated across the life-course and in a range of health and disease contexts, and that DNAm is profoundly altered in association with variation in gestational age and that this may contribute to white matter connectivity in the neonatal period.

Lay Abstract

Early life factors, such as birth weight or gestational age at birth, have been associated with vulnerability and resilience to a range of diseases and problems that emerge throughout life. This was first observed in relation to cardiovascular disease and has since been linked to brain health such as psychiatric disorders and neurodevelopmental problems. This is underpinned by alterations to brain structure that are in evidence in both early life and into adulthood. Many studies have investigated how these early life factor influence brain structure in early life, but few have investigated this in older age.

DNA methylation is an epigenetic mechanism that may mediate this relationship between early life and subsequent vulnerability. Altered DNA methylation changes how genes are expressed. In development, this helps to establish different cell types, despite all cells having the same genetic sequence. However, it can also contribute to adverse health outcomes. It is responsive to environmental exposures in later life such as smoking, and in the early life it is responsive to factors such as maternal breastfeeding, or gestation length and birth weight.

This thesis presents three studies that investigate contributions of early life and DNA methylation to brain structure and function. In the first study, I explore the impact of birth weight on brain structure in participants aged 73 years old. I found that larger birth weight corresponded to larger brain size, and larger cortical surface area. However, birth weight was not associated with age-associated brain structure, such as tissue loss. In the second study I examined the previously published literature that had reported associations between DNA methylation and brain imaging findings, as measured by magnetic resonance imaging (MRI). This study indicated that DNA methylation is associated with brain structure and function across life, and in a variety of health and disease contexts. In the final study, I found that there

were widespread alterations to DNA methylation associated with gestational age at birth in neonatal saliva, a tissue that holds promise for non-invasive sampling at multiple timepoints. Further, I found that this DNA methylation was associated with measures of brain structural connectivity.

This thesis demonstrates that early life exerts a life-long influence on brain structure, DNA methylation is associated with brain structure and function throughout life, and that a profound early life stressor results in a profound alteration to DNA methylation, which contributes to brain connectivity in early life.

Declaration

I declare that the content of this thesis is my own work and that all contributions and collaborations have been explicitly acknowledged in the text. No material presented here has been submitted for any other degree or professional qualification.

Emily N. W. Wheater

March 2021

Acknowledgements

I would like to thank my supervisors, Professor James Boardman, Dr Mark Bastin and Dr Simon Cox. They have provided guidance and support but have also had faith in me and I, in turn, have had complete faith in them. I would also like to thank Professor Joanna Wardlaw who, as my thesis chair, has provided many a timely insight.

I have been very fortunate to work alongside many talented scientists throughout my PhD. I would like to thank Dr Manuel Blesa, Dr Paola Galdi, Gillian Lamb, Dr Gemma Sullivan, Dr David Stoye, and Kadi Vaher. Manuel, Paola, Gemma and David all deserve special thanks for their generosity with their knowledge and time, for their words of encouragement, and for tactical trips to purchase afternoon snacks at various key moments. They really did keep me going. I would also like to thank Dr Riccardo Marioni and Dr Daniel McCartney for sharing their expertise in all things pertaining to DNA methylation. I could not have done it without them.

The work in this thesis was supported by a PhD studentship in Translational Neuroscience, funded by the Wellcome Trust. I thank Wellcome for their support, and Professors Deary, ffrench-Constant, Kind, Lawrie, Price, and Wardlaw for giving me this opportunity. I would also like to thank Dr Jane Haley for her kindness and indefatigable support.

Thank you to my parents, John and Bella. My mind ever boggles at the collective knowledge and experience shared between these two, and I am grateful that I continue to benefit from it. To Dad I owe an early curiosity about science (“What *do* those funny symbols all mean?” I never did find out). From Mum I continue to learn the true meaning of attention to detail, and I hope that one day I will achieve her mastery of the comma (unlikely – but one must have something to aim for). Thank you to my sister, Kitty, who is a true champion and has seen me through some tight spots.

The final words of thanks must be to my partner, and teammate, Piran. You have supported me from near and from far, and always with your characteristic practicality, intelligence, and care. You are the greatest gift. Thank you.

Table of Contents

Chapter 1. Introduction

1.1 Early life influences life-long health outcomes

1.1.1 Developmental Origins of Health and Disease

The Developmental Origins of Health and Disease (DOHaD) hypothesis states that the origins of noncommunicable diseases of middle and later life, such as cardiovascular and metabolic disease, lie in responses to adverse early life experiences, such as undernutrition. This hypothesis arose from observations that areas which experienced high levels of infant and neonatal mortality were also likely to exhibit high levels of hypertension and stroke in adults (Barker and Osmond, 1986). Subsequent studies demonstrated that low birth weight (an indicator of the intrauterine environment) is associated with an increased risk of developing metabolic and cardiovascular disease throughout life (Barker, 2004; Belbasis et al., 2016).

1.1.2 Early life influences brain health throughout life

Early life adversity has been linked to vulnerability to cardiovascular and metabolic disease in later life, but also to developing subsequent psychiatric disorders such as Major Depressive Disorder (MDD) and schizophrenia (SCZ) (Fatemi and Folsom, 2009; Gałecki and Talarowska, 2018; Thompson et al., 2001). In utero events have a lasting impact on neurocognitive outcomes. A study following the Dutch Hunger Winter of 1944-45, found that prenatal nutrition was associated with coronary heart disease, but also with cognition in later life (De Rooij et al., 2010). Cognition and risk of developing dementia and stroke in later life is further influenced by early life cognition, but whether these relationships are established early in development and then preserved throughout life, or whether early life factors differentially affect ageing process

remains poorly understood (Backhouse et al., 2015; Tucker-Drob, 2019; Whalley et al., 2006).

1.1.3 Fetal growth affects brain health: birth weight

Variation in birth weight, an indicator of fetal growth, is associated with neurological and psychiatric outcomes in later life (O'Donnell and Meaney, 2017). Low birth weight (LBW) (<2500 g) was found to be a risk factor for developing depression in later life in men (Thompson et al., 2001). LBW has been linked to depressive symptoms in adolescent girls (Van Lieshout and Boylan, 2010). Very LBW (VLBW) (<1500 g) is associated with cognitive deficits in executive functioning and intelligence quotient (IQ) in early life and these effects are preserved into adulthood (Eryigit Madzwamuse et al., 2015). Birth weight variation, including within the normal range, is associated with cognitive ability throughout life, and is associated with a risk of dementia (Jefferis et al., 2002; Matte et al., 2001; Mosing et al., 2018; Shenkin et al., 2004, 2001). LBW has been associated with schizophrenia, and personality disorders (Schlotz and Phillips, 2009). Variation within normal birthweight (2500 g – 4000 g) has likewise been found to contribute to deficits in neurocognitive development, including increased vulnerability to developing schizophrenia (Abel et al., 2010; Wade et al., 2014). Brain volumes have also been shown to mediate the association between birth weight and depression in UK Biobank participants (Ye et al., 2020). This suggests that the alterations in risk for neuropsychiatric and cognitive deficits that are associated with birth weight variation have identifiable brain structural correlates, inferred from neuroimaging.

1.1.4 Fetal growth affects brain health: preterm birth

Preterm birth is defined as birth under 37 weeks of gestation (full-term is birth at 40 weeks gestation), and affects around 15 million births globally per year, accounting for 10% of all births. While it is the leading cause of infant death,

survival following preterm birth has improved rapidly over the decades. However, improved survival has led to a corresponding increase in the prevalence of long-term adverse effects following preterm birth, particularly adverse neurodevelopmental sequalae (Saigal and Doyle, 2008). Cerebral palsy affects 5 -10% of infants born preterm, and gestational age at birth is associated with increased risk of developing attention deficit hyperactivity disorder (ADHD), autism spectrum disorders (ASD), and reduced IQ (Agrawal et al., 2018; Burnett et al., 2011; Franz et al., 2018; Mackay and Smith, 2011; Nosarti et al., 2012; Trønnes et al., 2014; Van Lieshout et al., 2018). The prevalence of special educational needs decreases with the length of gestation, and this trend continues into the term range (37 – 40 weeks gestation) (Johnson et al., 2010; Mackay et al., 2010). Elevated risk of neurodevelopmental disability in comparison to term born infants is apparent even in infants born late preterm (34-36 weeks) and moderately preterm (32-33 weeks) (Johnson et al., 2015). These cognitive and attentional deficits do not just affect early life but extend throughout childhood and into adolescence and adulthood (Breeman et al., 2016, 2015; Linsell et al., 2018). Adolescents and adults born preterm manifest an increased likelihood of receiving psychiatric diagnoses in adolescents and adulthood (Nosarti et al., 2012). The impact of preterm birth on neurological and neuropsychiatric health extends throughout life into adulthood, and these effects are likely to persist into older age.

1.2 Magnetic Resonance Imaging

1.2.1 Magnetic Resonance Imaging to assess brain structure and function

Alterations to brain structure are a likely neuroanatomical substrate for the observed neurodevelopmental and cognitive sequalae of preterm birth or variation in birth weight. Magnetic resonance imaging (MRI) is a non-invasive way of measuring the brain throughout life. It can provide quantitative measurements of brain structure and function. Structural MRI is used to assess

gross anatomical features and provides quantitative measures such as tissue volume measurements; diffusion MRI is used to infer white matter microstructure; functional MRI measures blood-oxygen level dependent (BOLD) signal. BOLD is sensitive to the hemodynamic response - changes in the ratio of oxygenated versus deoxygenated haemoglobin. fMRI data can be used to infer neuronal activity, due to the correspondence between neuronal activity (and increased metabolic demand) and increases in blood flow and oxygenation levels (Heeger and Ress, 2002). From patterns of neuronal activity, functional connectivity (connectivity of the brain that is defined by a temporal relationship, rather than a spatial or anatomical one) can be measured. This may be achieved through monitoring brain activity during rest (resting-state connectivity) or during tasks. The latter aims to identify brain networks underlying cognitive or emotional functioning, such as working memory or emotional processing, by measuring activity in response to tasks designed to isolate those functions. MRI, therefore, provides useful insights into the structure and functioning of the living brain.

1.2.2 Structural MRI

MRI capitalises on the electromagnetic properties of hydrogen protons. Protons possess a positive charge, mass and spin, and generate a magnetic field as a result of these properties. Usually, the magnetic fields of protons in a tissue are randomly oriented in relation to each other. However, in the presence of a strong magnetic field (B_0), such as those in an MRI scanner, these will align, with the majority aligning in the lowest energy state (parallel) and some aligning in the high-energy orientation (anti-parallel). Radio frequencies (RF) are then applied, and protons in the low energy state flip to the high energy state, with their magnetic fields anti parallel to the applied magnetic field. When the radio frequency is removed these high-energy protons relax to the low energy state and emit RF energy. This is detected by the scanner and used to generate an image.

The time-course over which RF energy is emitted, by protons reverting to the parallel orientation with B_0, is denoted T1, or the spin-lattice relaxation time, and is dependent on the strength of the applied magnetic field and proton density of the tissue. In T1-weighted (T1w) imaging fat appears bright, due to the rapid realignment of protons with B_0, while water appears dark (Paus et al., 2001).

Magnetic fields of excited protons (following the RF pulse) interact and are in phase. Following the removal of the pulse the spins dephase. The time-course over which these dipoles diphase with each other is denoted T2, or spin-spin relaxation time. T2 is longer in free water, but in tissues T2 relaxation is quicker. In T2-weighted (T2w) imaging tissues low in water such as fat appear dark, due to long T2, while grey matter appears bright dark (Paus et al., 2001).

T1 and T2 relaxation times form the basis of most structural MRI protocols. T1-weighted and T2-weighted structural MRI are sensitive to the proton density of tissues and therefore provide contrast between grey and white matter, and cerebrospinal fluid (CSF). Grey matter is composed of cell bodies of neurons, unmyelinated axons, and glial cells. White matter is formed of bundles of axons that connect regions of the brain. Axons become myelinated during post-natal development, which is critical for the fast and efficient transmission of electrical signals in the brain, giving this tissue its white colour. In combination with tissue segmentation, structural MRI can be used to provide quantitative measurements which include: brain tissue volumes, such as total brain volume (TBV), grey matter volume (GMV), white matter volume (WMV); burden of pathology such as white matter hyperintensities (WMH), such as white matter hyperintensity volume; and cortical morphology, such as cortical thickness, volume, and surface area. WMH are age-associated white matter lesions, that may be focal or multifocal, and appear as hyperintense signal on T2w MRI or on fluid-attenuated inversion recovery (FLAIR) imaging. They are associated with axonal

loss and demyelination, and increased interstitial fluid (Wardlaw et al., 2015). Intracranial volume (ICV) can also be ascertained from structural MRI.

1.2.3 Diffusion MRI

Diffusion MRI (dMRI) generates contrast based on the diffusion of water molecules in tissues and can be used to observe white matter microstructure (Le Bihan and Johansen-Berg, 2012). When unconstrained, water diffuses in a Brownian (random) manner. In the brain, however, the diffusion of water may be constrained by tissues, cell membranes, myelin, and macromolecular cellular components. This results in a contrast based on the motion of water molecules, for example, whether in a Brownian manner as it does in the ventricles, or in a highly constrained way as it does in axons. Due to its sensitivity to tissue microstructure, such as cell membrane integrity or myelination, dMRI can provide insights into white matter pathology or dysmaturation.

1.2.4 Diffusion tensor imaging

The diffusion tensor model represents the movement of diffusion of water molecules in a 3D matrix with three eigenvectors and corresponding eigenvalues. These eigenvalues describe the magnitude of diffusion occurring along three principal orthogonal axes. This model can be visualised as an ellipsoid (Figure 1). In isotropic diffusion the magnitude of diffusion along each of these axes (described by the eigenvalues) is approximately equal ($\lambda_1 \approx \lambda_3 \approx \lambda_3$), resulting in a spherical ellipsoid. This type of water molecule diffusion occurs in CSF in the ventricles. Anisotropic diffusion occurs when at least one of the eigenvalues, representing the magnitude of water diffusion occurring along the principal axes, has a different value from the others ($\lambda_1 > \lambda_3 > \lambda_3$). This results in directionality to the water diffusion. Water diffusion is directional in axons and dendrites, where diffusion is constrained by cell membranes, myelin, and macromolecular structures such as cell cytoskeleton. The signal obtained from

diffusion MRI is therefore affected by tissue architecture which varies across health and disease states. A common set of diffusion parameters are calculated from the eigenvalues: mean diffusivity (MD), axial diffusivity (AD), radial diffusivity (RD), and fractional anisotropy (FA). MD is the mean of the diffusivity along all three axes; AD refers to diffusion along the principal axis; RD is the average of the diffusion along the remaining two axes. The directionality of water diffusion is quantified through FA, which has values 0 to 1, where 0 represents isotropic diffusion and 1 corresponding to diffusion in only one direction. FA may approach 1 in large white matter tracts where there are many myelinated axons and where there is a high degree of directional coherence among fibres.

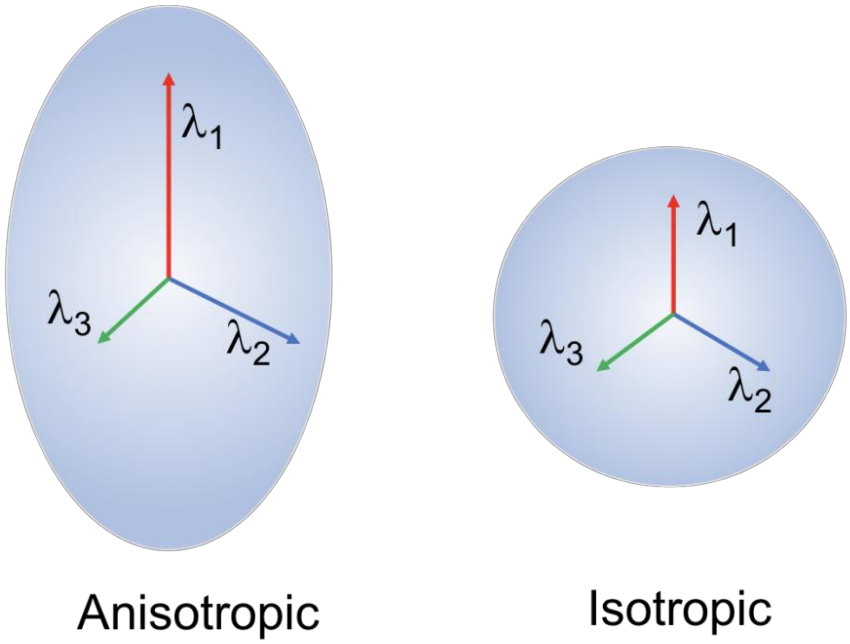

Figure 1. The diffusion tensor model represents water diffusion as an ellipsoid with three eigenvectors representing the 3 principal axes of diffusion and three eigenvalues representing the magnitude of diffusion. Anisotropic diffusion is represented on the left; isotropic diffusion is represented on the right.

1.2.5 Neurite Orientation and Dispersion Density Imaging

The diffusion tensor imaging (DTI) model is a powerful tool for identifying clinically relevant microstructural alterations, but its accuracy can be reduced by crossing fibres within a voxel. Other, more advanced methods, such as neurite orientation and dispersion density imaging (NODDI), can address these limitations, by modelling tissue compartments such as the intra-neurite and extra-neurite space found in grey and white matter, and non-tissue compartments such as CSF in each voxel (Figure 2) (Zhang et al., 2012). CSF follows an isotropic Gaussian water diffusion displacement pattern. Hindered diffusion, following an anisotropic Gaussian water diffusion displacement pattern, is assumed to take place in extra-neurite space, including extra-cellular space and neuronal cell bodies and glial cells. Restricted diffusion, which follows a non-Gaussian water diffusion displacement pattern, is assumed to take place in intra-neurite contexts, within axonal or dendritic membranes. NODDI provides CSF volume fraction (ISO), which refers to the isotropic water fraction, and also the following diffusion-based metrics of tissue microstructure: orientation dispersion index (ODI) and neurite density index (NDI). NDI denotes the intra-neurite volume fraction within a voxel, while ODI describes tract complexity or neurite fanning.

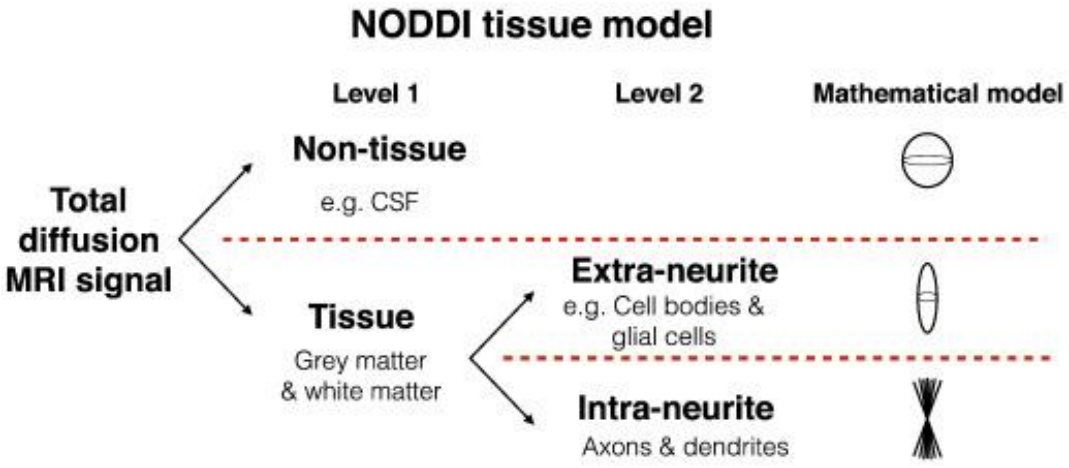

Figure 2. NODDI biophysical model where different water molecule diffusion patterns are used to generate a biophysical model of tissue and non-tissue fractions. Reproduced with permission (Tariq et al., 2016).

1.2.6 Global dMRI measures of white matter microstructure

Variance in water diffusion parameters is shared among major white matter tracts in both neonates and adults, and so generalised metrics of global white matter microstructure can be derived that are informative of alterations to the white matter tissue that are not tract-specific (Alloza et al., 2016; Cox et al., 2016; Penke et al., 2010; Telford et al., 2017). Peak width skeletonised metrics are histogram-based measures of global white matter microstructure based on the values of diffusion metrics of voxels within the white matter skeleton, which is created by skeletonising DTI data using tract based spatial statistics (TBSS) (Smith et al., 2006). The peak width skeletonised value is calculated as the difference between the value of the 5^{th} percentile and the 95^{th} percentile within the skeleton (Figure 3) (Baykara et al., 2016). Histogram analysis is thought to be effective at capturing diffuse white matter injury (Tofts et al., 2004). Alternatively, a general factor approach involves modelling variance shared between the white matter tracts in both the adult and neonatal brain (Alloza et al., 2016; Cox et al., 2016; Penke et al., 2010; Telford et al., 2017). General factors may be derived through either principal component analysis (PCA) or factor analytic approaches. The PCA approach provides a measure that captures maximal variance across all the tracts. Factor analysis, in contrast, excludes tract-specific error variance from the factor score, and models the reliable common variance across tracts. Despite these different statistical bases, the two methods produce very similar measures which are highly collinear with each other.

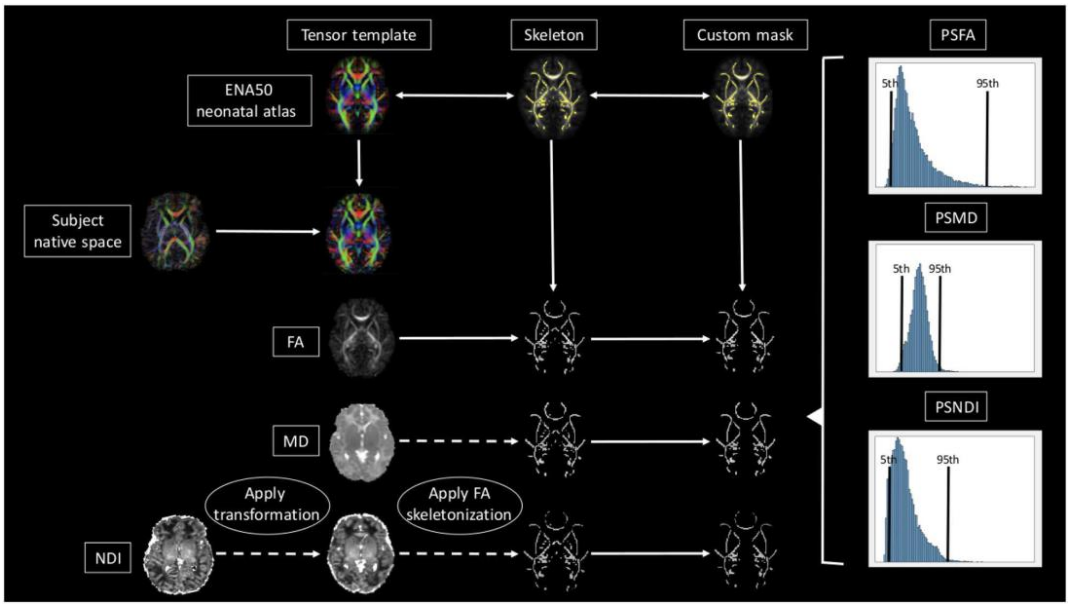

Figure 3. Schematic of the derivation of peak width skeletonised water diffusion metrics from neonatal dMRI data. Reproduced with permission (Blesa et al., 2020).

1.2.7 Brain injury following preterm birth

Both diffusion and structural MRI modalities have provided insight into brain tissue alterations that occur as a consequence of early birth, or with variation in birth weight.

White matter injury and dysmaturation of both the white and grey matter and impaired cortical development of the preterm brain form the 'encephalopathy of prematurity' (Volpe, 2019, 2009). Preterm birth results in abnormal brain growth, increased ventricle volume and decreased cortical surface area and a reduction in cortical folding and gyrification in the neonatal period (Engelhardt et al., 2014; Kapellou et al., 2006; Padilla et al., 2015; Shimony et al., 2016; Volpe, 2019). Neuronal/axonal disease resulting from disrupted maturation affects the thalamus, basal ganglia, cerebral cortex, brainstem and cerebellum (Volpe, 2009). Grey matter neuronal loss involves reductions in cortical and subcortical

grey matter volume and reduced cortical surface area (Back and Miller, 2014; Boardman and Counsell, 2020; Kapellou et al., 2006; Makropoulos et al., 2016). These findings demonstrate a dose-dependent effect, whereby increasing prematurity (lower gestational age) is associated with reduced brain tissue volumes (Bouyssi-Kobar et al., 2016). While many studies have reported reductions in both regional and total brain volumes in relation to decreasing gestational age, abnormal growth following preterm birth may also be associated with increases, as well as decreases, in brain growth. For example, primary visual, motor and somatosensory cortices were found to be larger in infants with younger gestational age at birth when scanned at term equivalent age (Alexander et al., 2019). These alterations may be related to the increased sensory inputs experienced by neonates born preterm, as a result of care and environments in neonatal intensive care units. The extent of grey matter abnormality is associated with the severity of white matter injury (Pierson et al., 2007).

White matter is especially vulnerable to injury in the neonatal brain due to the loss of premyelinating oligodendrocytes, and a resultant failure to myelinate axons (Back and Miller, 2014). Preterm infants show decreased white matter volumes in comparison to term born infants (Makropoulos et al., 2016). White matter injury in preterm infants may be localised such as in periventricular leukomalacia (PVL), a focal necrotic brain injury, or it may be diffuse. This results in dysconnectivity of developing brain structural networks (Galdi et al., 2020).

Diffuse white matter injury, inferred from diffusion MRI, is a hallmark of preterm brain dysmaturation and correlates with the cognitive and behavioural deficits observed (Boardman et al., 2010). The summary statistics obtained from the DTI model have identified microstructural alterations in white matter in neonates (Hüppi et al., 1998). The white matter of preterm born infants is characterised by

reduced FA and a corresponding increase in MD when scanned at term equivalent age (Anjari et al., 2007; Rose et al., 2008). This reflects a loss of directional coherence and increase in water diffusion in the white matter of preterm infants, and has been linked to neurodevelopmental impairments (Counsell et al., 2008). Neonatal NODDI imaging has shown that in normal maturation NDI increases in the white matter, and ODI increases in grey matter; preterm birth is associated with reduced white matter NDI and reduced cortical ODI (Batalle et al., 2019; Blesa et al., 2020; Eaton-Rosen et al., 2015; Kunz et al., 2014). Histogram analysis has been applied to DTI and NODDI metrics in a neonatal cohort; PSMD and peak width neurite density index (PSNDI) were both shown to classify preterm and term born infants with good accuracy at 81% and 77% respectively (Blesa et al., 2020). PSNDI has further been shown to be associated with IL-8 – a cytokine that is dysregulated in histologic chorioamnionitis and is implicated in human brain injury (Sullivan et al., 2020). In the neonatal period, a general factor of FA (gFA) increases with gestational age at birth (Telford et al., 2017).

White matter injury, the hall mark of preterm brain injury, is thought to underlie the neurocognitive deficits exhibited by those born preterm from infancy into adulthood. White matter volume was demonstrated to be a determinant of adolescent IQ in preterm infants (Northam et al., 2011). White matter connectivity alterations in relation to preterm birth are associated with cognitive outcomes: interhemispheric temporal lobe connectivity is predictive of language impairments in adolescents born preterm, and thalamocortical connectivity predicts cognition in children born preterm (Ball et al., 2015; Northam et al., 2012). Increased FA in the neonatal period, amongst preterm born children, has been linked to working memory at 5 years old (Ullman et al., 2015).

1.2.8 MRI findings from late life

In late life, brain structure is likely the product of developmental processes and also changes that occur as a result of ageing. The latter include the increasing prevalence of WMH, loss of white matter microstructural integrity, and tissue loss following atrophy.

Total brain volume, as well as white matter volume follows a U-shaped trajectory across life, increasing in size throughout infancy and childhood, and reducing in size with age, due to age-associated brain tissue atrophy (Hedman et al., 2012). Atrophy affects both the grey and white matter, but the degree to which each tissue is affected and whether this changes with age is unclear. In old age, brain volumes are a product of maximal prior brain size and tissue loss that has occurred with age (Vågberg et al., 2017). In late life, brain tissue atrophy can be inferred both from longitudinal imaging, but also by controlling brain tissue volumes for ICV, which is age invariant once maximal size is reached (Royle et al., 2013). At its maximal size the brain fills the intracranial cavity, making ICV an archaeological measure of brain size prior to disease or age-related tissue loss. Brain tissue loss in old age is associated with declining cognitive function, and degenerative diseases such as Alzheimer's disease (Johnson et al., 2012; Ritchie et al., 2015b).

Loss of white matter integrity can be captured through both microstructural alterations inferred from diffusion MRI, and white matter hyperintensity burden - a pathology captured by structural MRI. WMH are an MRI hallmark of cerebrovascular disease in old age and are associated with cognitive decline in late life (Arvanitakis et al., 2016). The prevalence of WMH increases with age, and they are associated with an increased risk of stroke and dementia (Debette and Markus, 2010; Wardlaw et al., 2015). WMH are associated with loss of myelin and axons (Gouw et al., 2011). Reductions in white matter FA and increases in MD are associated with cognitive decline in later life (Ritchie et al.,

2015a). NDI is sensitive to age in the developing brain from childhood to late adolescence and increases with maturation (Genc et al., 2017). However, in late life, a general factor of NDI (gNDI) and gFA display negative associations with increasing age (Cox et al., 2016). In late life, gFA is associated with information processing speed and intelligence (Penke et al., 2012, 2010). Peak width skeletonised mean diffusivity (PSMD) has been associated with cognitive processes in older-cohorts, both in a healthy ageing context and in disease, such as multiple sclerosis and small vessel disease (Baykara et al., 2016; Deary et al., 2019; Low et al., 2020; Vinciguerra et al., 2019). In cohorts that exhibit both focal and diffuse white matter injury, such as that observed in multiple sclerosis or small vessel disease, this histogram-based measurement has been shown to capture diffuse white matter injury (Low et al., 2020; Vinciguerra et al., 2019).

1.2.9 Evidence for brain alterations in association with preterm birth and birth weight in later life

As survival following preterm birth has improved, it has become possible to investigate its effects on brain structure beyond early life. This has revealed that the influence of early life factors on brain structure is in evidence in adolescents and adults, not just in early childhood. In adolescence, preterm born subjects have reduced brain volumes in comparison to term subjects (Nosarti et al., 2002). Preterm-born adults exhibit white matter alterations such as reduced fibre density, reduced white matter FA, and increased white matter MD (Allin et al., 2011; Eikenes et al., 2011; Menegaux et al., 2020). Within preterm groups these measures of white matter microstructural integrity were associated with general cognitive ability.

The brain exhibits alterations in structure in association with variation even within the normal birth weight range. Brain tissue volumes, including total brain, white matter and grey matter volumes, are positively associated with increasing

birth weight in late life (Muller et al., 2016, 2014). Increases in birth weight, even within the normal range, is positively associated with cortical surface area in adults and adolescents (Figure 4) (Raznahan et al., 2012; Walhovd et al., 2012). In adults aged 78 years, frontal white matter FA is associated with birthweight (Shenkin et al., 2009a). However, the impact of birth weight on global measures of white matter microstructure, and cortical morphology in late life has not previously been investigated.

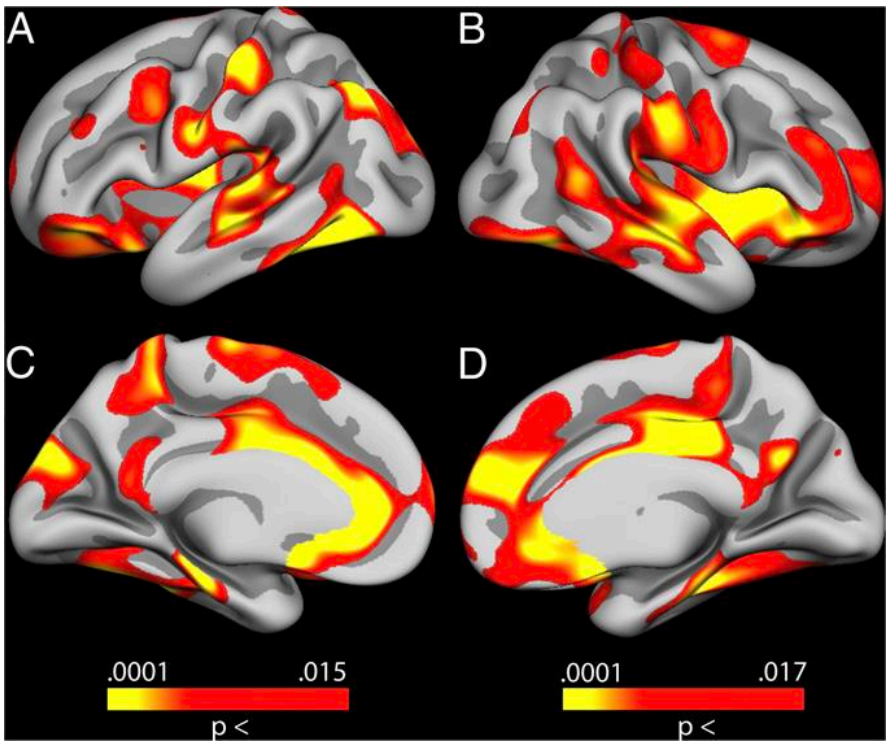

Figure 4. Heat maps showing the associations of birth weight on cortical surface area in adolescents and young adults. A) Lateral left hemisphere, B) Lateral right hemisphere, C) Medial left hemisphere, D) Medial right hemisphere. Reproduced with permission (Walhovd et al., 2012).

1.1 Epigenetics

1.3.1 Epigenetics regulate the output of the genome

In multicellular organisms, the underlying genetic sequence between cells does not vary. However, there is a great deal of variety in cell morphology and function within individuals. The establishment of distinct cellular identities within multicellular organisms is enabled by the differential spatial and temporal regulation of the output of the genome. This is facilitated by epigenetics, which is defined by Adrian Bird as: “the structural adaptation of chromosomal regions so as to register, signal or perpetuate altered activity states” (Bird, 2007). Structural adaptations may refer to molecular mechanisms that modify the structure of the DNA molecule, such as DNA methylation (DNAm) and chromatin remodelling through histone modifications, but not the underlying sequence of nucleotides (Figure 5). Such modifications modulate a region’s accessibility to transcriptional machinery such as RNA polymerases and transcription factors, thus regulating the output of the genome. Epigenetic modifications are developmentally dynamic, responsive to environmental inputs, and are thought to mediate the effects of early life exposures and health outcomes.

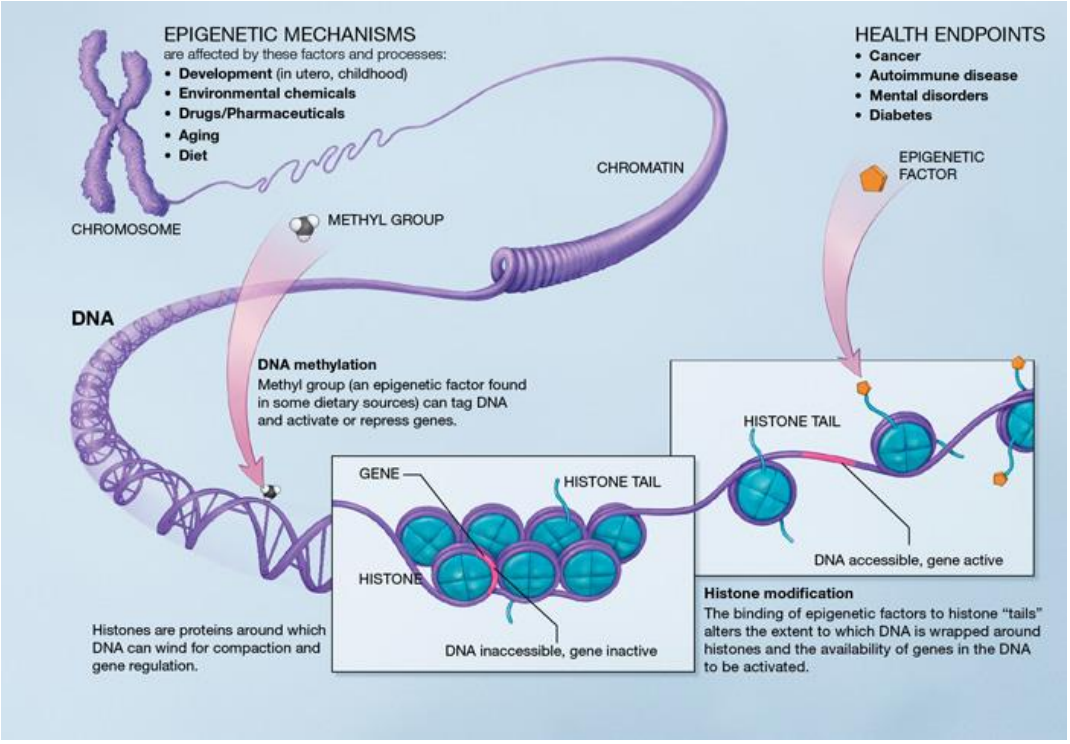

Figure 5. Epigenetic modifications, such as DNA methylation and histone modifications, provide a biological mechanistic link between environmental exposures and developmental effects and clinical phenotypes. (National Institutes of Health: https://commonfund.nih.gov/epigenomics/figure)

1.3.2 DNA methylation

DNAm is one such epigenetic possible mechanism proposed within the DOHAD paradigm to mechanistically link genome and environmental interactions to give rise to phenotype (Gluckman et al., 2010). DNAm is the addition, by DNA methyltranferases (DNMTs), of a methyl group at the 5C position of the pyramindine ring of cytosine residues in DNA (Figure 6). The addition of methyl groups (hypermethylation) generally corresponds to a reduction in gene expression, while the removal of them (hypomethylation) corresponds to an increase in gene expression (Smith and Meissner, 2013). The addition of methyl groups is thought to alter gene expression through several mechanisms. First,

the presence of methyl groups on the DNA molecule alters the accessibility of binding sites both for transcription factors and also interacts with chromatin remodelling factors to modulate the packaging of DNA onto histone proteins (Moore et al., 2013). The methyl group of 5'methylcytosine can become oxidised to form hydroxymethylcytosine. This modification is also prevalent in the human genome, and while its functional role is not well understood there is evidence that its presence corresponds to an increase in expression (Jin et al., 2011).

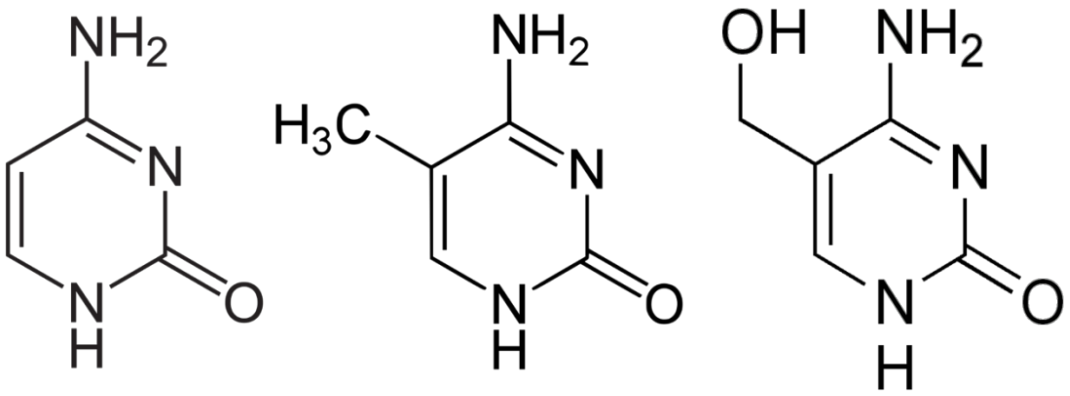

Figure 6. Cytosine (left), methylcytosine showing the addition of a methyl group at the 5C position (middle), and hydroxymethylcytosine showing the oxygenated modification of the methylated cytosine (right).

DNAm is not distributed evenly across the genome and primarily occurs within cytosine-phosphate-guanine (CpG) sequence contexts. This is a cytosine followed by a guanine nucleotide in the 5' -> 3' direction ('p' denotes the phosphoric bond between the two residues). CpGs are depleted from the genome in general due to their high mutation rate, but they are enriched at CpG Islands (10% of CpG dinucleotides occur in these contexts). Promoters are often found within CpG Islands and these are usually unmethylated, indicating that they have functional importance in the regulation of gene expression.

1.3.3 DNA methylation in development

DNAm is an important mechanism in developmental programming. It is the mechanism by which maternal or paternal imprinting of genes occurs, and is crucial in Barr body formation (inactivation of one of the X chromosomes in females) (Chow and Heard, 2009). In the early stages of embryonic development DNAm is completely ablated (Morgan et al., 2005; Reik, 2007) During gestation, genes involved in developmental processes usually become increasingly methylated (repressed), while those that are tissue specific and are involved in establishing distinct cellular identities tend to become less methylated and more active (Slieker et al., 2015). These processes contribute to cell differentiation *in utero* (Khavari et al., 2010).

1.3.4 Measuring DNA methylation

DNAm can be measured using several technologies with varying resolutions. Most of these make use of the bisulfite conversion of methylated cytosine to uracil (Olkhov-Mitsel and Bapat, 2012). Bisulfite sequencing measures DNAm at a single genomic region. Treatment with sodium bisulfite deaminates unmethylated cytosine converting it to uracil but leaves 5-methcytosine and 5-hydroxymethyl cytosine unaltered. The DNA, now containing uracil, is then amplified using PCR which inserts thymine nucleotides where there were unmethylated cytosines. This is then detected through DNA sequencing.

DNAm can also be measured at scale, across many loci using microarray technology, such as the Illumina arrays. There have, to date, been several generations of this technology with varying coverage across the genome. The 27k array measured DNAm at approximately 27,000 sites; the 450k array measured DNAm at approximately 450,000 sites; and the EPIC array measured DNAm at approximately 850,000 sites. These arrays also rely on the bisulfite conversion and single nucleotide extensions with fluorescently labelled nucleotides. Two types of probes are found on the Illumina arrays for measuring

DNAm; the two chemistries used to probe methylation status at loci are illustrated in Figure 7. In the Infinium I assay, two probes are used per CpG: one which measures unmethylated cytosine, and one which measures methylated cytosine. Single nucleotide extension will occur at the unmethylated allele if the cytosine residue has been converted to a thymine, through the combined steps of the bisulfite conversion and subsequent amplification of the DNA through PCR. Conversely, single nucleotide extensions will occur at the methylated allele if the cytosine remains unconverted. In the Infinium II assay, one probe is used to measure both methylated cytosine and unmethylated cytosine. The two are distinguished through the use of nucleotides labelled with different fluorophores which results in signal in two colour channels indicating methylation status. The resulting intensities that are detected from these two methods are used to estimate the beta value, which ranges from 0 to 1. While the presence of a methyl group on a cytosine residue is a binary state, the continuous scale used is a reflection of the measurement using DNA from multiple cells. This ability to measure DNAm across many loci makes DNAm an accessible epigenetic modification for study at the population level.

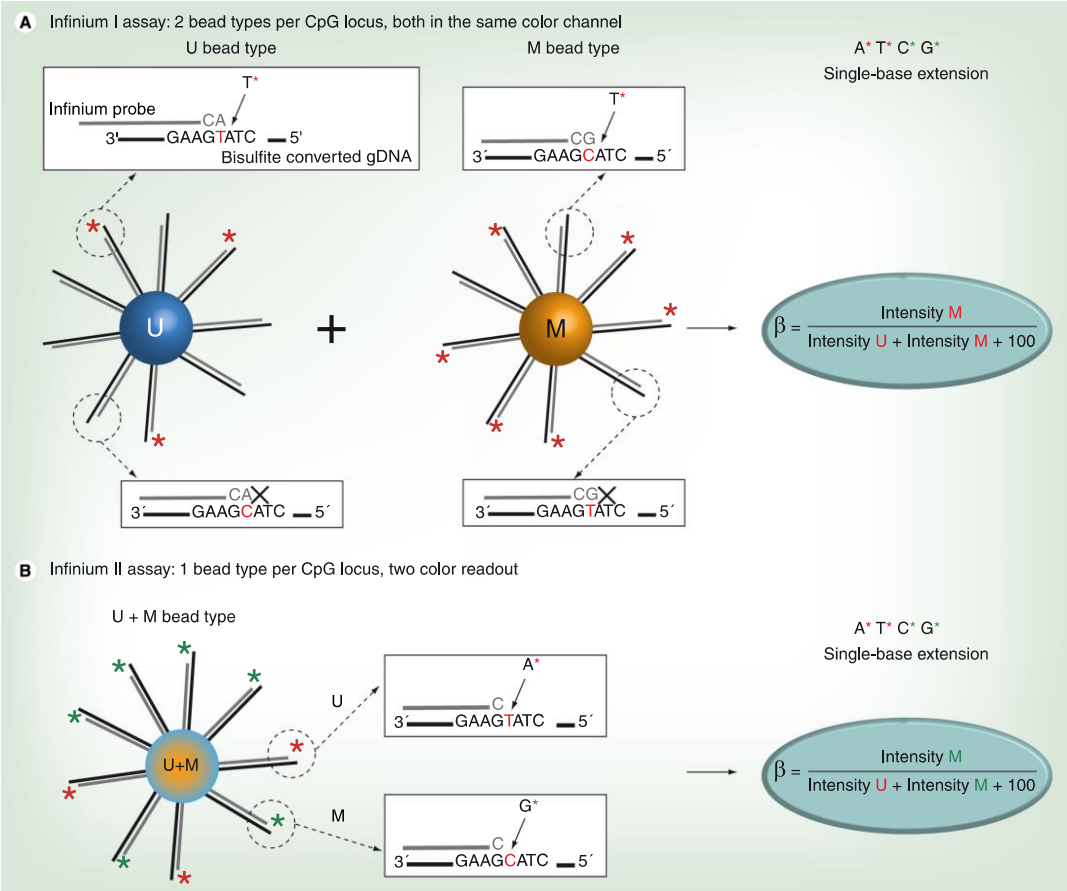

Figure 7. Two chemistries employed on Illumina microarrays to measure DNAm. A) Two different probes are utilised; one which measures unmethylated DNA, and one which measures methylated DNA. Reproduced with permission (Dedeurwaerder et al., 2011).

1.3.5 DNA methylation and pathology

The brain is sensitive to perturbations in expression of neurodevelopmental genes, and DNAm dysregulation is a key feature of several neurodevelopmental disorders (Kubota et al., 2015)(Rangasamy et al., 2013). Rett Syndrome is a neurodevelopmental disorder characterised by a regression of development and intellectual disability in early childhood. It results from a loss of function mutation in the *MECP2* gene, which encodes a protein that binds to methylated CpG sites

and functions to repress expression from loci. The loss of function mutation reduces MECP2 protein binding to CpG sites, leading to widespread gene expression dysregulation. Fragile X syndrome results from an expansion of a CGG trinucleotide repeat, within the *FMR1* gene promoter, resulting in increased methylation at this gene region and a corresponding reduction in expression of the gene.

Angelman's syndrome arises due to a loss of function mutation or deletion of the maternal allele of the *UBE3A* gene, and paternal imprinting of the remaining allele. This imprinting is neuronal-specific, thereby leaving no functioning copy of the gene in the central nervous system. These disorders, where the dysregulation of DNAm plays a key role in their aetiology, demonstrate the impact of DNAm on brain health/structure

1.3.6 DNA methylation and the environment

DNAm is dynamic across development and throughout life and is responsive to environmental factors, both post-natal and *in utero*. In adults, it has been demonstrated to be affected by BMI, age, and lifestyle factors such as smoking and alcohol (Hamilton et al., 2019; Hannum et al., 2013; Horvath, 2013; Joehanes et al., 2016; Liu et al., 2018; Wahl et al., 2017). Offspring methylome is sensitive to in utero environmental factors, such as maternal stress, smoking, and alcohol intake (Cao-Lei et al., 2014; Joubert et al., 2016; Portales-Casamar et al., 2016). Collectively, these studies demonstrate that DNAm is responsive to environmental exposures known to influence brain development and later health outcomes. DNAm is a likely mechanism to link genetic and environment to produce a phenotype.

1.3.7 DNA methylation and preterm birth and birth weight

Various studies have investigated the impact of early life stressors on the neonatal methylome. In the neonatal period, this has been largely been carried

out in cord blood. Differences in methylation in the neonates have been observed in relation to birth weight and gestational age (Bohlin et al., 2016; Hannon et al., 2019; Küpers et al., 2019; Merid et al., 2020; Schroeder et al., 2011). Widespread differential DNAm in association with gestational age at birth has been consistently demonstrated in cord blood, and also in a study of gestational age in fetal brain tissue (Spiers et al., 2015). Preterm birth is associated with differential methylation in saliva samples at protein coding genes implicated in neurodevelopment, and DNAm has been associated with tract shape and white matter microstructure in the neonatal period (Sparrow et al., 2016).

While the effects of early life adversity on brain structure appear to be in evidence beyond childhood, epigenetic signatures are less stable. The DNAm signature of early life adversity may be widespread, but it is consistently found to attenuate throughout life (Cruickshank et al., 2013; Simpkin et al., 2015). This suggested that early life effects are generally lost from the methylome. However, transient epigenetic signals may produce lasting effects on phenotype through developmental programming at a critical timepoint.

1.3.8 DNA methylation tissue sampling

A challenge of DNAm analysis is the selection of tissue to sample, from which DNAm is subsequently measured. Ideally, the tissue of interest itself would be sampled; however, for many tissues, including the brain, this is unfeasible due to the invasive nature of sample collection (biopsy). Alternatively, post-mortem tissue may be used, as it was in a study of the effects of gestational age on fetal brain tissue (Spiers et al., 2015). These tissues are very rare, can only provide data for one time point, making them unsuited to large scale longitudinal epidemiological studies of a population. There are further uncertainties regarding the effect that death itself may have on the methylome. Surrogate tissues, which are minimally invasive to collect, have therefore become the

mainstay of *in vivo* DNAm research. These surrogate tissues are typically blood, saliva, or buccal cell (cheek swab) samples, or cord blood, collected at time of birth, for the neonatal population.

Cord blood, like fetal brain tissue, can only be sampled at one time point, while saliva or blood may offer more opportunities for non-invasive longitudinal sampling. Brain and buccal epithelial cells (the main cellular component of saliva) are derived from the ectoderm germ layer, and therefore share embryonic lineage, and buccal cells may be more informative than blood for non-blood based phenotypes (Lowe et al., 2013; Theda et al., 2018). Comparisons of DNAm in cord blood, saliva and brain tissue indicate that saliva DNAm may be more representative of DNAm in brain tissue than blood, though this may depend on the genomic region being studied (Braun et al., 2019; Smith et al., 2015). In a study of the neonatal population, a further consideration is the need to avoid causing undue distress to the infant. Saliva sampling therefore provides several potential advantages over blood sampling in this population.

1.4 Scope of the thesis: statement of hypotheses

Early life factors are known to influence brain structure and brain health, and there is increasing evidence of this in late life. However, there remains uncertainty about whether brain structural alterations, particularly to white matter microstructure and cortical morphology, in relation to variation in birth weight are preserved throughout life into older age. Epigenetic mechanisms, including DNAm, have been proposed as likely mechanisms by which environmental and genetic factors give rise to health endpoints, such as neurodevelopmental or psychiatric disorders. Despite this, the role of differential DNAm in brain structure and function is unclear.

Within the neonatal period, DNAm associations with gestational age have been investigated in cord blood and has revealed widespread differential methylation

across the gestational age continuum. However, the generalisability of findings from this tissue to other readily available samples that would enable non-invasive longitudinal sampling and, further, it's potential contribution to MRI markers of brain dysmaturation following preterm birth, is not known.

The aims of this thesis are therefore as follows: to characterise the associations between birth weight and later life brain structure and connectivity; to evaluate the evidence that DNAm is implicated in brain structure and function across the life-course; to investigate the impact of gestational age at birth on the neonatal methylome and its association with brain connectivity. To this end, I present three results chapters that test the following hypotheses:

1) that birth weight is associated with i) global white matter microstructure and ii) brain volumes in later life;
2) that DNAm is associated with brain imaging in health and disease contexts across the life-course;
3) that gestational age at birth is associated with differential methylation in the neonatal period, and that this differential methylation associates with neonatal MR neuroimaging measures of global white matter microstructure.

I test the first hypothesis, in Chapter 2, using data from a subset of the Lothian Birth Cohort of 1936 (LBC1936). These participants were born in hospital, and therefore had their birth weights recorded at the time of birth, and also had multimodal MRI data from scans at ~73 years of age (Deary et al., 2007; Wardlaw et al., 2011). In this study I investigated the effect of birth weight variation on brain volumes and pathology, and white matter microstructure. Due to the potentially confounding effects of cardiovascular disease (also associated with birth weight) and overall body size (with a likely genetic origin) I investigate the potential roles of these factors in this relationship. I further investigate the

effects of birth weight on cortical morphology in late life, and control for the effects of atrophy.

I test the second hypothesis, in Chapter 3, by carrying out a systematic review of literature, published up until March 2018, where associations between structural, diffusion and functional MRI features with DNAm were tested. This review summarises DNAm-MRI associations across the life-course in a range of contexts including healthy participants and clinical populations.

I test the final hypotheses, in Chapter 4, using data from the Theirworld Edinburgh Birth Cohort (TEBC). Participants were neonates born preterm and term and had multimodal MRI obtained at the same time point as saliva samples and detailed clinical histories (Boardman et al., 2020). I investigated the differential DNAm in association with gestational age at birth in neonatal saliva, and the associations between a global measure of differential DNAm with MRI markers of brain dysmaturation.

Chapter 2: Birth weight is associated with brain tissue volumes seven decades later but not with age-associated changes to brain structure

Chapter Introduction

In this chapter brain structural alterations in association with variation in birth weight are investigated using data from an older age cohort. Previous work has shown that brain volumes are positively associated with birth weight in older age, but not white matter hyperintensities. However, the impact of birth weight on global white matter microstructure in this age group has not previously been investigated. In addition, while birth weight is associated with cortical structure in adolescents and early adulthood this has not been replicated in old age. I test the hypotheses that birth weight is associated with white matter microstructure and brain volumes in late life. I further investigate whether the previously observed regional patterning of cortical surface associations with birth weight are evident in older age, and whether this might be accounted for by head size.

This analysis uses a sample of participants from the Lothian Birth Cohort 1936 who had both birth record and MRI data at age 73. Birth weight data was collected from hospital records at time of birth.

This work is currently under review at *NeuroImage: Clinical* (https://doi.org/10.1101/2020.08.27.270033). As first author I designed and carried out the statistical analysis and drafted and wrote the manuscript.

Recruitment of participants to the study, gathering birth weight data from hospital records, MRI pre-processing and QC, subsequent white matter and cortical processing to derive brain structural and diffusion outcome variables, and sample collection were carried out by the LBC team.

Abstract

Birth weight, an indicator of fetal growth, is associated with cognitive outcomes in early life (which are predictive of cognitive ability in later life) and risk of metabolic and cardiovascular disease across the life course. Brain health in older age, indexed by MRI features, is associated with cognitive performance, but little is known about how variation in normal birth weight impacts on brain structure in later life. In a community dwelling cohort of participants in their early seventies we tested the hypothesis that birthweight is associated with the following MRI features: total brain (TB), grey matter (GM) and normal appearing white matter (NAWM) volumes; whiter matter hyperintensity (WMH) volume; a general factor of fractional anisotropy (gFA) and peak width skeletonised mean diffusivity (PSMD) across the white matter skeleton. We also investigated the associations of birthweight with cortical surface area, volume and thickness. Birthweight was positively associated with TB, GM and NAWM volumes in later life ($\beta \geq 0.194$), and with regional cortical surface area but not gFA, PSMD, WMH volume, or cortical volume or thickness. These positive relationships appear to be explained by larger intracranial volume rather than by age-related tissue atrophy, and are independent of body height and weight in adulthood. This suggests that larger birthweight is associated with increased brain tissue reserve in older life, rather than a resilience to age-related changes in brain structure, such as tissue atrophy or WMH volume.

2.1 Introduction

The Developmental Origins of Health and Disease hypothesis, formulated by David Barker, posits that the fetal development influences health and disease risk throughout the life course (Barker, 2004). Birth weight, an indicator of fetal growth, is associated with cardiovascular disease risk, and neurological and psychiatric outcomes from early life into adulthood, as well as early life cognitive outcomes (Geelhoed and Jaddoe, 2010; O'Donnell and Meaney, 2017; Sacchi et al., 2020; Shenkin et al., 2001). Higher cognitive ability in early life is associated with reduced risk of dementia and cognitive decline in later life (Bourne et al., 2007; Dekhtyar et al., 2015; Richards et al., 2004). Brain tissue reserve (indexed by maximal brain size) and age-associated changes to brain structure are two important neuroanatomical contributors to cognition in older age (Cox et al., 2019a; Royle et al., 2013; Tucker-Drob, 2019; van Loenhoud et al., 2018). Identifying potential determinants of cognitive and brain ageing is of paramount importance, and the nature of brain reserve that a higher birthweight might confer has been underexplored. In this study we have focused on the relationship between birth weight and metrics of brain structure known to be associated with cognition and cognitive decline in later life (Cox et al., 2019a; Ritchie et al., 2015c). It is unclear whether birth weight is a marker of preserved differentiation (differences in how much brain tissue an individual has to begin with), differentiated preservation (differences in decline), or both (Tucker-Drob, 2019).

Birth weight within the normal range (2.5 – 4.5 kg) correlates with cognitive performance in childhood (Pearson's r ~ 0.17), and this influence may extend into adulthood and later life (Grove et al., 2017; Shenkin et al., 2009b, 2004). Birth weight also demonstrates a relationship with brain volume (β ~ 0.17), and with a regional patterning of positive associations across the cortical surface area in a cohort of young adults and adolescents – the authors of this study suggested that the regional effects of birth weight on cortical surface area may

be due to head size or body size, but this was not explicitly tested (Walhovd et al., 2012). Importantly, the association between birth weight and brain tissue volumes and intracranial volume is evident in later life (Muller et al., 2016, 2014). However, the distinct contributions of anthropometric variables such as height, weight and head size remain unclear. Studies on diffusion MRI and birth weight have found white matter alterations in adolescents born with very low birth weight (<1500g), compared to those who were born normal birth weight life, and birth weight has been found to have a positive association with frontal white matter fractional anisotropy in later (Shenkin et al., 2009a; Skranes et al., 2007; Vangberg et al., 2006). However, little is known about the impact of birth weight variation on white matter microstructure in later life. Below the normal range birth weight is linked to a range of neurobiological correlates that extend into adolescence including reduced white matter microstructural integrity, and deviations in cortical thickness (both region dependent thickening and thinning), and volumetric alterations that may be associated with reduced cognitive function (Bjuland et al., 2013; de Bie et al., 2011; Eikenes et al., 2011; Hadaya and Nosarti, 2020; Karolis et al., 2017).

To better understand the value of birth weight value as a perinatal indicator of later life brain health, it is important to establish the neurobiological correlates of birth weight into older age. We investigated the following global measures, each of which is reliably associated with cognitive ability in later life with modest effect sizes: total brain (TB), grey matter (GM) and normal appearing white matter (NAWM) which are also linked to cognition, as well as white matter hyperintensity (WMH) volume, a marker of cerebrovascular disease in older age, is associated with cognitive decline (Arvanitakis et al., 2016; Au et al., 2006; Cox et al., 2019a; Pietschnig et al., 2015; Royle et al., 2013; Wiseman et al., 2018). In older age, brain volume may be affected both by the degree of tissue atrophy that has occurred and by maximal healthy brain size (indexed by intracranial volume (ICV), an archaeological measure of maximal brain volume that is

invariant with age (Blatter et al., 1995; Royle et al., 2013; Vågberg et al., 2017). To investigate the effects of age-related atrophy on associations between birth weight and brain volumes, we controlled for ICV (Royle et al., 2013). Controlling current brain size for ICV, either as a covariate in analysis or expressed as a proportion, is a well validated measure of the tissue atrophy that has taken place since the brain reached maximal size (van Loenhoud et al., 2018). As birth weight is also associated with greater adult height and weight, we controlled for these variables to investigate whether a relationship with brain volumes may be due to overall body dimension, rather than to a specific effect on brain or head growth (O'Brien et al., 2006; Sørensen et al., 1999). We selected two global measures of white matter microstructure: gFA, which reflects the pattern of covariance of FA values among white matter pathways of the brain and is correlated with preterm birth, ageing, and cognitive functioning in older age, and PSMD, which is effective at capturing diffuse pathology in otherwise normal appearing white matter (Baykara et al., 2016; Cox et al., 2019a, 2016; Deary et al., 2019; Telford et al., 2017; Vinciguerra et al., 2019). We further investigated regional associations between birth weight and cortical thickness, volume and surface area and explicitly tested the contribution of head size and body size.

To test the hypothesis that birthweight is associated with brain macrostructure and white matter microstructure in older age, we linked these MRI features of brain structure at 73 years of age with perinatal data using a well-characterised single-year-of-birth cohort of healthy community dwelling-older adults (the Lothian Birth Cohort 1936). To understand *how* birth weight has an impact on brain structure we considered the potential roles of i) body size ii) age-related brain tissue atrophy, and iii) cardiovascular and metabolic disease, which is also linked to low birth weight and may mediate the relationship between birth weight and brain structure.

2.2 Materials and Methods

2.2.1 Participants

Data were collected from the Lothian Birth Cohort 1936 (LBC1936), a longitudinal study of aging comprising individuals who were born in 1936. They mostly took part in the Scottish Mental Survey 1947 (SMS1947) and most were resident in Edinburgh and its surrounding area (the Lothians) at about age 70 years when recruitment for follow-up testing began. The recruitment, brain imaging, and cognitive testing protocols for the LBC1936 have been reported previously in detail (Deary et al., 2007; Taylor et al., 2018; Wardlaw et al., 2011).

At Wave 2, 866 participants returned (mean age = 72.5 years, SD = 0.7 years), 728 of whom underwent brain structural and diffusion MRI, upon which the current study is based. Ethical approval for the LBC1936 study came from the Multi-Centre Research Ethics Committee for Scotland (MREC/01/0/56; 07/MRE00/58) and the Lothian Research Ethics Committee (LREC/2003/2/29). All participants, who were volunteers and received no financial or other reward, completed a written consent form before any testing took place.

2.2.2 Birth weight

Birth weight was retrieved from original archival hospital records from the time of birth, accessed from the Lothian Health Service Archive at the Centre for Research Collections in the University of Edinburgh. Participants were born at the Edinburgh hospitals Royal Maternity Simpson Memorial Hospital (n = 74), Elsie Inglis Memorial Maternity Hospital (n = 60), Bellshill Maternity Hospital in Lanarkshire (n =2) and Aberdeen Maternity Hospital (n = 1). Birth weight was recorded in the original records in lb and oz and subsequently converted to grams. Analysis was performed with birth weight as a continuous variable.

2.2.3 Cardiovascular health covariates

During a structured medical history interview at Wave 2, participants were asked whether they had a history of cardiovascular disease or stroke, or had received a diagnosis from a doctor of diabetes, hypercholesterolemia, or hypertension. They were also asked about their smoking history (current/ex/never). BMI (kg/m^2) was calculated from height (cm) and weight (kg) which were measured at the same time as the medical interview.

2.2.4 Brain MRI acquisition and processing

Whole-brain structural and diffusion tensor MRI data were acquired by using a 1.5 T GE Signa Horizon scanner (General Electric, Milwaukee, WI, USA) located at the Brain Research Imaging Centre, University of Edinburgh, soon after cognitive testing and plasma collection. T1-, T2-, T2* and FLAIR-weighted MRI sequences were collected and co-registered (voxel size = 1 × 1 × 2 mm). Intracranial (ICV), total brain (TB), grey matter (GM), total white matter and white matter hyperintensity (WMH) volumes were measured using a semi-automated multispectral fusion method for segmentation of brain tissue volumes from the four structural scans, that is, T2-, T1-, T2*- and FLAIR-weighted MRI, (Wardlaw et al., 2011) (Valdés Hernández et al., 2010). Normal-appearing white matter volume (NAWM) was calculated as the difference between total white matter and WMH volumes.

The diffusion MRI protocol employed a single-shot spin-echo echo-planar diffusion-weighted sequence in which diffusion-weighted volumes (b = 1000 s mm^{-2}) were acquired in 64 non-collinear directions, together with seven T2-weighted volumes (b = 0 s mm^{-2}). This protocol was run with 72 contiguous axial slices with a field of view of 256 × 256 mm, an acquisition matrix of 128 × 128 and 2 mm isotropic voxels (Wardlaw et al., 2011). From these data we derived a factor of general fractional anisotropy (gFA) from quantitative tractography and peak width skeletonised mean diffusivity (PSMD).

Probabilistic neighbourhood tractography, an automatic tract segmentation method with good reproducibility, was implemented in the TractoR package for R (http://www.tractor-mri.org. uk) (Clayden et al., 2011). The following 12 tracts of interest in each were segmented using this method: the genu and splenium of the corpus callosum, the bilateral rostral cingulum cingulate gyri, the bilateral arcuate, uncinate, and inferior longitudinal fasciculi, and the bilateral anterior thalamic radiations. Tract average FA was derived as the average of all voxels contained within the tract mask weighted by connection probability.

PSMD is the 95th percentile minus the 5th percentile of an individual's MD within the white matter skeleton. Automatic calculation of PSMD followed the procedure described by Baykara et al. (2016) (Baykara et al., 2016). Diffusion MRI data were processed using the standard Tract-based Spatial Statistics (TBSS) pipeline in FSL. First, all participants' FA volumes were linearly and non-linearly registered to the standard space FMRIB 1-mm FA template. Second, a white matter skeleton was created from the mean of all registered FA volumes. This was achieved by searching for maximum FA values in directions perpendicular to the local tract direction in the mean FA volume. An FA threshold of 0.2 was applied to the mean FA skeleton to exclude predominantly non-white matter voxels. Third, MD volumes were projected onto the mean FA skeleton and further thresholded at an FA value of 0.3 to reduce CSF partial volume contamination using the skeleton mask provided by Baykara et al. (2016) (Baykara et al., 2016). Finally, PSMD was calculated as the difference between the 95th and 5th percentiles of the voxel-based MD values within each subject's MD skeleton (Deary et al., 2019). We opted for this metric instead of a general factor of MD based on prior work indicating its stronger associations with cognitive functioning than gMD (Baykara et al., 2016; Deary et al., 2019; Penke et al., 2010).

Finally, each of the T1-weighted volumes were processed using FreeSurfer v5.1. Following visual quality control in which the outputs for each participant were inspected for aberrant surface meshes, skull stripping and tissue segmentation failures, their estimated cortical surfaces were registered to the 'fsaverage' template, yielding a measure of regional volume, surface area and thickness at each of 327,684 vertices across the cortical mantle.

2.2.5 Statistical Analyses

Unless otherwise stated, all analyses were conducted in R 3.4.3 (R Core Team 2015). We conducted t-tests of continuous variables (age, weight, height, BMI, age 11 IQ) and χ^2 tests of categorical variables (sex, smoking status, diagnosis of hypertension, hypercholesterolemia or diabetes, cardiovascular disease and stroke history) between the cohort subsample with birth weight data and those without birth weight data. For regression models we report standardised regression coefficients and corrected p-values for multiple comparisons using the False Discovery Rate (FDR; Benjamini and Hochberg, 2007). A general factor of white matter tract FA was calculated using confirmatory factor analysis in *lavaan* (Rosseel, 2012). A latent factor was estimated from the mean FA of the 12 segmented white matter tracts. Each model included residual correlations between the left and right versions of the bilateral tracts, and also the residual correlation between the splenium and the genu of the corpus callosum. Standardised tract loadings on a general factor of FA (gFA) were > 0.4. Average variance explained = 31.4% Model fit statistics: Tucker Lewis Index= 0.961, Comparative Fit Index = 0.972, root mean square error of approximation = 0.043, standardised root mean square residual = 0.031, $X^2(48)= 106.341$, p <0.001. Tract loadings are reported in Table 1. A standardised factor score was extracted from the model for subsequent analysis. WMH volume was log transformed to meet the assumptions of homoscedasticity and normality of error distribution for linear regression.

Table 1. Tract loadings on general factor of fractional anisotropy

Tract	Standardised loadings.
Splenium	0.425
Genu	0.624
LArc	0.613
RArc	0.606
LATR	0.600
RATR	0.585
LCing	0.520
RCing	0.530
LUnc	0.634
RUnc	0.661
LILF	0.437
RILF	0.416

Note. the genu and splenium of the corpus callosum, LArc – Left arcuate, RArc – right arcuate, LATR – left anterior thalamic radiation, RATR – right anterior thalamic radiation, LCing – Left cingulum bundle, RCing – Right cingulum bundle, LUnc – left uncinate, RUnc – right uncinate, LILF – left inferior longitudinal fasciculus, RILF – right inferior longitudinal fasciculus.

Initially, we conducted linear regression models of birth weight and global brain image features, with a separate model for each of TB, GM, NAWM and WMH volumes, and PSMD and gFA as the outcome variable. Sex and age in days at MRI acquisition were included as covariates in all models. These models were then conducted with the inclusion of anthropometric covariates height and weight to isolate unique effects of birth weight from late life body size. Pearson correlations were calculated for birth weight with height and weight in later life. Next, because associations between smaller brain volumes in later life with

lower birth weight may be explained by increased atrophy in later life, or by having a smaller maximal brain size, prior to age-associated atrophy, we re-ran the associations using the global brain volumes (TB, GM, NAWM, WMH) with ICV as a covariate in addition to age at scan and sex. ICV is a reliable archaeological metric for estimating maximal healthy brain size (Royle et al., 2013). There are several potential ways of controlling for ICV: one is to express brain volumes as a proportion (i.e. a ratio of volume to ICV), and another is to include ICV as a covariate in analysis (O'Brien et al., 2011). For completeness we have included regression results for analysis using the proportion method.

Due to the relationship between birthweight and cardiovascular disease in later life, and the association between cardiovascular disease and brain structural outcomes, we conducted a set of models adjusting for age and sex and the following health covariates to control for the potential influence on results of cardiovascular and metabolic disease risk: Body Mass Index (BMI), hypertension, diabetes, hypercholesterolemia, smoking status (three categories: current, ex and never), and cardiovascular disease history.

Associations between birth weight and cortical measures (volume, thickness and surface area) were investigated in vertex-wise analyses across cortical mantle, using data smoothed at 20 FWHM to the FreeSurfer average surface (brainstem removed). Age and sex were included as covariates in all models. We additionally included height and weight to control for adult body size. In a separate analysis ICV was included in addition to age and sex to investigate whether the effect of birth weight on brain volumes was accounted for by larger head size/maximal brain size. Cortical volume, thickness and surface area vertex-wise analyses were performed across the average surface with linear models to investigate the effect of birth weight on cortical surface area using the SurfStat toolbox (http://www.math.mcgill.ca/keith/surfstat) for Matrix Laboratory R2018a (The MathWorks Inc., Natick, MA), for which 130 participants had

complete MRI, birth weight and covariate data. Results are reported in the form of t-statistics and FDR-corrected q-maps displayed on the 'fsaverage' cortical surface.

2.2.6 Data sharing

LBC 1936 data supporting the findings of this paper are available from the corresponding author upon reasonable request. LBC1936 data are not publicly available due to them containing information that could compromise participant consent and confidentiality. Reasonable requests for original image data will be considered through the Brain Images of Normal Subjects (BRAINS) image bank governance process: www.brainsimagebank.ac.uk (Job et al., 2017). Code used for analysis is available at: https://github.com/ENWWheater/MRI_Birthweight_LothianBirthCohort1936.

2.3 Results

2.3.1 Cohort

One hundred and thirty-seven participants of the Lothian Birth Cohort 1936 (LBC1936), a cohort of community dwelling older participants, had both birth weight recorded and structural and diffusion MRI, out of a total of 866 participants in the second wave of data collection (Table 2). In this sample there were no cases of dementia or Parkinson's disease. Six participants were low birth weight (<2500g); no participants were high birth weight (>4500g). There were no significant differences between those who had both MRI and birth weight data and those who did not in terms of age 11 IQ, age at MRI scan, sex, height, weight, BMI, smoking, hypertension, hypercholesterolemia, diabetes, cardiovascular disease history, or stroke history (all p values >0.05) (see Table 2).

Table 2. Characteristics of participants in sample, and those outside of sample from Wave 2 of LBC1936 data collection.

Total N	**137**	**LBCW2 N = 729**	TESTS
Female/Male	63/74	355/374	χ^2 = 0.2397; p = 0.624459
Age 11 IQ	99.84 (41.98 – 126.27)	100.83 (38.48 – 129.88)	T = -0.72485; p = 0.4694
Mean age (range) / years	72.6 (71.1 – 74.1)	72.5 (70.9 – 74.00	T = 1.05; p = 0.2942
Mean birth weight (range) /g **≤2500** **2501-3000** **3001-3500** **3501-4000** **4001-4500**	3346 (1843 – 4423) 6 22 58 40 11	- - - - - -	
Mean height (range) /cm	166.0 (146.0 – 185.5)	166.5 (143.1 – 195.5)	T = -0.061; p = 0.5458
Mean weight (range) / kg	78.35 (50 – 116.8)	77.28 (41.20 – 195.5)	0.76; p = 0.4454
Mean BMI (range)	28.37 (19.32 – 45.65)	27.84 (16.67 – 51.01)	T = 1.2; p = 0.2264
Smoking (current/ex/never)	14/55/68	62/320/347	χ^2 = 0.8603; p = 0.6504
Hypertension (yes/no)	66/71	359/370	χ^2= 0.0529 p = 0.818145
Hypercholesterolemia (yes/no)	62/75	294/435	χ^2 = 1.1561; p = 0.282284
Diabetes diagnosis (yes/no)	21/116	74/655	χ^2 = 3.1655; p = 0.07521
Cardiovascular disease history (yes/no)	43/94	207/522	χ^2 = 0.5027; p = 0.478315
Stroke history (yes/no)	11/126	44/685	χ^2 = 0.7706; p = 0.38

Note. Summary of descriptive data for LBC 1936 sample for those with MRI and BW data included in this analysis, and for those LBC wave 2 participants who were not included in the analysis. BMI: body-mass index. Hypertension, hypercholesterolemia, diabetes, cardiovascular and stroke history were obtained by participant self-report in a structured medical interview. Far right column contains test statistics and p values for comparisons between the two groups.

2.3.2 Birth weight is associated with brain volumes but not atrophy

We first performed linear regression models corrected for age and sex to test the association between birth weight and the following brain MRI features: total brain (TB), grey matter (GM), normal appearing white matter (NAWM), and white matter hyperintensity (WMH) volumes, a general factor of fractional anisotropy (gFA) and peak width skeletonised mean diffusivity (PSMD). The results of age- and sex-corrected associations between birth weight and global brain measures are presented in Table 3. Individuals with a higher birth weight showed generally higher later life TB ($\beta = 0.259$, $p < 0.001$), GM ($\beta = 0.194$, $p = 0.009$), and NAWM ($\beta = 0.293$, $p < 0.001$) volumes, all of which survived false discovery rate (FDR) multiple comparison correction. However, birth weight was not significantly associated with WMH, or diffusion metrics of white matter microstructure: gFA or PSMD ($\beta \geq -0.051$, $p > 0.555$).

Next, we investigated whether the effect of birth weight on brain volumes was accounted for by larger body size by controlling for height and weight in addition to age at scan and sex. Following adjustment for height and weight, TB and NAWM volumes remained significantly associated with birth weight, though the strength of the association was reduced by 27% and 23%, respectively. GM volume was no longer significantly associated with birth weight (effect size was attenuated by 31.9%). Birth weight was significantly associated with later life height (Pearson's $r = 0.209$, $p = 0.006$) but not with later life weight ($r = 0.137$, $p = 0.739$).

Results for associations between global volumetric measures corrected for ICV are presented in Table 3. ICV is strongly correlated with TB, GM and NAWM volumes (Pearson's $r \geq 0.835$, $p < 0.001$) but not with WMH volume (Pearson's $r = 0.066$ $p = 0.086$; see Figure 1). When we included ICV as a covariate for all

global volumetric measures, we found no significant associations between birth weight and TB volume ($\beta \leq |0.076|$, $p \geq 0.107$). Results were nearly identical when height and weight were also included in the model ($\beta \leq |0.072|$, $p \geq 0.137$). The associations magnitudes and p-values were also similar when these global MRI volumes were expressed as a proportion of ICV (Table 4; ($\beta \leq |0.149|$, $p > 0.070$)).

As the inclusion of ICV as a covariate attenuated the relationship between birth weight and brain volumes, we performed an *a posteriori* regression to verify the association between birth weight and ICV directly. ICV was significantly associated with birthweight ($\beta = 0.174$; $p = 0.009$) in a linear regression that included age at MRI, sex, height and weight as covariates.

Figure 1. Correlation matrix showing Pearson's r correlations between brain MRI features and birth weight, age at MRI, height and weight, and point biserial correlations between these variables and sex.

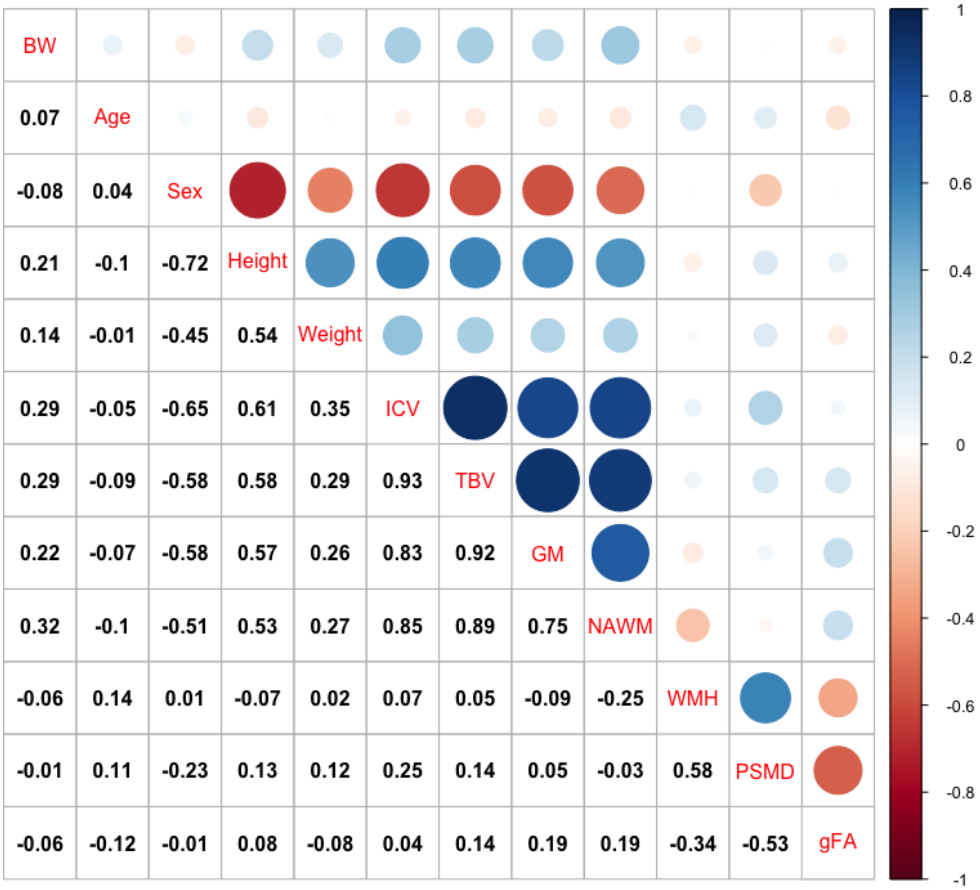

Note BW: birth weight; ICV: intracranial volume; TBV: total brain volume; GM: grey matter volume; NAWM: normal appearing white matter; WMH: white matter hyperintensity volume; PSMD: peak width skeletonized mean diffusivity; gFA: general factor of fractional anisotropy.

Table 3. Associations between birth weight and global brain structure at age 73.

	Adjusted for sex and age		Adjusted for sex, age, height and weight		Adjusted for sex, age and ICV		Adjusted for sex, age, ICV, height and weight	
Metric	*β*	*p*	*β*	*p*	*β*	*p*	*β*	*p*
TB	**0.259**	**<0.001**	**0.190**	**0.011**	0.028	0.442	0.024	0.518
GM	**0.194**	**0.009**	0.132	0.078	0.001	0.979	-0.007	0.900
NAWM	**0.293**	**<0.001**	**0.226**	**0.003**	0.076	0.107	0.072	0.137
WMH	-0.041	0.636	-0.017	0.851	-0.047	0.609	-0.025	0.790
gFA	-0.051	0.555	-0.094	0.280	-	-	-	-
PSMD	-0.037	0.657	0.013	0.883	-	-	-	-

Note. Standardised regression coefficients between birth weight and volumetric/white matter microstructure MRI measures in models adjusted for: sex and age at MRI; sex, age at MRI, height and weight; sex, age at MRI and ICV; and sex, age at MRI, ICV, height and weight. Bold typeface denotes FDR $q < 0.05$. TB: total brain volume; GM: grey matter volume; NAWM: normal appearing white matter volume; WMH: white matter hyperintensity volume; gFA: general factor of fractional anisotropy; PSMD: peak width skeletonised mean diffusivity; ICV: intracranial volume.

Table 4. Associations between birth weight and the ratio of global brain volumetric MRI measures as a proportion of intracranial volume, correcting for age and sex

	β	*p*
TB/icv	0.006	0.937
GM/icv	-0.074	0.379
NAWM/icv	0.149	0.080
WMH/icv	-0.094	0.273

Note. Standardised regression coefficients between birth weight and volumetric MRI measures expressed as a ratio with ICV. Bold typeface denotes FDR $q < 0.05$. TB: total brain volume; GM: grey matter volume; NAWM: normal appearing white matter volume; WMH: white matter hyperintensity volume.

2.3.2 Relationship between birth weight and brain structure is independent of cardiovascular risk factors and cardiovascular disease history

When we additionally corrected the associations between birth weight and global brain measures for cardiovascular risk factors and self-report history of cardiovascular disease (Table 5), the initial age- and sex- corrected findings (in Table 2) were modestly attenuated by up to 8.5% (this being the attenuation of effect for NAWM). The associations for birthweight remained significant for TB (β = 0.245, p = 0.00170), GM (β = 0182, p = 0.0188 and NAWM (β = 0.268, p = 0.000754). Associations with WMH, gFA and PSMD remained small and non-significant (β ≤|0.05|, p ≥ 0.5). In a sensitivity analysis including stroke as a covariate did not substantially alter the results (Table 6), though it marginally attenuated the association between GM and birth weight, which was non-significant after FDR correction (B = 0.172, p = 0.031). The size of the attenuation of the effect when stroke was added as a covariate was 5.5%. In a non-stroke sub-group (n = 126) analysis birth weight and GM were still significantly associated (β = 0.203, p = 0.011).

Table 5. Associations between birth weight and volumetric MRI measures correcting for age, sex, cardiovascular risk factors and cardiovascular disease history.

	β	*p*
TB	**0.245**	**0.002**
GM	**0.182**	**0.019**
NAWM	**0.268**	**<0.001**
WMH	-0.035	0.701
gFA	-0.053	0.547
PSMD	-0.016	0.850

Note. Standardised regression coefficients between birth weight and volumetric/white matter microstructure MRI measures. Bold typeface denotes FDR $q < 0.05$. TB: total brain volume; GM: grey matter volume; NAWM: normal appearing white matter volume; WMH: white matter hyperintensity volume; gFA: general factor of fractional anisotropy; PSMD: peak width skeletonised mean diffusivity.

Table 6. Associations between birth weight and volumetric MRI measures correcting for age, sex, cardiovascular risk factors and cardiovascular disease and stroke history.

	β	*p*
TB	**0.233**	**0.004**
GM	0.172	0.031
NAWM	**0.262**	**0.001**
WMH	-0.049	0.598
gFA	-0.060	0.503
PSMD	0.010	0.910

Note. Standardised regression coefficients between birth weight and volumetric/white matter microstructure MRI measures. Bold typeface denotes FDR $q < 0.05$. TB: total brain volume; GM: grey matter volume; NAWM: normal appearing white matter volume; WMH: white matter hyperintensity volume; gFA: general factor of fractional anisotropy; PSMD: peak width skeletonised mean diffusivity.

2.3.3 Associations between birth weight and regional grey matter measures

Vertex wise analysis revealed positive associations between birth weight and surface area on the bilateral temporal (inferior and middle), cingulate (anterior and posterior segments) and anterior frontal (inferior frontal and frontopolar), supramarginal and medial occipital cortices, as well as evidence for associations in the motor and somatosensory cortices and right-sided medial and lateral orbitofrontal, posterior fusiform, angular gyrus and supramarginal gyrus (Figure 2A). These associations were partially attenuated when correcting for height and weight: mean attenuation = 19.21%, SD = 8.67, max = 52.53% (Figure 2B). Controlling for ICV, in a model that was adjusted for age and sex, rendered the regional patterning of

birth weight on regional cortical surface area non-significant: mean attenuation = 48.0%, SD = 13.81, max = 98.43% (Figure 2C). There were no significant associations between birth weight and cortical thickness or cortical volume.

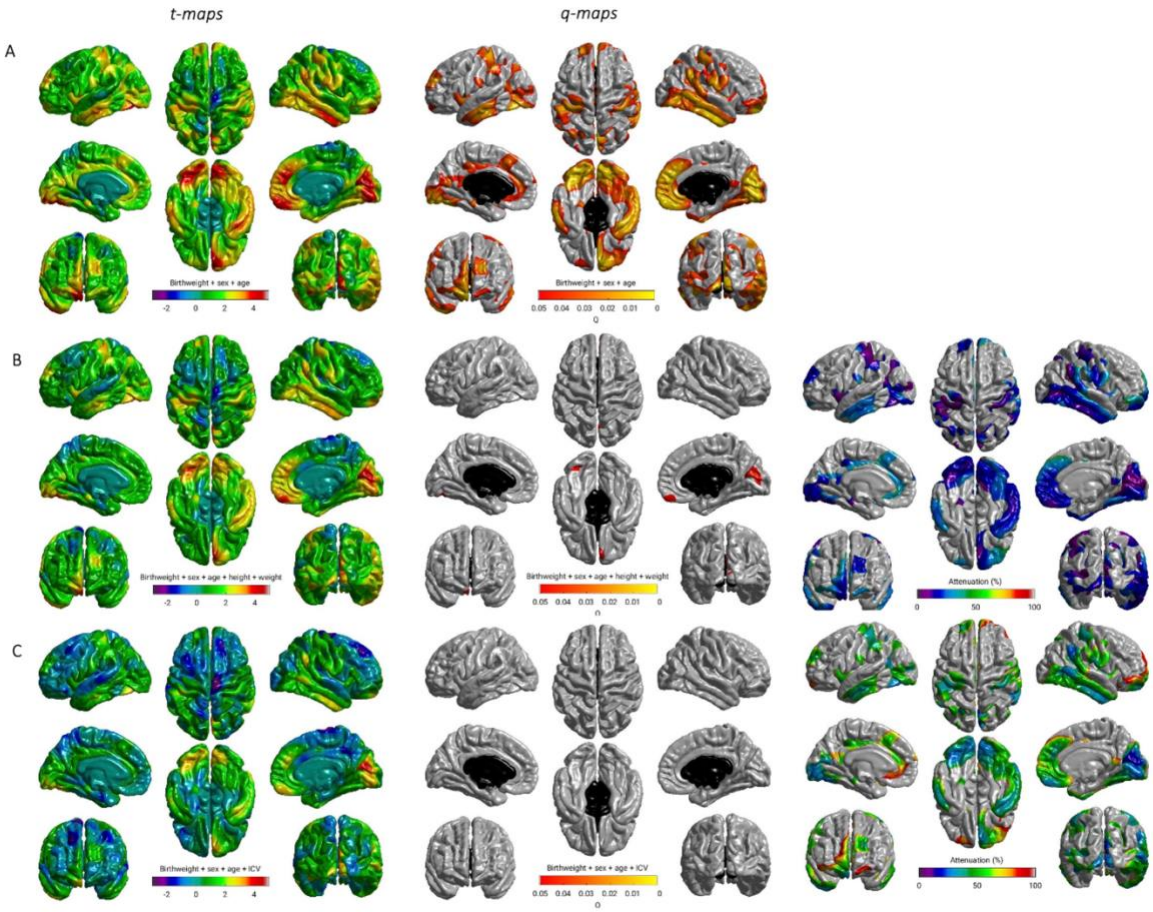

Figure 2. Regional distribution of associations between birth weight and cortical surface area: A) adjusted for sex and age; B) adjusted for age, sex, height and weight; C) adjusted for age, sex, and ICV. T maps (left); FDR q values (middle), far right (B and C) shows the percentage attenuation between the model shown in A, and the additionally adjusted models shown in B and C.

2.4 Discussion

In this well-characterised cohort of older community-dwelling adults, we report that higher birth weight is associated with larger TB, GM and NAWM volumes seven decades later. Importantly, these associations become non-significant with inclusion of ICV as a covariate, whereas associations with WMH, a brain marker of older age neurodegenerative processes among healthy adults, were null. This suggests that the association between birth weight and brain tissue volumes are likely due to the influence of brain size in early life, rather than brain tissue atrophy in later life. This indicates that higher birthweight may be associated with brain reserve in older age, in a pattern consistent with preserved differentiation rather than differentiated preservation.

Birth weight is positively correlated with adult height and weight and so we controlled for these to test whether the positive associations between birthweight and brain volumes were due to overall body size (Eide et al., 2005; Sørensen et al., 1999). Controlling for the effects of these anthropometric indices attenuated the effects between brain volumes and birth weight, but as both TB and NAWM volumes remained significantly positively associated with birth weight when height and weight were controlled for, this relationship appears largely independent of these indices. This was not the case for GM volume, although the effect size attenuation was modest. Given known associations between low birth weight and cardiovascular outcomes, and between cardiovascular risk factors and brain structural outcomes, we included these as covariates in a supplementary analysis and found that, although there was a modest attenuation of the effect (by up to 8.6%), results were robust (Cox et al., 2019b; Debette et al., 2011; Osmond et al., 1993; Song et al., 2020). In analyses of cortex associations, we found a strikingly similar pattern of positive associations between cortical surface area to that observed, by Walhovd et al. 2012, in a cohort of young adults and adolescents (Walhovd et al., 2012). These regional variations of cortical surface area in association with birth weight are

in line with the patterning of differential scaling seen as a function of TB volume, and may reflect asymmetric tissue scaling with overall brain dimension rather than an altered developmental trajectory (either maladaptive or compensatory) (Jäncke et al., 2019; Reardon et al., 2018). Walhovd et al. 2012 suggested that this effect might be partly driven by being physically larger and here we directly tested this hypothesis. The effect was partially attenuated by controlling for height and weight (by about 20%) which was sufficient for many of the associations across the cortical surface to become non–significant, though several areas still survived FDR correction. The attenuations of effect when controlling for height and weight were modest in comparison to the attenuations observed when controlling for ICV alone. In our analysis of cortical surface area, the magnitude of attenuation was on average around 50% when controlling for ICV. This is consistent, again, with our global brain tissue findings that the associations between birth weight and brain measures 73 years later are attributable to having a bigger head, rather than due to being physically bigger overall. However, like Walhovd et al. 2012, we found no significant relationship between either cortical thickness or volume with birth weight. Taken together, our results indicate a specific association between birth weight and maximal healthy brain size that is independent of its relationship to overall body size as measured by height and weight.

Despite consistent findings that low birth weight is associated with diffuse white matter injury from the neonatal period through to early adulthood, captured by measures of white matter microstructure, we did not observe a relationship between birth weight and WMH volume or global measures white matter microstructure in late life (Pascoe et al., 2019; Telford et al., 2017). However, in our study the birth weight range of the participants was largely normal and an association between birth weight and white matter microstructure was not evident. This supports the theory that the observed associations between low birth weight or preterm birth and white matter microstructure is the product of perturbation during a limited developmental

window which coincides with specific biological and environmental exposures, but those susceptibilities are not apparent for individuals in the normal birth weight range (Boardman and Counsell, 2020).

Our study has some limitations. Due to the historical nature of the birth data, we do not have reliable and precise information about gestational age at birth, and so we could not estimate the prevalence of fetal growth restriction (indicated by being small for gestational age) in our sample. Birth weight reflects fetal growth, which is influenced by genetic factors, uteroplacental function, and a range of prenatal exposures including maternal health. A previous study showed a significant association between birth weight and cortical surface area even when controlling for parental height (as an indicator of genetic contributors to growth), which suggests that the relationship we observed between birth weight and brain structure is likely independent of genetic growth potential (Walhovd et al., 2016). Height and weight in this sample were obtained only in older age rather than in midlife for instance, it is possible that head size is simply a more stable indicator of overall body size than height or weight. There are modest decreases in height that occur from midlife onwards and which accelerate around 70 years of age, due to stooping and flattening of intervertebral discs. However, the Pearson's correlations between birth weight and adult height reported in this sample ($r = 0.21$; Supplementary Figure 1) are of a very similar magnitude to those reported for a large group of men and women in the age group 56-70 years old (Ylihärsilä et al., 2007). In this study we have used a relatively small sample due to the availability of detailed birth data. However, our findings with regards to the positive associations between birth weight and brain tissue volumes in later life and regional cortical surface area are consistent with other studies in both adolescents and adults in late life (Muller et al., 2016, 2014; Walhovd et al., 2012). We have provided additional analysis of the impact of birth weight on more detailed measures of white matter microstructure and integrity, as well as demonstrating that the regional effects observed in cortical surface area persist into older age and are likely

due to the associations between birth weight on head growth and maximal head size; these relationships are likely established in early life. Within the LBC1936 participants we compared age 11 IQ (as an indicator of potential early life differences) of those with and without birth weight and MRI data, and found no significant difference between the two groups. This was also the case for the covariates included in our analysis, indicating that our sample is representative of the LBC1936 as a whole. This does not preclude the possibility that there were systematic differences in the characteristics of the women who gave birth in hospital in the 1930s compared to those who did not. In addition, the LBC1936 have higher cognitive ability based on their age 11 scores on the Moray House Test relative to the rest of the population that sat the test in 1947 (Johnson et al., 2010; Johnson and Deary, 2011). They are also likely to be of higher educational achievement and socioeconomic status (Johnson et al., 2011). Generalization of these results to other groups must be performed with caution. We expect that, due to this range restriction, the effect sizes reported here are likely to be underestimates of the true effect sizes that would be observed in the wider population. There is a low occurrence of low birth weight (<2.5kg) in this older age cohort, which is likely to be the result of survivor bias, and reflects the advancement in care and subsequent survival of infants born with low birth weight since 1936. It is, however, striking that these effects relating to variation in birthweight, within a largely normal range, are still detectable among such a relatively healthy group and across seven decades of life. This suggests that this variable may have valuable explanatory power with regards to the epidemiology of cognitive ageing.

Cognitive function and the emergence of cognitive impairment in older age are products of peak cognitive function (preserved differentiation) and the rate of decline that occurs in later life (differential preservation) (Tucker-Drob, 2019). Our results indicate that higher birth weight associates with increased brain volumes in later life in a manner consistent with preserved differentiation. We did not find an association between birth weight and age

associated brain neuroimaging features such as white matter hyperintensity volume or tissue atrophy. This suggests that birth weight is not related to differential preservation. However, analysis of longitudinal MRI neuroimaging would be required to gain temporal resolution and measures of atrophic rate, to distinguish between atrophy that began early and proceeded slowly and that which began late and proceeded quickly. Despite this, our results echo observations of other contributors to brain structure, such as education, and of cognition: cognitive ability in early life is a predictor of cognitive ability in later life, but does not seem to protect against age related cognitive decline or pathology, and similarly correlates of brain structure are often found to be predictive of baseline, but not of trajectory of age related decline (Gow et al., 2011; Ritchie et al., 2017). Maximal healthy brain size, estimated by ICV, has previously been demonstrated to modify the emergence of clinical symptoms for dementia, in a manner consistent with brain volume reserve effects, while birth size is significantly correlated with NART performance (an indicator of earlier, crystallized cognitive ability) at 80 years old (Shenkin et al., 2009b; Wolf et al., 2004). We found no evidence that the relationship between birth weight and brain volumes was accounted for by brain tissue atrophy, or cardiovascular risk factors in later life. The relationships between birth weight and brain tissue volumes and cortical surface area were attenuated by ICV. As the majority of ICV growth occurs in early childhood (achieving 95% of maximal size by 5 years old) we suggest that the relationship is established in early life (Sgouros et al., 1999).

Birth weight demonstrates a modest, positive association with brain tissue reserve in later life, which is likely established in early life. It is not a protective factor against either brain tissue atrophy or pathology in later life (indicated by WMH volume and white matter microstructure measured through diffusion MRI). Our results support a developmental origin of brain tissue reserve that survives into old age.

Chapter Conclusion

This study has demonstrated that birth weight is associated with greater brain volumes and regional cortical surface area brain structure in later life, but not with metrics that are associated with ageing, such as atrophy and white matter microstructure. These results support the developmental origins of the relationship between early life factors and brain structure in later life. This lays the foundation for the following chapters, where I investigate the role that DNA methylation plays in brain structure and function, and how it is affected by variation in gestational age.

Chapter 3. DNA methylation and brain structure and function across the life-course: a systematic review

Chapter Introduction

In the previous chapter, I provided evidence that early life factors, indexed by variation in birth weight, exerts an influence on brain structure in late life, supporting a developmental origin in brain structural changes in older age.

The brain is thought to be extremely sensitive to perturbations in gene regulation. Despite this, the role of differential DNAm, an epigenetic mechanism that regulates gene expression, in brain structure and function is not well understood. In this chapter, I examine the evidence that DNA methylation is associated with brain structure and function across life, in non-malignant contexts, by carrying out a systematic review of papers that report associations between DNAm and brain MRI. I test the hypothesis that DNAm is associated with brain imaging in health and disease contexts across the life-course.

This chapter has appeared as a manuscript in *Neuroscience and Biobehavioural Reviews.* As first author, I designed the protocol, developed the search terms, carried out the search and subsequent screening, data extraction, and synthesis, and drafted and wrote the manuscript. Dr David Stoye was the second reviewer, and also carried out screening, and double-extracted a portion of the data.

Abstract

MRI has enhanced our capacity to understand variations in brain structure and function conferred by the genome. We identified 60 studies that report associations between DNA methylation (DNAm) and human brain structure/function. Forty-three studies measured candidate loci DNAm; seventeen measured epigenome-wide DNAm. MRI features included region-of-interest and whole-brain structural, diffusion and functional imaging features. The studies report DNAm-MRI associations for: neurodevelopment and neurodevelopmental disorders; major depression and suicidality; alcohol use disorder; schizophrenia and psychosis; ageing, stroke, ataxia and neurodegeneration; post-traumatic stress disorder; and socio-emotional processing. Consistency between MRI features and differential DNAm is modest. Sources of bias: variable inclusion of comparator groups; different surrogate tissues used; variation in DNAm measurement methods; lack of control for genotype and cell-type composition; and variations in image processing. Knowledge of MRI features associated with differential DNAm may improve understanding of the role of DNAm in brain health and disease, but caution is required because conventions for linking DNAm and MRI data are not established, and clinical and methodological heterogeneity in existing literature is substantial.

3.1 Introduction

A growing number of studies have investigated associations between epigenetic signatures and neuroimaging markers of human disease, behaviour and cognition. This area of research is motivated by the understanding that epigenetic processes contribute to brain development, ageing and disease, and they may mediate interaction between genomic predisposition and environmental pressures that modify brain structure and function.

The term epigenetics refers to a set of molecular mechanisms that modulate the function of the genome in different cell types without altering the genome itself. DNA methylation (DNAm) is one such mechanism whereby a methyl group is covalently added to cytosine residues in a Cytosine-phosphate-Guanine context (CpG). This is thought to alter the accessibility of a locus to transcriptional machinery or modifying proteins, thereby influencing gene expression (Jones, 2012). However, DNA methylation may also occur after an initial change in gene expression and function as a form of longer-term control.

The pathogenesis of several genetic diseases with neurological phenotypes involve DNAm dysregulation. Rett syndrome is a severe neurological disorder characterised by regression of acquired skills, stereotypic movements, microcephaly, seizures, and intellectual disability. It results from a loss of function mutation in the X-linked methyl-CpG binding protein 2 gene (*MECP2*), which is a chromatin associated protein required for normal neuronal function throughout life. The loss of function mutation in *MECP2* serves to reduce the binding affinity of MECP2 to methylated DNA with effects on regulation of gene expression at transcriptional and post-transcriptional levels (Lyst and Bird, 2015). Angelman syndrome is characterised by cognitive impairment, movement or balance disorder, typical abnormal behaviours, and impaired speech and language. It arises from a mutation or deletion of the maternal ubiquitin protein ligase 3A gene (*UBE3A*)

and the neuronal tissue specific paternal imprinting of the gene that silences the paternal allele (Rangasamy et al., 2013). Fragile X syndrome arises due to CGG triplet expansion within the *FMR1* gene promoter which becomes hypermethylated and results in a reduction of gene expression (Wijetunge et al., 2013). In addition to these genetic neurological disorders associated with DNAm dysregulation, variation in DNAm has been implicated in the pathogenesis of a number of complex neurodevelopmental, neurological and psychiatric diseases including autism, schizophrenia, and problems associated with trauma and stress (De Rubeis et al., 2014; Grayson and Guidotti, 2013; Klengel et al., 2014; Oberlander et al., 2008; Palumbo et al., 2018).

DNAm may be modifiable by environmental factors including physiological and emotional stress, child abuse, nutritional deprivation, and other lifestyle factors that operate from fetal life to old age (Cao-Lei et al., 2015; Del Blanco and Barco, 2018; Gouin et al., 2017; Heijmans et al., 2008; Joehanes et al., 2016; McGowan et al., 2009; Provenzi et al., 2018; Vidal et al., 2014). As such, it has been proposed that environmentally-induced changes in DNAm may enable short-term survival adaptation, but may also induce adaptations that contribute to impaired development of neural networks and increased risk of pathology (Gluckman et al., 2010; Hoffmann et al., 2017).

Structural, diffusion and functional brain MRI enable the parsing of complex behavioural traits and diseases onto quantitative indicators of brain structure and function. Such imaging endophenotypes have been used to demonstrate the impact of common genetic variants on brain health and disease, but the role of DNAm in contributing to brain structure and / or function, as opposed to being a consequence of changes in structure or function, is less certain (Elliott et al., 2018). To obtain a comprehensive overview of the extent to which differential DNAm associates human behaviour and disease we performed a systematic review of studies that have analysed DNAm with quantitative brain MRI data. By doing so we aimed to provide a

comprehensive summary of what is known about DNAm-MRI associative relationships across the life course, and to identify image features associated with differential DNAm. Finally, we captured sources of heterogeneity in the extant literature to better inform the development of methods and conventions for analysing DNAm with MRI data.

3.2 Materials and methods

We performed a systematic literature search based on the PRISMA framework, according to a pre-registered protocol on PROSPERO (CRD42018090928).

3.2.1 Search strategy

Scopus, Web of Science, MEDLINE and EMBASE (via OVID) were searched in March 2018 to identify studies that integrated DNA methylation and human *in vivo* MRI. The search was composed of three OR clusters that contained terms relating to the key domains, which were combined with AND: MRI neuroimaging AND Brain AND DNA methylation. Bibliographies were searched for additional studies. There were no language restrictions on the search.

Systematic review search strategy:

OVID (Embase and Medline)

Epigenetics keywords

1. (DNA methyl* OR methylation Epigen* OR Methylome OR CpG OR CGI OR “bisulfite
adj1 (conversion OR treatment OR pyrosequencing OR sequencing)”).mp OR
Headings:
2. DNA methylation/ OR Epigenomics/ OR CpG Islands/ OR Exp epigenesis, genetic/
3. 1 OR 2
Brain:
Keywords:
4. “small worldness” OR Connectome OR Connectivity OR Myelin* OR “white matter”
OR “Brain volume” OR “cortical connectivity” OR “graph theor*” OR topology OR
cereb* OR (Connect* adj5 (brain or neur*)).mp
Headings:
5. White matter/ OR Neural Pathways/ OR Brain Mapping/ or exp Brain/
6. 4 OR 5

MRI Keywords

7. (MRI OR DTI OR fMRI OR dMRI OR “Magnetic Resonance Imaging” OR “Diffusion
Tensor Imaging” OR “Diffusion Magnetic Resonance Imaging” OR “functional Magnetic Resonance Imaging” OR dtMRI OR “diffusion tensor Magnetic Resonance
Imaging”).mp
8. Exp Neuroimaging/ OR Exp Magnetic Resonance Imaging/
9. 7 OR 8
10. 3 AND 6 AND 9

Web of Science

TS = (("DNA methyl*" OR methylation or Epigen* OR Methylome OR "CpG Island$" OR
"CpG" OR “bisulfite adj (conversion OR treatment OR pyrosequencing OR sequencing)”)
AND ("small world$" OR "graph theor*" or topology or connectome OR connectivity OR
connect* adj (brain OR neur*) OR "brain volume" OR "Neural pathways" OR "Brain

Mapping" OR "Cerebral Cortex" OR "cortical connectivity" OR Brain OR "Visual Cortex" OR
“White matter” OR “Myelin$” OR hippocamp* OR amygdal* or hypothalam* OR thalam*
OR cereb* OR cortex OR cortical OR Neuro*) AND ("Magnetic Resonance Imaging" OR
"Diffusion Tensor Imaging" OR "Diffusion Magnetic Imaging" OR MRI OR DTI OR
Neuroimaging OR "functional MRI" OR fMRI OR "functional Magnetic resonance imaging"
OR “functional MRI” OR dtMRI OR dMRI OR “diffusion tensor Magnetic resonance
imaging”))

Scopus

TITLE-ABS-KEY (("DNA methyl*" OR methylation OR epigen* OR methylome OR "CpG
Island$" OR "CpG" OR "bisulfite adj (conversion OR treatment OR pyrosequencing OR
sequencing)") AND ("small world$" OR connectome OR topology OR "graph
theor*" OR connectivity OR "connect* adj (brain OR neur*)" OR "brain volume" OR "Neural pathways" OR "Brain Mapping" OR "Cerebral Cortex" OR "cortical
connectivity" OR brain OR "Visual Cortex" OR "White
matter" OR "Myelin*" OR "hippocamp*" OR "amygdal*" OR "cortex" OR "cortical" OR
"Neuro*" OR hypothalam* OR thalam* OR cereb*) AND ("Magnetic Resonance
Imaging" OR "Diffusion Tensor Imaging" OR "Diffusion Magnetic
Imaging" OR mri OR dti OR neuroimaging OR fmri OR "functional Magnetic Resonance
Imaging" OR "functional MRI")

3.2.2 Screening and study selection

Search results were imported to EndNote X8 prior to removal of duplicates and retrieval of full texts prior to import to Covidence software (https://www.covidence.org/home). Screening was carried out by ENWW and DQS independently and studies were included if they met the following criteria: report of primary results; recruited human participants of any age with *in vivo* neuroimaging and DNAm; investigated the relationship between brain imaging using MRI and epigenome-wide or loci specific DNAm. Exclusion criteria: no original data reported (reviews, abstracts, letters, and grey literature as defined by Grey Literature International Committee Guidance); no test of association between brain imaging findings and DNA methylation; analysis was carried out in animals or in post-mortem human tissue; DNAm-MRI analyses of central nervous system malignancy.

3.2.3 Data extraction

ENWW extracted data for all included studies and DQS duplicated extraction for a subset of 25%. Extraction included: participant characteristics, study design, method of DNAm ascertainment, MRI modality and image feature(s) of interest, and statistical method, consideration of cell sub-type composition includes cell sorting techniques or statistical methods to estimate and control for cell sub type composition and consideration of genotype or ancestry. The total number of participants per phenotypic category were estimated. Due to participant overlap in some studies, the largest study population reported was used to estimate the total number of participants.

3.2.4 Risk of bias assessment

In the absence of a validated quality assessment tool for studies linking DNAm with MRI data, we extracted data on study characteristics that might affect risk of bias: design, presence / absence of a comparator group; DNA source; candidate or epigenome-wide approach for evaluating differential DNAm; ascertainment of cell type composition; consideration of genotype; image processing methodology; and region-of-interest versus whole brain

MRI analysis, and considered their prevalence in the epigenetic-neuroimaging literature.

3.2.5 Data synthesis

We provide a narrative synthesis structured around the type of association between DNAm and image feature, target population characteristics, tabulated, and categorised by disease.

3.3 Results

3.3.1 Overview of the literature

Figure 1 is the PRISMA flow chart of study identification and inclusion. Our search strategy yielded 3442 in total: 3438 resulting from the search and an additional 4 papers were identified post search and were included. After removal of duplicates and exclusions at screening, 336 articles were eligible for full text evaluation. Of the full text articles that were screened for eligibility for inclusion, 276 were removed due to lack of eligibility. In total, 60 studies were included in this review (estimated 6775 participants): 34 (57%) included a control or comparator group. Table 1 summarises diseases and conditions in phenotypic categories, number of participants per category, MRI modality, and method used to analyse DNAm (EWAS or candidate loci). All studies report populations from resource rich settings: United States (25), United Kingdom (3), Germany (4), Switzerland (4), Germany and Switzerland (1), South Korea (7), Canada (3), Italy (2), Japan (1), China (2), Singapore (2), Republic of Ireland (2), Australia (2), Spain (1), Sweden (1).

Figure 1. PRISMA flow diagram of studies

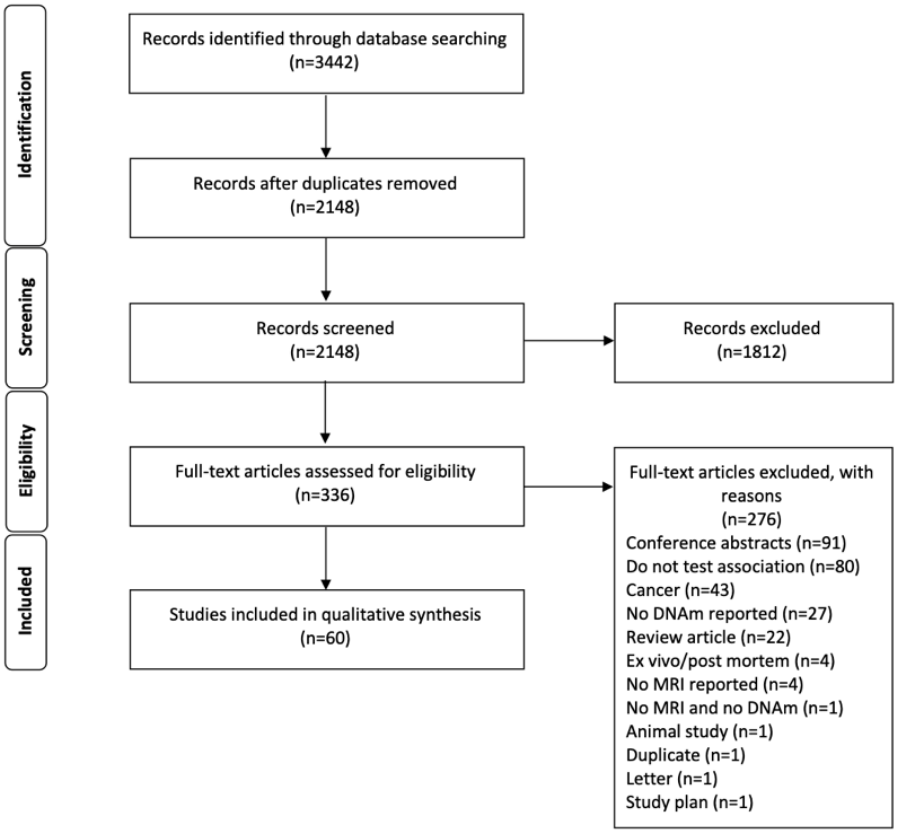

3.3.2 DNA methylation

All studies used surrogate tissues to probe methylation status: blood (n=46); saliva (n=12); one study reported using both blood and saliva, and one reported using blood/saliva/buccal cells (Ismaylova et al., 2017; Nikolova et al., 2014). The majority of studies did not report adjustments for cell type composition of samples used to estimate DNAm (n=48).

Forty-three studies used a candidate gene analysis approach and 17 performed an epigenome-wide association study (EWAS). The majority of included studies that used a candidate gene approach measured methylation using bisulfite pyrosequencing (n=36). Three studies measured methylation at a candidate gene using the EpiTYPER® system (Haas et al., 2016; Shelton et al., 2017, 2016). One study carried out a restriction enzyme digest and sequencing to measure DNAm at a candidate site (McMillan et al.,

2015). Three studies measured DNAm using Illumina arrays, and used the output to inform candidate gene DNAm-MRI analyses (Sadeh et al., 2016; Walton et al., 2014; Wiemerslage et al., 2017). Overall, nineteen candidate loci were studied. *SLC6A4* (Na+/Cl- Dependent Serotonin Transporter) was the gene of interest in 11 studies; *BDNF* (member of nerve growth factor family), *FKBP5* (member of the immunophilin family) and *OXTR* (oxytocin receptor) were selected as candidate genes in four studies; *NR3C1* (glucocorticoid receptor) in three studies; *FMR1* (FMRP Translational Regulator 1), *COMT* (enzyme involved in catecholamine degradation) and *DAT/SLC6A3* (Na^+/K^+ dependent dopamine transporter) in two studies. The following genes were selected candidates in one study: *OXT* (encodes oxytocin and neurophysin 1 precursor protein)*, C9orf72* (thought to be a transcriptional regulator in the brain), *CACNA1C* (voltage gated calcium channel), *DRD2* (dopamine receptor), *KLF13* (transcription regulator), *NCAPH2/LMF2* (encoding both a non-SMC subunit of the condensin II complex and a lipase maturation factor protein from the same locus), *PPM1G* (member of the PP2C family of Ser/Thr protein phosphatases), *HTR3A* (member of the ligand-gated ion channel receptor superfamily), *SKA2* (Spindle And Kinetochore Associated Complex Subunit 2), *SOD* (superoxide dismutase) and *TESC* (tescalcin – regulates cell pH by controlling H+/Na+ exchange across the plasma membrane).

All of the EWAS studies used Illumina Infinium arrays to measure DNAm: Illumina HumanMethylation27 (n=6), Illumina 450 (n=13), and Illumina EPIC (n=1). These arrays measure methylation at 27 578, 485 512 and 866 836 CpG sites respectively. Five studies investigated DNAm age, a method that uses a subset of CpG sites associated with age to investigate age and age acceleration (Chouliaras et al., 2018; Davis et al., 2017; Hodgson et al., 2017; Raina et al., 2017; Wolf et al., 2016).

Of studies which only report DNAm at candidate genes, two reported that the sample used to measure DNAm was mononuclear blood cells (lymphocytes

and monocytes) (Chouliaras et al., 2018; Ursini et al., 2011) whereas none of the studies that measured DNAm by bisulfite pyrosequencing reported correction for cell type composition. 12 of the 20 studies which used Illumina arrays performed a correction for cell type composition. Only one study reported direct counting of cell types included in their samples (Freytag et al., 2017).

3.3.3 Magnetic Resonance Imaging

The majority of studies used 3T MRI scanners (n = 42); five studies used 1.5T scanners; five included participants scanned at 1.5T and 3T scanners; and eight studies did not report field strength. Many included studies carried out functional MRI (n=29), of which three studies also carried out structural analysis. Structural MRI, to investigate volumes, cortical morphology, and conventional clinical MRI measures, was used in 26 studies. Diffusion MRI to measure properties of white matter microstructure was used in nine studies, and MR angiography was used in one.

3.3.3.4 MRI features associated with DNAm across studies

Table 2 shows 10 MRI features that are associated with differential DNAm in two or more studies. The image features are: hippocampal volume (n=11); hippocampal functional connectivity/activity (n=4); amygdala functional connectivity/activity (n=9); PFC functional connectivity/activity (n=8); regional FA measures (n=6); cortical thickness (n=6); regional diffusion metrics (AxD/MD/RD) (n=5); global FA (n=2); and cortical volume (n=2). For most of these, differential DNAm occurred at different loci. However, amygdala functional connectivity/activity was associated with differential DNAm in *SLC6A4* in six studies, and *OXTR* in two studies. PFC connectivity/activity was associated with DNAm in *BDNF* in two studies. Hippocampal volume was associated with *FKBP5* DNAm in two studies. Activation within the prefrontal cortex in working memory tasks were associated with *COMT* DNAm in two studies. The studies all employed a candidate gene approach

to DNAm analysis and directions of association were mixed across the studies.

Six studies tested an association between *SLC6A4* methylation and amygdala reactivity. Four out of five studies that reported associations between *SLC6A4* methylation and the emotional face processing task assessed by fMRI in response to threat stimuli found positive associations with amygdala reactivity and connectivity (Ismaylova et al., 2018; Nikolova et al., 2014; Schneider et al., 2018; Swartz et al., 2017). One study investigated resting state functional connectivity and reported a positive association between *SLC6A4* methylation and amygdala coupling with the salience network (Muehlhan et al., 2015). However, in a further study that investigated *SLC6A4* methylation and brain activity in the context of both resting state connectivity and the emotional face processing task, there were no significant associations reported with regard to the amygdala either with regards to whole brain analysis or amygdala region-of-interest analysis (Ismaylova et al., 2017).The sixth study that reported an association between *SLC6A4* and amygdala connectivity was also task-based fMRI, and used a visual emotional attention shifting paradigm (Frodl et al., 2015).These papers assessed DNAm within the promoter region of the *SLC6A4* gene, with the exception of Schneider et al. 2018, where a retrotransposon element, AluJb, was studied.

Two studies reported significant associations between *OXTR* methylation and amygdala connectivity (Puglia et al., 2015; Ziegler et al., 2015). Each study used a different fMRI task paradigm: the first used a task employing words involving social phobia relevant verbal stimuli in a cohort of patients with social anxiety disorder (Ziegler et al., 2015); and the second used an emotional face- matching block-design task in a group of healthy study participants (Puglia et al., 2015). Both studies measured DNAm in blood, but each targeted a different region of the *OXTR* gene in bisulfite sequencing. Ziegler et al. 2015 targeted exon 3 of the OXTR gene due to previous work

demonstrating an association between methylation in this region and social cognition (Unternaehrer et al., 2012; Ziegler et al., 2015). Puglia et al. 2015 targeted a single CpG site at position -934 relative to the transcription start site, where methylation had previously been associated with autism spectrum disorder (Gregory et al., 2009; Puglia et al., 2015). The directions of associations reported in these two studies were mixed and may be explained by the variations in study design and participant characteristics.

Two studies reported significant associations between *BDNF* methylation and PFC functional connectivity (Moser et al., 2015; Ursini et al., 2016). Moser et al. performed DNAm-MRI analysis in a combined group of analysis of study participants with PTSD, sub-threshold PTSD and healthy control women, and assessed neural response to a Modified Crowell Procedure (Moser et al., 2015). The second study reported *BDNF* DNAm associations with PFC activity during a working memory task in a healthy group of study participants (Ursini et al., 2016). Both of these studies measured DNAm at different regions of the *BDNF* gene. Ursini et al. 2016 measured *BDNF* DNAm in blood at a region containing the rs6265 SNP, which lies in a coding region of the gene, which may interact with environmental factors to modulate risk for schizophrenia, while Moser et al. 2015 measured *BDNF* promoter DNAm in saliva, where methylation has been associated with trauma associated psychiatric disease in children (Moser et al., 2015; Ursini et al., 2016). The directions of associations reported in these studies were mixed.

Two studies reported associations between *FKBP5* methylation and hippocampal volume (Klengel et al., 2013; Resmini et al., 2016). In study participants with childhood trauma related PTSD there was a negative correlation between *FKBP5* methylation in blood and right hippocampal head volume (Klengel et al., 2013). In patients with Cushing's syndrome there was a positive association between *FKBP5* methylation in blood and bilateral hippocampal volume (Resmini et al., 2016). Both of these studies measured DNAm at glucocorticoid responsive regions of the *FKBP5* gene but report

significant associations in different regions. Klengel et al. 2013 reported significant associations with intron 7, while Resmini et al. 2016 reports a significant association with a CpG site within intron 2 (Klengel et al., 2013; Resmini et al., 2016).

Two studies reported associations between *COMT* DNAm and PFC activation during working memory tasks (Ursini et al., 2011; Walton et al., 2014). The two studies assessed brain activity during different working memory tasks: the *n*-back task (Ursini et al., 2011); and the Sternberg Item Recognition task (Walton et al., 2014). The *COMT* gene encodes two isoforms of the catechol-O-methyltransferase enzyme: one soluble and one membrane bound, each with their own promoters, with the membrane bound isoform being the form most commonly found in the brain. Positive associations between *MB-COMT* promoter DNAm in blood and activity in the left dlPFC and vlPFC (Broca's area 45) during the Sternberg Item Recognition task were found in a group of participants including healthy controls and schizophrenia patients (Walton et al., 2014). In the second study of healthy participants significant negative associations were reported between methylation at *COMT* rs4680 SNP in blood and activity in the bilateral PFC (BA 45/14 and BA47) during the *n*-back task in participants homozygous for the Val/Val allele at the rs4680 *COMT* SNP (Ursini et al., 2011). The difference in direction of associations reported by these two studies may be explained by the variations in study design and participant characteristics.

3.3.4 Associations between DNAm and MRI features categorised by phenotype

3.3.4.1 Neurodevelopment and neurodevelopmental disorders

Table 3 summarises eight studies that focused on neurodevelopment: typical development; the impact of early life stress on young adulthood; *BDNF* polymorphism in early life; ADHD; preterm brain injury; hippocampal sclerosis

in mesial temporal lobe epilepsy; birthweight discordance between twins and its impact on cortical anatomy. Four of the eight studies included a comparison group, and four were case series. Two studies report data from the Growing up towards Healthy Outcomes in Singapore (GUSTO) cohort study (Chen et al., 2015; Guillaume et al., 2018).

Two studies used a candidate gene approach and both reported positive associations, but between different MRI features and different genes: the first between DNAm at the *SLC6A4* promoter and cortical thickness in an uncontrolled case series of 102 children with ADHD (Park et al., 2015); and the second between DNAm at *FKBP5* introns and dlPFC activation during the go no-go task in a case series of young adults with a history of early life stress exposure (Harms et al., 2017). The remaining six studies used the Illumina 450k array to measure DNAm, and all reported significant associations between DNAm at multiple loci and features including fractional anisotropy (FA), sub-cortical ROI volumes, cortical thickness, volume and surface area (Casey et al., 2017; Chen et al., 2015, 2018; Guillaume et al., 2018; Long et al., 2017; Sparrow et al., 2016). Two studies reported associations between DNAm at *SMOC2* and MRI brain imaging features (Chen et al., 2018; Guillaume et al., 2018). Guillaume et al. 2018 performed an EWAS in neonates and report an association between DNAm at this gene and FA in the left ventrolateral thalamus (Guillaume et al., 2018). Chen et al. 2018 reported differential methylation and discordance in twin pairs discordant for ADHD diagnosis, and identified six probes associated with the *SMOC2* gene which were differentially methylated and were associated with differences in striatum (among 48 probes that were differentially methylated with regard to striatum volume) (Chen et al., 2018). *SMOC2* encodes SPARC-related modular calcium binding protein 2.

Two studies reported an association between neonatal water diffusion properties and DNAm (Guillaume et al., 2018; Sparrow et al., 2016). In a case control study of preterm infants and term born controls principal

component analysis of saliva DNAm identified a component that was associated with shape of the right corticospinal tract (Sparrow et al., 2016); and in neonates from the GUSTO cohort study there was an association between umbilical cord blood DNAm at the *SMOC2* gene and FA in the left ventrolateral thalamus (Guillaume et al., 2018).

3.3.4.2 Major depressive disorder (MDD) and suicidality

Table 4 describes 10 studies of MDD and 1 of suicidality. Seven studies had overlapping participants: five have some overlapping participants from an outpatient psychiatric clinic of Korea University Anam Hospital and community controls (Choi et al., 2015; K. Han et al., 2017; K. M. Han et al., 2017; Na et al., 2016; Won et al., 2016); and two other studies had overlapping participants (Booij et al., 2015; Frodl et al., 2015). Nine studies included a comparator group and 2 were case series of individuals with familial risk for MDD.

Ten of eleven studies used a candidate gene approach based on blood samples and one carried out EWAS on salivary DNA. Five candidate genes were studied in the context of MDD: *SLC6A4* (n=5), *BDNF* (n=2), *TESC* (n=1), *FKBP5* (n=1) and *CACNA1C* (n=1). The single EWAS study reported an association between DNAm age and hippocampal volume, noting that DNAm mediated the effect of cortisol on hippocampal volume (Davis et al., 2017).

All four fMRI studies were task based. Two used the emotional face processing paradigm to investigate amygdala reactivity in relation to the *SLC6A4 AluJb* element or its promoter, and both report significant correlations between activation and *SLC6A4* DNAm among cases (Schneider et al., 2018; Swartz et al., 2017). Another study reported a correlation between DNAm at the *SLC6A4* and limbic system activation during a visual emotional attention shifting task in an analysis which pooled MDD cases and controls (Frodl et al., 2015). Together these studies suggest that *SLC6A4*

methylation positively correlates with limbic system reactivity in response to threat or negative emotional stimuli. However, these studies measured and reported *SLC6A4* methylation at different sites, and analysed them differently. For example, Frodl et al used a summary mean measure across 11 CpG sites in the promoter, Swartz et al calculated a residualised change score from 20 CpG sites, and Schneider et al calculated mean methylation at the AluJb element of the promoter from 6 CpG sites (Frodl et al., 2015; Schneider et al., 2018; Swartz et al., 2017). The fourth fMRI study investigated brain responses to images that were associated with suicidal means in relation to DNAm in the *CACNA1C* transcription factor binding site, and reported differential brain activation in association with DNAm at two CpGs (Kim et al., 2017).

3.3.4.3. Alcohol use disorder

Table 5 summarises 4 studies of alcohol use disorder, all of which investigated DNAm in candidate genes in relation to task-based fMRI. Two were case-control study designs and two were uncontrolled case series. Three candidate genes were assessed: *DRD2*, *SLC6A3/DAT* and *PPM1G*. Three different tasks were used: testing impulse control, reactivity to alcohol cues and processing of reward/punishment cues. Three of these studies measured DNAm in blood, and one in saliva. Three of the four studies reported positive correlations between functional activation in limbic system structures and DNAm among participants with alcohol use disorder (Bidwell et al., 2018; Ruggeri et al., 2015; Wiers et al., 2015). The remaining study found no significant correlations in the alcohol dependent cases, but did find negative correlations in functional activation in the nucleus accumbens and methylation at the *SLC6A3* promoter in the context of a monetary incentive delay task (Muench et al., 2018*)*.

3.3.4.4. Schizophrenia and psychosis

Table 6 summarises seven studies of schizophrenia and psychosis, all of which included a comparator group. Six of the included studies use data from

participants in the Mind Clinical Imaging Consortium (MCIC) all of whom have MRI, DNAm and SNP data available (Deng et al., 2016; Hass et al., 2015; Hu et al., 2018; Liu et al., 2015; Walton et al., 2014; Wang et al., 2017).

The majority of these studies measured blood DNAm on the Illumina HumanMethylation27 array (n=4), and one study carried out a candidate gene analysis on blood *MB-COMT* DNAm. Five of these used the Illumina HumanMethylation27 array, and two carried out bisulfite pyrosequencing of two genes: *OXTR* and *MB-COMT*. fMRI was the most commonly used modality (n=5), followed by sMRI (n=3). Of these, one study used both modalities. fMRI tasks included: a sensorimotor task and the Sternberg Item Recognition Paradigm for working memory (Hu et al., 2018; Walton et al., 2014). Two studies did not report the fMRI paradigm (Deng et al., 2016; Wang et al., 2017).

3.3.4.5. Ageing, stroke, ataxia and neurodegeneration

Table 7 summarises eight studies that investigated aspects of ageing, including healthy ageing, Alzheimer's disease, minor cognitive impairment, stroke, WMH burden and *C9orf72* expansion and Fragile X Associated Tremor Ataxia Syndrome (FXTAS).

Imaging modalities used were as follows: dMRI (n=2), sMRI (n=5) d/sMRI (n=1). All studies used blood samples to measure DNAm. Five studies carried out candidate gene analysis and three measured DNAm in an epigenome-wide manner. The candidate genes studied were: *C9orf72* (n=1), *NCAPH2/LMF2* (n=1), *FMR1* (n=2), *SOD* (n=1). Two studies carried out a longitudinal analysis as well as a cross-sectional analysis (McMillan et al., 2015; Swartz et al., 2017). One of these showed, in a group of 11 *C9orf72* expansion patients, that there was more rapid grey matter atrophy in the right hippocampus, right thalamus and left middle frontal cortex where there was decreased methylation in the expansion region (McMillan et al., 2015). The other found in 87 study participants that increases in SLC6A4 promoter methylation corresponded to increases in amygdala reactivity in response to

threat related stimuli in task-based fMRI (Swartz et al., 2017). Two studies that investigated associations between *FMR1* methylation and brain imaging in women with FXTAS had overlapping participants (Shelton et al., 2017, 2016). The three EWAS studies investigated DNAm age in relation to its associations with brain imaging features (Chouliaras et al., 2018; Hodgson et al., 2017; Raina et al., 2017). Two of these three studies investigated dMRI: one found a negative association of FA with epigenetic age acceleration, while the other found a negative association between global mean diffusivity (MD) and Hannum age and a positive association between FA and Hannum age (Chouliaras et al., 2018; Hodgson et al., 2017). In an analysis with sMRI a positive association was found between WMH burden category and DNAm age acceleration (Raina et al., 2017).

3.3.4.6. Post-traumatic stress disorder

Table 8 summarises seven studies that were carried out in participants with PTSD (Table 6). Several studies had overlapping participants. Three studies report associations in an overlapping group of participants: PTSD cases and non-PTSD controls, where the case population was mothers who have experienced interpersonal violence (IPV) (Moser et al., 2015; Schechter et al., 2017, 2015). Two further studies had overlapping participants – a cohort of trauma exposed veterans (Sadeh et al., 2016; Wolf et al., 2016). An additional group of veterans was also studied in relation to PTSD (McNerney et al., 2018). A further study recruited women who had experienced early life trauma to investigate associations between DNAm and sMRI features (Klengel et al., 2013). Five candidate genes were studied: *NR3C1* (n=2), *SKA2* (n=1), *BDNF* (n=1), *FKBP5* (n=1), *5HT3A* (n=1). All three modalities were employed to investigate neuroimaging features: dMRI (n=1), sMRI (n=3), fMRI (n=3). Overlap in study populations lay between two studies which measured DNAm using the Illumina 450k array (Sadeh et al., 2016; Wolf et al., 2016). Wolf et al. (2016) carried out analysis of DNAm age while Sadeh et al. (2016) carried out a candidate gene analysis of *SKA2* (Sadeh et al., 2016; Wolf et al., 2016). McNerney et al. (2018) measured DNAm at the

NR3C1 gene using bisulfite pyrosequencing (McNerney et al., 2018). All three of the articles investigating a population of mothers who have experienced IPV studied candidate genes: *NR3C1, BDNF* and *5HT3A* (Moser et al., 2015; Schechter et al., 2017, 2015). All three used fMRI, with two using the same task (Modified Crowell procedure), and one using a unique task video stimulus depicting neutral, menacing, and male-female prosocial interactions (Moser et al., 2015). The two studies that reported on IPV PTSD mothers in relation to the modified Crowell procedure showed positive associations between DNAm at *NR3C1* and *BDNF* and cluster activation in vmPFC OFC posterior cingulate cortex (Moser et al., 2015; Schechter et al., 2015).

3.3.4.7. Miscellaneous: healthy adults, socio-emotional processing, Cushing's syndrome

Two of the included studies in this section investigated patient populations, and the remainder reported healthy participants. One case-control study investigated DNAm-MRI in Cushing's Syndrome patients, and another case series study investigated social anxiety disorder (Resmini et al., 2016; Ziegler et al., 2015). Both studies discovered significant correlations between DNAm and neuroimaging findings. Fourteen studies in this section adopt a candidate gene analysis approach, with 1 being epigenome-wide (Table 9). The candidate genes studied were: *COMT* (n=1)*, OXTR* (n=3)*, NR3C1* (n=1)*, SLC6A4* (n=5)*, OXT* (n=1)*, FKBP5* (n=1)*, KLF13* (n=1), BDNF (n=1). DNAm was measured in the following tissues: saliva (n=3); blood (n=10); blood/saliva/buccal (n=1); saliva and blood (n=1). Two MRI modalities are represented in this section: sMRI (n=3), and fMRI (n=10), and two studies used both modalities (s/fMRI (n=2). fMRI tasks included: N back task, social phobia associated verbal stimuli, emotional perspective, emotional attribution, social perception, emotional face processing, responses to high calorie versus low calorie foods.

The three studies that investigated associations with *OXTR* methylation measured DNAm at two different positions: one in exon 3 and the other two at a CpG site -934 base pairs upstream of the TSS which has consistent methylation across blood and brain tissues (Jack et al., 2012; Puglia et al., 2015; Rubin et al., 2016; Ziegler et al., 2015). While these studies all used fMRI, they also used different tasks: social phobia related verbal stimuli, the emotional face matching task, and the social perception task (where objects move in ways to suggest animacy or random movement). One study investigated *OXTR* DNAm in exon 3, which had previously been implicated in social cognition, in a patient population with social anxiety disorder (Ziegler et al., 2015). The other two investigated healthy participants; one of these was in the context of social perception and individual variability in social perception (displays of animacy) (Jack et al., 2012; Puglia et al., 2015).

Five papers analysed associations between *SLC6A4* methylation and neuroimaging features. They included fMRI (n=4) and sMRI (n=2). fMRI studies used resting state and/or emotional face processing tasks. Ismaylova et al. (2017) estimated DNAm from three different surrogate tissues: blood, saliva, and buccal cells and reported that right lateral parietal area (RLP) resting state connectivity with the lateral occipital cortex and frontal poles has a positive association with *SLC6A4* DNAm (Ismaylova et al., 2017). Muehlhan et al. (2015) found positive associations between functional coupling between amygdala and nodes of the salience network with DNAm of the *SLC6A4* promoter in blood (Muehlhan et al., 2015). In the emotional face processing task, two studies report positive association between *SLC6A4* methylation and amygdala reactivity/connectivity in response to threat/fear related faces. Nikolova et al reported a positive relationship between saliva DNAm at *SLC6A4* and left amygdala reactivity to threat stimuli, while Ismaylova et al reported that twins with higher saliva DNAm at *SLC6A4* display greater connectivity between ACC and left amygdala (Ismaylova et al., 2018; Nikolova et al., 2014). The two studies that used sMRI both found positive associations between DNAm at *SLC6A4* and grey matter volumes

(Dannlowski et al., 2014; Ismaylova et al., 2017). However, they did not replicate each other by identifying the same brain regions as being associated even when using the same tissue to estimate DNAm.

3.4 Discussion

This systematic review of 60 studies involving approximately 6775 participants suggests that differential DNAm may be associated with MRI features of brain structure and / or function for conditions / diseases within the following categories: neurodevelopment and neurodevelopmental disorders; MDD and suicidality; alcohol use disorder; schizophrenia and psychosis; ageing, stroke, ataxia and neurodegeneration; post-traumatic stress disorder; healthy adults and socio-emotional processing. We found that 10 image features were associated with differential DNAm in two or more of the 60 studies. However, quantitative synthesis of DNAm-MRI associations was not possible due to the lack of consistency in DNAm findings, and / or heterogeneity in image features across studies. While the results presented here could provide new insights into the role of DNAm in health and disease across the life course, caution is required because the clinical and methodological heterogeneity of included studies was large. We identified the following sources of methodological heterogeneity and potential sources of bias: variable inclusion and characterisation of comparator groups in study designs; use of different tissues as a surrogate for brain; variation in methods for estimating DNAm and ascertainment of cell type composition; lack of control for genotype; and variations in image processing methodology and selected MRI features.

3.4.1 Study populations and comparator group validity

Twenty-six studies (43%) did not include a comparator group, and some others recruited cases and controls but combined the groups in DNAm-MRI analysis or restricted DNAm-MRI analysis to one group only. These issues limit inference about disease association. Several aspects of study design that are fundamental to good epidemiology should be adopted in future

DNAm-MRI studies to reduce potential sources of bias and enable maximum inference. These include detailed descriptions of participant selection, the population from which they were selected, and the method used to select. Not only is this important for understanding case definition, but also because research participation is influenced by social class, education, and ethnicity, and some of these factors may influence DNAm (Stafford et al., 2013). The same descriptive standards should be applied to comparator groups to ensure clinical validity, and attention should be given to matching comparator groups for ethnicity and age because both affect DNAm (Fraser et al., 2012; Heyn et al., 2013; Horvath, 2013; Talens et al., 2010)(Hannum et al 2013).

3.4.2 Surrogate tissues for brain DNAm and cell composition

Surrogate tissues include blood and saliva buccal cell samples. This is important when interpreting data because of tissue and cell heterogeneity in DNAm patterns. Buccal cells, a major cell type found in saliva, have been proposed to have more validity than blood as a surrogate tissue for brain since they have a common embryological cell lineage, both being derived from the ectoderm germ layer (Smith et al., 2015). One study that ascertained DNAm from three sample types (blood, saliva, buccal - buccal cells and saliva samples are collected differently) found that DNAm obtained from non-blood surrogate tissues most strongly associated with brain processes in living humans in the context of fMRI study (Ismaylova et al., 2017). This is consistent with a previous study in postmortem brain tissue in animal models, which found that saliva and brain are more similar in their DNA methylation patterns than are blood and brain (Lowe et al., 2013). Surrogate tissues have heterogeneous cell compositions which can impact the DNAm signature of the sample: blood comprises lymphocytes, neutrophils, basophils, monocytes and eosinophils; and saliva contains predominantly buccal cells but can include leukocytes. Crucially, the compositions of both surrogates are influenced by disease status. Hence, adjustment for cell composition should be considered in DNAm analysis.

3.4.3 Candidate gene versus epigenome-wide approaches

Forty-three included studies in this review used a candidate gene analysis approach, with candidacy most often rooted in knowledge or hypotheses about the biological underpinnings of the target disease. The majority of candidate gene studies focused on promoter regions, which risks neglect of other important regulatory regions, because it limits research to currently understood genomic elements that have a clear role in gene expression regulation.

Although there are inherent sources of bias in the candidate approach, it has been suggested that candidate gene studies can provide a useful starting point for hypothesis construction for example by investigating candidates that have emerged from the GWAS literature (Nikolova and Hariri, 2015). However, we did not find that candidate selection was based on the GWAS literature in the majority of studies. For example, *SLC6A4* was the candidate gene in eleven studies. *SLC6A4* encodes a serotonin transporter responsible for serotonin re-uptake from the synapse, and is one of the targets for the serotonin reuptake inhibitor class of antidepressants. Despite the importance of this gene product in the pharmacology of depression, recent GWAS studies report no association between candidate polymorphisms at *SLC6A4* (or a number of other candidate genes) and major depression (Border et al., 2019). This suggests that candidate genes that encode important pharmacological targets are not necessarily aetiologically significant. This is not to say that the methylation status of these genes is irrelevant: for example, it could be useful for investigating medication response, or as a biomarker. Frodl et al carried out an DNAm-MRI analysis with medication status as a covariate, and but found that this did not modify their findings regarding *SLC6A4* methylation and brain function in MDD patients and controls, while Booij et al have reported differential methylation at the *SLC6A4* promoter in association SSRI exposure (Booij et al., 2015; Frodl et al., 2015). In a human population of MDD no difference was found in methylation between medication free subjects and those on medication in a

post mortem study (Sabunciyan et al., 2012). These uncertainties suggest that further research into association between medication exposure and DNAm is warranted, and that hypothesis formation around candidate genes should be explicit in terms of theorised mechanism of disease or biomarker development. Further, mechanistic studies are crucial to aid our understanding of the interaction between DNAm and disease or therapy.

The rationales given for the selection of candidate genes for DNAm-MRI analysis were varied. Several studies selected candidates based on prior unbiased analyses in relation to phenotype (Kim et al., 2017; Ruggeri et al., 2015; Sadeh et al., 2016). For example, both *PP1MG* and *SKA2* were identified in EWAS analyses (Ruggeri et al., 2015; Sadeh et al., 2016), and *CACNA1C* was identified from a hypothesis free Methyl-Seq (Kim et al., 2017). Other candidate genes were chosen because they have a strong genetic link to the patient population being studied, such as *C9orf72* expansion in ALS-clinic patients and *FMR1* in FXTAS patients (McMillan et al., 2015; Shelton et al., 2017, 2016). For the most part candidate genes were selected because their gene products are considered key components of a pathway of relevance to a condition or phenotype studied. *NR3C1* and *FKBP5*, the genes that encode the glucocorticoid receptor and FK506 binding protein (which regulates glucocorticoid receptor sensitivity), are both involved in cortisol signalling and were selected in studies investigating stress response or stress related neuropsychiatric conditions such as PTSD or MDD, or in Cushing's Syndrome where cortisol is known to be dysregulated. *BDNF*, which encodes for brain derived neurotrophic factor, was studied in association to MDD, PTSD and working memory. *COMT* encodes catechol-O-methyltransferase, an enzyme that degrades catecholamines such as dopamine, epinephrine and norepinephrine, was the candidate gene in studies investigating DNAm-MRI in the context of working memory in schizophrenia and in healthy participants. *OXTR* encodes the receptor for oxytocin and was selected in studies that investigated an aspect of emotional or social processing. *SLC6A4* encodes the serotonin reuptake

transporter and is a target for the serotonin reuptake inhibitor class of anti-depressants. It was the selected candidate gene in studies of MDD and ADHD patients and emotional processing, and resting state amygdala activity.

Seventeen studies used an EWAS approach. There was no overlap between differentially methylated regions identified using this method versus the selected candidate gene approach for any of the phenotypic categories, which highlights the value of epigenome-wide approaches for unbiased investigation of the putative role of DNAm in brain structure and / or function. However, one study which employed an epigenome-wide approach to DNAm analysis identified *COMT* and *SLC6A3* as being negatively associated with right amygdala volume in neonates homozygous for *BDNF* rs6265 Met/Met allele (Chen et al., 2015). Both of these genes were selected as candidates in other studies but associations were reported in different populations with regards to age and clinical background, and with different image features (Muench et al., 2018; Ursini et al., 2011; Walton et al., 2014; Wiers et al., 2015). Many of the studies that utilised epigenome wide methods for measuring DNAm did not go on to report on individual loci. In future studies whole genome-based approaches could play an important role in generating novel candidates and pathways for future research that could provide mechanistic insight into pathogenesis.

3.4.4 Interindividual variability, effect of genotype, and temporal stability

Sources of variability that are crucial for understanding of how changes in DNAm associate with endophenotypes include interindividual variability which may be stochastic, genetic or environmental in origin, and temporal stability (Lancaster et al., 2018). Twin studies are useful for separating genetic and environmental contributions to variability, and several are included in the DNAm-MRI literature to date (Casey et al., 2017; Chen et al., 2018; Ismaylova et al., 2018). Twenty-four studies controlled for genotypic

effects, for example by covarying for single nucleotide polymorphisms (SNPs), or for the first PC of the variance in genome wide genetic data. This is because variation in DNAm may be explained partly by common genetic variation, such as a SNP that removes a methylation site. Therefore, genotyping in DNAm-MRI analyses is necessary for determining whether epigenetic associations with brain structure and function are genotype-specific, or whether associations are independent of genotype.

The stability of some epialleles varies over time with dynamic methylation and demethylation at CpG sites occurring in typical development and ageing, and in response to environmental exposures (Lancaster et al., 2018). Only fifteen studies reported the timing of DNAm sampling in respect to MRI acquisition; we suggest that this information is included in future studies because it is required to compare study populations and interpret phenotypic associations. Longitudinal investigation could be used to establish the temporal stability of methylation at a genomic region or site, the impact of medication, and for assessing potential causal relationships.

All of the included studies carried out cross-sectional analysis and two additionally carried out longitudinal analysis. Three other studies performed mediation analysis to assess causal relationships (Casey et al., 2017; Freytag et al., 2017; Harms et al., 2017). Studies designed to investigate association or causation should report the magnitude of differential DNAm between groups since the described changes in DNAm are often small and the biological relevance of these remains uncertain. Ultimately however, differential DNAm-MRI data will need to be interpreted in the wider context of mechanistic studies of gene expression in order to make inferences about causality. For example, experiments that demonstrate changes in gene expression associated with the differential methylation patterns reported from DNAm-MRI studies would be an important first step in dissecting causality, although it is important to note that changes in DNAm may actually occur as a consequence of changes in gene expression.

3.4.5 Neuroimaging considerations

Structural and functional quantitative neuroimaging features have been included in this review, assessed using sMRI, fMRI and dMRI. Others have emphasised the importance of selecting image features that represent a deficient or pathological phenotype when investigating associations between DNAm and MRI (Lancaster et al., 2018). Five DNAm-MRI associations recurred in two or more studies (*SLC6A4* and amygdala reactivity; *OXTR* and amygdala reactivity; *BDNF* and PFC function; *FKBP5* and hippocampal volume; *COMT* and *PFC* function), and a narrative synthesis of these demonstrates that there were mixed directions of associations, which may be explained by the variation in where in a genomic region DNAm was measured and in which tissue, in tasks employed during fMRI and in participant characteristics. A variety of fMRI paradigms have been used to probe brain function in this field, such as resting state and emotional processing, and dMRI studies have used different diffusion gradient encoding schemes and strengths (b-values) to measure the mobility of water molecules *in vivo*. A further layer of complexity is added in terms of differences in image processing pipelines such as CIVET (http://www.bic.mni.mcgill.ca/ServicesSoftware/CIVET), FreeSurfer (https://surfer.nmr.mgh.harvard.edu) and SPM (https://www.fil.ion.ucl.ac.uk/spm) for sMRI; and voxel based methods e.g. TBSS (https://fsl.fmrib.ox.ac.uk/fsl/fslwiki/TBSS) or tractography methods e.g. probabilistic neighbourhood tractography (http://www.tractor-mri.org.uk/tractography) for analysis of dMRI (Ad-Dab'bagh et al., 2006; Anblagan et al., 2015; Bastin et al., 2010; Clayden et al., 2007, 2006; Fischl, 2012; Smith et al., 2006). In the future, it will be necessary to form consensus and harmonisation about the optimal acquisition protocols and analysis pipelines to allow findings from different groups to be combined more readily. Initiatives such as the ENIGMA consortium which aims to understand brain structure, function and disease using brain imaging and genetic data from groups around the world are an important step in this direction.

3.4.6 Strengths and limitations

This systematic review has several strengths. It was based on a predefined protocol and followed standard guidelines with rigorous screening of >3,400 articles and without language or publication year restrictions. Our analysis was based on 60 studies examining healthy individuals and a wide range of neurological and psychiatric diseases in more than 6,000 patients across the life course. This provided a detailed overview of a growing body of literature linking DNAm and MRI data types, and enabled us to identify the key sources of methodological variation that should be addressed as standards and conventions in DNAm-MRI analyses become established.

Our study also has limitations. First, there was substantial clinical and methodological heterogeneity which prohibited quantitative synthesis for any single phenotype category, or MRI feature. Second, in the absence of validated tools for assessing quality and risk of bias in DNAm-MRI analyses, we were unable to evaluate these issues quantitively.

3.4.7 Conclusion

There is some evidence of association between differential DNAm and human brain structure and / or function across the life course. However, varied methodologies used to acquire and analyse DNAm-MRI data prevent quantitative synthesis. The development of standards and conventions for studies linking DNAm with MRI data is required, with particular focus on: detailed case and comparator group definition; surrogate tissue type; adjustment for cell composition and common genetic variation; consistent approaches to DNAm estimation using whole genome approaches; and use of image acquisition protocols, analysis pipelines and image feature selection that best support pooled analyses that are likely to be required to achieve statistical power for EWAS-neuroimaging studies. In summary, this review has found that: differential DNAm is associated with image features of brain structure and function in health and disease across the life course (using data from over 6,000 individuals); evidence that differential DNAm is

associated with specific image features is modest; and it has identified specific sources of sample and methodological heterogeneity in existing DNAm-MRI analyses. We anticipate that identification of these will expedite rational development of analytic methods in this emerging field so that researchers might more rapidly design studies that support causal inference.

Chapter Conclusion

In this chapter I have provided a comprehensive overview of DNAm-MRI associations. Associations were reported across a range of contexts in terms of disease/health, development and age. However, the current evidence linking DNAm to brain structure and function is modest, and substantial sources of heterogeneity precluded quantitative synthesis. It has indicated areas of bias such as a lack of control for cell type, and genetic background. This work indicates that epigenome wide approaches have potential for the identification of target genes for future study and may expedite target discovery by providing empirical rationale. It further emphasises the value of MRI features that are implementable across cohorts.

Abbreviations used in tables:

ACR, anterior corona radiata
AD, alcohol dependence
AxD, axial diffusivity
ADC, apparent diffusion coefficient
aMCI, amnesic mild cognitive impairment
BCC, body of the corpus calllosum
CC, corpus callosum
CLASP, Constrained Laplacian-based Automated Segmentation with Proximities
CSF, cerebral spinal fluid
CST, corticospinal tract
DG, dentate gyrus
DMR, differentially methylated region
FA, fractional anisotropy
FXTAS, Fragile X Associated Tremor Ataxia Syndrome
GCC, genu of corpus callosum
GM, grey matter
HC, healthy controls
HS, hippocampal sclerosis
IFG, inferior frontal gyrus
IT, inferior temporal
MD, mean diffusivity
MDD, major depressive disorder
MFG, middle frontal gyrus
mOFC, medial orbitofrontal cortex
MRF, Markov Random Field
MTLE, mesial temporal lobe epilepsy
NAcc, nucleus accumbens
NR, not reported
PCR, posterior corona radiata
PHC, parahippocampal cingulum
PNT, probabilistic neighbourhood tractography
PTR, posterior thalamic radiation
RD, radial diffusivity
RLP, right lateral parietal area
RS, resting state
SFG, superior frontal gyrus
STG, superior temporal gyrus
TBSS, tract-based spatial statistics
vlPFC, ventrolateral prefrontal cortex
vlThalamus, ventrolateral thalamus
WB, whole brain
WMH, white matter hyperintensities

Gene names

SKA2, Spindle and Kinetochore Associated Complex Subunit 2
SLC6A4, Solute Carrier Family 6 Member 4
BDNF, Brain Derived Neurotrophic Factor
FKBP5, FK506 Binding Protein 51
OXTR, Oxytocin Receptor
NR3C1, Nuclear Receptor Subfamily 3 Group member 1
FMR1, Fragile X Mental Retardation 1
COMT, Catecholamine Transferase
DAT/SLC6A3, Dopamine Transporter/Solute Carrier Family 6 Member 3
OXT, Oxytocin/Neurophysin 1 Prepropeptide
C9orf72, Chromosome 9 Open Reading Frame 72
CACNA1C, Calcium Voltage-Gated Channel Subunit Alpha1 C
DRD2, Dopamine Receptor 2
KLF13, Kruppel Like Factor 13
NCAPH2, Non-SMC Condensin II Complex Subunit H2
LMF2, Lipase Maturation Factor 2
PPM1G, Protein Phosphatase Magnesium Dependent 1 Gamma
HTR3A, 5-Hydroxytryptamine Receptor 3A
SOD, Superoxide Dismutase
TESC, Tescalcin

Table 1. Overview of studies

Disease or condition, number of studies	**Number of participants**	**MRI modality (structural, functional, diffusion)**	**Epigenetic method: Epigenome-wide (EW) or candidate (candidate loci)**
Neurodevelopment and neurodevelopmental disorders† n=8	715	5 sMRI 1 fMRI 2 dMRI	6 EW 2 candidate (*SLC6A4, FKBP5)*
Major depressive disorder and suicidality n=11	922§	4 sMRI 4 fMRI 2 dMRI 1 sMRI/dMRI	1 EW 10 candidate (*BDNF, SLC6A4, FKPB5, CACNA1C, TESC)*
Alcohol use disorder n=4	921	4 fMRI	0 EW 4 candidate *(PPM1G, DAT/SLC6A3, DRD2)*
Schizophrenia and psychosis n=7	456§	2 sMRI 4 fMRI 1 sMRI/fMRI	5 EW 3 candidate (*OXTR, BDNF, COMT)*
Ageing, stroke, ataxia and neurodegeneration n=8	1456§	5 sMRI 2 dMRI 1 sMRI/dMRI	3 EW 5 candidate *(C9orf72, FMR1, SOD, NCAPH2/LMF2)*
Post-traumatic stress disorder n=7	450§	3 sMRI 3 fMRI 1 dMRI	1 EW 6 candidate *(SKA2, NR3C1, HTR3A, BDNF, FKBP5)*
Miscellaneous‡ n=15	1855	3 sMRI 10 fMRI 2 sMRI/fMRI	1 EW 14 candidate *(COMT, OXTR, NR3C1, SLC6A4, OXT, FKBP5, KLF13, BDNF)*

†Includes studies of typical development, twin birth weight discordance, *BDNF* Val66Met polymorphism, preterm birth, early life stress, attention deficit hyperactivity disorder, medial temporal lobe epilepsy

‡Healthy adults, emotion processing, social anxiety disorder, Cushing's syndrome

§Estimate due to possible sample overlap within phenotypic category.

Table 2. Associations between image features and DNAm

Image Feature (number of studies)	**Differential DNAm: gene or feature**
Global fractional anisotropy (n=2)	DNAm age (Horvath) DNAm age (Hannum)
Regional fractional anisotropy (n = 6) ▪ Corpus callosum ▪ Ventrolateral thalamus ▪ Right anterior corona radiata ▪ Right parahippocampal cingulum	 *SLC6A4* *FMR1* DNAm age (Hannum) *SMOC2* *BDNF* *TESC*
Regional radial, mean or axial diffusivity (n = 5) ▪ Inferior and middle cerebellar peduncle ▪ Corpus Callosum ▪ Right anterior corona radiata ▪ Right parahippocampal cingulum	 *FMR1* DNAm age (Hannum) *SLC6A4* *BDNF* *TESC*
Amygdala functional connectivity (n=9)	*SLC6A4* *SLC6A4* *SLC6A4* *SLC6A3/DAT* *SLC6A4* *OXTR* *OXTR* *SLC6A4* *SLC6A4*
Hippocampal functional connectivity (n = 4)	*SLC6A4* Cluster of genes identified through EWAS (Wang et al 2017)* Cluster of genes identified through EWAS (Hu et al 2018)* *BDNF*

Prefrontal cortex functional connectivity (n = 8)	*FKBP5* *MB-COMT* *BDNF* *NR3C1* *HTR3A* *COMT* *SLC6A4* *BDNF*
Hippocampal volume (n = 11)	*BDNF* *SLC6A4* *TESC* DNAm age (Horvath) Cluster of genes identified through EWAS (Hass et al 2015)* *OXTR* DNAm age (Hannum) *FKBP5* *NR3C1-1F* *SLC6A4* *FKBP5*
Cortical volume (n = 2)	Cluster of genes identified through EWAS (Casey et al 2017)* Cluster of genes identified through EWAS (Liu et al 2015)*
Cortical thickness (n = 6)	*SLC6A4* *BDNF* *FKBP5* *FMR1* *SKA2* Independent component of DNAm (Freytag et al 2017)
PFC (volume/thickness) (n = 2)	*OXTR* *SKA2*

*See Tables 3-9 for list of genes included in clusters identified by EWAS

Table 3. Neurodevelopment and neurodevelopmental disorders

Author, Country	Sample characteristics ▪ condition ▪ Cases (male); controls (male) ▪ Age	▪ Epigenome-wide/candidate, platform ▪ Tissue sampled ▪ Correction for cell sub-type distribution ▪ Consideration of genotype	▪ MRI field strength ▪ Modality ▪ Image feature(s) ▪ Analysis method	Main Findings
Chen et al., 2015 Singapore †	▪ *BDNF* Val66Met polymorphism in GUSTO study ▪ 237 cases (133M) ▪ Mean gestational age 38.7 weeks	▪ Epigenome-wide: Illumina 450 array ▪ Umbilical cord blood ▪ Cell type composition: NR ▪ Consideration of genotype: yes	▪ 1.5T ▪ Structural, T2 ▪ Volume of total brain and 18 ROIs ▪ MRF model segmentation	▪ 19% of total variable CpGs were significantly associated with the volume of the left hippocampus for Val/Val neonates. ▪ 5% of total variable CpGs were associated with left hippocampal volume in the Met/Val genotype group ▪ 3% of total variable CpGs were significant in the Met/Met genotype group.
Park et al., 2015 South Korea	▪ ADHD ▪ 102 participants (77M) ▪ Mean age 8.9 years	▪ Candidate: *SLC6A4* promoter (185bp region) ▪ Blood ▪ Cell type composition: NR ▪ Consideration of genotype: yes	▪ 3T ▪ Structural, T1 ▪ Cortical thickness ▪ CLASP algorithm (Kim et al., 2005)	▪ Negative association between DNAm of *SLC6A4* CpGs 5-8 in the promoter region and cortical thickness in the right STG, middle occipital gyrus, lingual gyrus, inferior occipital gyrus, precentral gyrus, MTG, cuneus, and cingulate gyrus.
Sparrow et al., 2016 United Kingdom	▪ Preterm birth ▪ 36 preterm infants (<32 weeks'	▪ Epigenome-wide: Illumina 450 array ▪ Saliva ▪ Cell type composition: no	▪ 3T ▪ Diffusion ▪ Tract shape in 8 major tracts.	▪ 95% of the variance in the preterm methylome was explained by 23 principal components; the 6th principal component explained 2.9% of the variance of DNAm data in the preterm group and was associated with right CST topology.

	gestation); 36 term controls ▪ Mean age at assessment: 39.7 weeks for controls and; 40.0 weeks for cases	▪ Consideration of genotype: yes	▪ Probabilistic Neighbourhood Tractography (PNT)	
Casey et al., 2017 Canada	▪ Cortical anatomy in monozygotic twin cohort ▪ 52 twin pairs (22M) ▪ Mean age 15.7 years	▪ Epigenome-wide: Illumina 450 array ▪ Saliva ▪ Cell type composition: yes ▪ Consideration of genotype: NR	▪ 3T ▪ Structural, T1 ▪ Cortical thickness, surface area, volume ▪ CIVET automated analysis pipeline	▪ 23 probes mediate the relationship between birthweight discordance and cortical volume, including annotated probes found in 13 genes: *PRPF3, RELN, EXOC2, LEFTY2, CAST, SNK1G2, TRIM5, ABR, TNF, C6orf10, FREM2, GABPA* and *EFNA5*; 15 probes mediate the relationship between birthweight discordance and cortical surface area, including annotated probes found in 9 genes: *TMCO3, TRIM15, KDM2A, EPDR1, PARP14, PBLD, RELN, ACACA* and *CASZ1.* ▪ No probes significantly mediated the relationship between birthweight discordance and cortical thickness discordance.
Long et al., 2017 China	▪ HS in MTLE ▪ Cases n=30 (18M); controls n = 30 (18M) ▪ Cases mean 25.3 years; controls mean 28.2 years	▪ Epigenome-wide: Illumina 450 array ▪ Blood ▪ Cell type composition: NR ▪ Consideration of genotype: NR	▪ Image acquisition: NR ▪ Hippocampal sclerosis on conventional MRI	Subgroup analysis: MTLE patients with (n = 9) or without HS (n = 14). ▪ From top 10 differentially methylated probes: DNAm in *SLC12A7, SRC*, *PLIN5* had a positive association with HS*;* DNAm in *PCNT, CEACAM21, PCGF3, BAT2* displayed a negative association with HS. ▪ Genes from top 10 positively associated with HS: *RASAL3*, *PFDN6:WDR46*, *UBN1:GLYR1*, *TRIM49*, *ACVR1B*. ▪ Genes from the top 10 negatively associated with HS: *SPIRE2*, *NKD1*, *TNFRSF11B*

Harms et al., 2017 United States	▪ Early life stress exposure on adult outcome ▪ 33 participants (15M) ▪ Mean age 20.5 years	▪ Candidate: *FKBP5*, CpG sites in intron 7, 5, and 2 ▪ Saliva ▪ Cell type composition: NR ▪ Consideration of genotype: NR	▪ 3T ▪ fMRI task: go-no go task ▪ dlPFC activation ▪ Analysis of Functional NeuroImages	▪ Negative association between DNAm of intron 5 of FKBP5 and activation in the dlPFC in the go no-go task. ▪ CpG8 of intron 5 mediates the relationship between childhood stress and dlPFC activation.
Chen et al., 2018 United States	▪ ADHD ▪ 15 monozygotic twin pairs (12M), discordant for ADHD ▪ Mean 9.7 years	▪ Epigenome-wide: Illumina 450 array ▪ Blood ▪ Cell type composition: yes ▪ Consideration of genotype: yes	▪ 1.5T ▪ Structural, T1 ▪ Cerebral cortex, cerebellum, caudate, putamen, thalamus volumes ▪ FreeSurfer	Subset of 14 MZ twins: Of the 67 genes with intrapair probe DNAm which associated with volume discordance in the cerebellum, 49 were negatively associated. Of the 48 genes associated with the striatum, 38 were negatively associated, while of the 78 associated with the thalamus 44 were negatively associated.
Guillaume et al., 2018 Singapore †	▪ GUSTO birth cohort ▪ 114 participants ▪ 7-10 days post birth	▪ Epigenome-wide: Illumina 450 array ▪ Umbilical cord blood ▪ Cell type composition: yes ▪ Consideration of genotype: NR	▪ 1.5T, ▪ Diffusion ▪ FA ▪ Voxel based comparison of FA maps	EWAS a significant association between probe cg19641625 in the *SMOC2* gene locus, with FA in the left vlThalamus.

† Overlapping cohorts (GUSTO study)

Table 4. Major depressive disorder and suicidality

Author, Country	Sample characteristics ▪ Condition ▪ Cases (male); controls (male) ▪ Age	▪ Epigenome-wide/candidate, platform ▪ Tissue sampled ▪ Correction for cell sub-type distribution ▪ Consideration of genotype	▪ MRI field strength ▪ Modality ▪ Image feature(s) ▪ Analysis method	Main Findings
Choi et al., 2015 South Korea †	▪ MDD ▪ Cases, n=60 (13M); controls, n=53 (17M) ▪ Cases, mean 41.9 years; controls, mean 41.2 years	▪ Candidate: *BDNF*, 4 CpGs in the promoter region ▪ Blood ▪ Cell type composition: NR ▪ Consideration of genotype: NR	▪ 3T ▪ Diffusion ▪ FA/RD/AxD of 7 white matter tracts ▪ Tract Based Spatial Statistics (TBSS)	▪ Cases: negative association between DNAm of CpG4 and FA of the right ACR, AxD of right ACR is negatively associated with *BDNF* DNAm. RD was not significantly associated with *BDNF* DNAm. ▪ Controls: no significant positive associations.
Booij et al., 2015 Republic of Ireland ‡	▪ MDD ▪ Cases, n=33 (10M); controls, n=36 (15M) ▪ Cases, mean 40.3 years; controls, mean 35.3 years	▪ Candidate: *SLC6A4*, CpGs 5-15 found 214–625 bp upstream of the gene promoter ▪ Blood ▪ Cell type composition: NR ▪ Consideration of genotype: yes	▪ 3T ▪ Structural, T1 ▪ Whole hippocampal and sub-hippocampal volumes ▪ FreeSurfer	▪ Whole group: negative predictive value of hippocampal volume and sub-volumes (CA2/3 and DG, and CA1) and *SLC6A4* DNAm (average and site specific – CpG 5&6, CpG 11&12)

Frodl et al., 2015 Republic of Ireland ‡	▪ MDD ▪ Cases, n=25(7M); controls, n=35(13M) ▪ Cases, mean 41.6 years; controls, mean 35.6	▪ Candidate: *SLC6A4*, promoter ▪ Blood ▪ Cell type composition: NR ▪ Consideration of genotype: NR	▪ 3T ▪ fMRI task: Visual emotional attention shifting ▪ Whole brain ▪ SPM8	▪ Whole group: when shifting from emotional valence to geometric properties there is a negative association between DNAm and activation in the right Rolandic operculum and insula, right superior temporal lobe, and pons; when shifting from negative to neutral emotional valence, there is positive association between DNAm and activation in the left anterior insula and inferior frontal operculum ▪ Controls: When looking at emotionally negative stimuli versus neutral stimuli, there was a positive association between DNAm and more activation in the bilateral hippocampus, left inferior operculum, fusiform gyrus and amygdala regions.
Na et al., 2016 South Korea †	▪ MDD ▪ Cases, n=65 (11M); controls, n=65 (15M) ▪ Cases, mean 42.5 years; controls mean 40.3 years	▪ Candidate: *BDNF*, 4 CpGs in the promoter region ▪ Blood ▪ Cell type composition: NR ▪ Consideration of genotype: yes	▪ 3T ▪ Structural, T1 ▪ Cortical thickness ▪ FreeSurfer	▪ Cases: negative association between CpG2/4 and cortical thickness in the right rostral middle frontal, mOFC cortical thicknesses and left lingual, STG and SFG cortices. Negative association between CpG2 and cortical thickness in the right IT and pericalcarine and left rostral middle frontal cortices. Negative association between CpG4 and cortical thickness in the right cuneus, precuneus and post central cortices and left frontal pole cortices. ▪ Controls: no significant associations found.
Won et al., 2016 South Korea †	▪ MDD ▪ Cases, n=35 (10M); controls, n=49 (15M) ▪ Cases, mean 40.3 years; controls mean 41.1 years	▪ Candidate: *SLC6A4*, 5 CpGs in the promoter ▪ Blood ▪ Cell type composition: NR ▪ Consideration of genotype NR	▪ 3T ▪ Diffusion ▪ FA/MD/AxD/RD ▪ TBSS	▪ Cases: negative association between *SLC6A4* DNAm and FA/AxD in the BCC (medication naïve). ▪ Controls: negative association between *SLC6A4* DNAm and GCC FA, and positive association with RD. ▪ Associations between BCC FA/AxD and CpG3 DNAm are higher in the cases compared to controls.

K. Han et al., 2017 South Korea †	▪ MDD ▪ Cases, n=114 (24M); controls, n=88 (27M) ▪ Cases, mean 43.5 years; controls, mean 39.9 years	▪ Candidate: *FKBP5*, intron 7 rs1360780, 2 CpGs investigated ▪ Blood ▪ Cell type composition: NR ▪ Consideration of genotype: yes	▪ 3T ▪ Structural, T1 ▪ GM volumes/cortical thickness of 14 cortical/subcortical regions ▪ FreeSurfer	▪ *FKBP5* C homozygote group (patients and controls) (n = 118): positive association between DNAm of CpG1 and cortical thickness in the right transverse frontopolar gyrus.
Kim et al., 2017 South Korea	▪ Suicidality ▪ Cases (suicide attempters), n=14 (1M), controls, n=22 (9M) ▪ Cases, mean 31.9 years, controls, 33.6 years	▪ Candidate: *CACNA1C*, 11 CpG sites in DMR in a transcription factor binding site ▪ Blood ▪ Cell type composition: NR ▪ Consideration of genotype: NR	▪ 3T ▪ fMRI task: participants shown pictures of facial emotion and objects relating to suicidal means ▪ Activation in 4 left hemisphere regions ▪ SPM5	▪ Cases: in knife vs neutral landscape contrast positive association between CpG4/6 DNAm and brain activation in the left thalamus, MFG, IFG. ▪ Controls: positive association between CpG6 DNAm and activation in the left MFG and IFG.
K. M. Han et al., 2017 South Korea †	▪ MDD ▪ Cases, n=84 (13M); controls, n=61(17M) ▪ Cases, mean 43.4 years; controls, mean 38.6 years	▪ Candidate: *TESC,* rs7294919 locus ▪ Blood ▪ Cell type composition: NR ▪ Consideration of genotype: yes	▪ 3T ▪ Diffusion ▪ Structural ▪ Diffusion parameters of the PHC ▪ Hippocampal subfield volumes ▪ Global PNT	▪ Cases: negative association of FA and positive association of RD with CpG3 DNAm in right PHC. ▪ Controls: no significant associations.

Swartz et al., 2017 United States	▪ Family history of depression ▪ Cases n=94 (51M); controls n=89(46M); ▪ Wave 1, mean 13.5 years; wave 2, mean 15.6 years	▪ Candidate: *SLC6A4* - 20 CpG sites in promoter region ▪ Blood ▪ Cell type composition: NR ▪ Consideration of genotype: yes	▪ 3T ▪ fMRI task: emotional face processing ▪ Amygdala reactivity ▪ SPM8	▪ Subgroup (n=87), longitudinal analysis: *SLC6A4* promoter DNAm increases over time is associated with increases in left centromedial amygdala reactivity when participants viewed faces with fearful expressions in contrast to geometric shapes.
Davis et al., 2017 United States	▪ High/low familial MDD risk among females ▪ High risk, n=24; low risk, n=22 ▪ High risk, mean 12.9 years; low risk, mean 12.1 years	▪ Epigenome-wide: Illumina EPIC, Horvath DNAm age ▪ Saliva ▪ Cell type composition: yes ▪ Correction of genotype: NR	▪ 1.5T/3T ▪ Structural, T1 ▪ Hippocampal and amygdala volumes ▪ FreeSurfer	Whole group analysis: ▪ Negative associations between DNAm age residual and left hippocampal volume. ▪ Accelerated DNAm age mediates the effect of cortisol on left hippocampal volume.
Schneider et al., 2018 Germany	▪ MDD ▪ Cases, n=137 (57M); controls, n=189 (83M) ▪ Cases, mean 37.4 years; controls, mean 35.6 years	▪ Candidate: *SLC6A4* AluJb element ▪ Blood ▪ Cell type composition: NR ▪ Consideration of genotype: yes	▪ 3T ▪ fMRI task: emotional face processing (threat/fearful faces) ▪ Amygdala reactivity ▪ SPM8	▪ Whole group analysis: Significant interaction of amygdala activity with DNAm and diagnosis. ▪ Cases: positive association between AluJb DNAm and activity in the right amygdala. No effect of DNAm on bilateral amygdala reactivity ▪ Controls: no significant associations

† Overlapping cohorts
‡ Overlapping cohorts

Table 5. Alcohol use disorder

Author, Country	Sample characteristics ▪ Condition ▪ Cases (male); controls (male) ▪ Age	▪ Epigenome-wide/candidate, platform ▪ Tissue sampled ▪ Correction for cell sub-type distribution ▪ Consideration of genotype	▪ MRI field strength ▪ Modality ▪ Image feature(s) ▪ Analysis method	Main Findings
Ruggeri et al., 2015 United Kingdom	▪ Alcohol exposure (IMAGEN cohort) ▪ n=499(222M) ▪ Mean age 14 years	▪ Candidate: *PPM1G*, 3' UTR ▪ Blood ▪ Cell type composition: NR ▪ Consideration of genotype: yes	▪ 3T ▪ fMRI task: stop signal task - impulse control ▪ BOLD responses in 2 ROIs ▪ MarsBaR (SPM8)	Subset of whole sample (n=393) ▪ Positive association between *PPM1G* DNAm and BOLD response in the right subthalamic nucleus in the stop success versus go success contrast ▪ No association with right IFG activation
Wiers et al., 2015 United States	▪ Alcohol dependence ▪ Cases n=38 (M); controls, n=17 (M) ▪ Cases, mean age 44.4 years; controls, mean 42.7 years	▪ Candidate: *SLC6A3/DAT* - 12 CpG sites in promoter region (-1037 to -829) ▪ Blood ▪ Cell type composition: NR ▪ Consideration of genotype: NR	▪ 3T ▪ fMRI task: cue reactivity task, alcohol elicited response ▪ Reactivity in 4 ROIs ▪ MarsBaR (SPM8)	▪ Cases: positive association between alcohol elicited amygdala reactivity (in contrast to soft drink) and *DAT* DNAm found only in cases with low depression scores (n=29)
Bidwell et al., 2018	▪ Alcohol dependence ▪ 383 (238M)	▪ Candidate: *DRD2,* 6 CpGs in promoter	▪ 3T ▪ fMRI task: cue reactivity task,	▪ ROI analysis: Positive association between DRD2 DNAm and alcohol elicited activation in striatum: right NAcc, bilateral putamen and bilateral caudate.

United States	▪ Mean age 30.1 years (range 21-56)	region (-126 to -189) ▪ Saliva ▪ Cell type composition: NR ▪ Consideration of genotype: NR	alcohol elicited response ▪ BOLD contrasts of 10 ROIs and WB analysis ▪ SPM8	▪ WB analysis: positive associations between DRD2 DNAm and alcohol elicited response in: left superior temporal, middle temporal, insula, postcentral, supramarginal, putamen regions.
Muench et al., 2018 United States	▪ Alcohol dependence ▪ Cases, n=45(35M); controls, n=45 (22M) ▪ Cases: mean 43.3 years; controls: 36.2 years	▪ Candidate: *SLC6A3/DAT*, 48 CpGs ▪ Blood ▪ Cell type composition: NR ▪ Consideration of genotype: NR	▪ 3T ▪ fMRI task: Monetary incentive delay task ▪ BOLD responses in bilateral NAcc ▪ AFNI	▪ Cases: no significant associations ▪ Controls: negative association between SLC6A3 promoter DNAm and NAcc activation during the anticipation of both high and low monetary loss. The effects were driven by 2 CpGs located at positions -1,001 and -993 from the TSS in the promoter of *SLC6A3*.

Table 6. Schizophrenia and psychosis

Author, Country	Sample characteristics ▪ Condition ▪ Cases (male); controls (male) ▪ Age	▪ Epigenome-wide/candidate, platform ▪ Tissue sampled ▪ Correction for cell sub-type distribution ▪ Consideration of genotype	▪ MRI field strength ▪ Modality ▪ Image feature(s) ▪ Analysis method	Main Findings
Walton et al., 2014 United States †	▪ Schizophrenia or schizophreniform disorder ▪ Cases, n=82(62M); controls, n=102(62M) ▪ Cases, mean 33.8 years; controls 32.7 years	▪ Candidate: *MB-COMT*, 864bp upstream from TSS of membrane bound isoform of *COMT* ▪ Blood ▪ Cell type composition: NR ▪ Consideration of genotype: yes	▪ 1.5T and 3T ▪ fMRI task: Sternberg item recognition paradigm - working memory task. ▪ BOLD response in dlPFC and exploratory whole brain analysis ▪ fMRIB (FSL)	Whole group: ▪ ROI analysis: positive association between *MB-COMT* promoter DNAm and left dlPFC activation; ▪ Whole brain analysis: positive association between *MB-COMT* promoter methylation and left dlPFC and vlPFC (BA45), left premotor and primary sensory cortex. No effect in R dlPFC. No effect of diagnosis.
Liu et al., 2015 United States †	▪ Schizophrenia, schizophreniform or schizoaffective disorder ▪ Cases, n=94; controls, n=106 ▪ Cases, mean 34.7 years;	▪ Epigenome-wide: Illumina Infinium HumanMethylation 27 Array ▪ Blood ▪ Cell type composition: NR ▪ Consideration of genotype: NR	▪ 1.5T and 3T ▪ Structural, T1 ▪ Volumes of cortical and subcortical regions ▪ FreeSurfer	▪ Negative association between the 7th DNAm component and the 1st brain volume component: Brain volume component - left cerebellar cortex, right cerebellar cortex Methylation component - *C1orf65, MCCC1, EPHA3, CDX1, RAET1L, LR8, STMN2, GATA4, NALP6, KCNK10, ADRA1D, NPDC1, MCHR1*

	controls, mean 32.5 years			
Hass et al., 2015 United States †	▪ Schizophrenia ▪ Cases, n=103 (75M); Controls, n=111(71M) ▪ Cases: mean 34.6 years; controls, mean 32.1 years	▪ Epigenome-wide: Illumina Infinium HumanMethylation 27 Array ▪ Blood ▪ Cell type composition: yes ▪ Consideration of genotype: yes	▪ 1.5T and 3T ▪ Structural, T1 ▪ fMRI: Sternberg Item Recognition Paradigm - working memory task. ▪ Hippocampal volume, STG thickness ▪ Working memory load dependent neural activity (percentage BOLD signal change) in the dlPFC ▪ FreeSurfer ▪ fMRIB (FSL)	▪ Alterations in the DNAm state of genes within the hsa-miR-219a-5p targets are associated with hippocampal volume changes (has-miR-219a-5p target gene set: *KIAA0182, PKNOX1, TRAF7, CBFA2T3, EPHA4, MKNK2, DDAH1, ESR1, AKAP13, PHACTR2, SLC31A1, KBTBD8, ADD2, ERGIC1, RBM24, KIAA0240, NEK6, THRB, SCN5A, TGFBR2, FZD4, SEMA4G)* ▪ STG thickness: miR-513 gene set sig enriched (NES = 1.7636) with an FDR q value of 0.2404 (based on positive association between DNAm data and phenotype) ▪ None of the predicted miRNA target gene sets was significantly enriched in association with working-memory load-dependent neural activity in the dlPFC.

Deng et al., 2016 United States †	▪ Schizophrenia ▪ Case, n=80(60M); Controls, n=104 (66M) ▪ Cases, mean 34 years; controls, mean 32 years	▪ Epigenome-wide: Illumina Infinium HumanMethylation 27 Array ▪ Tissue sampled: blood ▪ Cell type composition: NR ▪ Consideration of genotype: NR	▪ NR ▪ fMRI ▪ NR ▪ NR	▪ Small concordance between fMRI data and DNAm data. ▪ Prediction accuracy of schizophrenia cases was improved by incorporating the two data types versus prediction models using one or the other.
Rubin et al., 2016 United States	▪ Schizophrenia and Bipolar disorder ▪ Case, n=167(75M); controls, n=75(37M) ▪ Age Schizophrenia: Women (n=22): mean 39 years; Men (n=35): mean 22 years Schizoaffective disorder: Women (n=19) mean 37 years; Men (n=15) mean 38 years Bipolar disorder: Women (n=51) mean 36 years;	▪ Candidate: *OXTR* - methylation measured at a site 934bp upstream of TSS ▪ Blood ▪ Cell type composition: NR ▪ Consideration of genotype: NR	▪ 3T ▪ Structural, T1 ▪ Volumes of prefrontal regions and temporal limbic regions ▪ FreeSurfer	▪ Schizophrenia: positive association between OXTR DNAm and volumes of the left OFC, and right fusiform gyrus and negative association with the right hippocampus. ▪ Bipolar disorder: positive association between DNAm and right parahippocampal gyrus volume. ▪ Schizoaffective disorder (men): Negative association between *OXTR* DNAm and left MFG volume. ▪ Controls: negative association between *OXTR* DNAm and left amygdala, right MFG and IFG volumes.

	Men (n=25) mean 26 years Controls: Women (n=38) mean 36 years; Men (n=37) mean 39 years			
Wang et al., 2017 United States †	▪ Schizophrenia ▪ Cases, n=80(60M); Controls, n=104 (66M) ▪ Cases: mean 34 years; controls mean 32 years	▪ Epigenome-wide: Illumina Infinium HumanMethylation 27 Array ▪ Blood ▪ Cell type composition: NR ▪ Consideration of genotype: NR	▪ NR ▪ fMRI ▪ NR ▪ NR	▪ Positive association between fMRI and DNAm modules in cases. ▪ Associations in controls do not reach statistical significance. ▪ DNAm module: *ANKRD15, ATP6V0A4, C1orf116, C1orf172, C21orf56, CCNA1, CREB3L3, FLJ11017, HOXA4, HTN3, KIF27, LDHD, PAGE5, PDIA2, RCBTB2, RPL26L1, TMEM100* ▪ fMRI module: midcingulate area, parahippocampal gyrus, postcentral gyrus, supramarginal gyrus, angular gyrus, precuneus, superior temporal gyrus
Hu et al., 2018 United States †	▪ Schizophrenia ▪ Cases, n=79; controls, n=104 ▪ Age: NR	▪ Epigenome-wide: Illumina Infinium HumanMethylation 27 Array ▪ Blood ▪ Cell type composition: NR ▪ Consideration of genotype: NR	▪ Field Strength: NR ▪ fMRI task: Sensorimotor task ▪ NR ▪ NR	▪ Positive association between DNAm and fMRI data ▪ DNAm: 31 CpG sites that correspond to 30 genes ▪ fMRI (7 ROIs): left inferior frontal gyrus (pars triangularis), left hippocampus, right inferior occipital gyrus, bilateral fusiform gyrus, right middle temporal gyrus, left inferior temporal gyrus

† Mind Clinical Imaging Consortium

Table 7. Ageing, stroke, ataxia and neurodegeneration

Author, Country	Sample characteristics ▪ Condition ▪ Cases (male); controls (male) ▪ Age	▪ Epigenome-wide/candidate, platform ▪ Tissue sampled ▪ Correction for cell sub-type distribution ▪ Consideration of genotype	▪ MRI field strength ▪ Modality ▪ Image feature(s) ▪ Analysis method	Main Findings
McMillan et al., 2015 United States	▪ *C9orf72* expansion ▪ Cases, n=20; Controls, n=25 ▪ Cases: mean 61.9 years; controls: mean 6138 years	▪ Candidate: *C9orf72* ▪ Blood ▪ Cell type composition: NR ▪ Consideration of genotype: NR	▪ 3T ▪ Structural, T1 ▪ Grey matter density ▪ Randomise (FSL)	▪ *C9orf72* expansion group: positive association between *C9orf72* DNAm and grey matter density in the right hippocampus and thalamus and left premotor cortex. ▪ Longitudinal analysis (n=11): GM atrophy progresses more rapidly over time with decreased *C9orf72* DNAm in patients with *C9orf72* expansion
Shelton et al., 2016 Australia †	▪ Fragile X associated tremor ataxia syndrome (FXTAS) ▪ Cases, n=19F; controls, n=17F ▪ Cases: mean 39.4 years; controls, mean 39.8 years	▪ Candidate: FMR1 - exon 1 CpG1 and CpG2; intron 1 CpG6/7, CpG8/9; CpG10-12 ▪ Blood ▪ Cell type composition: NR ▪ Consideration of genotype: NR	▪ 3T ▪ Structural, T1 ▪ Regional cortical thickness from bilateral MFG and SFG and inferior parietal gyrus ▪ FreeSurfer	▪ Premutation group: positive associations between methylation of *FMR1* CpG6/7 or CpG1 or CpG10-12 and of cortical thickness in the left inferior parietal gyrus, middle frontal gyrus, and right middle frontal gyrus, superior frontal gyrus. Negative association between methylation in the intronic region with white matter hyperintensities. ▪ Controls: negative associations between FMR1 DNAm at CpGs 2, 6/7, 10–12 and cortical thickness in frontal lobe regions: left middle frontal gyrus and right superior frontal gyrus

Zhou et al., 2016 China	▪ Cerebral infarction ▪ Cases, n=83(45M); controls, n=94(52M) ▪ Cases: mean 61.6 years; controls: mean 61.6 years	▪ Candidate: Extracellular *SOD* ▪ Blood ▪ Cell type composition: NR ▪ Consideration of genotype: NR	▪ Field strength: NR ▪ MR Angiography ▪ Area of cerebral infarction; cerebral arteriosclerosis ▪ Analysis: NR	▪ Dependence between large/small area of cerebral infarction and extent of extracellular *SOD* DNAm. ▪ Negative but non-significant association between arteriosclerosis severity and extracellular *SOD* DNAm
Shinagawa et al., 2016 Japan	▪ Alzheimer's/aMCI ▪ Cases 58(27M): AD, n=30; aMCI n=28 ▪ Cases, mean 71.9 years	▪ Candidate: *NCAPH2/LMF2* promoter – representative CpG site ▪ Blood ▪ Cell type composition: NR ▪ Consideration of genotype: NR	▪ 1.5T ▪ Structural, T1 ▪ VBM Grey matter/ VSRAD Z-score (hippocampal atrophy grade) ▪ SPM8, DARTEL/VSRAD	▪ Extent of grey matter atrophy non-significant for associations with NCAPH/LMF2 promoter DNAm. ▪ Positive association between DNAm of *NCAPH2/LMF2* and severity of hippocampal atrophy.
Hodgson et al., 2017 United States	▪ Ageing ▪ Cases N=376 ▪ Mean 45.5years	▪ Epigenome-wide: Illumina 450 array, Horvath DNAm age ▪ Blood ▪ Cell type composition: yes ▪ Consideration of genotype: yes	▪ 3T ▪ Diffusion ▪ FA ▪ TBSS	▪ Negative association of FA with epigenetic age acceleration.

Raina et al., 2017 United States	▪ Cerebral white matter hyperintensities ▪ N=713(257M) ▪ Mean age at MRI was 61.8 years; mean age at DNA sampling 59.3 years	▪ Epigenome-wide; Illumina 450k array, Hannum/Horvath DNAm age ▪ Blood ▪ Cell type composition: yes ▪ Consideration of genotype: yes	▪ 1.5T ▪ Structural, T1/T2 ▪ White matter hyperintensities ▪ Non-automated counting	▪ Positive association between WMH burden and DNAm age acceleration: high WMH burden category was associated with DNAm age acceleration, whereas low WMH burden was not. ▪ No individual probe reached significance in any analysis.
Shelton et al., 2017 Australia †	▪ FXTAS ▪ Cases n=20 F; controls, n=20F ▪ Cases mean 40.1 years; controls mean 39.1 years	▪ Candidate: *FMR1* – exon 1 CpG1 and CpG2; intron 1 CpG6/7, CpG8/9; CpG10-12 ▪ Blood ▪ Cell type composition: NR ▪ Consideration of genotype: NR	▪ 3T ▪ Diffusion ▪ FA, MD in ROIs ▪ TBSS (FSL)	▪ Premutation group: negative association between inferior and middle cerebellar peduncle's MD and CpG1 ▪ Control: negative association between BCC FA and CpG6/7
Chouliaras et al., 2018 United Kingdom	▪ N = 47(39M) ▪ Cognitively intact, mean 72.8 years; cognitively impaired, mean 72.3 years (s.d. 6.02)	▪ Epigenome-wide: Illumina 450k array, Horvath/Hannum DNAm age ▪ Blood ▪ Cell type composition: yes ▪ Consideration of genotype: NR	▪ 3T ▪ Structural, T1/ ▪ Diffusion ▪ total brain, hippocampal, CSF, GM volumes, WMH ▪ FA, MD ▪ Voxel wise statistical analysis, BIANCA (WMH detection)/ FSL	▪ No associations were observed between the Horvath epigenetic clock and any of the imaging variables tested ▪ Candidate gene testing did not find any associations that survived correction for multiple comparisons. ▪ Negative association between global MD and Hannum age, and positive association between global FA and Hannum age.

† Overlapping cohort

Table 8. Post-traumatic stress disorder

Author, Country	Sample characteristics ▪ Condition ▪ Cases (male); controls (male) ▪ Age	▪ Epigenome-wide/candidate, platform ▪ Tissue sampled ▪ Correction for cell sub-type distribution ▪ Consideration of genotype	▪ MRI field strength ▪ Modality ▪ Image feature(s) Analysis method	Main Findings
Klengel et al., 2013 United States	▪ Childhood trauma related PTSD ▪ Cases n=56(F) ▪ Cases, mean age 28.5 mean years	▪ Candidate: *FKBP5* - 4 intronic regions, CpG island of TSS and a region upstream of the TSS ▪ Blood ▪ Cell type composition: NR ▪ Consideration of genotype: yes	▪ 3T ▪ Structural, T1 ▪ Amygdala/Hippocampal volume ▪ Amygdala and hippocampal segmentation (Pruessner et al., 2000)	▪ Negative association between FKBP5 (mean at intron 7 bin 2) DNAm and right hippocampal head volume in a subset of the cohort (n=34).
Moser et al., 2015 Switzerland †	▪ Inter-personal violence related PTSD ▪ Controls, n= 20F; Subthreshold PTSD, n = 8F; IPV-PTSD diagnosis, n = 18F ▪ Age - (sample of 68 mothers with	▪ Candidate: *BDNF* mean methylation of 4 CpGs found in exon IV ▪ Saliva ▪ Cell type composition: NR ▪ Consideration of genotype: NR	▪ 3T ▪ fMRI task: Modified Crowell Procedure ▪ Contrast of brain activity when mothers watched their own and unfamiliar children during scenes of separation vs play ▪ SPM8	Whole group analysis: ▪ Positive associations between *BDNF* promoter mean methylation and DNAm and cluster activation in the following clusters: in left vmPFC, OFC, sgACC; right vmPFC, OFC; posterior cingulate cortex. ▪ Negative associations between *BDNF* promoter mean methylation and cluster activation in the following clusters: right hippocampus, right parahippocampal gyrus, right fusiform gyrus; left precuneus; right precuneus; left cerebellum; right STG.

	saliva): Mean 34.3 years (s.d. 5.8 years)			
Schechter et al., 2015 Switzerland †	▪ Inter-personal violence related PTSD ▪ Cases, n=28; controls n=17 ▪ Cases, median 35.1 years; controls, median 35.5 years	▪ Candidate: *NR3C1* – mean methylation of 13 CpGs ▪ Saliva ▪ Cell type composition: NR ▪ Consideration of genotype: NR	▪ 3T ▪ fMRI task: Modified Crowell Procedure ▪ Batch programming based on SPM8	Whole group analysis: ▪ Positive associations between DNAm of *NRC31* and cluster activation in vmPFC OFC, right gyrus rectus; left dlPFC; left dlPFC, left precentral gyrus; dmPFC; left precuneus, posterior cingulate cortex ▪ Spearman's correlations between each of the 13 CpG sites and neural activity in prefrontal cortex regions during separation vs. play did not reach statistical significance
Sadeh et al., 2016 United States ‡	▪ PTSD ▪ Cases: a subset (n=145) of cohort size n=200(182M) ▪ Mean 31.8 years	▪ Candidate: *SKA2*–3' UTR. (Illumina probe cg13989295) ▪ Illumina 450 array ▪ Blood ▪ Cell type composition: yes ▪ Consideration of genotype: yes	▪ 3T ▪ Structural, T1 ▪ Cortical thicknesses ▪ FreeSurfer	▪ Negative associations between *SKA2* DNAm and cortical thickness in prefrontal regions: left frontal pole, SFG and rostral middle frontal gyrus; right frontal pole, SFG, and right OFC/IFG pars orbitalis and rostral MFG. ▪ Mediation was significant for right OFC and rostral MFG cluster, and for left prefrontal cluster. Mediation effect not significant for the right frontal pole/SFG cluster, though direction of association was consistent.
Wolf et al., 2016 United States ‡	▪ PTSD ▪ Cases, n=281(247M) ▪ Cases, mean age 31.9 years	▪ Epigenome-wide: Illumina 450 array, Horvath/Hannum DNAm age Blood ▪ Cell type composition: yes ▪ Consideration of genotype: yes	▪ 3T ▪ Diffusion ▪ FA/RD/MD/AxD in right frontal cortex, left frontal cortex, genu of corpus callosum ▪ FreeSurfer/TBSS	Subset (n=241): ▪ Accelerated Hannum DNAm age associated with decreased FA, increased RD and MD in genu of corpus callosum ▪ Positive association between DNAm age acceleration and RD and MD in genu of corpus callosum ▪ Negative association between DNAn age acceleration and FA in the genu of corpus callosum. ▪ No associations found with Horvath DNAm age.

Schechter et al., 2017 Switzerland †	▪ Inter-personal violence related PTSD ▪ Cases, n=18F; controls, n=17F ▪ Cases, mean age 33.5 years; controls, mean 35.6 years	▪ Candidate: serotonin receptor 3A methylation (*HTR3A*) – 7 CpG sites in the promoter region ▪ Saliva ▪ Cell type composition: NR ▪ Consideration of genotype: NR	▪ Field strength: NR ▪ fMRI task: video stimuli depicting neutral, menacing, and male-female prosocial interactions. ▪ Neural activity in maternal brain regions association with emotion regulation ▪ Batch programming based on SPM8	▪ Negative association between DNAm at CpG 2 III site and neural activity in response to menacing vs prosocial stimuli: dorsomedial PFC, dACC, bilateral dorsolateral prefrontal gyrus, left prefrontal gyrus, left temporal pole, left STG, left MTG; posterior cingulate cortex; left cuneus, V1; cerebellum; right brainstem. ▪ Negative association between DNAm at *5HT3A* CpG 2 III site and neural activity in response to menacing vs neutral stimuli: dmPFC, left dlPFC, left temporal pole, left middle temporal gyrus.
Mcnerney et al., 2018 United States	▪ Veterans risk of meeting PTSD diagnostic criteria ▪ Cases, n= 67 (59M) ▪ Cases, mean 46 years	▪ Candidate: *NR3C1-1F* – promoter binding sites for transcription factor NGF1A ▪ Saliva ▪ Cell type composition: NR ▪ Consideration of genotype: NR	▪ 3T ▪ Structural, FSPGR ▪ Intracranial volume and hippocampal volume ▪ FreeSurfer	▪ Positive associations between hippocampal volume and DNAm of *NR3C1* gene in low scorers on the PTSD checklist (Civilian version 4; PCL-C), unlikely to meet PTSD diagnostic criteria). ▪ Associations were not significant for those who scored highly on the PCL-C.

† Overlapping cohort
‡ Overlapping cohort

Table 9. Miscellaneous: healthy adults, emotion processing, social anxiety disorder, Cushing's syndrome.

Author, Country	Sample characteristics ▪ Condition ▪ Cases (male); controls (male) ▪ Age	▪ Epigenome-wide/candidate, platform ▪ Tissue sampled ▪ Correction for cell sub-type distribution ▪ Consideration of genotype	▪ MRI field strength ▪ Modality ▪ Image feature(s) ▪ Analysis method	Main Findings
Ursini et al., 2011 Italy	▪ Healthy participants ▪ Cases, n=84(32M) ▪ Cases, mean age 25.9 years	▪ Candidate: *COMT* rs4680 (C2) and gene promoter (3 CpGs in the promoter) ▪ Peripheral blood mononuclear cells ▪ Cell type composition: NR ▪ Consideration of genotype: yes	▪ 3T ▪ fMRI task: N-back task–working memory ▪ BOLD responses in the bilateral prefrontal cortex ▪ SPM5	Val/Val genotype: ▪ Negative association between C2 DNAm and bilateral PFC (BA 45/13 and BA47) activity during task ▪ Increased stress and lower C2 DNAm related to greater activity in bilateral PFC (BA10/47; BA44/45) during working memory task ▪ No significant relationship was found between DNAm of sites in the COMT promoter or in LINE-1 and working memory related PFC activity in any other genotype group or in the whole sample.
Jack et al., 2012 United States	▪ Healthy participants ▪ Cases, n=42(23M) ▪ Cases, mean age 21.9 years	▪ Candidate: *OXTR*-coding strand including site -934 ▪ Blood (mononuclear cells) ▪ Cell type composition: NR ▪ Consideration of genotype: NR	▪ 3T ▪ fMRI task: social perception task (animacy versus random movement) ▪ whole brain: BOLD activity ▪ FSL (FEAT)	▪ *OXTR* DNAm positively associated with activity in left STG, supramarginal gyrus, and right dACC. ▪ Controlling for sex: *OXTR* DNAm positively associated with activity in the left STG and right dACC. No difference between men and women.

Vukojevic et al., 2014 Switzerland	▪ Healthy participants ▪ Cases, n=72(25M) ▪ Cases, median age 23 years	▪ Candidate: *NR3C1* CpG3 ▪ Saliva ▪ Cell type composition: NR ▪ Consideration of genotype: NR	▪ 3T ▪ fMRI task: N-back task–working memory task ▪ Brain activation ▪ SPM8	▪ Women: no significant associations between *NR3C1* CpG3 DNAm and brain activation during fMRI task. ▪ Men: positive associations between DNAm at *NR3C1* CpG3 and brain activity related to successful recognition of previously seen pictures: right hemisphere pars orbitalis, right hemisphere pars triangularis of the inferior frontal gyrus; near superior temporal cortex; left hemisphere cuneus, left hemisphere pericalcarine; near superior frontal cortex.
Nikolova et al., 2014 United States	▪ Healthy participants, Discovery set n=80(38M); replication set: 96 (48M) ▪ Discovery set mean age 19.7 years; replication set 13.6 years	▪ Candidate: *SLC6A4*; 20 CpG sites in promoter region ▪ Discovery: saliva ▪ Replication: blood ▪ Cell type composition: NR ▪ Consideration of genotype: yes	▪ 3T ▪ fMRI task: emotional faces processing ▪ BOLD - amygdala reactivity to threat (angry/fearful faces vs shapes). ▪ SPM8	▪ Positive association between *SLC6A4* DNAm and left amygdala reactivity in response to threat stimuli; right amygdala did not reach statistical significance. ▪ The CpG with the strongest association across both hemispheres is CpG14. ▪ Findings consistent in discovery and replication sets
Dannlowski et al., 2014 Germany	▪ Healthy participants ▪ Cases, n=189(90M) ▪ Two independent samples: sample 1 n=94(42M); sample 2 n=95(46M) ▪ Sample 1 mean age 36.9 years;	▪ Candidate: *SLC6A4* AluJb element – mean methylation of 8 investigated sites ▪ Blood ▪ Cell type composition: NR ▪ Genotype: yes	▪ Field strength: NR ▪ Structural, T1 ▪ VBM-ROI volumes: hippocampus, anterior cingulate cortex, amygdala ▪ VBM – whole brain. ▪ VBM8/SPM8	▪ Positive association between AluJb DNAm in the *SLC6A4* gene and bilateral hippocampal grey matter volume in ROI analysis in both samples. In sample 1 peak coordinates cluster extended into the bilateral amygdala. This was not the case in sample 2, but was the case in the combined sample. ▪ Whole brain analysis: positive association clusters where a positive association is also found: bilateral insula, right putamen, amygdala and caudate, and left superior occipital gyrus, bilateral hippocampus. ▪ No areas showed a negative association between DNAm rates and grey matter volume.

	sample 2 mean age 34.2 years			
Puglia et al., 2015 United States	▪ Healthy participants ▪ Cases, n=98(42M) ▪ Cases, mean age 22.8 years	▪ Candidate: *OXTR* CpG site at position -934 relative to TSS ▪ Peripheral blood mononuclear cells ▪ Cell type composition: NR ▪ Consideration of genotype: NR	▪ 3T ▪ fMRI task: emotional face matching task. ▪ BOLD - ROI analysis ▪ PPI/FEAT (FSL)	▪ Positive association between *OXTR* DNAm and BOLD in the left amygdala in Faces versus Ovals. No association in right amygdala. ▪ Higher *OXTR* DNAm predicted decreased levels of functional connectivity on tasks involving affect appraisal and emotion regulation between right amygdala and brain regions involved in emotional regulation including insular cortex, cingulate cortex, orbitofrontal cortex as well as regions associated with face perception e.g fusiform gyrus. Left amygdala showed no significant voxels.
Ziegler et al., 2015 Germany	▪ Social anxiety disorder ▪ Cases, n=25(F) ▪ Cases, mean age 28.8 years	▪ Candidate: *OXTR* gene exon 3 ▪ Blood ▪ Cell type composition: NR ▪ Consideration of genotype: yes	▪ 3T ▪ fMRI task: social phobia related verbal stimuli ▪ Amygdala responsiveness ▪ SPM8	▪ In SAD patients (n=25F): negative association between *OXTR* DNAm and amygdala responsiveness in social phobia vs negative words or neutral words.
Muehlhan et al., 2015 Germany	▪ Healthy participants ▪ Cases, n=74(45M) ▪ Cases (male), mean age 23.6	▪ Candidate: *SLC6A4*- mean methylation score at the promoter ▪ Blood	▪ 3T ▪ fMRI: resting state ▪ SPM12	Positive associations between *SLC6A4* DNAm and amygdala RS functional coupling with nodes of the salience network: ▪ Right amygdala: right SMA and left dACC, left putamen and left insula, right IFG, right putamen, right insula ▪ Left amygdala: right dACC, left ACC, left SMA

	years; cases (female), mean age 23.2 years	▪ Cell type composition: NR ▪ Consideration of genotype: yes		
Ursini et al., 2016 Italy	▪ Healthy participants ▪ Cases, n=141 ▪ Age: NR	▪ Candidate: *BDNF* - rs6265 methylation status ▪ Blood ▪ Cell type composition: NR ▪ Consideration of genotype: yes	▪ 3T ▪ fMRI task: N-back task, working memory ▪ SPM8	Analysis carried out in 141 healthy subjects: ▪ Positive association between *BDNF* rs6265 DNAm and left prefrontal activity ▪ Val/Val genotype: greater DNAm is associated with reduced activity in the PFC (BA46) subjects with hypoxia related obstetric complications (assessed using the McNeil-Sjöström Scale) compared to those without. ▪ Val/Met genotype: lower DNAm is associated with reduced activity in the prefrontal cortex (BA46) in subjects with hypoxia related obstetric complications compared to those without.
Haas et al., 2016 United States	▪ Healthy participants ▪ Cases, n=121(52M) ▪ Cases, mean age 21.3 years	▪ Candidate: *OXT* - average *OXT* DNA methylation across nine CpG sites ▪ Saliva ▪ Cell type composition: NR ▪ Consideration of genotype: NR	▪ 3T ▪ Structural, T1 ▪ fMRI task: Emotional perspective taking task; Emotion attribution task ▪ VBM - SPM8	▪ Emotional perspective task: Negative association between *OXT* DNAm and activity in the R superior temporal sulcus during emotional perspective taking; ▪ Emotion attribution task: negative association in the emotion attribution between *OXT* DNAm and activity in: right STS, right fusiform gyrus/middle occipital gyrus, right inferior frontal gyrus; left fusiform; ▪ Negative association between *OXT* DNAm and grey matter volume in right fusiform gyrus
Resmini et al., 2016 Spain	▪ Cushing's syndrome ▪ Cases, n=32; controls, n=32 ▪ Cases: mean age 45 years;	▪ Candidate: *FKBP5* - intronic regions ▪ Blood ▪ Cell type composition: NR ▪ Consideration of genotype: yes	▪ 3T ▪ Structural, T1 ▪ Hippocampal volume ▪ FreeSurfer	▪ Cases: positive association between Intron 2 region 2 CpG3 DNAm and bilateral hippocampal volume

	controls, mean age 44 years			
Ismaylova et al., 2017 Canada	▪ Healthy participants ▪ Cases 40(14M) ▪ At time of blood sampling: 27 ▪ At time of saliva/buccal sampling: mean 33.7 years	▪ Candidate: S*LC6A4* – promoter mean methylation score of 10 CpG sites ▪ (blood/saliva/buccal) ▪ Cell type composition: NR ▪ Consideration of genotype: NR	▪ 3T ▪ fMRI task: Emotional face processing task ▪ fMRI resting state ▪ Structural, T1 ▪ WB analysis and 10 ROIs grey matter volumes, functional connectivity ▪ VBM/SPM12/Conn functional connectivity toolbox	▪ Positive associations between *SLC6A4* promoter DNAm and grey matter volumes, which varied by tissue type: - Blood: right superior frontal grey matter; - Saliva: left superior frontal gyrus; - Buccal cells: left superior frontal gyrus, left inferior frontal gyrus, right ACC. ▪ Positive association between blood *SCL6A4* DNAm and RS connectivity between: RLP and bilateral frontal poles and SFG; RLP and left lateral occipital cortex ▪ Positive associations between buccal *SLC6A4* promoter DNAm and RS connectivity between the RLP with right lateral occipital cortex and right angular gyrus, ACC, right frontal pole and mPFC ▪ No significant associations were found for task-based fMRI
Wiemerslage et al., 2017 Sweden	▪ Orexigenia among healthy participants ▪ Cases, n=23(all M) ▪ Cases, mean age 26 years	▪ Candidate: *KLF13* - cg07814318 probe methylation ▪ Blood ▪ Cell type composition: yes ▪ Consideration of genotype: NR	▪ 3T ▪ fMRI resting state and task: virtual high or low-calorie food ▪ WB ▪ SPM8	▪ Negative associations between *KLF13* DNAm and neural activity in response to images high calorie food in comparison to images of low-calorie foods in: left claustrum and insula, bilateral cingulate gyrus, right precentral gyrus and claustrum, right MFG, SFG and medial FG. ▪ Positive associations between DNAm and RS activity in the right caudate and putamen, left lingual gyrus and fusiform gyrus.

Ismaylova et al., 2018 Canada	▪ Fronto-limbic brain responses to sadness/fear ▪ Cases, n=96 monozygotic twins (21M pairs) ▪ Cases, mean age 15 years	▪ Candidate: *SLC6A4* – promoter CpG 5-14 ▪ Saliva ▪ Cell type composition: NR ▪ Consideration of genotype: NR	▪ 3T ▪ fMRI task: Emotional face processing task ▪ ROI functional connectivity ▪ SPM8/CONN toolbox	▪ Sad condition: Positive association between *SLC6A4* DNAm and OFC activation. Positive association between methylation and functional connectivity between left amygdala and the ACC and the left amygdala and the right OFC ▪ Fearful condition: positive association between *SLC6A4*methylation and functional connectivity between ACC and both the left amygdala and left insula.
Freytag et al., 2017 Germany/ Switzerland	▪ Healthy cohort n=533(222M) of whom 514 have imaging. ▪ Mean age at MRI: mean 22.9 years; mean age at blood sampling 23.9 years	▪ Epigenome-wide: Illumina 450 array ▪ Blood ▪ Cell type composition: Methylomic profiling sample: yes; Replication cohort: none reported ▪ Consideration of genotype: yes	▪ 1.5T/3T ▪ Structural, T1 ▪ Cortical thickness ▪ FreeSurfer	▪ Independent component analysis (ICA) applied to decompose methylation profiles. ▪ Negative association between the second independent component (ICA2) DNAm and cortical thickness. ICA2 DNAm partially mediates the relationship between chronological age and global cortical thickness. ▪ Negative association between ICA2 and F6 (identified through exploratory factor analysis (EFA) of variation in cortical thicknesses); F6 accounts for 4% of variance in cortical thickness measures - spatial pattern comprising mainly temporal areas (loadings >0.3) with highest loadings in L and R temporal poles and entorhinal cortices.

Chapter 4. Association between preterm birth, differential DNA methylation and brain dysmaturation in neonates

Chapter Introduction

In the previous two chapters, I have shown that early life experiences influence brain structure in late life, and that DNAm, in relation to a variety of health and disease contexts, is associated with brain structure and function throughout the life-course, including neurodevelopment.

Alterations in DNAm in response to gestational age at birth have been observed in cord blood, but this tissue type is limited to time of birth. Other tissues, such as saliva, provide opportunities for non-invasive longitudinal sampling. Furthermore, DNAm in saliva has previously been linked to white matter tract shape and microstructure. In this chapter, I test the hypotheses that gestational age at birth is associated with differential DNAm of neonatal saliva, and that this is associated with neonatal MR neuroimaging measures of white matter microstructure.

Data is drawn from the Theirworld Edinburgh Birth Cohort, with neonatal participants who were recruited antenatally to the study. Saliva samples for measuring DNA, and brain MRI were obtained at the same time point.

This work is presented as a paper entitled “DNA methylation and brain dysmaturation in preterm infants” and is in submission. As first author I designed and carried out the analysis and drafted and wrote the manuscript. I also carried out the pre-processing of the DNAm data. Dr Manuel Blesa

performed the pre-processing of MRI data and generated the peak width skeletonised diffusion metrics. DNA extraction and measurement of DNAm was performed at the Edinburgh Clinical Research Facility. Recruitment of participants to the study, and MRI and sample collection was carried out by members of the Jennifer Brown Research Laboratory.

Abstract

Preterm birth is associated with dysconnectivity of structural brain networks and is a leading cause of neurocognitive impairment in childhood. Variation in DNA methylation (DNAm) is associated with early exposure to extrauterine life but there has been little research exploring its relationship with brain development.

Using genome-wide DNA methylation data from saliva of 258 neonates, we investigated the impact of gestational age on the methylome and performed functional analysis to identify enriched gene sets from probes that contributed to differentially methylated probes (DMPs) or regions (DMRs). We tested the hypothesis that variation in DNAm could underpin the association between preterm birth and atypical brain development by linking DMPs with measures of white matter connectivity derived from diffusion MRI metrics: peak width of skeletonised mean diffusivity (PSMD), fractional anisotropy (PSFA) and neurite density index (PSNDI).

Gestational age at birth was associated with widespread differential methylation, with genome-wide significant associations observed for 8,898 CpG probes ($p<3.6x10^{-8}$) and 1,775 differentially methylated regions. Functional analysis identified 14 enriched gene ontology terms pertaining to cell-cell contacts and cell-extracellular matrix contacts. Principal component analysis of probes with genome-wide significance revealed a first principal component (PC1) that explained 23.5% of variance in DNAm, and this was negatively associated with gestational age at birth. PC1 was associated with PSMD ($\beta=0.344$, $p=2.55x10^{-7}$) and PSNDI ($\beta=0.360$, $p=5.07x10^{-5}$), but not with PSFA ($\beta=-0.017$, $p=0.802$); these relationships mirrored the imaging metrics' associations with gestational age at birth.

Gestational age at birth has a profound and widely distributed effect on the neonatal saliva methylome. Enriched gene ontology terms related to cell-cell contacts reveal pathways that could mediate the effect of early life

environmental exposures on development. Finally, associations between differential DNAm and image markers of white matter tract microstructure suggest that variation in DNAm may provide a link between preterm birth and the dysconnectivity of developing brain networks that characterises atypical brain development in preterm infants.

4.1 Introduction

Preterm birth, defined as birth at <37 weeks of gestation, affects around 11% of births worldwide and is a leading cause of neurodevelopmental and cognitive problems that extend across the life course (Chawanpaiboon et al., 2019). These include autism spectrum disorder, social difficulties, language impairment, ADHD, reduced IQ, educational underachievement, and psychiatric diagnoses (Agrawal et al., 2018; Burnett et al., 2011; Franz et al., 2018; Johnson et al., 2015, 2010; Mackay et al., 2010; Nosarti et al., 2012; Van Lieshout et al., 2018).

The neural phenotypes that underlie long-term functional impairment include diffuse white matter injury and subsequent dysmaturation of white matter and grey matter neuroaxonal structures, collectively termed the 'encephalopathy of prematurity (Volpe, 2009). A consequence of the encephalopathy is generalised dysconnectivity of developing structural networks, which can be inferred from diffusion MRI (dMRI) and neurite orientation dispersion and density imaging (NODDI) during the neonatal period (Ball et al., 2015; Pietsch et al., 2019; Tariq et al., 2016; Telford et al., 2017; Zhang et al., 2012). Specifically, normal maturation is characterized by a reduction in mean diffusivity (MD) and increases in both fractional anisotropy (FA) and neurite density index (NDI) in white matter; but MD is increased and FA and NDI are decreased in preterm infants at term equivalent age, compared with healthy controls infants born at term (Boardman and Counsell, 2020). These changes reflect an increase in water content and a decrease in white matter organization in preterm infants. Peak width of skeletonised mean diffusivity (PSMD) is a method for histogram-based calculation of MD distribution across the entire white matter skeleton; it provides a measure of generalized white matter microstructure, is robust to scanner variation, and is predictive of cognition in later life (Baykara et al., 2016; Deary et al., 2019; Wei et al., 2019). In previous work we extended the histogram model to neonatal data and included other dMRI and NODDI metrics. We found that PSMD and PSNDI are altered in preterm infants at term equivalent age, and that

histogram-based measures have utility for investigating upstream determinants of dysmaturation such as systemic inflammation (Blesa et al., 2020; Sullivan et al., 2020).

The mechanisms that link the environmental stress of preterm birth with atypical brain development are uncertain. Variation in DNA methylation (DNAm) is a possible mechanism; DNAm is involved in the regulation of gene expression and cell fate during fetal brain development (Spiers et al., 2015). Alterations in DNAm contribute to the pathogenesis of neurodevelopmental disorders such as Rett syndrome, Immunodeficiency, Centromeric region instability, Facial anomalies [ICE] syndrome, and Angleman and Prader-Willi syndromes (Lyst and Bird, 2015; Rangasamy et al., 2013; Weemaes et al., 2013). There is growing evidence that differential DNAm can mediate the effect of environmental pressures on brain structure and function across the life course (Sparrow et al., 2016; Wheater et al., 2020). The neonatal methylome is sensitive to prenatal factors such as maternal smoking, maternal body mass index, as well as birth weight (Joubert et al., 2016; Küpers et al., 2019; Sharp et al., 2017). It is altered in association with co-morbidities of preterm birth, and there is some evidence for legacy differences in the methylome two decades after preterm birth (Cruickshank et al., 2013; Everson et al., 2020, 2019; Sparrow et al., 2016). A meta-analysis investigating DNAm from umbilical cord blood identified widespread differential methylation associated with gestational age at birth across the gestational age range of 27-42 weeks, as measured on the Illumina 450k array (Merid et al., 2020). However, due to differences in the cellular composition of samples, epigenetic signatures observed in different tissues are likely to be distinct (Armstrong et al., 2014). The main cellular component of saliva, buccal epithelium, may be more representative of the brain than umbilical cord blood because of ectodermal origin (Braun et al., 2019; Lowe et al., 2013; Smith et al., 2015).

Here, our first aim was to determine whether gestational age at birth was associated with variation in the salivary methylome and to characterise the biological pathways implicated in the DNAm response to preterm birth. Our second aim was to investigate whether the DNAm signal of preterm birth explains variance in measures of white matter microstructure. We tested the hypotheses that gestational age at birth is associated with widespread differential methylation, and that DNAm contributes to variance in peak width skeletonised metrics of white matter connectivity, apparent during the neonatal period.

4.2 Materials and methods

4.2.1 Participants

Preterm and term born infants delivered at the Royal Infirmary of Edinburgh, UK were recruited to the Theirworld Edinburgh Birth Cohort, a longitudinal study designed to investigate the effect of preterm birth on brain development (Boardman et al., 2020). Cohort exclusion criteria were major congenital malformations, chromosomal abnormalities, congenital infection, overt parenchymal lesions (cystic periventricular leukomalacia, hemorrhagic parenchymal infarction) or post-hemorrhagic ventricular dilatation. Ethical approval has been obtained from the National Research Ethics Service, South East Scotland Research Ethics Committee (11/55/0061, 13/SS/0143 and 16/SS/0154). Informed consent was obtained from a person with parental responsibility for each participant. The study was conducted according to the principles of the Declaration of Helsinki. DNAm data were available from 258 neonates, 214 of whom also had successful dMRI acquisition.

4.2.2 DNA extraction and methylation measurement

Saliva obtained at term equivalent age was collected in Oragene OG-575 Assisted Collection kits, by DNA Genotek, and DNA extracted using prepIT.L2P reagent (DNA Genotek, Ontario, Canada). DNA was bisulfite converted and methylation levels were measured using Illumina

HumanMethylationEPIC BeadChip (Illumina, San Diego, CA, USA) at the Edinburgh Clinical Research Facility (Edinburgh, UK). The arrays were imaged on the Illumina iScan or HiScan platform and genotypes were called automatically using GenomeStudio Analysis software version 2011.1 (Illumina). DNAm was analysed in two batches.

4.2.3 DNA Methylation pre-processing

Raw intensity (.idat) files were read into R environment (version 3.4.4) using minfi. wateRmelon and minfi used for preprocessing, quality control and normalisation (Aryee et al., 2014; Pidsley et al., 2013). The pfilter function in wateRmelon was used to exclude: samples with 1 % of sites with a detection p-value greater than 0.05; sites with beadcount <3 in 5% of samples; and sites with 1% of samples with detection p value >0.05. Cross hybridising probes and probes targeting single nucleotide polymorphisms with overall minor allele frequency ≥0.05 were also removed (McCartney et al., 2016). Control probes (n = 59) were also removed. Samples were removed if there was a mismatch between predicted sex (minfi) and recorded sex (n = 3). Data was danet normalised which includes background correction and dye bias correction (Pidsley et al., 2013). Saliva contains different cells types, including buccal epithelial cells and leukocytes. Epithelial cell proportions were estimated with epigenetic dissection of intra-sample heterogeneity with the reduced partial correlation method implemented in the R package EpiDISH (Zheng et al., 2018). Data from one of each twin pair was removed randomly (n=20).

4.2.4 MRI acquisition

This study incorporates data from two phases of MRI acquisition. MRI was obtained at the same appointment as saliva sample collection for DNAm analysis. Structural and diffusion MRI were performed on 93 infants using a MAGNETOM Verio 3T clinical MRI scanner (Siemens Healthcare GmbH, Erlangen, Germany) and 12-channel phased-array head coil, which were used to acquire: dMRI employed a protocol consisting of 11 T2- and 64

diffusion-weighted (b = 750 s/mm^2) single-shot spin-echo echo planar imaging (EPI) volumes acquired with 2 mm isotropic voxels (TE = 106 ms and TR = 7300 ms).

For the second phase (n=121), structural and diffusion MRI were performed on 121 infants using a MAGNETOM Prisma 3T clinical MRI scanner (Siemens Healthcare GmbH, Erlangen, Germany) and 16-channel phased-array pediatric head and neck coil were used to acquire dMRI in two separate acquisitions: the first consisted of 8 baseline volumes (b=0 s/mm^2 [b0]) and 64 volumes with b=750s/mm^2; the second consisted of 8 b0, 3 volumes with b=200 s/mm^2, 6 volumes with b=500s/mm^2 and 64 volumes with b = 2500 s/mm^2. An optimal angular coverage for the sampling scheme was applied.(Caruyer et al., 2013) In addition, an acquisition of 3 b0 volumes with an inverse phase encoding direction was performed. All dMRI volumes were acquired using single-shot spin-echo EPI with 2-fold simultaneous multislice and 2-fold in-plane parallel imaging acceleration and 2 mm isotropic voxels; all three diffusion acquisitions had the same parameters (TR/TE 3500/78.0ms). Images affected by motion artifact were re-acquired multiple times as required; dMRI acquisitions were repeated if signal loss was seen in 3 or more volumes.

Infants were fed and wrapped and allowed to sleep naturally in the scanner without sedation. Pulse oximetry, electrocardiography and temperature were monitored. Flexible earplugs and neonatal earmuffs (MiniMuffs, Natus) were used for acoustic protection. All scans were supervised by a doctor or nurse trained in neonatal resuscitation. Structural images were reported by an experienced pediatric radiologist (A.J.Q.)

4.2.5 dMRI pre-processing

Diffusion images that were acquired on the MAGNETOM Verio scanner were denoised using a Marchenko-Pastur-PCA-based algorithm (Tournier et al., 2019; Veraart et al., 2016a, 2016b); eddy current distortion and head

movement were corrected using outlier replacement (Andersson et al., 2016; Andersson and Sotiropoulos, 2016; Smith et al., 2004); bias field inhomogeneity correction was performed by calculating the bias field of the mean b0 volume and applying the correction to all the volumes (Tustison et al., 2010). FA and MD were calculated from the dMRI data.

The two dMRI acquisitions from the MAGNETOM Prisma scanner were first concatenated and then denoised using a Marchenko-Pastur-PCA-based algorithm (Tournier et al., 2019; Veraart et al., 2016a, 2016b); eddy current, head movement and EPI geometric distortions were corrected using outlier replacement and slice-to-volume registration (Andersson et al., 2017, 2016; Andersson and Sotiropoulos, 2016; Smith et al., 2004); bias field inhomogeneity correction was performed by calculating the bias field of the mean b0 volume and applying the correction to all the other volumes (Tustison et al., 2010). From the dMRI data we calculated the three eigenvalues and eigenvectors of the water diffusion tensor, and NODDI (Bingham distribution) parametric maps using cuDIMOT (intracellular volume fraction [NDI] and the overall orientation dispersion index [ODI_{TOT}]) (Hernandez-Fernandez et al., 2019; Tariq et al., 2016; Zhang et al., 2012). FA and MD were calculated using single-shell data to match the Verio scanner.

4.3.6 Peak width of skeletonized water diffusion parameters

All the subjects were registered to the Edinburgh Neonatal Atlas (ENA50) using DTI-TK (Blesa et al., 2020). The diffusion tensor derived maps of each subject (FA and MD) were calculated after registration; NDI was then propagated to the template space using the previously calculated transformations. The data was skeletonized using the ENA50 skeleton and then multiplied by a custom mask. Finally, the peak width of the histogram of values computed within the skeletonized maps was calculated as the difference between between the 95th and 5th percentiles (Baykara et al., 2016; Blesa et al., 2020).

4.2.7 Epigenome-wide association analyses

Unless otherwise stated, analysis was completed in R version 3.4.4 (RCoreTeam, 2020). Surrogate variable analysis of the data matrix was carried out, in order to adjust for potential confounders such as batch, using the sva function in the *sva* package in R (Leek et al., 2012; Leek and Storey, 2007). A fully adjusted model was specified prior to SVA to retain signal explained by biological variables of interest: CpG ~ Gestational age at birth + Gestational age at scan + Birthweight z score + Maternal smoking + Sex + Epithelial cells. SVA identified 17 significant surrogate variables which were subsequently included in the analysis.

EWAS was performed using the *limma* package in R (Ritchie et al., 2015). Beta values of each of 776084 CpG sites were regressed (as dependent variables) on gestational age at birth using linear regression. Covariates were added to adjust for sex, birthweight z score, gestational age at sample collection, maternal smoking, estimated epithelial cell proportions and surrogate variables. A significance threshold of 3.6×10^{-8} was selected, which represents genome-wide significance (Saffari et al., 2018).

4.2.8 Differentially methylated region analysis

Differentially methylated regions were assessed using the dmrff function in the *dmrff* package in R (Suderman et al., 2018). Here a differentially methylated region is a region containing two or above sites separated by ≤500 bp with EWAS analysis $p \leq 0.05$ and methylation changes in a consistent direction. Following dmrff's subregion selection step, DMRs with Bonferroni-adjusted $p \leq 0.05$ were significant.

4.2.9 Gene set testing

Gene set enrichment analysis was carried out using the GO and KEGG databases, and using the gometh function in *missMethyl* package, which controls for multiple probe bias (Maksimovic et al., 2020). Sites that reached genome-wide significance in EWAS, and those that contributed to differentially methylated regions, were included in this analysis.

4.2.10 Principal component analysis

Principal components analysis (PCA) was conducted on CpG probes that reached genome-wide significance, using the *prcomp* function in R. CpGs were pre-corrected for the effects of biological covariates and surrogate variables via linear regression. The scree plot was visually inspected in order to select a principal component (eigenvalue >1) to be carried forward for subsequent analysis.

4.2.11 Linear regression between DNAm and PS metrics

Pearson's correlation coefficient was used to assess the relationship between the first PC identified from PCA and gestational age at birth. This PC was used in linear regression models, as an independent variable, to test the associations between PSMD, PSNDI and PSFA with DNAm, conducted in R version 4.0.1 (RCoreTeam, 2020). In models testing PSMD and PSFA, MRI scanner was included as a binary covariate as MRI data from both phases of data collection were included. PSNDI was only available for one phase of data collection and so it was not necessary to include scanner as a covariate. We report standardised regression coefficients and p-values.

4.2.12 Data availability

The atlas with templates can be found at https://git.ecdf.ed.ac.uk/jbrl/ena and the code necessary to calculate histogram-based metrics is at https://git.ecdf.ed.ac.uk/jbrl/psmd. Requests for original image data will be considered through the BRAINS governance process: www.brainsimagebank.ac.uk (Job et al., 2017). DNA methylation data are deposited in NCBI's Gene Expression Omnibus.

4.3 Results

4.3.1 Cohort

DNAm data were collected from 311 neonates. Twenty-nine did not meet DNAm preprocessing QC criteria and were excluded. One participant with a congenital abnormality was removed, as were three participants whose sex predicted from DNAm data did not match their recorded sex. This group of 278 neonates included 20 sets of twins. After random removal of one twin from each set there was no evidence of imbalance for birthweight (t=-0.157, p=0.88), or sex (χ^2=0.417, p=0.52). The study group consisted of 258 neonates: 155 participants were preterm and 103 were controls born at full term, see Table 1 for participant characteristics. Among the preterm infants, 38(25%) had bronchopulmonary dysplasia (defined as need for supplementary oxygen ≥36 weeks gestational age), 9(6%) developed necrotising enterocolitis requiring medical or surgical treatment, and 31(20%) had an episode of postnatal sepsis defined as either blood culture positivity with a pathogenic organism, or physician decision to treat for ≥5 days in the context of growth of coagulase negative staphylococcus from blood or a negative culture. Of the 258 participants with DNAm data, 214 also had MRI data.

Table 1. Participant characteristics

	Preterm infants (n=155)	**Term infants** (n=103)
Gestational age at birth/weeks (range)	28.84 (23.28 – 34.84)	39.7 (36.42 – 42.14)
Gestational age at scan/weeks (range)	40.56 (37.70 -45.14)	42.27 (39.84 – 47.14)
Birth weight/g (range)	1177 (500 – 2100)	3482 (2346 – 4670)
Birth weight z-score (range)	-0.19 (range -3.13 – 1.58)	0.43 (range -2.30 – 2.96)
Sex: Female (%)	75 (48)	44 (43)
Maternal folate supplementation in pregnancy (%)	136 (88)	86 (83)
Maternal age (years)	31.1 (17–44)	33.7 (19–48)
Maternal tobacco smoker in pregnancy (%)	29 (19)	2 (2)

4.3.2 Widespread differential saliva DNAm in association with gestational age at birth

We conducted an epigenome-wide association study whereby CpG methylation at 776,084 sites was regressed on gestational age at birth, controlling for birthweight z-score, infant sex, gestational age at sample collection, maternal smoking, estimated epithelial cell proportion and surrogate variables. Differential methylation in relation to gestational age at birth was identified at 8,898 CpG sites at genome-wide significance ($p<3.6x10^{-8}$), Fig. 1. Of these, 4258 (47.8%) sites demonstrated a positive association with gestational age, while 4,640 (52.1%) were negatively associated. The genomic inflation factor was 1.72. Following Bonferroni adjustment, 1775 DMRs corresponding to 4,672 CpG sites were significant $p<0.05$. Of these, 11 had ten or more CpG sites contributing to the DMR. The largest DMR mapped to a genomic region that encodes two genes: *NNAT* and *BLCAP.* The 29 probes mapped to this region were all located within islands and positively associated with gestational age at birth, indicating that longer gestation corresponds to hypermethylation. Of the 10 most significant DMPs, 3 probes were localised to the *IRX4* gene, 1 probe to the *GAL3ST4* gene, and 1 to *LOXL4* (Table 2; Fig. 2). The probes with the largest absolute

magnitude effect size (top 5 hypermethylated and hypomethylated) mapped to the following genes: *IRX2, SMIM2, INTS1, HEATR2, ZBP1* and *UBXN11*, Table 3.

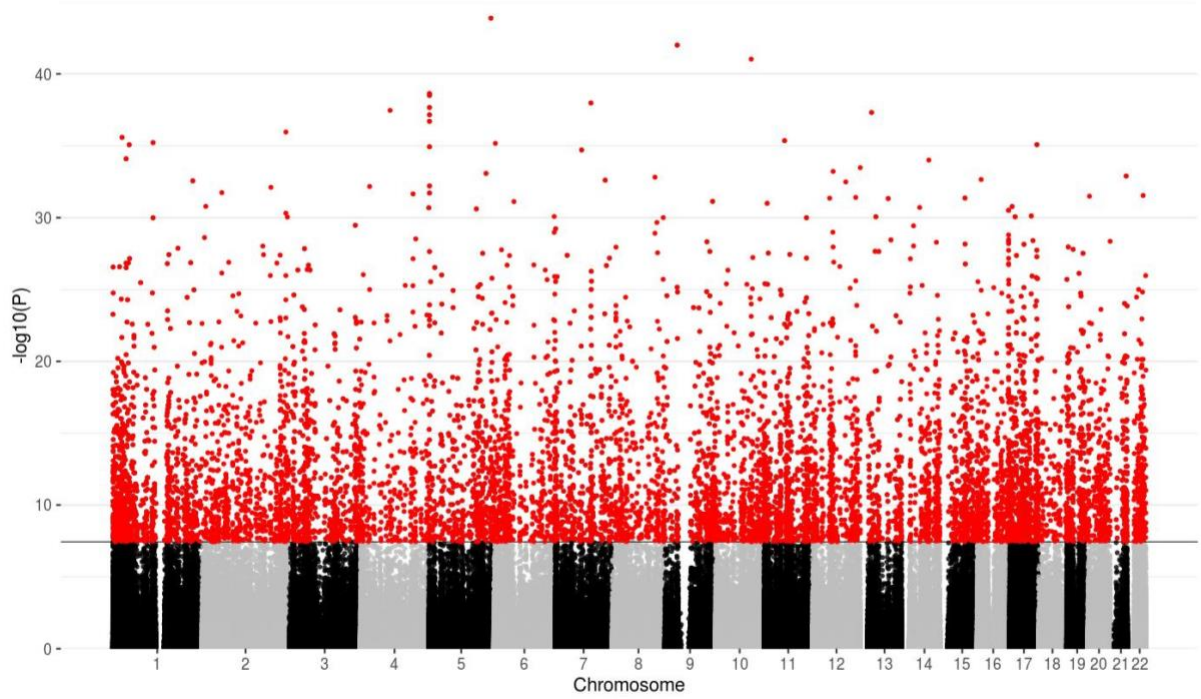

Figure 1. Manhattan plot for the association between gestational age at birth and DNA methylation, following adjustment for covariates and surrogate variables. The solid horizontal line shows the genome-wide significance level and red dots above this line represent probes that are significant at this threshold ($p<3.6x10^{-8}$).

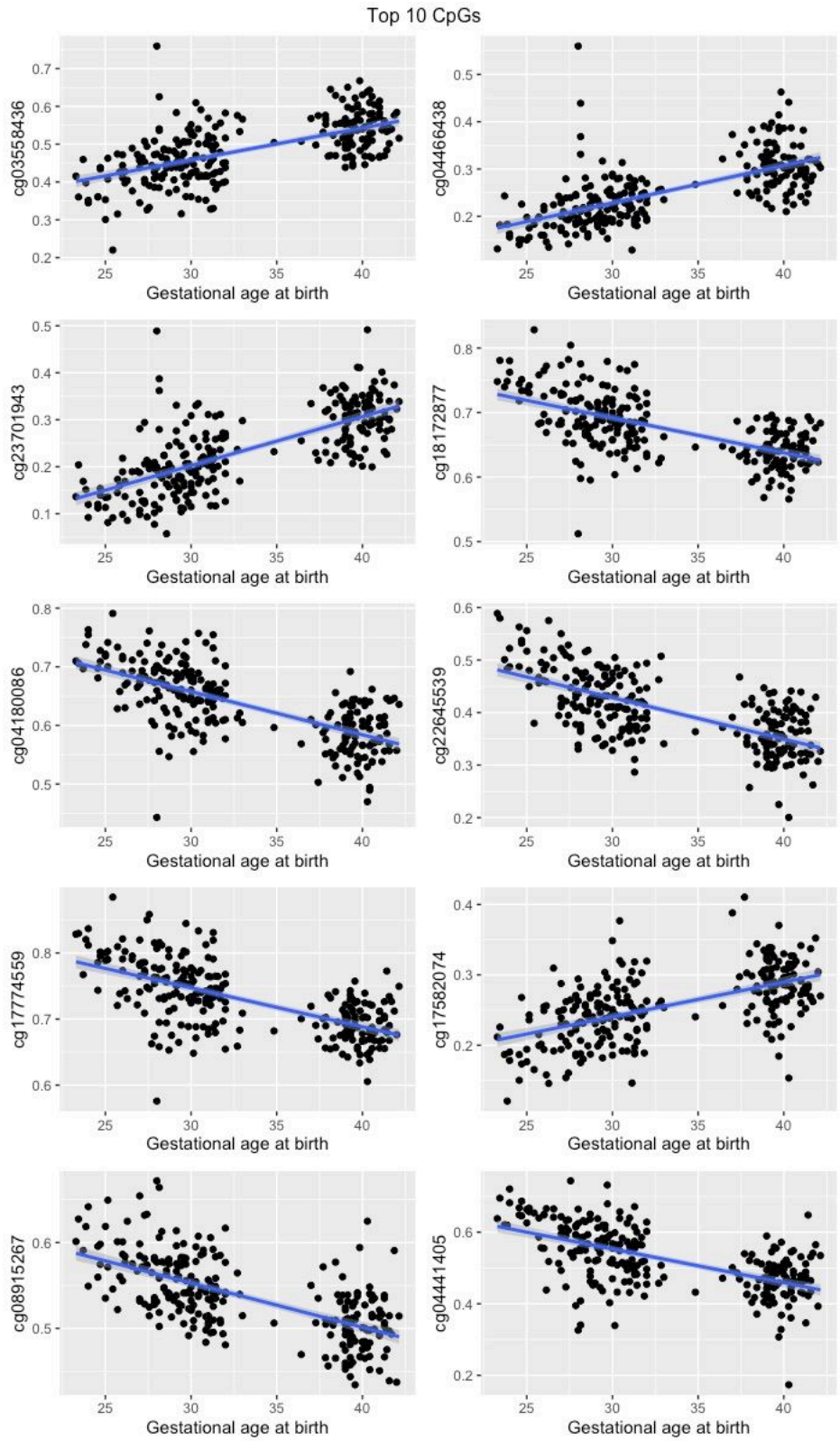

Figure 2. Scatter plots showing the relationship between the beta values of top ten most significant CpG probes and gestational age at birth in weeks, with 95% confidence intervals.

Table 2. Top ten most significant probes associated with gestational age at birth.

Probe	Chromosome	*p* value	Gene	Direction of effect	Coefficient*	Relation to island
cg03558436	5	$1.32x10^{-44}$	-	+	0.01017	Open Sea
cg04466438	9	$9.91x10^{-43}$	-	+	0.00755	Open Sea
cg23701943	10	$9.38x10^{-42}$	*LOXL4*	+	0.01045	Open Sea
cg18172877	5	$2.31x10^{-39}$	*IRX4*	-	-0.00611	Island
cg04180086	5	$3.16x10^{-39}$	*IRX4*	-	-0.00736	Island
cg22645539	7	$1.06x10^{-38}$	*GAL3ST4*	-	-0.00816	North Shelf
cg17774559	5	$2.15x10^{-38}$	*IRX4*	-	-0.00634	Island
cg17582074	4	$3.44x10^{-38}$	-	+	0.00526	Open Sea
cg08915267	13	$4.83x10^{-38}$	-	-	-0.00517	North Shelf
cg04441405	5	$6.99x10^{-38}$	-	-	-0.01101	Island

[a]Coefficient corresponds to methylation change per week of gestation.

Table 3. Top ten probes with the largest absolute magnitude of association with gestational age at birth.

Probe	Chromosome	P value	Gene	Direction of effect	Coefficient[a]	Relation to island
cg10402321	1	2.61×10^{-36}	*UBXN11*	-	-0.01147	Open Sea
cg04441405	5	6.99×10^{-38}	-	-	-0.01101	Island
cg07167946	5	1.93×10^{-32}	*IRX4*	-	-0.00984	Island
cg14670058	13	7.96×10^{-23}	*SMIM2*	-	-0.00910	Open Sea
cg07803375	7	3.54×10^{-22}	*HEATR2*	-	-0.00909	North Shelf
cg16051275	6	6.77×10^{-36}	-	+	0.01234	Open Sea
cg11460314	20	3.35×10^{-20}	*ZBP1*	+	0.01246	Open Sea
cg04118102	17	8.71×10^{-31}	-	+	0.01314	South Shelf
cg17368297	16	1.14×10^{-25}	-	+	0.01409	Open Sea
cg14576951	7	5.95×10^{-30}	*INTS1*	+	0.01409	Island

[a]Coefficient corresponds to methylation change per week of gestation.

4.3.3 Pathways implicated in functional testing

Based on the 8898 sites that met the genome-wide significance threshold ($p<3.6x10^{-8}$), no KEGG terms remained significant following FDR correction for multiple comparisons. Two Gene Ontology terms were enriched following FDR correction: one for anchoring (GO:0070161; q=0.0047) and one for adherens junction (GO:0005912; q=0.0047). In an analysis that incorporated all 11,790 distinct CpGs from both EWAS and DMR analysis, 14 GO terms were enriched, Table 4.

Table 4. Gene ontology (GO) terms that were significantly enriched in an analysis of all probes that contributed to DMPs and DMRs.

Gene ontology	Term	P value	Type	Description
GO:0005912	**adherens junction**	**0.0000188754**	**Cellular component**	**A cell-cell junction composed of the epithelial cadherin-catenin complex.**
GO:0005925	focal adhesion	0.0055801772	Cellular component	A cell-substrate junction that anchors the cell to the extracellular matrix and that forms a point of termination of actin filaments.
GO:0007155	cell adhesion	0.0134553303	Biological process	The attachment of a cell, to another cell or to the extracellular matrix, via cell adhesion molecules.
GO:0007167	enzyme linked receptor protein signalling pathway	0.0132658055	Biological process	A series of molecular signals initiated by the binding of an extracellular ligand to a receptor on the target cell plasma membrane, where the receptor possesses catalytic activity or is closely associated with an enzyme such as a protein kinase, and ending with regulation of a downstream cellular process, e.g. transcription
GO:0007169	transmembrane receptor protein tyrosine kinase signalling pathway	0.0074164416	Biological process	A series of molecular signals, initiated by the binding of an extracellular ligand to a tyrosine kinase receptor on the target cell plasma membrane, ending with regulation of a downstream cellular process.
GO:0022610	biological adhesion	0.0107477439	Biological process	The attachment of a cell to a substrate, another cell, including intracellular attachment between membrane regions.
GO:0030029	actin filament-based process	0.0229891956	Biological process	Any cellular process that depends upon, or alters, the actin cytoskeleton (comprising actin filaments and their associated proteins).
GO:0030036	actin cytoskeleton organization	0.0288732105	Biological process	The assembly, arrangement of constituent parts, or disassembly of cytoskeletal structures comprising actin filaments and their associated proteins.
GO:0030054	cell junction	0.0087863792	Cellular component	Forms a specialized region of connection between two or more cells, or between a cell and the extracellular matrix, or between two membrane-bound components of a cell, such as flagella.
GO:0030055	cell-substrate junction	0.0072626482	Cellular component	A cell junction between a cell and the extracellular matrix.
GO:0034330	cell junction organization	0.0460818115	Biological process	The assembly, arrangement of constituent parts, or disassembly of a cell junction. A cell junction is a specialized region of connection between two cells or between a cell and the extracellular matrix
GO:0045296	cadherin binding	0.0025438358	Molecular function	Interacting selectively and non-covalently with cadherin, a type I membrane protein involved in cell adhesion.
GO:0050839	cell adhesion molecule binding	0.0025438358	Molecular function	Interacting selectively and non-covalently with a cell adhesion molecule.
GO:0070161	**anchoring junction**	**0.0000188754**	**Cellular component**	**A cell junction that mechanically attaches a cell, and its cytoskeleton, to neighbouring cells or the extracellular matrix.**

Terms in bold were enriched in an analysis of 8898 genome-wide significant DMPs

4.3.4 Gestational age at birth is associated with metrics of white matter microstructure in neonates

DNAm and PSMD and PSFA were both available for 214 infants and DNAm and PSNDI were available for the 121 infants from phase 2. Gestational age at birth was significantly associated with PSMD (β=-0.602, $p<2x10^{-16}$) and PSNDI (β=-0.594, $p=2.17x10^{-9}$), but not with PSFA (β=-0.005 p=0.933), Fig. 3A and 3B; Table 5.

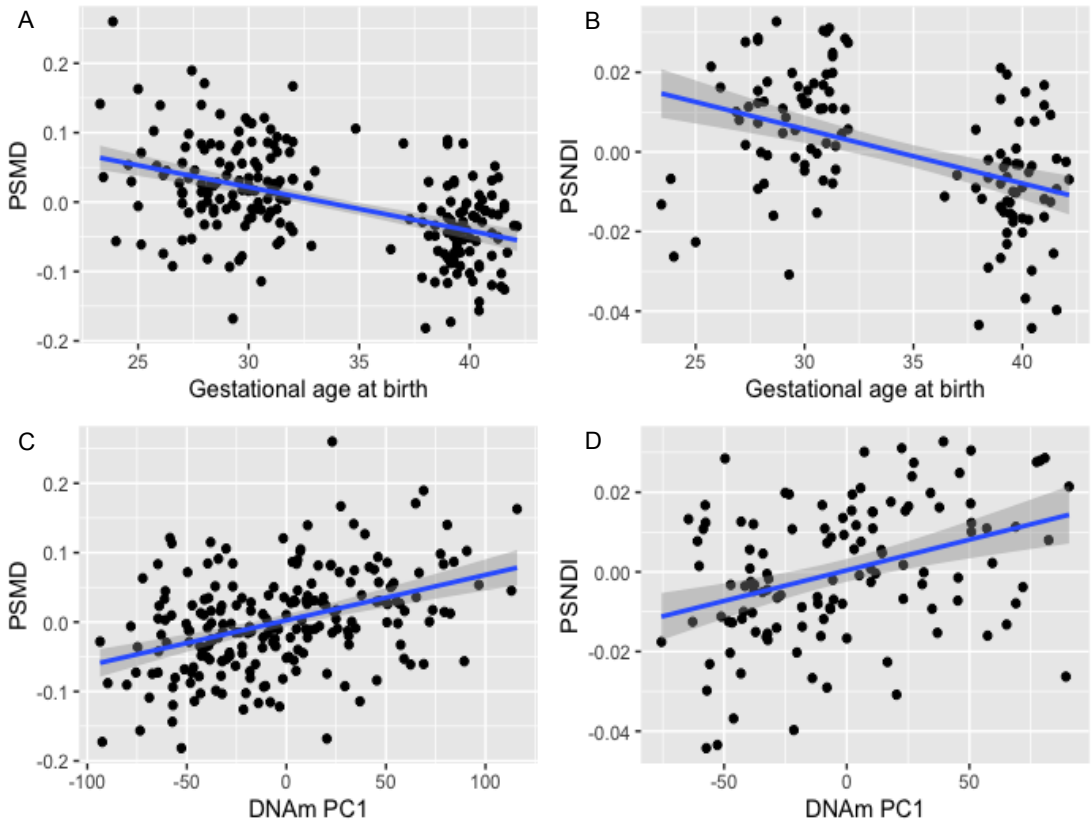

Figure 3. Scatter plots with 95% confidence intervals, showing the relationships between gestational age at birth and DNAm with peak width skeletonised mean diffusivity and neurite density index. The associations between gestational age and PSMD and PSNDI are shown in A and B, respectively. The relationships between DNAm PC1 and PSMD and PSNDI are shown in C and D, respectively. PS metrics are residualised for gestational age at scan; PSMD is additionally residualised for scanner

4.3.5 Differential DNAm is associated with white matter microstructure

The first unrotated PC derived from the 8,898 genome-wide significant CpGs accounted for 23.5% of the variance, the second PC accounted for 2.5%, Fig. 4A. There was no evidence of batch effects in the PCs (Fig. 5).

PC1 was significantly correlated with gestational age at birth (r=-0.622; $p<2.2x10^{-16}$), Fig. 4B. PC1 was also positively associated with PSNDI (β=0.365, $p=3.79x10^{-5}$), and in models adjusted for scanner it was positively associated with PSMD (β=0.350, $p=7.31x10^{-10}$) but not PSFA (β=-0.035, $p=0.511$), (Fig. 3C and 3D;Table 5). All models were adjusted for gestational age at scan.

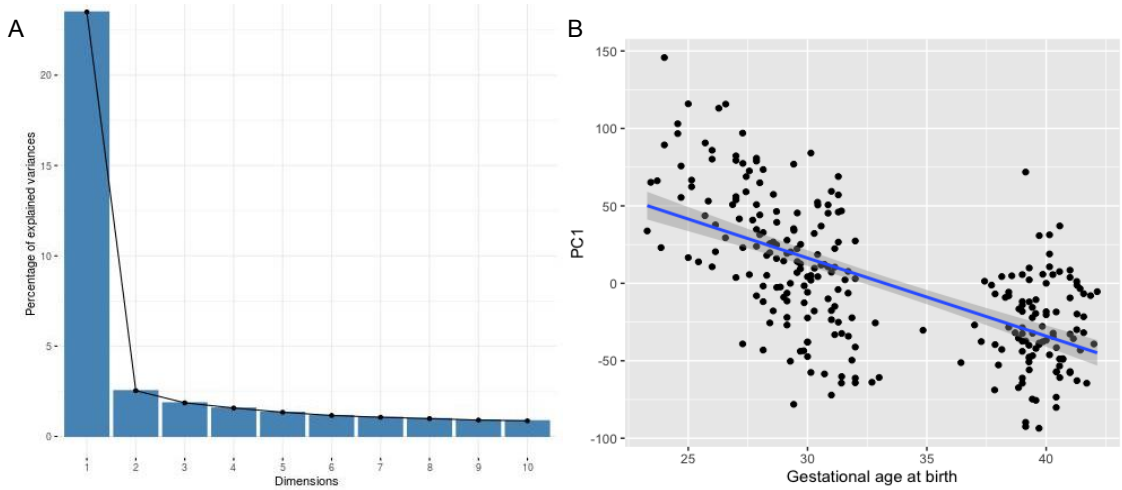

Figure 4. Variation in DNAm probes selected by EWAS captured by principal component, and the relationship with gestational age. Fig 3A, scree plot showing sharp elbow after the first PC, accounting for 23.5% of variance. Fig 3B, scatter plot showing relationship between gestational age at birth and PC1 (r=-0.622) with 95% confidence interval.

Figure 5. Batch effects have been successfully removed from the residualised DNAm data based on the top 2 PCs derived from 8,898 CpG probes that reached genome-wide significance.

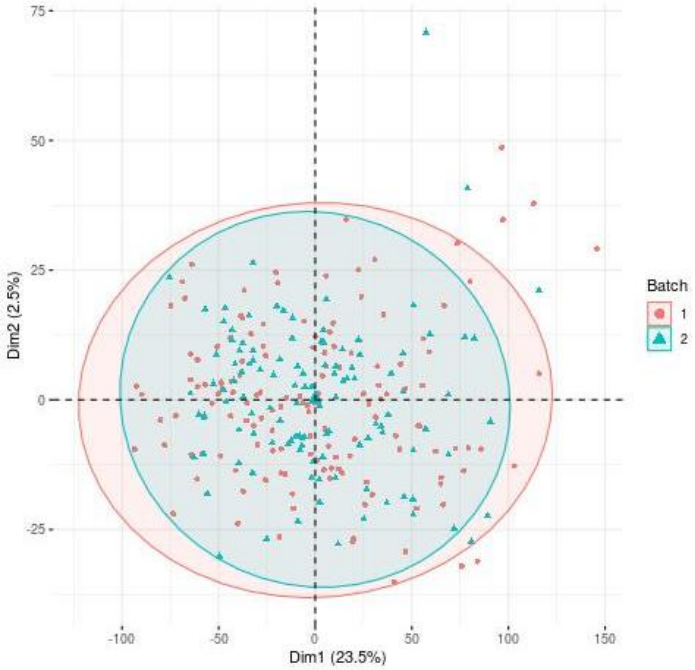

Table 5. Associations between global metrics of white matter microstructure, DNAm first principal component (left) and gestational age (right)

PS metric	**Metric ~ PC1 DNAm + Gestational age at scan + scanner variable[a]**		**Metric ~ Gestational age at birth + Gestational age at scan + scanner variable[a]**	
	β	*p*	β	*p*
PSFA	-0.035	0.511	-0.005	0.933
PSMD	0.350	**7.31×10^{-10}**	**-0.602**	**$< 2 \times 10^{-16}$**
PSNDI	0.365	**3.79×10^{-5}**	**-0.594**	**2.17×10^{-9}**

[a]scanner variable was included in the model for PSFA and PSMD but not PSNDI because NODDI imaging was carried out for a subset using a single MRI scanner (n=121). Bold print signifies significant associations.

4.4 Discussion

By studying a unique database of DNA linked to brain imaging in a population of preterm infants and healthy controls, we have identified extensive differential methylation in association with gestational age at birth and revealed an association between the principal axis of methylation variation and brain dysmaturation within the same sample. Differentially methylated regions and probes were distributed widely across the genome, indicating that gestation duration is associated with global perturbations to the neonatal methylome. Gene enrichment analysis of changes associated with gestational age identified gene sets pertaining to cell contacts and cytoskeleton. A single principal component that explained 23.5% of the variance in differential DNAm linked to preterm birth was closely associated with markers of generalised dysconnectivity across the white matter skeleton.

The data are consistent with studies that have reported associations between length of gestation and genome-wide variation in DNAm within fetal brain and umbilical cord blood (Bohlin et al., 2016; Merid et al., 2020; Spiers et al., 2015); widely distributed variation is reported in association with postmenstrual age at sampling of preterm infants (a proxy for GA at birth) (Everson et al., 2020). The signature we identified in saliva sampled at term equivalent age included 234 probes that were previously shown to be differentially methylated in association with GA in a meta-analysis of umbilical cord blood samples that reported 8,899 gestation-dependent CpGs (Merid et al., 2020). The limited overlap could be explained by differences in cellular composition of assessed tissues, different array types used to measure DNAm, or due to the time of sampling. Cord blood is collected at birth and so methylation changes at this time reflect fetal maturity and/or prenatal experience, whereas the methylation signature at term equivalent age reflects the allostatic load of early postnatal experiences as well as the prenatal environment. We chose to sample at term equivalent age because postnatal co-morbidities of preterm birth and NICU care practices such as painful stress exposures alter DNAm profiles, and because cumulative

DNAm variations over this time period may link exposure to behavioural outcome in preterm infants (Everson et al., 2019; Fontana et al., 2021; Provenzi et al., 2018).

Functional analyses of DMPs identified two enriched gene ontology terms, for adherens and anchoring junctions. When distinct probes that contributed to both DMPs and DMRs were combined, gene ontology analysis identified an additional 14 terms related to cell-cell adhesion, cell adhesions with the extracellular matrix, and signalling from the extracellular membrane; 12 of these were also identified in the meta-analysis of gestational age effects on DNAm obtained at birth from umbilical cord blood (Merid et al., 2020). The most significant DMR mapped to a site encoding two genes including *NNAT*, which encodes the neural fate initiator neuronatin, the expression of which decreases throughout development (Lin et al., 2010); there was a positive association with increasing gestational age at birth. Hypomethylation of *NNAT* is associated with a corresponding increase in expression of neuronatin (Numata et al., 2012). Furthermore, the candidacy of *NNAT* as a gene of interest whose expression may be modified by perinatal exposures is supported by previous EWAS of gestational age, maternal body mass index, maternal smoking, and schizophrenia (Battram et al., 2021; Bohlin et al., 2016; Hannon et al., 2019, 2016; Sharp et al., 2017, 2015; Spiers et al., 2015).

Probes that demonstrated the largest magnitude of effect in association with gestational age mapped to genes previously associated with gestational age or maternal risk factors in EWAS (Battram et al., 2021). Hypermethylated genes include: *ZBP1,* which was identified in EWAS investigating gestational age and hypertensive disorders of pregnancy (Bohlin et al., 2016; Hannon et al., 2019; Kazmi et al., 2019); *INTS1,* which has been identified in EWAS of gestational age, hypertensive disorders of pregnancy, maternal body-mass-index, birth weight and breastfeeding duration (Bohlin et al., 2016; Kazmi et al., 2019; Küpers et al., 2019; Odintsova et al., 2019; Sharp et al., 2015;

Spiers et al., 2015). Hypomethylated genes included: *UBXN11,* which was identified in studies of gestational age (Bohlin et al., 2016; Spiers et al., 2015); and *IRX4.* Three of the ten most significant DMPs mapped to the *IRX4* gene, all of which displayed a negative association with gestational age at birth. *IRX4* is associated with cardiac development in vertebrates, including humans (Bruneau et al., 2000). Its homologues have been implicated in retinal axon guidance in zebrafish, and neural patterning in *Xenopus,* and it has been identified in previous EWAS of hypertensive disorders of pregnancy and prenatal maternal stress (Garriock et al., 2001; Jin et al., 2003; Kazmi et al., 2019; Rijlaarsdam et al., 2016).

The novel pathways and genes implicated by EWAS studies of gestational age could provide a strong empirical basis for the selection of genes in targeted analyses in association with neuroimaging (Wheater et al., 2020). For example, one of the genes identified in our EWAS has been implicated in neurodevelopmental disorders; biallelic mutations in *INTS1* have been associated with a rare neurodevelopmental syndrome characterised by intellectual disability (Krall et al., 2019; Oegema et al., 2017; Zhang et al., 2020).

We used metrics of generalised white matter connectivity to assess relationships between DNAm and brain development because generalised dysconnectivity of structural networks is a hallmark of the preterm brain dysmaturation (Galdi et al., 2020; Telford et al., 2017; Volpe, 2009). PSNDI and PSMD were strongly associated with the first principal component of GA-dependent variation in DNAm, but PSFA was not. This suggests that variations in DNAm could contribute to the higher variability in water content and intra-axonal volume that characterise preterm brain dysmaturation (Blesa et al., 2020). We have previously reported that differential DNAm is associated with FA of the genu of the corpus callosum and tract shape of the right corticospinal tract (Sparrow et al., 2016); it is most likely that we did not observe an association between neither GA nor DNAm with PSFA because

this metric is subject to histogram shift, meaning that although there are groupwise differences in FA values across the skeleton, the spread of values is the same (Blesa et al., 2020). Associations between GA at birth and both DNAm and image markers of dysconnectivity, and between DNAm and image features, suggest that differential DNAm may contribute, in part, to the relationship between GA and brain network dysconnectivity in preterm infants.

Strengths of this study are that we studied a population of preterm and control infants across the gestational age range of 23 to 42 weeks, who were uniquely phenotyped with DNAm and dMRI. We sampled after the period of NICU care in order to capture the allostatic load of preterm birth. We measured DNAm from neonatal saliva samples, which has consistency with brain DNAm patterns and is non-invasive. The Illumina EPIC platform provided extensive coverage of the methylome (850,000 sites) and we controlled for cell composition. Finally, we used an image phenotype that is robust to scanner variation (Baykara et al., 2016). There are some limitations. First, control for cell composition was based on estimation of cell proportions rather than measurement, so we cannot rule out the possibility that some of the signal identified was related to variation in cell composition. Second, mediation analysis to assess causation was not possible because the association between the DNAm PC1 and PS metrics might result from the DNAm PC being derived from CpG sites that are associated with gestational age, so variance attributable to the mediating variable cannot be assumed. This could be addressed by out-of-sample validation, which will require other neonatal cohorts with both methylome and dMRI data. There was also some evidence of inflation of test statistics based on the genomic inflation factor. However, genomic inflation factor is thought to provide an overestimate of inflation and corrections based on it may be overly conservative (van Iterson et al., 2017). The value of the genomic inflation factor was also similar to those previously reported in neonatal cohorts (Merid et al., 2020). In addition, visual inspection of our results via Manhattan plots suggests that our finding,

of widespread differences in DNAm in relation to gestational age at birth, are in line with previous studies that have investigated this in cord blood and in fetal brain tissue (Merid et al., 2020; Spiers et al., 2015).

In conclusion, gestational age at birth is associated with profound and widely distributed perturbations to the neonatal saliva methylome at term equivalent age, which reflects the allostatic load of preterm birth itself and postnatal exposures during neonatal intensive care. Gene ontology terms related to cell-cell contacts were enriched, indicating that cell contacts and organisation are implicated in the phenotype. Associations between DNAm and PSMD and PSNDI suggest that variations in DNAm could contribute to white matter dysconnectivity commonly seen in preterm infants, and this analysis identified several genes and gene regions that could provide further insight into the molecular mechanisms by which early exposure to extrauterine life influences neurodevelopment.

Chapter Conclusion

This study has demonstrated widespread differential DNAm in association with gestational age in neonatal saliva samples at term equivalent age, and that this DNAm signature is associated with PSNDI and PSMD from MRI at the same time point. It was not associated with PSFA. Differential DNAm was observed at sites mapping to genes that have previously been implicated in heart development, neuronal development, and in EWAS of gestational age, and hypertensive disorders of pregnancy.

Chapter 5. Discussion

5.1 Summary of findings

In this thesis I have investigated life-course effects of early life factors on brain structure and the methylome. Previous work has demonstrated that early life events, such as fetal growth, exert an effect on brain health and structure throughout life. However, whether the effect of birth weight on brain structure in later life has its origins in development, or in alterations to age-related trajectories, is less clear – to which the work presented in Chapter 2 contributes novel insights. Further, while epigenetic processes are known to play a role in neurodevelopment, and DNAm dysregulation plays a role in neurodevelopmental disease – Chapter 3 offers a comprehensive overview of the extent to which DNAm and MRI findings associate across the life-course. Finally, while early life adversity, indexed by gestational age at birth, is associated with widespread differential DNAm in cord blood, the generalisability of this finding to other neonatal tissues which would enable longitudinal, non-invasive sampling is unknown, as is its association with white matter microstructure. The work in Chapter 4 addresses these uncertainties. Below, I summarise the main findings from these chapters.

5.1.1 Summary of Chapter 2

In Chapter 2, I tested the hypothesis that birth weight is associated with white matter microstructure and brain volumes in late life to further build on the knowledge of how birth weight exerts and effect on brain structure in later life. I found no evidence of an association between birth weight and global metrics of white matter microstructure such as gFA, or PSMD. I found that there was a positive association between birth weight and brain volumes (total brain, grey matter, white matter volumes), but there was no significant association with white matter hyperintensities. This finding was in line with previous work. Birth weight was not associated with brain volumetric

measures when controlling for ICV (a proxy for maximal brain size) which shows that in this cohort, birth weight was not associated with atrophy. Atrophy, white matter hyperintensities, and white matter microstructure are metrics that are associated with age and ageing; these results indicate that birth weight was not associated with a greater propensity towards age-associated alterations to brain structure. Cortical surface area was associated with birth weight in a pattern that was strikingly similar to that previously observed in adolescents and young adults, indicating that this relationship is established early in life and remains in aging. The regional distribution of effect may reflect a scaling phenomenon whereby regional surface areas scale differently as a function of overall brain size (Reardon et al., 2018). Results presented in Chapter 2 support this explanation, as the pattern of regional associations between cortical surface area and birth weight were attenuated when controlling for ICV – a measure of maximal brain size. Overall, these results suggest that birth weight is associated with brain structure in late life, and that this is established in early life, but is not associated with age-related changes to brain structure, indexed by white matter microstructure, white matter hyperintensities, and atrophy. This chapter provides evidence for an association with brain reserve (given, for example, the modest but robust association with brain size and cognitive functioning in adulthood) with a developmental origin, but not necessarily resilience to age-associated changes.

5.1.2 Summary of Chapter 3

In Chapter 3, I tested the hypothesis that DNAm is associated with brain imaging in health and disease contexts across the life-course. I identified 60 studies that had reported on DNAm and MR neuroimaging associations. These had been studied in a range of contexts, including neurodevelopment and neurodevelopmental disorders, major depression and suicidality, alcohol use disorder, schizophrenia and psychosis, ageing and degenerative and age-associated disorders, post-traumatic stress disorder, and socio-emotional processing in healthy participants. It incorporated structural,

diffusion, and both resting-state fMRI and task-based fMRI. The main finding of this chapter was that while there is modest evidence that DNAm and MR neuroimaging are associated across the life-course, this emerging field exhibits a great deal of methodological heterogeneity. This limited the value of a quantitative synthesis, and so a narrative synthesis was performed. Sources of this heterogeneity included: candidate gene and epigenome-wide approaches to measuring DNAm and subsequent analysis with brain imaging features; a wide range of candidate genes selected limiting the biological rationale for a quantitative synthesis; epigenome-wide feature selection; MRI modality and/or construct tested in association with DNAm. Narrative synthesis of the findings was categorised into phenotypic context, such as health/disease or developmental stage, and I further provided a synthesis of the more consistent DNAm-MRI associations tested. These were: associations between *SLC6A4* gene methylation and amygdala reactivity assessed using both resting-state and task-based fMRI; *OXTR* DNAm and amygdala reactivity in task-based fMRI; *BDNF* methylation and prefrontal cortex connectivity in task-based fMRI; *COMT* DNAm and prefrontal cortex reactivity during task-based fMRI; *FKBP5* DNAm and hippocampal volume. However, even within these relatively consistent studies, there remained insufficient similarity to enable a quantitative synthesis. In addition to the high degree of heterogeneity in the field, several sources of bias were identified. These included a lack of control for cell composition in statistical analysis, and lack of control for genetics. Overall, this study demonstrated that there is a growing body of evidence supporting modest DNAm-MRI associations in a range of health and disease contexts across the life-course.

5.1.3 Summary of Chapter 4

In Chapter 4, I tested the hypothesis that gestational age at birth is associated with differential methylation in the neonatal period and that this differential methylation associates with neonatal MR neuroimaging measures of white matter microstructure. I conducted an EWAS which showed that DNAm is profoundly altered in association with variation in gestational age in

neonatal term equivalent saliva samples. This corresponds with previous observations in other tissues such as cord blood and fetal brain, which likewise demonstrated widespread differential DNAm. However, saliva provides opportunities for non-invasive, longitudinal sampling. As well as identifying DMPs, I also identified many DMRs that were likewise distributed across the genome. The largest of the DMRs mapped to a genomic region that encodes the *NNAT* gene – a neural fate initiator. Gene sets related to actin cytoskeleton organisation and cell adhesions (to other cells of extracellular matrix) were enriched. These are processes that are fundamental to development, and not specific to individual organ systems. These findings demonstrate that genes related to neurodevelopment are differentially methylated in association with gestational age at birth, but also that genes and processes that are involved in the development of many organ systems are affected. A measure of the variance in DMPs was associated with white matter connectivity in the neonatal period, indicating that DNAm contributes, in part, to the relationship between GA and brain network dysconnectivity in preterm infants.

5.2 Interpretations and future work

5.2.1 Widespread differential methylation in the neonatal period

Differential DNAm identified through EWAS in early life in response to exposures such as birth weight and gestational age variation fetal alcohol disorder are consistently widespread across the genome (Bohlin et al., 2016; Hannon et al., 2019; Küpers et al., 2019; Merid et al., 2020; Portales-Casamar et al., 2016; Spiers et al., 2015). Although the differential DNAm observed in the study detailed in Chapter 4 likewise demonstrates a genome-wide effect in association with gestational age, important differences remain between this result and previous findings in cord blood. While cord blood DNAm provides a measure of time at birth, DNAm obtained at term equivalent age may encompass both the maturational stage at the time of birth, but also the allostatic load of a gamut of post-natal experiences such as

stressful or painful NICU exposures, nutrition, sepsis, or inflammation. These factors contribute to the brain dysmaturation phenotype observed following preterm birth (Blesa et al., 2019; Duerden et al., 2018; J. Schneider et al., 2018; Shah et al., 2008; Sullivan et al., 2020). DNAm may link these experiences to outcomes associated with preterm birth. For example, differential DNAm at the *SLC6A4* gene in association with NICU-stress has been linked to early outcomes in preterm infants, independently of gestational age at birth (Montirosso et al., 2016; Montirosso and Provenzi, 2015; Provenzi et al., 2015). Longitudinal observational studies designs, such as TEBC would be well placed to investigate these questions. The cross-sectional study reported in Chapter 4 of this thesis cannot readily distinguish between these two sources of variation. However, large sample sizes and longitudinal sampling (which is possible with a tissue such as saliva, but not with cord blood) would enable this line of enquiry.

The widespread nature differential DNAm is likely to reflect the profound effect that gestational age has on development, but this multidimensional finding also poses challenges for interpretation and subsequent downstream analysis with outcomes of interest such as MR neuroimaging phenotype. In Chapter 4, I carried out PCA to reduce the dimensionality of the data. This has the advantage of providing one measure of genome-wide differential DNAm to test for associations with measures of white matter microstructure. In Chapter 3, there were several other approaches taken with genome-wide data to test for associations with MRI. Five of the 17 studies that performed EWAS tested for associations with DNAm age (Chouliaras et al., 2018; Davis et al., 2017; Hannum et al., 2013; Hodgson et al., 2017; Horvath, 2013; Raina et al., 2017; Wolf et al., 2016). The feature of interest in these studies was epigenetic age acceleration – the residual values from the regression of predicted age onto chronological age. Despite many published associations between age acceleration and clinical outcomes of interest, including death, the biological mechanisms underlying it are not well understood. Further, as the accuracy of DNAm age predictors improve (i.e. correctly predict

chronological age), and by definition reducing residuals, this finding suggests that the phenomenon of DNAm age acceleration may simply be a result of prediction error, or confounding (Zhang et al., 2019).

EWAS and DMR analysis may play an important role in the identification of novel candidate genes and pathways, that would aid mechanistic insight into the brain's vulnerability and resilience to adverse environmental stimuli. Using EWAS as an empirical basis for candidate gene selection was employed by two studies identified in Chapter 3, (Ruggeri et al., 2015; Sadeh et al., 2016). For example, the *NNAT* gene, which was a DMR in the analysis presented in Chapter 4, is a neurodevelopmental gene that is implicated in a developmental/neurodegenerative disease (Lafora disease) where dysregulated gene expression is a key feature.
This study fits into a growing body of literature investigating early life stressors and DNAm-MRI associations. I identified several studies in Chapter 3 that explicitly investigated forms of early life stress, such as birth weight discordance in twins, preterm birth, and childhood stress, in relation to DNAm-MRI associations (Casey et al., 2017; Harms et al., 2017; Sparrow et al., 2016).

As the number of EWAS, investigating a variety of early life exposures, increases, findings from these studies can be triangulated to identify likely genes and pathways that are consistently dysregulated and may lead to the discovery of core processes that ultimately give rise to the lifelong vulnerability to poor health outcomes observed in relation to early life stress. DMR analysis described in chapter 4 identified a DMR associated with gestational age at birth which mapped to the *CASZ1* gene, which is involved in vascular assembly and blood pressure variation (Charpentier et al., 2013). EWAS of birth weight from participants in the UK Biobank identified several CpG sites associated with the *CASZ1* gene in adult blood samples (Madden et al., 2020). There is also evidence that DNAm, measured from adolescent saliva samples, of this gene may mediate the relationship between birth

weight discordance, in monozygotic twins, and discordance in cortical surface area (Casey et al., 2017). Improving the interpretability of findings in this way may contribute to mechanistic insights that ultimately enable evidence-based interventions.

A challenge for future research is the selection of interpretable DNAm variables that also reflect the underlying biology, to aid casual inference about the effect of exposures on neuroimaging or neurodevelopmental outcomes. EWAS studies such as that conducted in Chapter 4 and those identified in Chapter 3 may provide an empirical rationale for the selection of candidate genes which, in combination with a theoretical justification based on experimental work linking a gene with a certain process, should improve causal inference, and the efficiency of targets discovery for intervention to alleviate the neurodevelopmental costs of early life adversity.

5.2.3 White matter associations in older age

In this thesis I tested the hypothesis that birth weight is associated with generalised metrics of global white matter microstructure in late life. The rationale behind this hypothesis was that white matter microstructure is well established to be altered in the neonatal period in association with birth weight and gestational age, and in adults aged ~78 years, frontal FA was associated with birth weight (Shenkin et al., 2009a). However, global measures of white matter microstructure (gFA and PSMD) in the LBC1936 (detailed in Chapter 2) demonstrated no significant association with birth weight. There are several potential explanations for this observation. Any association with global white matter microstructure with birth factors may be obscured by ageing related effects differentially affecting specific tracts (Cox et al., 2016). It is possible that alterations in white matter microstructure in the neonatal period associated with birth weight or gestational age resolve in adulthood, such that they are no longer observable in later life. This may, in part, be due to the proportion of variance contributable to birth weight reducing as a myriad of life-course influences, including age, begin to explain

more of the variance. However, as preterm and low birth weight cohorts survive into adulthood there is mounting evidence that altered white matter microstructure in association with preterm birth and very low birth weight extends into adulthood (Allin et al., 2011; Eikenes et al., 2011; Menegaux et al., 2020).

It is likely that this finding reflects survivor bias in our older age cohort and the largely normal birth weight range represented. A systematic review and meta-analysis that investigated associations between very low birth weight (< 1500 g) and brain structure did not identify studies on cohorts in later life, suggesting that to date, survivor bias is a major limitation of this area of investigation (Farajdokht et al., 2017). This would suggest that within the normal birth weight range there is no impact on white matter microstructure, despite an association with white matter volume. This explanation is compatible with the observation that variation encompassing very low birth weight is associated with white matter microstructure alterations into adulthood. Further work in cohorts that are less effected by survivor bias would need to be performed to confirm that this finding is applicable across the whole range of birth weights.

Future studies into the impact of perinatal factors on brain structure into later life will benefit from perinatal data collection in recent decades. In addition, the widespread use of ultrasound to accurately measure gestational age may be used in combination with birth weight data to isolate the effects of maturation at time of birth, from those of intrauterine growth restriction indexed by being small for gestational age. The improved survival of those born preterm and with low birth weight will enable researchers to establish whether the finding that white matter microstructure and age associated brain structural changes are not associated with birth weight within the normal range, is also observed in birth weight variation outside the normal range in late-life cohorts.

5.3 Strengths & Limitations

In this thesis, I have used a cohort with accurate historical birth weight data, recorded at hospital births, in combination with multimodal MR neuroimaging to provide novel insights into the associations between birth weight and brain structure and connectivity in later life. This work has contributed novel insight relevant to the development origins theory of origins of brain ageing, by supporting a development origin of preserved differentiation in brain volumes and cortical surface area, rather than a differential preservation model.

By conducting a systematic review of DNAm-MRI associations I identified studies published between 2011-2018, which provides a detailed overview of associations across the life-course and encompassing multiple modalities of MRI and DNAm data. Neuroimaging-epigenetics is a relatively new field, and standards and conventions have not yet been established. By providing a comprehensive overview of the associations between DNAm and brain MRI across the life-course, sources of bias in the literature were identified and, as a result, informed recommendations for standards and conventions in imaging-epigenetics studies. These include controlling for cell type variation and genetics, and selection of MRI features that support pooled analyses.

I employed an unbiased approach to investigating the effects of gestational age on the neonatal methylome in saliva samples at term equivalent age, with extensive coverage using the Illumina EPIC microarray platform. Further, this sample was enriched for preterm infants, including those born extremely preterm (<28 weeks gestation). This work has contributed novel targets of interest for future studies and has further corroborated previous findings in other tissues.

Due to sample size limitations, I have not investigated sex-specific effects in this thesis. There is evidence that early life environment affects male and female neurodevelopmental outcomes and brain development differently (Carpenter et al., 2017; Johnson et al., 2015; Thompson et al., 2001). Sexual

dimorphism in DNAm may provide insight into the molecular underpinnings of sexually dimorphic risk and resilience (Boks et al., 2009; McCartney et al., 2019). Larger cohorts would enable sex-disaggregated analysis.

Environmental factors and also stochastic events contribute to variation in DNAm, but so does the underlying genetic sequence (Lancaster et al., 2018). In Chapter 3, I identified a lack of genetic control for studies involving DNAm features as a potential source of bias. DNAm variation in association with early life stress will best be understood within a genetic context, to parse the distinct contributions from the environment and genetics. This is a limitation also of the work presented in Chapter 4. Among the 8898 differentially methylated loci, identified by EWAS of gestational age on the neonatal methylome, were probes located at genes previously identified in a genome-wide association study of gestation duration and preterm birth (Zhang et al., 2017). This may indicate that EWAS is detecting differential methylation that has a genetic origin rather than being the result of environmental variation (Jia et al., 2019). Future work on DNAm data in the TEBC will benefit from genotyping, in order to distinguish between differential DNAm arising as a result of genetic variation, and that arising as a result of early life exposures.

The assumption that changes in DNAm result in alterations to gene regulation form the basis of the rationale for DNAm to be an interesting mechanism of study is. However, an important step towards demonstrating the functional significance of differential DNAm is to test this assumption through gene expression studies at both the mRNA level (applicable to genomic regions that are protein-encoding), as well as regulating RNAs such as long non-coding RNAs. Any future work should confirm that differential methylation is associated with a corresponding change in gene expression. Related to this, the methods described in this thesis to measure DNAm are all based on the bisulfite conversion of modified cytosine residues, and these methods cannot distinguish between two forms of modified cytosine: hydroxymethylcytosine (which is also abundant in humans) and

methylcytosine (Huang et al., 2010). These two cytosine modifications may regulate gene expression differently: methylation of cytosines within a gene promoter region is thought to reduce expression from that gene, while hydroxymethylation is thought to be an activator of expression (Jin et al., 2011; Williams et al., 2011). This limitation of the measurement methods for DNAm emphasises the need to confirm alterations to gene expression that may arise as a result of differential DNAm.

In Chapter 3 of this thesis, I demonstrated that all the studies identified that tested DNAm-MRI associations used surrogate tissues, that is, the DNAm signature studied was not measured from brain tissue, due to the invasive nature of tissue collection. Investigating brain DNAm from post-mortem or biopsy brain tissue may contribute to the understanding of concordance between surrogate tissue and the target tissue, and the representativeness of different surrogate tissues. Meta-analysis of DNAm data from neonatal cohorts might provide more accurate estimates of the concordance between tissue types, at different stages of development (Herzog et al., 2021). This would enable informed choice of surrogate tissue for the target organ, as well as aiding interpretability of findings. In addition, when selecting a candidate-gene based on data generated from EWAS or DMR analysis, investigation of expression patterns in the tissue of interest is warranted.

5.4 Conclusions

This thesis provides three original research studies that generated the following main findings:

- birth weight is associated with brain structure into late life, including brain tissue volumes and cortical surface area, but not on global white matter microstructure;
- DNAm and MRI neuroimaging are associated across the life-course and in a range of health and disease contexts;

- DNAm at term equivalent age is profoundly altered in association with variation in gestational age, and this variation in DNAm contributes to white matter connectivity in the neonatal period.

These results support early life as an important factor in future brain health, and that DNAm provides novel biological insight into the interaction between early life and brain structure and function, and thus facilitate novel therapeutic developments. Further, this thesis provides insights to guide future studies to expedite this process.

References

Abel, K.M., Wicks, S., Susser, E.S., Dalman, C., Pedersen, M.G., Mortensen, P.B., Webb, R.T., 2010. Birth Weight, Schizophrenia, and Adult Mental Disorder. Arch. Gen. Psychiatry 67, 923. https://doi.org/10.1001/archgenpsychiatry.2010.100

Ad-Dab'bagh, Y., Einarson, D., Lyttelton, O., Muehlboeck, J.-S., Mok, K., Ivanov, O., Vincent, R.D., Lepage, C., Lerch, J., Fombonne, E., Evans, A.C., 2006. The CIVET image-processing environment: a fully automated comprehensive pipeline for anatomical neuroimaging research. Proc. 12th Annu. Meet. Organ. Hum. Brain Mapp.

Agrawal, S., Rao, S.C., Bulsara, M.K., Patole, S.K., 2018. Prevalence of autism spectrum disorder in preterm infants: A meta-Analysis. Pediatrics 142. https://doi.org/10.1542/peds.2018-0134

Alexander, B., Kelly, C.E., Adamson, C., Beare, R., Zannino, D., Chen, J., Murray, A.L., Yen, W., Matthews, L.G., War, S.K., Anderson, P.J., Doyle, L.W., Seal, M.L., Spittle, A.J., Cheong, J.L.Y., Thompson, D.K., 2019. Changes in neonatal regional brain volume associated with preterm birth and perinatal factors 185, 654–663. https://doi.org/10.1016/j.neuroimage.2018.07.021

Allin, M.P.G., Kontis, D., Walshe, M., Wyatt, J., Barker, G.J., Kanaan, R.A.A., McGuire, P., Rifkin, L., Murray, R.M., Nosarti, C., 2011. White matter and cognition in adults who were born preterm. PLoS One 6, 1–9. https://doi.org/10.1371/journal.pone.0024525

Alloza, C., Cox, S.R., Duff, B., Semple, S.I., Bastin, M.E., Whalley, H.C., Lawrie, S.M., 2016. Information processing speed mediates the relationship between white matter and general intelligence in schizophrenia. Psychiatry Res. - Neuroimaging 254, 26–33. https://doi.org/10.1016/j.pscychresns.2016.05.008

Anblagan, D., Bastin, M.E., Sparrow, S., Piyasena, C., Pataky, R., Moore, E.J., Serag, A., Wilkinson, A.G., Clayden, J.D., Semple, S.I., Boardman, J.P., 2015. Tract shape modeling detects changes associated with preterm birth and neuroprotective treatment effects. NeuroImage Clin. 8, 51–58. https://doi.org/10.1016/j.nicl.2015.03.021

Andersson, J.L.R., Graham, M.S., Drobnjak, I., Zhang, H., Filippini, N., Bastiani, M., 2017. Towards a comprehensive framework for movement and distortion correction of diffusion MR images: Within volume movement. Neuroimage 152, 450–466. https://doi.org/10.1016/j.neuroimage.2017.02.085

Andersson, J.L.R., Graham, M.S., Zsoldos, E., Sotiropoulos, S.N., 2016. Incorporating outlier detection and replacement into a non-parametric framework for movement and distortion correction of diffusion MR images. Neuroimage 141, 556–572. https://doi.org/10.1016/j.neuroimage.2016.06.058

Andersson, J.L.R., Sotiropoulos, S.N., 2016. An integrated approach to correction for off-resonance effects and subject movement in diffusion MR

imaging. Neuroimage 125, 1063–1078. https://doi.org/10.1016/j.neuroimage.2015.10.019

Anjari, M., Srinivasan, L., Allsop, J.M., Hajnal, J. V., Rutherford, M.A., Edwards, A.D., Counsell, S.J., 2007. Diffusion tensor imaging with tract-based spatial statistics reveals local white matter abnormalities in preterm infants. Neuroimage 35, 1021–1027. https://doi.org/10.1016/j.neuroimage.2007.01.035

Armstrong, D.A., Lesseur, C., Conradt, E., Lester, B.M., Marsit, C.J., 2014. Global and gene-specific DNA methylation across multiple tissues in early infancy: Implications for children's health research. FASEB J. 28, 2088–2097. https://doi.org/10.1096/fj.13-238402

Arvanitakis, Z., Fleischman, D.A., Arfanakis, K., Leurgans, S.E., Barnes, L.L., Bennett, D.A., 2016. Association of white matter hyperintensities and gray matter volume with cognition in older individuals without cognitive impairment. Brain Struct. Funct. 221, 2135–2146. https://doi.org/10.1007/s00429-015-1034-7

Aryee, M.J., Jaffe, A.E., Corrada-Bravo, H., Ladd-Acosta, C., Feinberg, A.P., Hansen, K.D., Irizarry, R.A., 2014. Minfi: A flexible and comprehensive Bioconductor package for the analysis of Infinium DNA methylation microarrays. Bioinformatics 30, 1363–1369. https://doi.org/10.1093/bioinformatics/btu049

Au, R., Massaro, J.M., Wolf, P.A., Young, M.E., Beiser, A., Seshadri, S., D'Agostino, R.B., DeCarli, C., 2006. Association of white matter hyperintensity volume with decreased cognitive functioning: The Framingham Heart Study. Arch. Neurol. 63, 246–250. https://doi.org/10.1001/archneur.63.2.246

Back, S.A., Miller, S.P., 2014. Brain injury in premature neonates: A primary cerebral dysmaturation disorder? Ann. Neurol. 75, 469–486. https://doi.org/10.1002/ana.24132

Backhouse, E. V., McHutchison, C.A., Cvoro, V., Shenkin, S.D., Wardlaw, J.M., 2015. Early Life Risk Factors for Stroke and Cognitive Impairment. Curr. Epidemiol. Reports 172–179. https://doi.org/10.1007/s40471-015-0051-7

Ball, G., Pazderova, L., Chew, A., Tusor, N., Merchant, N., Arichi, T., Allsop, J.M., Cowan, F.M., Edwards, A.D., Counsell, S.J., 2015. Thalamocortical connectivity predicts cognition in children born preterm. Cereb. Cortex 25, 4310–4318. https://doi.org/10.1093/cercor/bhu331

Barker, D.J.P., 2004. The Developmental Origins of Adult Disease. J. Am. Coll. Nutr. 23, 588S-595S. https://doi.org/10.1080/07315724.2004.10719428

Barker, D.J.P., Osmond, C., 1986. Infant Mortality, Childhood Nutrition, and Ischaemic Heart Disease in England and Wales. Lancet 327, 1077–1081. https://doi.org/10.1016/S0140-6736(86)91340-1

Bastin, M.E., Munoz Maniega, S., Ferguson, K.J., Brown, L.J., Wardlaw, J.M., MacLullich, A.M., Clayden, J.D., 2010. Quantifying the effects of normal ageing on white matter structure using unsupervised tract shape modelling. Neuroimage 51, 1–10. https://doi.org/10.1016/j.neuroimage.2010.02.036

Batalle, D., Muircheartaigh, J.O., Makropoulos, A., Kelly, C.J., Dimitrova, R., Hughes, E.J., Hajnal, J. V, Zhang, H., Alexander, D.C., Edwards, A.D., Counsell,

S.J., 2019. Different patterns of cortical maturation before and after 38 weeks gestational age demonstrated by diffusion MRI in vivo. Neuroimage 185, 764–775. https://doi.org/10.1016/j.neuroimage.2018.05.046

Battram, T., Yousefi, P., Crawford, G., Prince, C., Babaei, M.S., Sharp, G., Hatcher, C., Vega-salas, M.J., Khodabakhsh, S., Whitehurst, O., Langdon, R., Ma-, L., Gaunt, T.R., Relton, C.L., Staley, J.R., Suderman, M., 2021. The EWAS Catalog: a database of epigenome-wide association studies. OSF Prepr. 2–5.

Baykara, E., Gesierich, B., Adam, R., Tuladhar, A.M., Biesbroek, J.M., Koek, H.L., Ropele, S., Jouvent, E., Chabriat, H., Ertl-Wagner, B., Ewers, M., Schmidt, R., de Leeuw, F.E., Biessels, G.J., Dichgans, M., Duering, M., 2016. A Novel Imaging Marker for Small Vessel Disease Based on Skeletonization of White Matter Tracts and Diffusion Histograms. Ann. Neurol. 80, 581–592. https://doi.org/10.1002/ana.24758

Belbasis, L., Savvidou, M.D., Kanu, C., Evangelou, E., Tzoulaki, I., 2016. Birth weight in relation to health and disease in later life: An umbrella review of systematic reviews and meta-analyses. BMC Med. 14. https://doi.org/10.1186/s12916-016-0692-5

Benjamini, Y., Hochberg, Y., 2007. Controlling the False Discovery Rate : A Practical and Powerful Approach to Multiple Testing. J. R. Stat. Soc. Ser. B (Statistical Methodol. 57, 289–300.

Bidwell, L.C., Karoly, H.C., Thayer, R.E., Claus, E.D., Bryan, A.D., Weiland, B.J., Yorkwilliams, S., Hutchison, K.E., 2018. DRD2 promoter methylation and measures of alcohol reward : functional activation of reward circuits and clinical severity. Addict. Biol. 24, 539–548. https://doi.org/10.1111/adb.12614

Bird, A., 2007. Perceptions of epigenetics. Nature 447, 396–398. https://doi.org/10.1038/nature05913

Bjuland, K.J., Løhaugen, G.C.C., Martinussen, M., Skranes, J., 2013. Cortical thickness and cognition in very-low-birth-weight late teenagers. Early Hum. Dev. 89, 371–380. https://doi.org/10.1016/j.earlhumdev.2012.12.003

Blatter, D.D., Bigler, E.D., Gale, S.D., Johnson, S.C., Anderson, C. V., Burnett, B.M., Parker, N., Kurth, S., Horn, S.D., 1995. Quantitative volumetric analysis of brain MR: Normative database spanning 5 decades of life. Am. J. Neuroradiol. 16, 241–251.

Blesa, M., Sullivan, G., Anblagan, D., Telford, E.J., Quigley, A.J., Sparrow, S.A., Serag, A., Semple, S.I., Bastin, M.E., Boardman, J.P., 2019. Early breast milk exposure modifies brain connectivity in preterm infants. Neuroimage 184, 431–439. https://doi.org/10.1016/j.neuroimage.2018.09.045

Blesa, M., Galdi, P., Sullivan, G., Wheater, E.N., 2020. Peak width of skeletonized water diffusion MRI in the neonatal brain. Front. Neurol. https://doi.org/10.3389/fneur.2020.00235/abstract

Boardman, J.P., Counsell, S.J., 2020. Factors associated with atypical brain development in preterm infants: insights from magnetic resonance imaging. Neuropathol. Appl. Neurobiol. 46, 413–421. https://doi.org/10.1111/nan.12589

Boardman, J.P., Craven, C., Valappil, S., Counsell, S.J., Dyet, L.E., Rueckert, D., Aljabar, P., Rutherford, M.A., Chew, A.T.M., Allsop, J.M., Cowan, F., Edwards, A.D., 2010. A common neonatal image phenotype predicts adverse neurodevelopmental outcome in children born preterm. Neuroimage 52, 409–414. https://doi.org/10.1016/j.neuroimage.2010.04.261

Boardman, J.P., Hall, J., Thrippleton, M.J., Reynolds, R.M., Bogaert, D., Davidson, D.J., Schwarze, J., Drake, A.J., Chandran, S., Bastin, M.E., Fletcher-Watson, S., 2020. Impact of preterm birth on brain development and long-term outcome: Protocol for a cohort study in Scotland. BMJ Open 10, 1–11. https://doi.org/10.1136/bmjopen-2019-035854

Bohlin, J., Håberg, S.E., Magnus, P., Reese, S.E., Gjessing, H.K., Magnus, M.C., Parr, C.L., Page, C.M., London, S.J., Nystad, W., 2016. Prediction of gestational age based on genome-wide differentially methylated regions. Genome Biol. 17, 1–9. https://doi.org/10.1186/s13059-016-1063-4

Boks, M.P., Derks, E.M., Weisenberger, D.J., Strengman, E., Janson, E., Sommer, I.E., Kahn, R.S., Ophoff, R.A., 2009. The relationship of DNA methylation with age, gender and genotype in twins and healthy controls. PLoS One 4, 21–23. https://doi.org/10.1371/journal.pone.0006767

Booij, L., Szyf, M., Carballedo, A., Frey, E., Morris, D., Dymov, S., Vaisheva, F., Ly, V., Fahey, C., Meaney, J., Gill, M., Frodl, T., 2015. DNA Methylation of the Serotonin Transporter Gene in Peripheral Cells and Stress-Related Changes in Hippocampal Volume: A Study in Depressed Patients and Healthy Controls. PLoS One 10, 1–14. https://doi.org/10.1371/journal.pone.0119061

Border, R., Johnson, E.C., Ph, D., Evans, L.M., Ph, D., Smolen, A., Ph, D., Berley, N., Sullivan, P.F., Keller, M.C., Ph, D., 2019. No Support for Historical Candidate Gene or Candidate Gene-by-Interaction Hypotheses for Major Depression Across Multiple Large Samples. Am. J. Psychiatry 176, 376–387. https://doi.org/10.1176/appi.ajp.2018.18070881

Bourne, V.J., Fox, H.C., Deary, I.J., Whalley, L.J., 2007. Does childhood intelligence predict variation in cognitive change in later life? Pers. Individ. Dif. 42, 1551–1559. https://doi.org/10.1016/j.paid.2006.10.030

Bouyssi-Kobar, M., Du Plessis, A.J., McCarter, R., Brossard-Racine, M., Murnick, J., Tinkleman, L., Robertson, R.L., Limperopoulos, C., 2016. Third Trimester Brain Growth in Preterm Infants Compared with in Utero Healthy Fetuses. Pediatrics 72, 145–146. https://doi.org/10.1097/01.ogx.0000513225.92648.a4

Braun, P.R., Han, S., Hing, B., Nagahama, Y., Gaul, L.N., Heinzman, J.T., Grossbach, A.J., Close, L., Dlouhy, B.J., Howard, M.A., Kawasaki, H., Potash, J.B., Shinozaki, G., 2019. Genome-wide DNA methylation comparison between live human brain and peripheral tissues within individuals. Transl. Psychiatry 9. https://doi.org/10.1038/s41398-019-0376-y

Breeman, L.D., Jaekel, J., Baumann, N., Bartmann, P., 2015. Preterm Cognitive Function Into Adulthood. Pediatrics 136. https://doi.org/10.1542/peds.2015-0608

Breeman, L.D., Jaekel, J., Baumann, N., Bartmann, P., Wolke, D., 2016. Attention problems in very preterm children from childhood to adulthood: the Bavarian Longitudinal Study 2, 132–140. https://doi.org/10.1111/jcpp.12456

Bruneau, B.G., Bao, Z.Z., Tanaka, M., Schott, J.J., Izumo, S., Cepko, C.L., Seidman, J.G., Seidman, C.E., 2000. Cardiac expression of the ventricle-specific homeobox gene Irx4 is modulated by Nkx2-5 and dHand. Dev. Biol. 217, 266–277. https://doi.org/10.1006/dbio.1999.9548

Burnett, A.C., Anderson, P.J., Cheong, J., Doyle, L.W., Davey, C.G., Wood, S.J., 2011. Prevalence of psychiatric diagnoses in preterm and full-term children, adolescents and young adults: A meta-analysis. Psychol. Med. 41, 2463–2474. https://doi.org/10.1017/S003329171100081X

Cao-Lei, L., Massart, R., Suderman, M.J., Machnes, Z., Elgbeili, G., Laplante, D.P., Szyf, M., King, S., 2014. DNA methylation signatures triggered by prenatal maternal stress exposure to a natural disaster: Project ice storm. PLoS One 9. https://doi.org/10.1371/journal.pone.0107653

Cao-Lei, L., Elgbeili, G., Massart, R., Laplante, D.P., Szyf, M., King, S., 2015. Pregnant women's cognitive appraisal of a natural disaster affects DNA methylation in their children 13 years later: Project Ice Storm. Transl. Psychiatry 5, e515-9. https://doi.org/10.1038/tp.2015.13

Carpenter, T., Grecian, S.M., Reynolds, R.M., 2017. Sex differences in early-life programming of the hypothalamic-pituitary-adrenal axis in humans suggest increased vulnerability in females: A systematic review. J. Dev. Orig. Health Dis. 8, 244–255. https://doi.org/10.1017/S204017441600074X

Caruyer, E., Lenglet, C., Sapiro, G., Deriche, R., 2013. Design of multishell sampling schemes with uniform coverage in diffusion MRI. Magn. Reson. Med. 69, 1534–1540. https://doi.org/10.1002/mrm.24736

Casey, K.F., Levesque, M.L., Szyf, M., Ismaylova, E., Verner, M.-P., Suderman, M., Vitaro, F., Brendgen, M., Dionne, G., Boivin, M., Tremblay, R.E., Booij, L., 2017. Birth Weight Discordance , DNA Methylation , and Cortical Morphology of Adolescent Monozygotic Twins. Hum. Brain Mapp. 38, 2037–2050. https://doi.org/10.1002/hbm.23503

Charpentier, M.S., Christine, K.S., Amin, N.M., Dorr, K.M., Kushner, E.J., Bautch, V.L., Taylor, J.M., Conlon, F.L., 2013. CASZ1 Promotes Vascular Assembly and Morphogenesis through the Direct Regulation of an EGFL7/RhoA-Mediated Pathway. Dev. Cell 25, 132–143. https://doi.org/10.1016/j.devcel.2013.03.003

Chawanpaiboon, S., Vogel, J.P., Moller, A.B., Lumbiganon, P., Petzold, M., Hogan, D., Landoulsi, S., Jampathong, N., Kongwattanakul, K., Laopaiboon, M., Lewis, C., Rattanakanokchai, S., Teng, D.N., Thinkhamrop, J., Watananirun, K., Zhang, J., Zhou, W., Gülmezoglu, A.M., 2019. Global, regional, and national estimates of levels of preterm birth in 2014: a systematic review and modelling analysis. Lancet Glob. Heal. 7, e37–e46. https://doi.org/10.1016/S2214-109X(18)30451-0

Chen, L.I., Pan, H., Tuan, A.N.H., Teh, L., MacIsaac, J.L., Mah, S.M., McEwen, L.M., Li, Y., Chen, H., Broekman, B.F.P., Buschdorf, J.P., Chong, Y.S., Kwek, K., Saw, S.M., Gluckman, P.D., Fortier, M. V., Rifkin-Graboi, A., Kobor, M.S., Qiu, A., Meaney, M.J., Holbrook, J.D., GUSTO Study Group, 2015. Brain-derived neurotrophic factor (BDNF) Val66Met polymorphism influences the association of the methylome with maternal anxiety and neonatal brain volumes. Dev. Psychopathol. 27, 137–150. https://doi.org/10.1017/S0954579414001357

Chen, Y.C., Sudre, G., Sharp, W., Donovan, F., Chandrasekharappa, S.C., Hansen, N., Elnitski, L., Shaw, P., 2018. Neuroanatomic, epigenetic and genetic differences in monozygotic twins discordant for attention deficit hyperactivity disorder. Mol. Psychiatry 23, 683–690. https://doi.org/10.1038/mp.2017.45

Choi, S., Han, K.-M., Won, E., Yoon, B.-J., Lee, M.-S., Ham, B.-J., 2015. Association of brain-derived neurotrophic factor DNA methylation and reduced white matter integrity in the anterior corona radiata in major depression. J. Affect. Disord. 172, 74–80. https://doi.org/10.1016/j.jad.2014.09.042

Chouliaras, L., Pishva, E., Haapakoski, R., Zsoldos, E., Mahmood, A., Filippini, N., Burrage, J., Mill, J., Kivima, M., Lunnon, K., Ebmeier, K.P., 2018. Peripheral DNA methylation, cognitive decline and brain aging: pilot findings from the Whitehall II imaging study. Epigenomics 10, 585–595. https://doi.org/10.2217/epi-2017-0132

Chow, J., Heard, E., 2009. X inactivation and the complexities of silencing a sex chromosome. Curr. Opin. Cell Biol. 21, 359–366. https://doi.org/10.1016/j.ceb.2009.04.012

Clayden, J.D., Bastin, M.E., Storkey, A.J., 2006. Improved segmentation reproducibility in group tractography using a quantitative tract similarity measure. Neuroimage 33, 482–492. https://doi.org/10.1016/j.neuroimage.2006.07.016

Clayden, J.D., Storkey, A.J., Bastin, M.E., 2007. A Probabilistic Model-Based Approach to Consistent White Matter Tract Segmentation. IEEE Trans. Med. Imaging 26, 1555–1561.

Clayden, J.D., Mu, S., Storkey, A.J., King, M.D., Bastin, M.E., Clark, C.A., 2011. TractoR : Magnetic Resonance Imaging and Tractography with R. J. Stat. Softw. 44, 1–18. https://doi.org/10.18637/jss.v044.i08

Counsell, S.J., Edwards, A.D., Chew, A.T.M., Anjari, M., Dyet, L.E., Srinivasan, L., Boardman, J.P., Allsop, J.M., Hajnal, J. V., Rutherford, M.A., Cowan, F.M., 2008. Specific relations between neurodevelopmental abilities and white matter microstructure in children born preterm. Brain 131, 3201–3208. https://doi.org/10.1093/brain/awn268

Cox, S.R., Ritchie, S.J., Tucker-drob, E.M., Liewald, D.C., Hagenaars, S.P., Davies, G., Wardlaw, J.M., Gale, C.R., Bastin, M.E., Deary, I.J., 2016. Ageing and brain white matter structure in 3,513 UK Biobank participants. Nat. Publ. Gr. 7, 13629. https://doi.org/10.1038/ncomms13629

Cox, S.R., Fawns-Ritchie, C., Tucker-Drob, E.M., Deary, I.J., 2019a. Brain imaging correlates of general intelligence in UK Biobank. Intelligence 76, 101376.

Cox, S.R., Lyall, D.M., Ritchie, S.J., Bastin, M.E., Harris, M.A., Buchanan, C.R., Fawns-Ritchie, C., Barbu, M.C., De Nooij, L., Reus, L.M., Alloza, C., Shen, X., Neilson, E., Alderson, H.L., Hunter, S., Liewald, D.C., Whalley, H.C., McIntosh, A.M., Lawrie, S.M., Pell, J.P., Tucker-Drob, E.M., Wardlaw, J.M., Gale, C.R., Deary, I.J., 2019b. Associations between vascular risk factors and brain MRI indices in UK Biobank. Eur. Heart J. 40, 2290–2299. https://doi.org/10.1093/eurheartj/ehz100

Cruickshank, M.N., Oshlack, A., Theda, C., Davis, P.G., Martino, D., Sheehan, P., Dai, Y., Saffery, R., Doyle, L.W., Craig, J.M., 2013. Analysis of epigenetic changes in survivors of preterm birth reveals the effect of gestational age and evidence for a long term legacy. Genome Med. 5. https://doi.org/10.1186/gm500

Dannlowski, U., Kugel, H., Redlich, R., Halik, A., Schneider, I., Opel, N., Grotegerd, D., Schwarte, K., Schettler, C., Ambree, O., Rust, S., Domschke, K., Arolt, V., Heindel, W., Baune, B.T., Suslow, T., Zhang, W., Hohoff, C., 2014. Serotonin transporter gene methylation is associated with hippocampal gray matter volume. Hum. Brain Mapp. 35, 5356–5367. https://doi.org/10.1002/hbm.22555

Davis, E.G., Humphreys, K.L., McEwen, L.M., Sacchet, M.D., Camacho, M.C., MacIsaac, J.L., Lin, D.T.S., Kobor, M.S., Gotlib, I.H., 2017. Accelerated DNA methylation age in adolescent girls: associations with elevated diurnal cortisol and reduced hippocampal volume. Transl. Psychiatry 7, e1223. https://doi.org/10.1038/tp.2017.188

de Bie, H.M.A., Oostrom, K.J., Boersma, M., Veltman, D.J., Barkhof, F., Delemarre-van de Waal, H.A., van den Heuvel, M.P., 2011. Global and regional differences in brain anatomy of young children born small for gestational age. PLoS One 6. https://doi.org/10.1371/journal.pone.0024116

De Rooij, S.R., Wouters, H., Yonker, J.E., Painter, R.C., Roseboom, T.J., 2010. Prenatal undernutrition and cognitive function in late adulthood. Proc. Natl. Acad. Sci. U. S. A. 107, 16881–16886. https://doi.org/10.1073/pnas.1009459107

De Rubeis, S., He, X., Goldberg, A.P., Poultney, C.S., Samocha, K., Cicek, A.E., Kou, Y., Liu, L., Fromer, M., Walker, S., Singh, T., Klei, L., Kosmicki, J., Shih-Chen, F., Aleksic, B., Biscaldi, M., Bolton, P.F., Brownfeld, J.M., Cai, J., Campbell, N.G., Carracedo, A., Chahrour, M.H., Chiocchetti, A.G., Coon, H., Crawford, E.L., Curran, S.R., Dawson, G., Duketis, E., Fernandez, B.A., Gallagher, L., Geller, E., Guter, S.J., Hill, R.S., Ionita-Laza, J., Jimenz Gonzalez, P., Kilpinen, H., Klauck, S.M., Kolevzon, A., Lee, I., Lei, I., Lei, J., Lehtimaki, T., Lin, C.F., Ma'ayan, A., Marshall, C.R., McInnes, A.L., Neale, B., Owen, M.J., Ozaki, N., Parellada, M., Parr, J.R., Purcell, S., Puura, K., Rajagopalan, D., Rehnstrom, K., Reichenberg, A., Sabo, A., Sachse, M., Sanders, S.J., Schafer, C., Schulte-Ruther, M., Skuse, D., Stevens, C., Szatmari, P., Tammimies, K., Valladares, O., Voran, A., Li-San, W., Weiss, L.A., Willsey, A.J., Yu, T.W., Yuen, R.K., Study, D.D.D., Homozygosity Mapping Collaborative for, A., Consortium, U.K., Cook, E.H., Freitag, C.M., Gill, M., Hultman, C.M., Lehner, T., Palotie, A., Schellenberg, G.D., Sklar, P., State, M.W., Sutcliffe, J.S., Walsh, C.A., Scherer,

S.W., Zwick, M.E., Barett, J.C., Cutler, D.J., Roeder, K., Devlin, B., Daly, M.J., Buxbaum, J.D., 2014. Synaptic, transcriptional and chromatin genes disrupted in autism. Nature 515, 209–215. https://doi.org/10.1038/nature13772

Deary, I.J., Gow, A.J., Taylor, M.D., Corley, J., Brett, C., Wilson, V., Campbell, H., Whalley, L.J., Visscher, P.M., Porteous, D.J., Starr, J.M., 2007. The Lothian Birth Cohort 1936 : a study to examine influences on cognitive ageing from age 11 to age 70 and beyond. BMC Geriatr. 12, 1–12. https://doi.org/10.1186/1471-2318-7-28

Deary, I.J., Ritchie, S.J., Muñoz Maniega, S., Cox, S.R., Valdés Hernández, M.C., Luciano, M., Starr, J.M., Wardlaw, J.M., Bastin, M.E., 2019. Brain Peak Width of Skeletonized Mean Diffusivity (PSMD) and Cognitive Function in Later Life. Front. Psychiatry 10, 1–10. https://doi.org/10.3389/fpsyt.2019.00524

Debette, S., Markus, H.S., 2010. The clinical importance of white matter hyperintensities on brain magnetic resonance imaging: Systematic review and meta-analysis. BMJ 341, 288. https://doi.org/10.1136/bmj.c3666

Debette, S., Seshadri, S., Beiser, A., Au, R., Himali, J.J., Palumbo, C., Wolf, P.A., DeCarli, C., 2011. Midlife vascular risk factor exposure accelerates structural brain aging and cognitive decline. Neurology 77, 461–468. https://doi.org/10.1212/WNL.0b013e318227b227

Dedeurwaerder, S., Defrance, M., Calonne, E., Denis, H., Sotiriou, C., Fuks, F., 2011. Evaluation of the Infinium Methylation 450K technology. Epigenomics 3, 771–784. https://doi.org/10.2217/epi.11.105

Dekhtyar, S., Wang, H.X., Scott, K., Goodman, A., Ilona, K., Herlitz, A., 2015. A life-course study of cognitive reserve in dementia - From childhood to old age. Am. J. Geriatr. Psychiatry 23, 885–896. https://doi.org/10.1016/j.jagp.2015.02.002

Del Blanco, B., Barco, A., 2018. Impact of environmental conditions and chemicals on the neuronal epigenome. Curr. Opin. Behav. Sci. 45, 157–165. https://doi.org/10.1016/j.cbpa.2018.06.003

Deng, S., Lin, D., Calhoun, V.D., Wang, Y., Member, S., 2016. Predicting Schizophrenia by Fusing Networks from SNPs , DNA Methylation and fMRI Data *. Conf. Proc. Annu. Int. Conf. IEEE Eng. Med. Biol. Soc. IEEE Eng. Med. Biol. Soc. Annu. Conf. 1447–1450. https://doi.org/10.1109/EMBC.2016.7590981

Duerden, E.G., Grunau, R.E., Guo, T., Foong, J., Pearson, A., Au-Young, S., Lavoie, R., Chakravarty, M.M., Chau, V., Synnes, A., Miller, S.P., 2018. Early procedural pain is associated with regionally-specific alterations in thalamic development in preterm neonates. J. Neurosci. 38, 878–886. https://doi.org/10.1523/JNEUROSCI.0867-17.2017

Eaton-Rosen, Z., Melbourne, A., Orasanu, E., Cardoso, M.J., Modat, M., Bainbridge, A., Kendall, G.S., Robertson, N.J., Marlow, N., Ourselin, S., 2015. Longitudinal measurement of the developing grey matter in preterm subjects using multi-modal MRI. Neuroimage 111, 580–589. https://doi.org/10.1016/j.neuroimage.2015.02.010

Eide, M.G., Øyen, N., Skjœrven, R., Nilsen, S.T., Bjerkedal, T., Tell, G.S., 2005. Size at birth and gestational age as predictors of adult height and weight. Epidemiology 16, 175–181. https://doi.org/10.1097/01.ede.0000152524.89074.bf

Eikenes, L., Løhaugen, G.C., Brubakk, A.M., Skranes, J., Håberg, A.K., 2011. Young adults born preterm with very low birth weight demonstrate widespread white matter alterations on brain DTI. Neuroimage 54, 1774–1785. https://doi.org/10.1016/j.neuroimage.2010.10.037

Elliott, L.T., Sharp, K., Alfaro-almagro, F., Shi, S., Miller, K.L., Douaud, G., Marchini, J., Smith, S.M., 2018. Genome-wide association studies of brain imaging phenotypes in UK Biobank. Nature 562, 210–216. https://doi.org/10.1038/s41586-018-0571-7

Engelhardt, E., Inder, T.E., Alexopoulos, D., Dierker, D.L., Hill, J., Essen, D. Van, Neil, J.J., 2014. Regional Impairments of Cortical Folding in Premature Infants. https://doi.org/10.1002/ana.24313

Eryigit Madzwamuse, S., Baumann, N., Jaekel, J., Bartmann, P., Wolke, D., 2015. Neuro-cognitive performance of very preterm or very low birth weight adults at 26 years. J. Child Psychol. Psychiatry Allied Discip. 56, 857–864. https://doi.org/10.1111/jcpp.12358

Everson, T.M., Marsit, C.J., Shea, T.M.O., Burt, A., Hermetz, K., Carter, B.S., Helderman, J., Hofheimer, J.A., Mcgowan, E.C., Neal, C.R., Pastyrnak, S.L., Smith, L.M., Soliman, A., 2019. Epigenome-wide Analysis Identifies Genes and Pathways Linked to Neurobehavioral Variation in Preterm Infants 1–13. https://doi.org/10.1038/s41598-019-42654-4

Everson, T.M., O'Shea, T.M., Burt, A., Hermetz, K., Carter, B.S., Helderman, J., Hofheimer, J.A., McGowan, E.C., Neal, C.R., Pastyrnak, S.L., Smith, L.M., Soliman, A., DellaGrotta, S.A., Dansereau, L.M., Padbury, J.F., Lester, B.M., Marsit, C.J., 2020. Serious neonatal morbidities are associated with differences in DNA methylation among very preterm infants. Clin. Epigenetics 12, 1–15. https://doi.org/10.1186/s13148-020-00942-1

Farajdokht, F., Sadigh-Eteghad, S., Dehghani, R., Mohaddes, G., Abedi, L., Bughchechi, R., Majdi, A., Mahmoudi, J., 2017. Very low birth weight is associated with brain structure abnormalities and cognitive function impairments: A systematic review. Brain Cogn. 118, 80–89. https://doi.org/10.1016/j.bandc.2017.07.006

Fatemi, S.H., Folsom, T.D., 2009. The Neurodevelopmental Hypothesis of Schizophrenia, Revisited. Schizophr. Bull. 35, 528–548. https://doi.org/10.1093/schbul/sbn187

Fischl, B., 2012. FreeSurfer. Neuroimage 62, 774–781. https://doi.org/10.1016/j.neuroimage.2012.01.021

Fontana, C., Marasca, F., Provitera, L., Mancinelli, S., Pesenti, N., Sinha, S., Passera, S., Abrignani, S., Mosca, F., Lodato, S., Bodega, B., Fumagalli, M., 2021. Early maternal care restores LINE-1 methylation and enhances neurodevelopment in preterm infants 1–16.

Franz, A.P., Bolat, G.U., Bolat, H., Matijasevich, A., Santo, I.S., Silveira, R.C., Procianoy, R.S., Rohde, L.A., Moreira-Maia, C.R., 2018. Attention-Deficit / Hyperactivity Disorder and Very Preterm / Very Low Birth Weight : A Meta-analysis. Pediatrics 141.

Fraser, H.B., Lam, L.L., Neumann, S.M., Kobor, M.S., 2012. Population-specificity of human DNA methylation. Genome Biol. 13. https://doi.org/10.1186/gb-2012-13-2-r8

Freytag, V., Carrillo-roa, T., Milnik, A., Samann, P.G., Vukojevic, V., Coynel, D., Demougin, P., Egli, T., Gschwind, L., Jessen, F., Loos, E., Maier, W., Riedel-heller, S.G., Scherer, M., Vogler, C., Wagner, M., Binder, E.B., Quervain, D.J. De, Papassotiropoulos, A., 2017. A peripheral epigenetic signature of immune system genes is linked to neocortical thickness and memory. Nat. Commun. 8. https://doi.org/10.1038/ncomms15193

Frodl, T., Szyf, M., Carballedo, A., Ly, V., Dymov, S., Vaisheva, F., Morris, D., Fahey, C., Meaney, J., Gill, M., Booij, L., 2015. DNA methylation of the serotonin transporter gene (SLC6A4) is associated with brain function involved in processing emotional stimuli. J. Psychiatry Neurosci. 40, 296–305. https://doi.org/10.1503/jpn.140180

Galdi, P., Blesa, M., Stoye, D.Q., Sullivan, G., Lamb, G.J., Quigley, A.J., Thrippleton, M.J., Bastin, M.E., Boardman, J.P., 2020. Neonatal morphometric similarity mapping for predicting brain age and characterizing neuroanatomic variation associated with preterm birth. NeuroImage Clin. 25, 102195. https://doi.org/10.1016/j.nicl.2020.102195

Gałecki, P., Talarowska, M., 2018. Neurodevelopmental theory of depression. Prog. Neuro-Psychopharmacology Biol. Psychiatry 80, 267–272. https://doi.org/10.1016/j.pnpbp.2017.05.023

Garriock, R.J., Vokes, S.A., Small, E.M., Larson, R., Krieg, P.A., 2001. Developmental expression of the Xenopus Iroquois-family homeobox genes, Irx4 and Irx5. Dev. Genes Evol. 211, 257–260. https://doi.org/10.1007/s004270100147

Geelhoed, J.J.M., Jaddoe, V.W.V., 2010. Early influences on cardiovascular and renal development. Eur. J. Epidemiol. 25, 677–692. https://doi.org/10.1007/s10654-010-9510-0

Genc, S., Malpas, C.B., Holland, S.K., Beare, R., Silk, T.J., 2017. Neurite density index is sensitive to age related differences in the developing brain. Neuroimage 148, 373–380. https://doi.org/10.1016/j.neuroimage.2017.01.023

Gluckman, P.D., Hanson, M.A., Buklijas, T., 2010. A conceptual framework for the developmental origins of health and disease. J. Dev. Orig. Health Dis. 1, 6–18. https://doi.org/10.1017/S2040174409990171

Gouin, J.P., Zhou, Q.Q., Booij, L., Boivin, M., Cote, S.M., Hebert, M., Ouellet-Morin, I., Szyf, M., Tremblay, R.E., Turecki, G., Vitaro, F., 2017. Associations among oxytocin receptor gene (OXTR) DNA methylation in

adulthood, exposure to early life adversity, and childhood trajectories of anxiousness. Sci. Rep. 7, 7446. https://doi.org/10.1038/s41598-017-07950-x

Gouw, A.A., Seewann, A., Van Der Flier, W.M., Barkhof, F., Rozemuller, A.M., Scheltens, P., Geurts, J.J.G., 2011. Heterogeneity of small vessel disease: A systematic review of MRI and histopathology correlations. J. Neurol. Neurosurg. Psychiatry 82, 126–135. https://doi.org/10.1136/jnnp.2009.204685

Gow, A.J., Johnson, W., Pattie, A., Brett, C.E., Roberts, B., Starr, J.M., Deary, I.J., 2011. Stability and Change in Intelligence From Age 11 to Ages 70, 79, and 87: The Lothian Birth Cohorts of 1921 and 1936. Psychol. Aging 26, 232–240. https://doi.org/10.1037/a0021072

Grayson, D.R., Guidotti, A., 2013. The dynamics of DNA methylation in schizophrenia and related psychiatric disorders. Neuropsychopharmacology 38, 138–166. https://doi.org/10.1038/npp.2012.125

Gregory, S.G., Connelly, J.J., Towers, A.J., Johnson, J., Biscocho, D., Markunas, C.A., Lintas, C., Abramson, R.K., Wright, H.H., Ellis, P., Langford, C.F., Worley, G., Delong, R., Murphy, S.K., Cuccaro, M.L., Persico, A., Pericak-Vance, M.A., 2009. Genomic and epigenetic evidence for oxytocin receptor deficiency in autism. BMC Med. 7. https://doi.org/10.1186/1741-7015-7-62

Grove, B.J., Lim, S.J., Gale, C.R., Shenkin, S.D., 2017. Birth weight and cognitive ability in adulthood: A systematic review and meta-analysis. Intelligence 61, 146–158. https://doi.org/10.1016/j.intell.2017.02.001

Guillaume, B., Wang, C., Poh, J., Shen, M.J., Ong, M.L., Tan, P.F., Karnani, N., Meaney, M., Qiu, A., 2018. Improving mass-univariate analysis of neuroimaging data by modelling important unknown covariates: Application to Epigenome-Wide Association Studies. Neuroimage 173, 57–71. https://doi.org/10.1016/j.neuroimage.2018.01.073

Haas, B.W., Filkowski, M.M., Cochran, R.N., Denison, L., Ishak, A., Nishitani, S., 2016. Epigenetic modification of OXT and human sociability. Proc. Natl. Acad. Sci. U. S. A. 113. https://doi.org/10.1073/pnas.1602809113

Hadaya, L., Nosarti, C., 2020. The neurobiological correlates of cognitive outcomes in adolescence and adulthood following very preterm birth. Semin. Fetal Neonatal Med. 25, 101117. https://doi.org/10.1016/j.siny.2020.101117

Hamilton, O.K.L., Zhang, Q., McRae, A.F., Walker, R.M., Morris, S.W., Redmond, P., Campbell, A., Murray, A.D., Porteous, D.J., Evans, K.L., McIntosh, A.M., Deary, I.J., Marioni, R.E., 2019. An epigenetic score for BMI based on DNA methylation correlates with poor physical health and major disease in the Lothian Birth Cohort. Int. J. Obes. 43, 1795–1802. https://doi.org/10.1038/s41366-018-0262-3

Han, K., Won, E., Sim, Y., Kang, J., Han, C., Kim, Y., Kim, S., Joe, S., Lee, M., Tae, W., Ham, B., 2017. Influence of FKBP5 polymorphism and DNA methylation on structural changes of the brain in major depressive disorder. Sci. Rep. 1–12. https://doi.org/10.1038/srep42621

Han, K.M., Won, E., Kang, J., Choi, S., Kim, A., Lee, M.S., Tae, W.S., Ham, B.J., 2017. TESC gene-regulating genetic variant (rs7294919) affects hippocampal subfield volumes and parahippocampal cingulum white matter integrity in major depressive disorder. J. Psychiatr. Res. 93, 20–29. https://doi.org/10.1016/j.jpsychires.2017.05.010

Hannon, E., Dempster, E., Viana, J., Burrage, J., Smith, A.R., Macdonald, R., St Clair, D., Mustard, C., Breen, G., Therman, S., Kaprio, J., Toulopoulou, T., Pol, H.E.H., Bohlken, M.M., Kahn, R.S., Nenadic, I., Hultman, C.M., Murray, R.M., Collier, D.A., Bass, N., Gurling, H., McQuillin, A., Schalkwyk, L., Mill, J., 2016. An integrated genetic-epigenetic analysis of schizophrenia: Evidence for co-localization of genetic associations and differential DNA methylation. Genome Biol. 17, 1–16. https://doi.org/10.1186/s13059-016-1041-x

Hannon, E., Schendel, D., Ladd-Acosta, C., Grove, J., Hansen, C.S., Hougaard, D.M., Bresnahan, M., Mors, O., Hollegaard, M.V., Bækvad-Hansen, M., Hornig, M., Mortensen, P.B., Børglum, A.D., Werge, T., Pedersen, M.G., Nordentoft, M., Buxbaum, J.D., Fallin, M.D., Bybjerg-Grauholm, J., Reichenberg, A., Mill, J., 2019. Variable DNA methylation in neonates mediates the association between prenatal smoking and birth weight. Philos. Trans. R. Soc. B Biol. Sci. 374. https://doi.org/10.1098/rstb.2018.0120

Hannum, G., Guinney, J., Zhao, L., Zhang, L., Hughes, G., Sadda, S.V., Klotzle, B., Bibikova, M., Fan, J.B., Gao, Y., Deconde, R., Chen, M., Rajapakse, I., Friend, S., Ideker, T., Zhang, K., 2013. Genome-wide Methylation Profiles Reveal Quantitative Views of Human Aging Rates. Mol. Cell Resour. 49, 359–367. https://doi.org/10.1016/j.molcel.2012.10.016

Harms, M.B., Birn, R., Provencal, N., Wiechmann, T., 2017. Early life stress , FK506 binding protein 5 gene (FKBP5) methylation , and inhibition-related prefrontal function: A prospective longitudinal study. Dev. Psychopathol. 29, 1895–1903. https://doi.org/10.1017/S095457941700147X

Hass, J., Walton, E., Wright, C., Beyer, A., Scholz, M., Turner, J., Liu, J., Smolka, M.N., Roessner, V., Sponheim, S.R., Gollub, R.L., Calhoun, V.D., Ehrlich, S., 2015. Associations between DNA methylation and schizophrenia-related intermediate phenotypes — A gene set enrichment analysis. Prog. Neuropsychopharmacol. Biol. Psychiatry 59, 31–39. https://doi.org/10.1016/j.pnpbp.2015.01.006

Hedman, A.M., van Haren, N.E.M., Schnack, H.G., Kahn, R.S., Hulshoff Pol, H.E., 2012. Human brain changes across the life span: A review of 56 longitudinal magnetic resonance imaging studies. Hum. Brain Mapp. 33, 1987–2002. https://doi.org/10.1002/hbm.21334

Heeger, D.J., Ress, D., 2002. What does fMRI tell us about neuronal activity? Nat. Neurosci. 3, 142–151. https://doi.org/10.1038/nrn730

Heijmans, B.T., Tobi, E.W., Stein, A.D., Putter, H., Blauw, G.J., Susser, E.S., Slagboom, P.E., Lumey, L.H., 2008. Persistent epigenetic differences associated with prenatal exposure to famine in humans. Proc. Natl. Acad. Sci. U. S. A. 105, 17046–17049. https://doi.org/10.1073/pnas.0806560105

Hernandez-Fernandez, M., Reguly, I., Jbabdi, S., Giles, M., Smith, S., Sotiropoulos, S.N., 2019. Using GPUs to accelerate computational diffusion MRI: From microstructure estimation to tractography and connectomes. Neuroimage 188, 598–615. https://doi.org/10.1016/j.neuroimage.2018.12.015

Herzog, E.M., Eggink, A.J., Willemsen, S.P., Slieker, R.C., Felix, J.F., Stubbs, A.P., Van Der Spek, P.J., Van Meurs, J.B.J., Heijmans, B.T., Steegers-Theunissen, R.P.M., 2021. The tissue-specific aspect of genome-wide DNA methylation in newborn and placental tissues: implications for epigenetic epidemiologic studies. J. Dev. Orig. Health Dis. 12, 113–123. https://doi.org/10.1017/S2040174420000136

Heyn, H., Moran, S., Hernando-Herraez, I., Sayols, S., Gomez, A., Sandoval, J., Monk, D., Hata, K., Marques-Bonet, T., Wang, L., Esteller, M., 2013. DNA methylation contributes to natural human variation. Genome Res. 23, 1363–1372. https://doi.org/10.1101/gr.154187.112

Hodgson, K., Carless, M.A., Kulkarni, H., Curran, J.E., Sprooten, E., Knowles, E.E., Mathias, S., Goring, H.H.H., Yao, N., Olvera, R.L., Fox, P.T., Almasy, L., Duggirala, R., Blangero, J., Glahn, D.C., 2017. Epigenetic Age Acceleration Assessed with Human White-Matter Images. J. Neurosci. 37, 4735–4743. https://doi.org/10.1523/JNEUROSCI.0177-17.2017

Hoffmann, A., Sportelli, V., Ziller, M., Spengler, D., 2017. Epigenomics of major depressive disorders and schizophrenia: Early life decides. Int. J. Mol. Sci. 18, 1–25. https://doi.org/10.3390/ijms18081711

Horvath, S., 2013. DNA methylation age of human tissues and cell types DNA methylation age of human tissues and cell types. Genome Biol. 144:R115. https://doi.org/doi:10.1186/gb-2013-14-10-r115

Hu, W., Lin, D., Cao, S., Liu, J., Chen, J., Calhoun, V.D., Wang, Y., Member, S., 2018. Adaptive Sparse Multiple Canonical Correlation Analysis With Application to Imaging (Epi)Genomics Study of Schizophrenia. IEEE Trans. Biomed. Eng. 65, 390–399. https://doi.org/10.1109/TBME.2017.2771483

Huang, Y., Pastor, W.A., Shen, Y., Tahiliani, M., Liu, D.R., Rao, A., 2010. The behaviour of 5-hydroxymethylcytosine in bisulfite sequencing. PLoS One 5, 1–9. https://doi.org/10.1371/journal.pone.0008888

Hüppi, P.S., Maier, S.E., Peled, S., Zientara, G.P., Barnes, P.D., Jolesz, F.A., Volpe, J.J., 1998. Microstructural Development of Human Newborn Cerebral White Matter Assessed in Vivo by Diffusion Tensor Magnetic Resonance Imaging. Pediatr. Res. 44, 584–590. https://doi.org/10.1203/00006450-199810000-00019

Ismaylova, E., Di Sante, J., Szyf, M., Nemoda, Z., Yu, W.J., Pomares, F.B., Turecki, G., Gobbi, G., Vitaro, F., Tremblay, R.E., Booij, L., 2017. Serotonin transporter gene promoter methylation in peripheral cells in healthy adults: Neural correlates and tissue specificity. Eur. Neuropsychopharmacol. 27, 1032–1041. https://doi.org/10.1016/j.euroneuro.2017.07.005

Ismaylova, E., Lévesque, M.L., Pomares, F.B., Szyf, M., Fahim, C., Vitaro, F., Brendgen, M., Dionne, G., Boivin, M., Tremblay, R.E., Booij, L., 2018. Serotonin transporter promoter methylation in peripheral cells and neural responses to negative stimuli : A study of adolescent monozygotic twins. Transl. Psychiatry 8. https://doi.org/10.1038/s41398-018-0195-6

Jack, A., Connelly, J.J., James, P., 2012. DNA methylation of the oxytocin receptor gene predicts neural response to ambiguous social stimuli. Front. Hum. Neurosci. 6, 1–7. https://doi.org/10.3389/fnhum.2012.00280

Jäncke, L., Liem, F., Merillat, S., 2019. Weak correlations between body height and several brain metrics in healthy elderly subjects. Eur. J. Neurosci. 50, 3578–3589. https://doi.org/10.1111/ejn.14501

Jefferis, B.J.M.H., Power, C., Hertzman, C., 2002. Birth weight, childhood socioeconomic environment, and cognitive development in the 1958 Brisith birth cohort study. BMJ 325:305.

Jia, T., Chu, C., Liu, Y., van Dongen, J., Papastergios, E., Armstrong, N.J., Bastin, M.E., Carrillo-Roa, T., den Braber, A., Harris, M., Jansen, R., Liu, J., Luciano, M., Ori, A.P.S., Roiz Santiañez, R., Ruggeri, B., Sarkisyan, D., Shin, J., Sungeun, K., Tordesillas Gutiérrez, D., van't Ent, D., Ames, D., Artiges, E., Bakalkin, G., Banaschewski, T., Bokde, A.L.W., Brodaty, H., Bromberg, U., Brouwer, R., Büchel, C., Burke Quinlan, E., Cahn, W., de Zubicaray, G.I., Ehrlich, S., Ekström, T.J., Flor, H., Fröhner, J.H., Frouin, V., Garavan, H., Gowland, P., Heinz, A., Hoare, J., Ittermann, B., Jahanshad, N., Jiang, J., Kwok, J.B., Martin, N.G., Martinot, J.L., Mather, K.A., McMahon, K.L., McRae, A.F., Nees, F., Papadopoulos Orfanos, D., Paus, T., Poustka, L., Sämann, P.G., Schofield, P.R., Smolka, M.N., Stein, D.J., Strike, L.T., Teeuw, J., Thalamuthu, A., Trollor, J., Walter, H., Wardlaw, J.M., Wen, W., Whelan, R., Apostolova, L.G., Binder, E.B., Boomsma, D.I., Calhoun, V., Crespo-Facorro, B., Deary, I.J., Hulshoff Pol, H., Ophoff, R.A., Pausova, Z., Sachdev, P.S., Saykin, A., Wright, M.J., Thompson, P.M., Schumann, G., Desrivières, S., 2019. Epigenome-wide meta-analysis of blood DNA methylation and its association with subcortical volumes: findings from the ENIGMA Epigenetics Working Group. Mol. Psychiatry. https://doi.org/10.1038/s41380-019-0605-z

Jin, S.G., Wu, X., Li, A.X., Pfeifer, G.P., 2011. Genomic mapping of 5-hydroxymethylcytosine in the human brain. Nucleic Acids Res. 39, 5015–5024. https://doi.org/10.1093/nar/gkr120

Jin, Z., Zhang, J., Klar, A., Chédotal, A., Rao, Y., Cepko, C.L., Bao, Z.Z., 2003. Irx4-mediated regulation of Slit1 expression contributes to the definition of early axonal paths inside the retina. Development 130, 1037–1048. https://doi.org/10.1242/dev.00326

Job, D.E., Dickie, D.A., Rodriguez, D., Robson, A., Danso, S., Pernet, C., Bastin, M.E., Boardman, J.P., Murray, A.D., Ahearn, T., Waiter, G.D., Staff, R.T., Deary, I.J., Shenkin, S.D., Wardlaw, J.M., 2017. A brain imaging repository of normal structural MRI across the life course: Brain Images of Normal Subjects (BRAINS). Neuroimage 144, 299–304. https://doi.org/10.1016/j.neuroimage.2016.01.027

Joehanes, R., Just, A.C., Marioni, R.E., Pilling, L.C., Reynolds, L.M., Mandaviya, P.R., Guan, W., Xu, T., Elks, C.E., Aslibekyan, S., Moreno-Macias, H., Smith, J.A., Brody, J.A., Dhingra, R., Yousefi, P., Pankow, J.S., Kunze, S., Shah, S.H., McRae, A.F., Lohman, K., Sha, J., Absher, D.M., Ferrucci, L., Zhao, W., Demerath, E.W., Bressler, J., Grove, M.L., Huan, T., Liu, C., Mendelson, M.M., Yao, C., Kiel, D.P., Peters, A., Wang-Sattler, R., Visscher, P.M., Wray, N.R., Starr, J.M., Ding, J., Rodriguez, C.J., Wareham, N.J., Irvin, M.R., Zhi, D., Barrdahl, M., Vineis, P., Ambatipudi, S., Uitterlinden, A.G., Hofman, A., Schwartz, J., Colicino, E., Hou, L., Vokonas, P.S., Hernandez, D.G., Singleton, A.B., Bandinelli, S., Turner, S.T., Ware, E.B., Smith, A.K., Klengel, T., Binder, E.B., Psaty, B.M., Taylor, K.D., Gharib, S.A., Swenson, B.R., Liang, L., Demeo, D.L., O'Connor, G.T., Herceg, Z., Ressler, K.J., Conneely, K.N., Sotoodehnia, N., Kardia, S.L.R., Melzer, D., Baccarelli, A.A., Van Meurs, J.B.J., Romieu, I., Arnett, D.K., Ong, K.K., Liu, Y., Waldenberger, M., Deary, I.J., Fornage, M., Levy, D., London, S.J., 2016. Epigenetic Signatures of Cigarette Smoking. Circ. Cardiovasc. Genet. 9, 436–447. https://doi.org/10.1161/CIRCGENETICS.116.001506

Johnson, K.A., Fox, N.C., Sperling, R.A., Klunk, W.E., 2012. Brain Imaging in Alzheimer Disease. Cold Spring Harb. Perspect. Med. 2. https://doi.org/10.1001/archneur.1979.00500440087021

Johnson, S., Hollis, C., Kochhar, P., Hennessy, E., Wolke, D., Marlow, N., 2010. Autism Spectrum Disorders in Extremely Preterm Children. J. Pediatr. 156, 525-531.e2. https://doi.org/10.1016/j.jpeds.2009.10.041

Johnson, S., Evans, T.A., Draper, E.S., Field, D.J., Manktelow, B.N., Marlow, N., Matthews, R., Petrou, S., Seaton, S.E., Smith, L.K., Boyle, E.M., 2015. Neurodevelopmental outcomes following late and moderate prematurity: A population-based cohort study. Arch. Dis. Child. Fetal Neonatal Ed. 100, F301–F308. https://doi.org/10.1136/archdischild-2014-307684

Johnson, W., Gow, A.J., Corley, J., Starr, J.M., Deary, I.J., 2010. Location in cognitive and residential space at age 70 reflects a lifelong trait over parental and environmental circumstances: The Lothian Birth Cohort 1936. Intelligence 38, 402–411. https://doi.org/10.1016/j.intell.2010.04.001

Johnson, W., Corley, J., Starr, J.M., Deary, I.J., 2011. Psychological and Physical Health at Age 70 in the Lothian Birth Cohort 1936: Links With Early Life IQ, SES, and Current Cognitive Function and Neighborhood Environment. Heal. Psychol. 30, 1–11. https://doi.org/10.1037/a0021834

Johnson, W., Deary, I.J., 2011. Placing inspection time, reaction time, and perceptual speed in the broader context of cognitive ability: The VPR model in the Lothian Birth Cohort 1936. Intelligence 39, 405–417. https://doi.org/10.1016/j.intell.2011.07.003

Jones, P.A., 2012. Functions of DNA methylation: islands, start sites, gene bodies and beyond. Nat. Rev. Genet. 13, 484–492. https://doi.org/10.1038/nrg3230

Joubert, B.R., Felix, J.F., Yousefi, P., Bakulski, K.M., Just, A.C., Breton, C., Reese, S.E., Markunas, C.A., Richmond, R.C., Xu, C.J., Küpers, L.K., Oh, S.S., Hoyo, C., Gruzieva, O., Söderhäll, C., Salas, L.A., Baïz, N., Zhang, H., Lepeule, J., Ruiz, C., Ligthart, S., Wang, T., Taylor, J.A., Duijts, L., Sharp, G.C., Jankipersadsing, S.A., Nilsen, R.M., Vaez, A., Fallin, M.D., Hu, D., Litonjua, A.A., Fuemmeler, B.F., Huen, K., Kere, J., Kull, I., Munthe-Kaas, M.C., Gehring, U., Bustamante, M., Saurel-Coubizolles, M.J., Quraishi, B.M., Ren, J., Tost, J., Gonzalez, J.R., Peters, M.J., Håberg, S.E., Xu, Z., Van Meurs, J.B., Gaunt, T.R., Kerkhof, M., Corpeleijn, E., Feinberg, A.P., Eng, C., Baccarelli, A.A., Benjamin Neelon, S.E., Bradman, A., Merid, S.K., Bergström, A., Herceg, Z., Hernandez-Vargas, H., Brunekreef, B., Pinart, M., Heude, B., Ewart, S., Yao, J., Lemonnier, N., Franco, O.H., Wu, M.C., Hofman, A., McArdle, W., Van Der Vlies, P., Falahi, F., Gillman, M.W., Barcellos, L.F., Kumar, A., Wickman, M., Guerra, S., Charles, M.A., Holloway, J., Auffray, C., Tiemeier, H.W., Smith, G.D., Postma, D., Hivert, M.F., Eskenazi, B., Vrijheid, M., Arshad, H., Antó, J.M., Dehghan, A., Karmaus, W., Annesi-Maesano, I., Sunyer, J., Ghantous, A., Pershagen, G., Holland, N., Murphy, S.K., Demeo, D.L., Burchard, E.G., Ladd-Acosta, C., Snieder, H., Nystad, W., Koppelman, G.H., Relton, C.L., Jaddoe, V.W.V., Wilcox, A., Melén, E., London, S.J., 2016. DNA Methylation in Newborns and Maternal Smoking in Pregnancy: Genome-wide Consortium Meta-analysis. Am. J. Hum. Genet. 98, 680–696. https://doi.org/10.1016/j.ajhg.2016.02.019

Kapellou, O., Counsell, S.J., Kennea, N., Dyet, L., Saeed, N., Stark, J., Maalouf, E., Duggan, P., Ajayi-Obe, M., Hajnal, J., Allsop, J.M., Boardman, J., Rutherford, M.A., Cowan, F., Edwards, A.D., 2006. Abnormal cortical development after premature birth shown by altered allometric scaling of brain growth. PLoS Med. 3, 1382–1390. https://doi.org/10.1371/journal.pmed.0030265

Karolis, V.R., Froudist-Walsh, S., Kroll, J., Brittain, P.J., Tseng, C.E.J., Nam, K.W., Reinders, A.A.T.S., Murray, R.M., Williams, S.C.R., Thompson, P.M., Nosarti, C., 2017. Volumetric grey matter alterations in adolescents and adults born very preterm suggest accelerated brain maturation. Neuroimage 163, 379–389. https://doi.org/10.1016/j.neuroimage.2017.09.039

Kazmi, N., Sharp, G.C., Reese, S.E., Vehmeijer, F.O., Lahti, J., Page, C.M., Zhang, W., Rifas-Shiman, S.L., Rezwan, F.I., Simpkin, A.J., Burrows, K., Richardson, T.G., Santos Ferreira, D.L., Fraser, A., Harmon, Q.E., Zhao, S., Jaddoe, V.W.V., Czamara, D., Binder, E.B., Magnus, M.C., Håberg, S.E., Nystad, W., Nohr, E.A., Starling, A.P., Kechris, K.J., Yang, I. V., Demeo, D.L., Litonjua, A.A., Baccarelli, A., Oken, E., Holloway, J.W., Karmaus, W., Arshad, S.H., Dabelea, D., Sørensen, T.I.A., Laivuori, H., Raikkonen, K., Felix, J.F., London, S.J., Hivert, M.F., Gaunt, T.R., Lawlor, D.A., Relton, C.L., 2019. Hypertensive Disorders of Pregnancy and DNA Methylation in Newborns: Findings from the Pregnancy and Childhood Epigenetics Consortium. Hypertension 74, 375–383. https://doi.org/10.1161/HYPERTENSIONAHA.119.12634

Khavari, D.A., Sen, G.L., Rinn, J.L., 2010. DNA methylation and epigenetic control of cellular differentiation. Cell Cycle 9, 3880–3883. https://doi.org/10.4161/cc.9.19.13385

Kim, J.S., Singh, V., Lee, J.K., Lerch, J., Ad-Dab'bagh, Y., MacDonald, D., Lee, J.M., Kim, S.I., Evans, A.C., 2005. Automated 3-D extraction and evaluation of the inner and outer cortical surfaces using a Laplacian map and partial volume effect classification. Neuroimage 27, 210–221. https://doi.org/10.1016/j.neuroimage.2005.03.036

Kim, Y.J., Park, H.J., Jahng, G.H., Lee, S.M., Kang, W.S., Kim, S.K., Kim, T., Cho, A.R., Park, J.K., 2017. A pilot study of differential brain activation to suicidal means and DNA methylation of CACNA1C gene in suicidal attempt patients. Psychiatry Res. 255, 42–48. https://doi.org/10.1016/j.psychres.2017.03.058

Klengel, T., Mehta, D., Anacker, C., Rex-Haffner, M., Pruessner, J.C., Pariante, C.M., Pace, T.W.W., Mercer, K.B., Mayberg, H.S., Bradley, B., Nemeroff, C.B., Holsboer, F., Heim, C.M., Ressler, K.J., Rein, T., Binder, E.B., 2013. Allele-specific FKBP5 DNA demethylation mediates gene-childhood trauma interactions. Nat. Neurosci. 16, 33–41. https://doi.org/10.1038/nn.3275

Klengel, T., Pape, J., Binder, E.B., Mehta, D., 2014. The role of DNA methylation in stress-related psychiatric disorders. Neuropharmacology 80, 115–132. https://doi.org/10.1016/j.neuropharm.2014.01.013

Krall, M., Htun, S., Schnur, R.E., Brooks, A.S., Baker, L., de Alba Campomanes, A., Lamont, R.E., Gripp, K.W., Schneidman-Duhovny, D., Innes, A.M., Mancini, G.M.S., Slavotinek, A.M., 2019. Biallelic sequence variants in INTS1 in patients with developmental delays, cataracts, and craniofacial anomalies. Eur. J. Hum. Genet. 27, 582–593. https://doi.org/10.1038/s41431-018-0298-9

Kubota, T., Miyake, K., Hariya, N., Mochizuki, K., 2015. Understanding the epigenetics of neurodevelopmental disorders and DOHaD. J. Dev. Orig. Health Dis. 6, 96–104. https://doi.org/10.1017/S2040174415000057

Kunz, N., Zhang, H., Vasung, L., Brien, K.R.O., Assaf, Y., Lazeyras, F., Alexander, D.C., Hüppi, P.S., 2014. Assessing white matter microstructure of the newborn with multi-shell diffusion MRI and biophysical compartment models. Neuroimage 96, 288–299. https://doi.org/10.1016/j.neuroimage.2014.03.057

Küpers, L.K., Monnereau, C., Sharp, G.C., Yousefi, P., Salas, L.A., Ghantous, A., Page, C.M., Reese, S.E., Wilcox, A.J., Czamara, D., Starling, A.P., Novoloaca, A., Lent, S., Roy, R., Hoyo, C., Breton, C. V., Allard, C., Just, A.C., Bakulski, K.M., Holloway, J.W., Everson, T.M., Xu, C.J., Huang, R.C., van der Plaat, D.A., Wielscher, M., Merid, S.K., Ullemar, V., Rezwan, F.I., Lahti, J., van Dongen, J., Langie, S.A.S., Richardson, T.G., Magnus, M.C., Nohr, E.A., Xu, Z., Duijts, L., Zhao, S., Zhang, W., Plusquin, M., DeMeo, D.L., Solomon, O., Heimovaara, J.H., Jima, D.D., Gao, L., Bustamante, M., Perron, P., Wright, R.O., Hertz-Picciotto, I., Zhang, H., Karagas, M.R., Gehring, U., Marsit, C.J., Beilin, L.J., Vonk, J.M., Jarvelin, M.R., Bergström, A., Örtqvist, A.K., Ewart, S., Villa, P.M., Moore, S.E., Willemsen, G., Standaert, A.R.L., Håberg, S.E., Sørensen, T.I.A., Taylor, J.A., Räikkönen, K., Yang, I. V., Kechris, K., Nawrot, T.S., Silver, M.J., Gong, Y.Y., Richiardi, L., Kogevinas, M., Litonjua, A.A., Eskenazi, B., Huen, K., Mbarek, H., Maguire, R.L., Dwyer, T., Vrijheid, M., Bouchard, L., Baccarelli,

A.A., Croen, L.A., Karmaus, W., Anderson, D., de Vries, M., Sebert, S., Kere, J., Karlsson, R., Arshad, S.H., Hämäläinen, E., Routledge, M.N., Boomsma, D.I., Feinberg, A.P., Newschaffer, C.J., Govarts, E., Moisse, M., Fallin, M.D., Melén, E., Prentice, A.M., Kajantie, E., Almqvist, C., Oken, E., Dabelea, D., Boezen, H.M., Melton, P.E., Wright, R.J., Koppelman, G.H., Trevisi, L., Hivert, M.F., Sunyer, J., Munthe-Kaas, M.C., Murphy, S.K., Corpeleijn, E., Wiemels, J., Holland, N., Herceg, Z., Binder, E.B., Davey Smith, G., Jaddoe, V.W.V., Lie, R.T., Nystad, W., London, S.J., Lawlor, D.A., Relton, C.L., Snieder, H., Felix, J.F., 2019. Meta-analysis of epigenome-wide association studies in neonates reveals widespread differential DNA methylation associated with birthweight. Nat. Commun. 10, 1–11. https://doi.org/10.1038/s41467-019-09671-3

Lancaster, K., Morris, J.P., Connelly, J.J., 2018. Neuroimaging Epigenetics: Challenges and Recommendations for Best Practices. Neuroscience 370, 88–100. https://doi.org/10.1016/j.neuroscience.2017.08.004

Le Bihan, D., Johansen-Berg, H., 2012. Diffusion MRI at 25 : Exploring brain tissue structure and function. Neuroimage 61, 324–341. https://doi.org/10.1016/j.neuroimage.2011.11.006

Leek, J.T., Storey, J.D., 2007. Capturing heterogeneity in gene expression studies by surrogate variable analysis. PLoS Genet. 3, 1724–1735. https://doi.org/10.1371/journal.pgen.0030161

Leek, J.T., Johnson, W.E., Parker, H.S., Jaffe, A.E., Storey, J.D., 2012. The SVA package for removing batch effects and other unwanted variation in high-throughput experiments. Bioinformatics 28, 882–883. https://doi.org/10.1093/bioinformatics/bts034

Lin, H.H., Bell, E., Uwanogho, D., Perfect, L.W., Noristani, H., Bates, T.J.D., Snetkov, V., Price, J., Sun, Y.M., 2010. Neuronatin promotes neural lineage in ESCs via Ca2+ signaling. Stem Cells 28, 1950–1960. https://doi.org/10.1002/stem.530

Linsell, L., Johnson, S., Wolke, D., Reilly, H.O., Morris, J.K., Kurinczuk, J.J., Marlow, N., 2018. Cognitive trajectories from infancy to early adulthood following birth before 26 weeks of gestation : a prospective , population-based cohort study 363–370. https://doi.org/10.1136/archdischild-2017-313414

Liu, C., Marioni, R.E., Hedman, A.K., Pfeiffer, L., Tsai, P.C., Reynolds, L.M., Just, A.C., Duan, Q., Boer, C.G., Tanaka, T., Elks, C.E., Aslibekyan, S., Brody, J.A., Kühnel, B., Herder, C., Almli, L.M., Zhi, D., Wang, Y., Huan, T., Yao, C., Mendelson, M.M., Joehanes, R., Liang, L., Love, S.A., Guan, W., Shah, S., McRae, A.F., Kretschmer, A., Prokisch, H., Strauch, K., Peters, A., Visscher, P.M., Wray, N.R., Guo, X., Wiggins, K.L., Smith, A.K., Binder, E.B., Ressler, K.J., Irvin, M.R., Absher, D.M., Hernandez, D., Ferrucci, L., Bandinelli, S., Lohman, K., Ding, J., Trevisi, L., Gustafsson, S., Sandling, J.H., Stolk, L., Uitterlinden, A.G., Yet, I., Castillo-Fernandez, J.E., Spector, T.D., Schwartz, J.D., Vokonas, P., Lind, L., Li, Y., Fornage, M., Arnett, D.K., Wareham, N.J., Sotoodehnia, N., Ong, K.K., Van Meurs, J.B.J., Conneely, K.N., Baccarelli, A.A., Deary, I.J., Bell, J.T., North, K.E., Liu, Y., Waldenberger, M., London, S.J., Ingelsson, E., Levy, D., 2018. A

DNA methylation biomarker of alcohol consumption. Mol. Psychiatry 23, 422–433. https://doi.org/10.1038/mp.2016.192

Liu, J., Julnes, P.S., Chen, J., Ehrlich, S., Walton, E., Calhoun, V.D., 2015. The association of DNA methylation and brain volume in healthy individuals and schizophrenia patients. Schizophr. Res. 169, 447–452. https://doi.org/10.1016/j.schres.2015.08.035.The

Long, H., Feng, L., Kang, J., Luo, Z., Xiao, W., Long, L., Yan, X.-X., Zhou, L., Xiao, B., 2017. Blood DNA methylation pattern is altered in mesial temporal lobe epilepsy. Sci. Rep. 7. https://doi.org/10.1038/srep43810

Low, A., Mak, E., Stefaniak, J.D., Malpetti, M., Nicastro, N., Savulich, G., Chouliaras, L., Markus, H.S., Rowe, J.B., O'Brien, J.T., 2020. Peak Width of Skeletonized Mean Diffusivity as a Marker of Diffuse Cerebrovascular Damage. Front. Neurosci. 14, 1–11. https://doi.org/10.3389/fnins.2020.00238

Lowe, R., Gemma, C., Beyan, H., Hawa, M.I., Bazeos, A., Leslie, R.D., Montpetit, A., Rakyan, V.K., Ramagopalan, S. V., 2013. Buccals are likely to be a more informative surrogate tissue than blood for epigenome-wide association studies. Epigenetics 8, 445–454. https://doi.org/10.4161/epi.24362

Lowe, R., Gemma, C., Beyan, H., Hawa, M.I., Bazeos, A., Leslie, R.D., Montpetit, A., Vardhman, K., Ramagopalan, S. V, Lowe, R., Gemma, C., Beyan, H., Hawa, M.I., Leslie, R.D., Montpetit, A., Rakyan, V.K., Ramagopalan, S. V, Lowe, R., Gemma, C., Beyan, H., Hawa, M.I., Bazeos, A., Leslie, R.D., Rakyan, V.K., Ramagopalan, S. V, 2013. surrogate tissue than blood for epigenome-Buccals are likely to be a more informative surrogate tissue than blood for epigenome-wide association studies. Epigenetics 8. https://doi.org/10.4161/epi.24362

Lyst, M.J., Bird, A., 2015. Rett syndrome: A complex disorder with simple roots. Nat. Rev. Genet. 16, 261–274. https://doi.org/10.1038/nrg3897

Mackay, D.F., Smith, G.C.S., Dobbie, R., Pell, J.P., 2010. Gestational Age at Delivery and Special Educational Need : Retrospective Cohort Study of 407 , 503 Schoolchildren 7, 1–10. https://doi.org/10.1371/journal.pmed.1000289

Mackay, D.F., Smith, G.C.S., 2011. Meta-analysis of the association between preterm delivery and intelligence 34, 209–216. https://doi.org/10.1093/pubmed/fdr024

Madden, R.A., Mccartney, D.L., Walker, R.M., Hillary, R.F., Bermingham, M.L., Rawlik, K., Morris, S.W., Campbell, A., Porteous, D.J., Deary, I.J., Kathryn, L., Hafferty, J., Mcintosh, A.M., Marioni, R.E., Hospital, R.E., Medicine, E., Epidemiology, C., Medicine, E., 2020. Birth weight associations with psychiatric and physical health, cognitive function, and DNA methylation differences in an adult population 44.

Makropoulos, A., Aljabar, P., Wright, R., Hüning, B., Merchant, N., Arichi, T., Tusor, N., Hajnal, J. V., Edwards, A.D., Counsell, S.J., Rueckert, D., 2016. Regional growth and atlasing of the developing human brain. Neuroimage 125, 456–478. https://doi.org/10.1016/j.neuroimage.2015.10.047

Maksimovic, J., Oshlack, A., Phipson, B., 2020. Gene set enrichment analysis for genome-wide DNA methylation data. bioRxiv 2020.08.24.265702. https://doi.org/10.1101/2020.08.24.265702

Matte, T.D., Bresnahan, M., Begg, M.D., Susser, E., 2001. Influence of variation in birth weight within normal range and within sibships on IQ at age 7 years: Cohort study. Br. Med. J. 323, 310–314. https://doi.org/10.1136/bmj.323.7308.310

McCartney, D.L., Walker, R.M., Morris, S.W., McIntosh, A.M., Porteous, D.J., Evans, K.L., 2016. Identification of polymorphic and off-target probe binding sites on the Illumina Infinium MethylationEPIC BeadChip. Genomics Data 9, 22–24. https://doi.org/10.1016/j.gdata.2016.05.012

McCartney, D.L., Hillary, R.F., Zhang, Q., Stevenson, A.J., Walker, R.M., Bermingham, M.L., Morris, S.W., Campbell, A., Murray, A.D., Whalley, H.C., Porteous, D.J., Evans, K.L., Chandra, T., Deary, I.J., McIntosh, A.M., Visscher, P.M., McRae, A.F., Marioni, R.E., 2019. An epigenome-wide association study of sex-specific chronological ageing. bioRxiv 1–11. https://doi.org/10.1101/606020

McGowan, P.O., Sasaki, A., D'Alessio, A.C., Dymov, S., Labonte, B., Szyf, M., Turecki, G., Meaney, M.J., 2009. Epigenetic regulation of the glucocorticoid receptor in human brain associates with childhood abuse. Nat. Neurosci. 12, 342–348. https://doi.org/10.1038/nn.2270

McMillan, C.T., Russ, J., Wood, E.M., Irwin, D.J., Grossman, M., McCluskey, L., Van Deerlin, V., Lee, E.B., 2015. C9orf72 promoter hypermethylation is neuroprotective. Am. Acad. Neurol. 84, 1622–1630.

McNerney, M.W., Sheng, T., Nechvatal, J.M., Lee, A.G., Lyons, M., Soman, S., Liao, C., Hara, R.O., Hallmayer, J., Taylor, J., Ashford, J.W., Yesavage, J., Adamson, M.M., 2018. Integration of neural and epigenetic contributions to posttraumatic stress symptoms: The role of hippocampal volume and glucocorticoid receptor gene methylation. PLoS One 13, e0192222. https://doi.org/10.1371/journal.pone.0192222

Menegaux, A., Hedderich, D.M., Bäuml, J.G., Manoliu, A., Daamen, M., Berg, R.C., Preibisch, C., Zimmer, C., Boecker, H., Bartmann, P., Wolke, D., Sorg, C., Stämpfli, P., 2020. Reduced apparent fiber density in the white matter of premature-born adults. Sci. Rep. 10, 1–13. https://doi.org/10.1038/s41598-020-73717-6

Merid, S.K., Novoloaca, A., Sharp, G.C., Küpers, L.K., Kho, A.T., 2020. Epigenome-wide meta-analysis of blood DNA methylation in newborns and children identifies numerous loci related to gestational age. Genome Med. 12, 1–17.

Montirosso, R., Provenzi, L., 2015. Implications of epigenetics and stress regulation on research and developmental care of preterm infants. JOGNN - J. Obstet. Gynecol. Neonatal Nurs. 44, 174–182. https://doi.org/10.1111/1552-6909.12559

Montirosso, R., Provenzi, L., Fumagalli, M., Sirgiovanni, I., Giorda, R., Pozzoli, U., Beri, S., Menozzi, G., Tronick, E., Morandi, F., Mosca, F., Borgatti, R., 2016. Serotonin Transporter Gene (SLC6A4) Methylation Associates With Neonatal Intensive Care Unit Stay and 3-Month-Old Temperament in Preterm Infants. Child Dev. 87, 38–48. https://doi.org/10.1111/cdev.12492

Moore, L.D., Le, T., Fan, G., 2013. DNA methylation and its basic function. Neuropsychopharmacology 38, 23–38. https://doi.org/10.1038/npp.2012.112

Morgan, H.D., Santos, F., Green, K., Dean, W., Reik, W., 2005. Epigenetic reprogramming in mammals. Hum. Mol. Genet. 14, 47–58. https://doi.org/10.1093/hmg/ddi114

Moser, D.A., Paoloni-giacobino, A., Stenz, L., Adouan, W., Rusconi-serpa, S., Ansermet, F., Dayer, A.G., 2015. BDNF Methylation and Maternal Brain Activity in a Violence-Related Sample 1–13. https://doi.org/10.1371/journal.pone.0143427

Mosing, M.A., Lundholm, C., Cnattingius, S., Gatz, M., Pedersen, N.L., 2018. Associations between birth characteristics and age-related cognitive impairment and dementia: A registry-based cohort study. PLoS Med. 15, 1–21. https://doi.org/10.1371/journal.pmed.1002609

Muehlhan, M., Kirschbaum, C., Wittchen, H., Alexander, N., 2015. Epigenetic Variation in the Serotonin Transporter Gene Predicts Resting State Functional Connectivity Strength Within the Salience-Network. Hum. Brain Mapp. 36, 4361–4371. https://doi.org/10.1002/hbm.22923

Muench, C., Wiers, C.E., Cortes, C.R., Momenan, R., Lohoff, F.W., 2018. Dopamine Transporter Gene Methylation is Associated with Nucleus Accumbens Activation During Reward Processing in Healthy but not Alcohol-Dependent Individuals. Alcohol. Clin. Exp. Res. 42, 21–31. https://doi.org/10.1111/acer.13526

Muller, M., Sigurdsson, S., Kjartansson, O., Gunnarsdottir, I., Thorsdottir, I., Harris, T.B., van Buchem, M., Gudnason, V., Launer, L.J., 2016. Late-life brain volume: a life-course approach. The AGES-Reykjavik study. Neurobiol. Aging 41, 86–92. https://doi.org/10.1038/s41395-018-0061-4.

Muller, M., Sigurdsson, S., Kjartansson, O., Jonsson, P. V., Garcia, M., von Bonsdorff, M.B., Gunnarsdottir, I., Thorsdottir, I., Harris, T.B., van Buchem, M., Gudnason, V., Launer, L.J., 2014. Birth size and brain function 75 years later. Pediatrics 134, 761–770. https://doi.org/10.1542/peds.2014-1108

Na, K.S., Won, E., Kang, J., Chang, H.S., Yoon, H.K., Tae, W.S., Kim, Y.K., Lee, M.S., Joe, S.H., Kim, H., Ham, B.J., 2016. Brain-derived neurotrophic factor promoter methylation and cortical thickness in recurrent major depressive disorder. Sci Rep 6, 21089. https://doi.org/10.1038/srep21089

Nikolova, Y.S., Koenen, K.C., Galea, S., Wang, C., Seney, M.L., Sibille, E., Williamson, D.E., Hariri, A.R., 2014. Beyond genotype: serotonin transporter epigenetic modification predicts human brain function. Nat. Neurosci. 17, 1153–1155. https://doi.org/10.1038/nn.3778

Nikolova, Y.S., Hariri, A.R., 2015. Can we observe epigenetic effects on human brain function? Trends Cogn. Sci. 19, 366–373. https://doi.org/10.1016/j.tics.2015.05.003

Northam, G.B., Liégeois, F., Chong, W.K., S. Wyatt, J., Baldeweg, T., 2011. Total brain white matter is a major determinant of IQ in adolescents born preterm. Ann. Neurol. 69, 702–711. https://doi.org/10.1002/ana.22263

Northam, G.B., Liegeois, F., Tournier, J., Croft, L.J., Johns, P.N., Chong, W.K., Wyatt, J.S., Baldeweg, T., 2012. Interhemispheric temporal lobe connectivity predicts language impairment in adolescents born preterm. Brain 135, 3781–3798. https://doi.org/10.1093/brain/aws276

Nosarti, C., Al-asady, M.H.S., Frangou, S., Stewart, A.L., Rifkin, L., Murray, R.M., 2002. Adolescents who were born very preterm have decreased brain volumes 1616–1623.

Nosarti, C., Reichenberg, A., Murray, R.M., Cnattingius, S., Lambe, M.P., Yin, L., MacCabe, J., Rifkin, L., Hultman, C.M., 2012. Preterm birth and psychiatric disorders in young adult life. Arch. Gen. Psychiatry 69. https://doi.org/10.1001/archgenpsychiatry.2011.1374

Numata, S., Ye, T., Hyde, T.M., Guitart-Navarro, X., Tao, R., Wininger, M., Colantuoni, C., Weinberger, D.R., Kleinman, J.E., Lipska, B.K., 2012. DNA methylation signatures in development and aging of the human prefrontal cortex. Am. J. Hum. Genet. 90, 260–272. https://doi.org/10.1016/j.ajhg.2011.12.020

O'Brien, L.M., Ziegler, D.A., Deutsch, C.K., Kennedy, D.N., Goldstein, J.M., Seidman, L.J., Hodge, S., Makris, N., Caviness, V., Frazier, J.A., Herbert, M.R., 2006. Adjustment for whole brain and cranial size in volumetric brain studies: A review of common adjustment factors and statistical methods. Harv. Rev. Psychiatry 14, 141–151. https://doi.org/10.1080/10673220600784119

O'Brien, L.M., Ziegler, D.A., Deutsch, C.K., Frazier, J.A., Herbert, M.R., Locascio, J.J., 2011. Statistical adjustments for brain size in volumetric neuroimaging studies: Some practical implications in methods. Psychiatry Res. 193, 113–122. https://doi.org/10.1016/j.pscychresns.2011.01.007.Statistical

O'Donnell, K.J., Meaney, M.J., 2017. Fetal origins of mental health: The developmental origins of health and disease hypothesis. Am. J. Psychiatry 174, 319–328. https://doi.org/10.1176/appi.ajp.2016.16020138

Oberlander, T.F., Weinberg, J., Papsdorf, M., Grunau, R., Misri, S., Devlin, A.M., 2008. Prenatal exposure to maternal depression, neonatal methylation of human glucocorticoid receptor gene (NR3C1) and infant cortisol stress responses. Epigenetics 3, 97–106. https://doi.org/10.4161/epi.3.2.6034

Odintsova, V. V, Hagenbeek, F.A., Suderman, M., Caramaschi, D., Beijsterveldt, C.E.M. Van, Kallsen, N.A., Ehli, E.A., Davies, G.E., Sukhikh, G.T., Fanos, V., Relton, C., Bartels, M., Boomsma, D.I., Dongen, J. Van, 2019. DNA Methylation Signatures of Breastfeeding in Buccal Cells Collected in Mid-Childhood. Nutrientsi 1–26.

Oegema, R., Baillat, D., Schot, R., van Unen, L.M., Brooks, A., Kia, S.K., Hoogeboom, A.J.M., Xia, Z., Li, W., Cesaroni, M., Lequin, M.H., van Slegtenhorst, M., Dobyns, W.B., de Coo, I.F.M., van den Berg, D., Verheijen, F.W., Kremer, A., van der Spek, P.J., Heijsman, D., Wagner, E.J., Fornerod, M., Mancini, G.M.S., 2017. Human mutations in integrator complex subunits link transcriptome integrity to brain development. PLoS Genet. 13, e1006923. https://doi.org/10.1371/journal.pgen.1006923

Olkhov-Mitsel, E., Bapat, B., 2012. Strategies for discovery and validation of methylated and hydroxymethylated DNA biomarkers. Cancer Med. 1, 237–260. https://doi.org/10.1002/cam4.22

Osmond, C., Barker, D.J.P., Winter, P.D., Fall, C.H.D., Simmonds, S.J., 1993. Early growth and death from cardiovascular disease in women. Br. Med. J. 307, 1519–1524. https://doi.org/10.1136/bmj.307.6918.1519

Padilla, N., Alexandrou, G., Blennow, M., Lagercrantz, H., Ådén, U., 2015. Brain Growth Gains and Losses in Extremely Preterm Infants at Term. Cereb. Cortex 25, 1897–1905. https://doi.org/10.1093/cercor/bht431

Palumbo, S., Mariotti, V., Iofrida, C., Pellegrini, S., 2018. Genes and Aggressive Behavior: Epigenetic Mechanisms Underlying Individual Susceptibility to Aversive Environments. Front. Behav. Neurosci. 12, 117. https://doi.org/10.3389/fnbeh.2018.00117

Park, S., Lee, J., Kim, J., Cho, D., Yun, H.J., Han, D.H., Cheong, J.H., Kim, B., 2015. Associations between serotonin transporter gene (SLC6A4) methylation and clinical characteristics and cortical thickness in children with ADHD. Psychol. Med. 45, 3009–3017. https://doi.org/10.1017/S003329171500094X

Pascoe, M.J., Melzer, T.R., Horwood, L.J., Woodward, L.J., Darlow, B.A., 2019. Altered grey matter volume, perfusion and white matter integrity in very low birthweight adults. NeuroImage Clin. 22, 101780. https://doi.org/10.1016/j.nicl.2019.101780

Paus, T., Collins, D.L., Evans, A.C., Leonard, G., Pike, B., Zijdenbos, A., 2001. Maturation of white matter in the human brain: A review of magnetic resonance studies. Brain Res. Bull. 54, 255–266.

Penke, L., Maniega, S.M., Murray, C., Gow, A.J., Valdes Hernandez, M.C., Clayden, J.D., Starr, J.M., Wardlaw, J.M., Bastin, M.E., Deary, I.J., 2010. A General Factor of Brain White Matter Integrity Predicts Information Processing Speed in Healthy Older People. J. Neurosci. 30, 7569–7574. https://doi.org/10.1523/JNEUROSCI.1553-10.2010

Penke, L., Maniega, S.M., Bastin, M.E., Valdés Hernández, M.C., Murray, C., Royle, N.A., Starr, J.M., Wardlaw, J.M., Deary, I.J., 2012. Brain white matter tract integrity as a neural foundation for general intelligence. Mol. Psychiatry 17, 1026–1030. https://doi.org/10.1038/mp.2012.66

Pidsley, R., Wong, C.C.Y., Volta, M., Lunnon, K., Mill, J., Schalkwyk, L.C., 2013. A data-driven approach to preprocessing Illumina 450 K methylation array data. BMC Genomics 14, 293. https://doi.org/10.1186/1471-2164-14-293

Pierson, C.R., Folkerth, R.D., Billiards, S.S., Trachtenberg, F.L., Drinkwater, M.E., Volpe, J.J., Kinney, H.C., 2007. Gray matter injury associated with periventricular leukomalacia in the premature infant. Acta Neuropathol. 619–631. https://doi.org/10.1007/s00401-007-0295-5

Pietsch, M., Christiaens, D., Hutter, J., Cordero-grande, L., Price, A.N., Hughes, E., Edwards, A.D., Hajnal, J. V, Counsell, S.J., Tournier, J., 2019. A framework for multi-component analysis of diffusion MRI data over the neonatal period. Neuroimage 186, 321–337. https://doi.org/10.1016/j.neuroimage.2018.10.060

Pietschnig, J., Penke, L., Wicherts, J.M., Zeiler, M., Voracek, M., 2015. Meta-analysis of associations between human brain volume and intelligence differences: How strong are they and what do they mean? Neurosci. Biobehav. Rev. 57, 411–432. https://doi.org/10.1016/j.neubiorev.2015.09.017

Portales-Casamar, E., Lussier, A.A., Jones, M.J., MacIsaac, J.L., Edgar, R.D., Mah, S.M., Barhdadi, A., Provost, S., Lemieux-Perreault, L.-P., Cynader, M.S., Chudley, A.E., Dubé, M.-P., Reynolds, J.N., Pavlidis, P., Kobor, M.S., 2016. DNA methylation signature of human fetal alcohol spectrum disorder. Epigenetics Chromatin 9, 25. https://doi.org/10.1186/s13072-016-0074-4

Provenzi, L., Fumagalli, M., Sirgiovanni, I., Giorda, R., Pozzoli, U., Morandi, F., Beri, S., Menozzi, G., Mosca, F., Borgatti, R., Montirosso, R., 2015. Pain-related stress during the Neonatal Intensive Care Unit stay and SLC6A4 methylation in very preterm infants. Front. Behav. Neurosci. 9, 1–9. https://doi.org/10.3389/fnbeh.2015.00099

Provenzi, L., Guida, E., Montirosso, R., 2018. Preterm behavioral epigenetics: A systematic review. Neurosci. Biobehav. Rev. 84, 262–271. https://doi.org/10.1016/j.neubiorev.2017.08.020

Pruessner, J.C., Li, L.M., Serles, W., Pruessner, M., Collins, D.L., Kabani, N., Lupien, S., Evans, A.C., 2000. Volumetry of Hippocampus and Amygdala with High-resolution MRI and Three-dimensional Analysis Software: Minimizing the Discrepancies between Laboratories. Cereb. Cortex 10, 433–442.

Puglia, M.H., Lillard, T.S., Morris, J.P., Connelly, J.J., 2015. Epigenetic modification of the oxytocin receptor gene influences the perception of anger and fear in the human brain. Proc. Natl. Acad. Sci. U. S. A. 112, 3308–3313. https://doi.org/10.1073/pnas.1422096112

Raina, A., Zhao, X., Grove, M.L., Bressler, J., Gottesman, R.F., Guan, W., Pankow, J.S., Boerwinkle, E., Mosley, T.H., Fornage, M., 2017. Cerebral white matter hyperintensities on MRI and acceleration of epigenetic aging: the atherosclerosis risk in communities study. Clin. Epigenetics 9, 1–9. https://doi.org/10.1186/s13148-016-0302-6

Rangasamy, S., D'Mello, S.R., Narayanan, V., 2013. Epigenetics, Autism Spectrum, and Neurodevelopmental Disorders. Neurotherapeutics 10, 742–756. https://doi.org/10.1007/s13311-013-0227-0

Raznahan, A., Greenstein, D., Lee, N.R., Clasen, L.S., Giedd, J.N., 2012. Prenatal growth in humans and postnatal brain maturation into late adolescence. Proc. Natl. Acad. Sci. U. S. A. 109, 11366–11371. https://doi.org/10.1073/pnas.1203350109

RCoreTeam, 2020. R: A language and environment for statistical computing. R Found. Stat. Comput. Vienna, Austria.

Reardon, P.K., Seidlitz, J., Vandekar, S., Liu, S., Patel, R., Park, M.T.M., Alexander-Bloch, A., Clasen, L.S., Blumenthal, J.D., Lalonde, F.M., Giedd, J.N., Gur, R.C., Gur, R.E., Lerch, J.P., Chakravarty, M.M., Satterthwaite, T.D., Shinohara, R.T., Raznahan, A., 2018. Normative brain size variation and brain shape diversity in humans. Science (80-.). 360, 1222–1227. https://doi.org/10.1126/science.aar2578

Reik, W., 2007. Stability and flexibility of epigenetic gene regulation in mammalian development. Nature 447, 425–432. https://doi.org/10.1038/nature05918

Resmini, E., Santos, A., Aulinas, A., Webb, S.M., Vives-Gilabert, Y., Cox, O., Wand, G., Lee, R.S., 2016. Reduced DNA methylation of FKBP5 in Cushing's syndrome. Endocrine 54, 768–777. https://doi.org/10.1007/s12020-016-1083-6

Richards, M., Shipley, B., Fuhrer, R., Wadsworth, M.E.J., 2004. Cognitive ability in childhood and cognitive decline in mid-life: Longitudinal birth cohort study. Br. Med. J. 328, 552–554. https://doi.org/10.1136/bmj.37972.513819.ee

Rijlaarsdam, J., Pappa, I., Walton, E., Bakermans-Kranenburg, M.J., Mileva-Seitz, V.R., Rippe, R.C.A., Roza, S.J., Jaddoe, V.W.V., Verhulst, F.C., Felix, J.F., Cecil, C.A.M., Relton, C.L., Gaunt, T.R., McArdle, W., Mill, J., Barker, E.D., Tiemeier, H., van IJzendoorn, M.H., 2016. An epigenome-wide association meta-analysis of prenatal maternal stress in neonates: A model approach for replication. Epigenetics 11, 140–149. https://doi.org/10.1080/15592294.2016.1145329

Ritchie, M.E., Phipson, B., Wu, D., Hu, Y., Law, C.W., Shi, W., Smyth, G.K., 2015. Limma powers differential expression analyses for RNA-sequencing and microarray studies. Nucleic Acids Res. 43, e47. https://doi.org/10.1093/nar/gkv007

Ritchie, S.J., Bastin, M.E., Tucker-Drob, E.M., Maniega, S.M., Engelhardt, L.E., Cox, S.R., Royle, N.A., Gow, A.J., Corley, J., Pattie, A., Taylor, A.M., Valdes Hernandez, M. d. C., Starr, J.M., Wardlaw, J.M., Deary, I.J., 2015a. Coupled Changes in Brain White Matter Microstructure and Fluid Intelligence in Later Life. J. Neurosci. 35, 8672–8682. https://doi.org/10.1523/JNEUROSCI.0862-15.2015

Ritchie, S.J., Dickie, D.A., Cox, S.R., Valdes Hernandez, M. del C., Corley, J., Royle, N.A., Pattie, A., Aribisala, B.S., Redmond, P., Muñoz Maniega, S.,

Taylor, A.M., Sibbett, R., Gow, A.J., Starr, J.M., Bastin, M.E., Wardlaw, J.M., Deary, I.J., 2015b. Brain volumetric changes and cognitive ageing during the eighth decade of life. Hum. Brain Mapp. 36, 4910–4925. https://doi.org/10.1002/hbm.22959

Ritchie, S.J., Booth, T., Valdés Hernández, M. del C., Corley, J., Maniega, S.M., Gow, A.J., Royle, N.A., Pattie, A., Karama, S., Starr, J.M., Bastin, M.E., Wardlaw, J.M., Deary, I.J., 2015c. Beyond a bigger brain: Multivariable structural brain imaging and intelligence. Intelligence 51, 47–56. https://doi.org/10.1016/j.intell.2015.05.001

Ritchie, S.J., Tucker-Drob, E.M., Cox, S.R., Dickie, D.A., Del C. Valdés Hernández, M., Corley, J., Royle, N.A., Redmond, P., Muñoz Maniega, S., Pattie, A., Aribisala, B.S., Taylor, A.M., Clarke, T.K., Gow, A.J., Starr, J.M., Bastin, M.E., Wardlaw, J.M., Deary, I.J., 2017. Risk and protective factors for structural brain ageing in the eighth decade of life. Brain Struct. Funct. 222, 3477–3490. https://doi.org/10.1007/s00429-017-1414-2

Rose, S.E., Hatzigeorgiou, X., Strudwick, M.W., Durbridge, G., Davies, P.S.W., Colditz, P.B., 2008. Altered white matter diffusion anisotropy in normal and preterm infants at term-equivalent age. Magn. Reson. Med. 60, 761–767. https://doi.org/10.1002/mrm.21689

Rosseel, Y., 2012. lavaan: An R Package fot Structural Equation Modeling. J. Stat. Softw. 48.

Royle, N.A., Booth, T., Valdés Hernández, M.C., Penke, L., Murray, C., Gow, A.J., Maniega, S.M., Starr, J., Bastin, M.E., Deary, I.J., Wardlaw, J.M., 2013. Estimated maximal and current brain volume predict cognitive ability in old age. Neurobiol. Aging 34, 2726–2733. https://doi.org/10.1016/j.neurobiolaging.2013.05.015

Rubin, L.H., Connelly, J.J., Reilly, J.L., Carter, C.S., Drogos, L.L., Pournaja, H., Ruocco, A.C., Keedy, S.K., Matthew, I., Tandon, N., Pearlson, G.D., Clementz, B.A., Tamminga, C.A., Gershon, E.S., Keshavan, M.S., Bishop, J.R., Sweeney, J.A., 2016. Sex and Diagnosis-Specific Associations Between DNA Methylation of the Oxytocin Receptor Gene With Emotion Processing and Temporal-Limbic and Prefrontal Brain Volumes in Psychotic Disorders. Biol. Psychiatry 1, 141–151. https://doi.org/10.1016/j.bpsc.2015.10.003

Ruggeri, B., Nymberg, C., Vuoksimaa, E., Lourdusamy, A., Wong, C.P., Carvalho, F.M., Jia, T., Cattrell, A., Macare, C., Banaschewski, T., Barker, G.J., Bokde, A.L., Bromberg, U., Buchel, C., Conrod, P.J., Fauth-Buhler, M., Flor, H., Frouin, V., Gallinat, J., Garavan, H., Gowland, P., Heinz, A., Ittermann, B., Martinot, J.L., Nees, F., Pausova, Z., Paus, T., Rietschel, M., Robbins, T., Smolka, M.N., Spanagel, R., Bakalkin, G., Mill, J., Sommer, W.H., Rose, R.J., Yan, J., Aliev, F., Dick, D., Kaprio, J., Desrivieres, S., Schumann, G., Consortium, I., 2015. Association of Protein Phosphatase PPM1G With Alcohol Use Disorder and Brain Activity During Behavioral Control in a Genome-Wide Methylation Analysis. Am. J. Psychiatry 172, 543–552. https://doi.org/10.1176/appi.ajp.2014.14030382

Sabunciyan, S., Aryee, M.J., Irizarry, R.A., Rongione, M., Webster, M.J., Kaufman, W.E., Murakami, P., Lessard, A., Yolken, R.H., Feinberg, A.P., Potash, J.B., Consortium, G., 2012. Genome-Wide DNA Methylation Scan in Major Depressive Disorder. PLoS One 7, e34451. https://doi.org/10.1371/journal.pone.0034451

Sacchi, C., Marino, C., Nosarti, C., Vieno, A., Visentin, S., Simonelli, A., 2020. Association of Intrauterine Growth Restriction and Small for Gestational Age Status with Childhood Cognitive Outcomes: A Systematic Review and Meta-analysis. JAMA Pediatr. 174, 772–781. https://doi.org/10.1001/jamapediatrics.2020.1097

Sadeh, N., Spielberg, J.M., Logue, M.W., Wolf, E.J., Smith, A.K., Lusk, J., Hayes, J.P., Sperbeck, E., Milberg, W.P., McGlinchey, R.E., Salat, D.H., Carter, W.C., Stone, A., Schichman, S.A., Humphries, D.E., Miller, M.W., 2016. SKA2 methylation predicts reduced cortical thickness in prefrontal cortex. Mol. Psychiatry 21, 299. https://doi.org/10.1038/mp.2016.10

Saffari, A., Silver, M.J., Zavattari, P., Moi, L., Columbano, A., Meaburn, E.L., Dudbridge, F., 2018. Estimation of a significance threshold for epigenome-wide association studies. Genet. Epidemiol. 42, 20–33. https://doi.org/10.1002/gepi.22086

Saigal, S., Doyle, L.W., 2008. An overview of mortality and sequelae of preterm birth from infancy to adulthood. Lancet 371, 261–269.

Schechter, D.S., Moser, D.A., Paoloni-Giacobino, A., Stenz, L., Gex-Fabry, M., Aue, T., Adouan, W., Cordero, M.I., Suardi, F., Manini, A., Sancho Rossignol, A., Merminod, G., Ansermet, F., Dayer, A.G., Rusconi-Serpa, S., 2015. Methylation of NR3C1 is related to maternal PTSD, parenting stress and maternal medial prefrontal cortical activity in response to child separation among mothers with histories of violence exposure. Front. Psychiatry 6, 1–12. https://doi.org/10.3389/fpsyg.2015.00690

Schechter, D.S., Moser, D.A., Pointet, V.C., Aue, T., Stenz, L., Paoloni-giacobino, A., Adouan, W., Manini, A., Suardi, F., Vital, M., Sancho, A., Cordero, M.I., Rothenberg, M., Rusconi, S., Dayer, A.G., 2017. The association of serotonin receptor 3A methylation with maternal violence exposure, neural activity, and child aggression. Behav. Brain Res. 325, 268–277. https://doi.org/10.1016/j.bbr.2016.10.009

Schlotz, W., Phillips, D.I.W., 2009. Fetal origins of mental health: Evidence and mechanisms. Brain. Behav. Immun. 23, 905–916. https://doi.org/10.1016/j.bbi.2009.02.001

Schneider, I., Kugel, H., Redlich, R., Grotegerd, D., Burger, C., Burkner, P.C., Opel, N., Dohm, K., Zaremba, D., Meinert, S., Schroder, N., Strassburg, A.M., Schwarte, K., Schettler, C., Ambree, O., Rust, S., Domschke, K., Arolt, V., Heindel, W., Baune, B.T., Zhang, W., Dannlowski, U., Hohoff, C., 2018. Association of Serotonin Transporter Gene AluJb Methylation with Major Depression, Amygdala Responsiveness, 5-HTTLPR/rs25531 Polymorphism, and

Stress. Neuropsychopharmacology 43, 1308–1316. https://doi.org/10.1038/npp.2017.273

Schneider, J., Duerden, E.G., Guo, T., Ng, K., Hagmann, P., Bickle Graz, M., Grunau, R.E., Chakravarty, M.M., Hüppi, P.S., Truttmann, A.C., Miller, S.P., 2018. Procedural pain and oral glucose in preterm neonates. Pain 159, 515–525.

Schroeder, J.W., Conneely, K.N., Cubells, J.C., Kilaru, V., Jeffrey Newport, D., Knight, B.T., Stowe, Z.N., Brennan, P.A., Krushkal, J., Tylavsky, F.A., Taylor, R.N., Adkins, R.M., Smith, A.K., 2011. Neonatal DNA methylation patterns associate with gestational age. Epigenetics 6, 1498–1504. https://doi.org/10.4161/epi.6.12.18296

Sgouros, S., Hockley, A.D., Goldin, J.H., Wake, M.J.C., Natarajan, K., 1999. Intracranial volume change in craniosynostosis. J. Neurosurg. 91, 617–625. https://doi.org/10.3171/jns.1999.91.4.0617

Shah, D.K., Doyle, L.W., Anderson, P.J., Bear, M., Daley, A.J., Hunt, R.W., Inder, T.E., 2008. Necrotizing Enterocolitis is Mediated by White Matter Abnormalities on Magnetic Resonance Imaging at Term. J. Pediatr. 153. https://doi.org/10.1016/j.jpeds.2008.02.033

Sharp, G.C., Lawlor, D.A., Richmond, R.C., Fraser, A., Simpkin, A., Suderman, M., Shihab, H.A., Lyttleton, O., McArdle, W., Ring, S.M., Gaunt, T.R., Smith, G.D., Relton, C.L., 2015. Maternal pre-pregnancy BMI and gestational weight gain, offspring DNA methylation and later offspring adiposity: Findings from the Avon Longitudinal Study of Parents and Children. Int. J. Epidemiol. 44, 1288–1304. https://doi.org/10.1093/ije/dyv042

Sharp, G.C., Salas, L.A., Monnereau, C., Allard, C., Yousefi, P., Everson, T.M., Bohlin, J., Xu, Z., Huang, R.C., Reese, S.E., Xu, C.J., Baïz, N., Hoyo, C., Agha, G., Roy, R., Holloway, J.W., Ghantous, A., Merid, S.K., Bakulski, K.M., Küpers, L.K., Zhang, H., Richmond, R.C., Page, C.M., Duijts, L., Lie, R.T., Melton, P.E., Vonk, J.M., Nohr, E.A., Williams-DeVane, C.L., Huen, K., Rifas-Shiman, S.L., Ruiz-Arenas, C., Gonseth, S., Rezwan, F.I., Herceg, Z., Ekström, S., Croen, L., Falahi, F., Perron, P., Karagas, M.R., Quraishi, B.M., Suderman, M., Magnus, M.C., Jaddoe, V.W.V., Taylor, J.A., Anderson, D., Zhao, S., Smit, H.A., Josey, M.J., Bradman, A., Baccarelli, A.A., Bustamante, M., Håberg, S.E., Pershagen, G., Hertz-Picciotto, I., Newschaffer, C., Corpeleijn, E., Bouchard, L., Lawlor, D.A., Maguire, R.L., Barcellos, L.F., Smith, G.D., Eskenazi, B., Karmaus, W., Marsit, C.J., Hivert, M.F., Snieder, H., Fallin, M.D., Melén, E., Munthe-Kaas, M.C., Arshad, H., Wiemels, J.L., Annesi-Maesano, I., Vrijheid, M., Oken, E., Holland, N., Murphy, S.K., Sørensen, T.I.A., Koppelman, G.H., Newnham, J.P., Wilcox, A.J., Nystad, W., London, S.J., Felix, J.F., Relton, C.L., 2017. Maternal BMI at the start of pregnancy and offspring epigenome-wide DNA methylation: Findings from the pregnancy and childhood epigenetics (PACE) consortium. Hum. Mol. Genet. 26, 4067–4085. https://doi.org/10.1093/hmg/ddx290

Shelton, A.L., Cornish, K.M., Kolbe, S., Clough, M., Slater, H.R., Li, X., Kraan, C.M., Bui, Q.M., Godler, D.E., Fielding, J., 2016. Brain structure and intragenic DNA methylation are correlated , and predict executive dysfunction in

fragile X premutation females. Transl. Psychiatry 6. https://doi.org/10.1038/tp.2016.250

Shelton, A.L., Cornish, K.M., Godler, D., Bui, Q.M., Kolbe, S., Fielding, J., 2017. White matter microstructure, cognition, and molecular markers in fragile X premutation females. Neurology 88, 2070–2088.

Shenkin, S.D., Starr, J.M., Pattie, A., Rush, M.A., Whalley, L.J., Deary, I.J., 2001. Birth weight and cognitive function at age 11 years: The Scottish Mental Survey 1932. Arch. Dis. Child. 85, 189–195. https://doi.org/10.1136/adc.85.3.189

Shenkin, S.D., Starr, J.M., Deary, I.J., 2004. Birth weight and cognitive ability in childhood: A systematic review. Psychol. Bull. 130, 989–1013. https://doi.org/10.1037/0033-2909.130.6.989

Shenkin, S.D., Bastin, M.E., MacGillivray, T.J., Deary, I.J., Starr, J.M., Wardlaw, J.M., 2009a. Birth parameters are associated with late-life white matter integrity in community-dwelling older people. Stroke 40, 1225–1228. https://doi.org/10.1161/STROKEAHA.108.527259

Shenkin, S.D., Deary, I.J., Starr, J.M., 2009b. Birth parameters and cognitive ability in older age: a follow-up study of people born 1921-1926. Gerontology 55, 92–98. https://doi.org/10.1159/000163444

Shimony, J.S., Smyser, C.D., Wideman, G., Alexopoulos, D., Hill, J., Harwell, J., Dierker, D., Essen, D.C. Van, Inder, T.E., Neil, J.J., 2016. Comparison of cortical folding measures for evaluation of developing human brain. Neuroimage 125, 780–790. https://doi.org/10.1016/j.neuroimage.2015.11.001

Shinagawa, S., Kobayashi, N., Nagata, T., Kusaka, A., 2016. Neuroscience Letters DNA methylation in the NCAPH2 / LMF2 promoter region is associated with hippocampal atrophy in Alzheimer ' s disease and amnesic mild cognitive impairment patients. Neurosci. Lett. 629, 33–37. https://doi.org/10.1016/j.neulet.2016.06.055

Simpkin, A.J., Suderman, M., Gaunt, T.R., Lyttleton, O., McArdle, W.L., Ring, S.M., Tilling, K., Davey Smith, G., Relton, C.L., 2015. Longitudinal analysis of DNA methylation associated with birth weight and gestational age. Hum. Mol. Genet. 24, 3752–3763. https://doi.org/10.1093/hmg/ddv119

Skranes, J., Vangberg, T.R., Kulseng, S., Indredavik, M.S., Evensen, K.A.I., Martinussen, M., Dale, A.M., Haraldseth, O., Brubakk, A.M., 2007. Clinical findings and white matter abnormalities seen on diffusion tensor imaging in adolescents with very low birth weight. Brain 130, 654–666. https://doi.org/10.1093/brain/awm001

Slieker, R.C., Roost, M.S., van Iperen, L., Suchiman, H.E.D., Tobi, E.W., Carlotti, F., de Koning, E.J.P., Slagboom, P.E., Heijmans, B.T., Chuva de Sousa Lopes, S.M., 2015. DNA Methylation Landscapes of Human Fetal Development. PLoS Genet. 11, 1–19. https://doi.org/10.1371/journal.pgen.1005583

Smith, S.M., Jenkinson, M., Woolrich, M.W., Beckmann, C.F., Behrens, T.E.J., Johansen-Berg, H., Bannister, P.R., De Luca, M., Drobnjak, I., Flitney,

D.E., Niazy, R.K., Saunders, J., Vickers, J., Zhang, Y., De Stefano, N., Brady, J.M., Matthews, P.M., 2004. Advances in functional and structural MR image analysis and implementation as FSL. Neuroimage 23, 208–219. https://doi.org/10.1016/j.neuroimage.2004.07.051

Smith, S.M., Jenkinson, M., Johansen-berg, H., Rueckert, D., Nichols, T.E., Mackay, C.E., Watkins, K.E., Ciccarelli, O., Cader, M.Z., Matthews, P.M., Behrens, T.E.J., 2006. Tract-based spatial statistics: Voxelwise analysis of multi-subject diffusion data. Neuroimage 31, 1487–1505. https://doi.org/10.1016/j.neuroimage.2006.02.024

Smith, Z.D., Meissner, A., 2013. DNA methylation: roles in mammalian development. Nat. Rev. Genet. 14, 204–220. https://doi.org/10.1038/nrg3354

Smith, A.K., Kilaru, V., Klengel, T., Mercer, K.B., Bradley, B., Conneely, K.N., Ressler, K.J., Binder, E.B., 2015. DNA extracted from saliva for methylation studies of psychiatric traits: Evidence tissue specificity and relatedness to brain. Am. J. Med. Genet. Part B Neuropsychiatr. Genet. 168, 36–44. https://doi.org/10.1002/ajmg.b.32278

Song, R., Xu, H., Dintica, C.S., Pan, K.Y., Qi, X., Buchman, A.S., Bennett, D.A., Xu, W., 2020. Associations Between Cardiovascular Risk, Structural Brain Changes, and Cognitive Decline. J. Am. Coll. Cardiol. 75, 2525–2534. https://doi.org/10.1016/j.jacc.2020.03.053

Sørensen, H.T., Sabroe, S., Rothman, K.J., Gillman, M., Steffensen, F.H., Fischer, P., Sørensen, T.I.A., 1999. Birth weight and length as predictors for adult height. Am. J. Epidemiol. 149, 726–729. https://doi.org/10.1093/oxfordjournals.aje.a009881

Sparrow, S., Manning, J.R., Cartier, J., Anblagan, D., Bastin, M.E., Piyasena, C., Pataky, R., Moore, E.J., Semple, S.I., Wilkinson, A.G., Evans, M., Drake, A.J., Boardman, J.P., 2016. Epigenomic profiling of preterm infants reveals DNA methylation differences at sites associated with neural function. Transl. Psychiatry 6, e716. https://doi.org/10.1038/tp.2015.210

Spiers, H., Hannon, E., Schalkwyk, L.C., Smith, R., Wong, C.C.Y., Donovan, M.C.O., Bray, N.J., Mill, J., 2015. Methylomic trajectories across human fetal brain development. Genome Res. 1–16. https://doi.org/10.1101/gr.180273.114.Freely

Stafford, M., Black, S., Shah, I., Hardy, R., Pierce, M., Richards, M., Wong, A., Kuh, D., 2013. Using a birth cohort to study ageing: representativeness and response rates in the National Survey of Health and Development. Eur. J. Ageing 10, 145–157. https://doi.org/10.1007/s10433-013-0258-8

Suderman, M., Staley, J.R., French, R., Arathimos, R., Simpkin, A., Tilling, K., 2018. Dmrff: Identifying differentially methylated regions efficiently with power and control. bioRxiv 1–26. https://doi.org/10.1101/508556

Sullivan, G., Galdi, P., Cabez, M.B., Borbye-Lorenzen, N., Stoye, D.Q., Lamb, G.J., Evans, M.J., Quigley, A.J., Thrippleton, M.J., Skogstrand, K., Chandran, S., Bastin, M.E., Boardman, J.P., 2020. Interleukin-8 dysregulation is

implicated in brain dysmaturation following preterm birth. Brain. Behav. Immun. 90, 311–318. https://doi.org/10.1016/j.bbi.2020.09.007

Swartz, J.R., Hariri, A.R., Williamson, D.E., 2017. An epigenetic mechanism links socioeconomic status to changes in depression-related brain function in high-risk adolescents. Mol. Psychiatry 22, 209–214. https://doi.org/10.1038/mp.2016.82

Talens, R.P., Boomsma, D.I., Tobi, E.W., Kremer, D., Jukema, J.W., Willemsen, G., Putter, H., Slagboom, P.E., Heijmans, B.T., 2010. Variation, patterns, and temporal stability of DNA methylation: considerations for epigenetic epidemiology. FASEB J. Res. Commun. 24, 3135–3144. https://doi.org/10.1096/fj.09-150490

Tariq, M., Schneider, T., Alexander, D.C., Gandini Wheeler-Kingshott, C.A., Zhang, H., 2016. Bingham-NODDI: Mapping anisotropic orientation dispersion of neurites using diffusion MRI. Neuroimage 133, 207–223. https://doi.org/10.1016/j.neuroimage.2016.01.046

Taylor, A.M., Pattie, A., Deary, I.J., 2018. Cohort Profile Update: The Lothian Birth Cohorts of 1921 and 1936. Int. J. Epidemiol. 47. https://doi.org/10.1093/ije/dyr197

Telford, E.J., Cox, S.R., Fletcher-Watson, S., Anblagan, D., Sparrow, S., Pataky, R., Quigley, A., Semple, S.I., Bastin, M.E., Boardman, J.P., 2017. A latent measure explains substantial variance in white matter microstructure across the newborn human brain. Brain Struct. Funct. 222. https://doi.org/10.1007/s00429-017-1455-6

Theda, C., Hwang, S.H., Czajko, A., Loke, Y.J., Leong, P., Craig, J.M., 2018. Quantitation of the cellular content of saliva and buccal swab samples. Sci. Rep. 8, 4–11. https://doi.org/10.1038/s41598-018-25311-0

Thompson, C., Syddall, H., Rodin, I., Osmond, C., Barker, D.J.P., 2001. Birth weight and the risk of depressive disorder in late life. Br. J. Psychiatry 179, 450–455. https://doi.org/10.1192/bjp.179.5.450

Tofts, P.S., Davies, G.R., Dehmeshki, J., 2004. Histograms: Measuring Subtle Diffuse Disease. Quant. MRI Brain 581–610. https://doi.org/10.1002/0470869526.ch18

Tournier, J.D., Smith, R., Raffelt, D., Tabbara, R., Dhollander, T., Pietsch, M., Christiaens, D., Jeurissen, B., Yeh, C.H., Connelly, A., 2019. MRtrix3: A fast, flexible and open software framework for medical image processing and visualisation. Neuroimage 202, 116137. https://doi.org/10.1016/j.neuroimage.2019.116137

Trønnes, H., Wilcox, A.J., Lie, R.T., Markestad, T., Moster, D., 2014. Risk of cerebral palsy in relation to pregnancy disorders and preterm birth: A national cohort study. Dev. Med. Child Neurol. 56, 779–785. https://doi.org/10.1111/dmcn.12430

Tucker-Drob, E.M., 2019. Cognitive Aging and Dementia: A Life-Span Perspective. Annu. Rev. Dev. Psychol. 1, 177–196. https://doi.org/10.1146/annurev-devpsych-121318-085204

Tustison, N.J., Avants, B.B., Cook, P.A., Zheng, Y., Egan, A., Yushkevich, P.A., Gee, J.C., 2010. N4ITK: Improved N3 bias correction. IEEE Trans. Med. Imaging 29, 1310–1320. https://doi.org/10.1109/TMI.2010.2046908

Ullman, H., Spencer-smith, M., Thompson, D.K., Doyle, L.W., Inder, T.E., Anderson, P.J., Klingberg, T., 2015. Neonatal MRI is associated with future cognition and academic achievement in preterm children. Brain 138, 3251–3262. https://doi.org/10.1093/brain/awv244

Unternaehrer, E., Luers, P., Mill, J., Dempster, E., Meyer, A.H., Staehli, S., Lieb, R., Hellhammer, D.H., Meinlschmidt, G., 2012. Dynamic changes in DNA methylation of stress-associated genes (OXTR , BDNF) after acute psychosocial stress. Transl. Psychiatry 2. https://doi.org/10.1038/tp.2012.77

Ursini, G., Bollati, V., Fazio, L., Porcelli, A., Iacovelli, L., Catalani, A., Sinibaldi, L., Gelao, B., Romano, R., Rampino, A., Taurisano, P., Mancini, M., Giorgio, A. Di, Popolizio, T., Baccarelli, A., Blasi, A. De, Blasi, G., Bertolino, A., 2011. Stress-Related Methylation of the Catechol- O -Methyltransferase Val 158 Allele Predicts Human Prefrontal Cognition and Activity. J. Neurosci. 31, 6692–6698. https://doi.org/10.1523/JNEUROSCI.6631-10.2011

Ursini, A.G., Cavalleri, T., Fazio, L., 2016. BDNF rs6265 methylation and genotype interact on risk for schizophrenia. Epigenetics 11, 11–23. https://doi.org/10.1080/15592294.2015.1117736

Vågberg, M., Granåsen, G., Svenningsson, A., 2017. Brain parenchymal fraction in healthy adults-a systematic review of the literature. PLoS One 12, 1–19. https://doi.org/10.1371/journal.pone.0170018

Valdés Hernández, M.D.C., Ferguson, K.J., Chappell, F.M., Wardlaw, J.M., 2010. New multispectral MRI data fusion technique for white matter lesion segmentation: Method and comparison with thresholding in FLAIR images. Eur. Radiol. 20, 1684–1691. https://doi.org/10.1007/s00330-010-1718-6

van Iterson, M., van Zwet, E.W., Heijmans, B.T., 't Hoen, P.A.C., van Meurs, J., Jansen, R., Franke, L., Boomsma, D.I., Pool, R., van Dongen, J., Hottenga, J.J., van Greevenbroek, M.M.J., Stehouwer, C.D.A., van der Kallen, C.J.H., Schalkwijk, C.G., Wijmenga, C., Zhernakova, S., Tigchelaar, E.F., Eline Slagboom, P., Beekman, M., Deelen, J., van Heemst, D., Veldink, J.H., van den Berg, L.H., van Duijn, C.M., Hofman, B.A., Isaacs, A., Uitterlinden, A.G., Jhamai, P.M., Verbiest, M., Suchiman, H.E.D., Verkerk, M., van der Breggen, R., van Rooij, J., Lakenberg, N., Mei, H., van Galen, M., Bot, J., Zhernakova, D. V., van 't Hof, P., Deelen, P., Nooren, I., Moed, M., Vermaat, M., Luijk, R., Bonder, M.J., van Dijk, F., Arindrarto, W., Kielbasa, S.M., Swertz, M.A., 't Hoen, P.B., 2017. Controlling bias and inflation in epigenome- and transcriptome-wide association studies using the empirical null distribution. Genome Biol. 18, 1–13. https://doi.org/10.1186/s13059-016-1131-9

Van Lieshout, R.J., Boylan, K., 2010. Increased depressive symptoms in female but not male adolescents born at low birth weight in the offspring of a national cohort. Can. J. Psychiatry 55, 422–430. https://doi.org/10.1177/070674371005500705

Van Lieshout, R.J., Ferro, M.A., Schmidt, L.A., Boyle, M.H., Saigal, S., Morrison, K.M., Mathewson, K.J., 2018. Trajectories of psychopathology in extremely low birth weight survivors from early adolescence to adulthood: a 20-year longitudinal study. J. Child Psychol. Psychiatry Allied Discip. 59, 1192–1200. https://doi.org/10.1111/jcpp.12909

van Loenhoud, A.C., Groot, C., Vogel, J.W., Van Der Flier, W.M., Ossenkoppele, R., 2018. Is intracranial volume a suitable proxy for brain reserve? Alzheimer's Res. Ther. 10, 1–12. https://doi.org/10.1186/s13195-018-0408-5

Vangberg, T.R., Skranes, J., Dale, A.M., Martinussen, M., Brubakk, A.-M., Haraldseth, O., 2006. Changes in white matter diffusion anisotropy in adolescents born prematurely. Neuroimage 32, 1538–1548. https://doi.org/10.1016/j.neuroimage.2006.04.230

Veraart, J., Fieremans, E., Novikov, D.S., 2016a. Diffusion MRI noise mapping using random matrix theory. Magn. Reson. Med. 76, 1582–1593. https://doi.org/10.1002/mrm.26059

Veraart, J., Novikov, D.S., Christiaens, D., Ades-aron, B., Sijbers, J., Fieremans, E., 2016b. Denoising of diffusion MRI using random matrix theory. Neuroimage 142, 394–406. https://doi.org/10.1016/j.neuroimage.2016.08.016

Vidal, A.C., Neelon, S.E.B., Liu, Y., Tuli, A.M., Fuemmeler, B.F., Hoyo, C., Murtha, A.P., Huang, Z., Schildkraut, J., Overcash, F., Kurtzberg, J., Jirtle, R.L., Iversen, E.S., Murphy, S.K., 2014. Maternal Stress, Preterm Birth, and DNA Methylation at Imprint Regulatory Sequences in Humans. Genet. Epigenetics 6, 37–44. https://doi.org/10.4137/GEG.S18067

Vinciguerra, C., Giorgio, A., Zhang, J., Di Donato, I., Stromillo, M.L., Tappa Brocci, R., Federico, A., Dotti, M.T., De Stefano, N., 2019. Peak width of skeletonized mean diffusivity (PSMD) as marker of widespread white matter tissue damage in multiple sclerosis. Mult. Scler. Relat. Disord. 27, 294–297. https://doi.org/10.1016/j.msard.2018.11.011

Volpe, J.J., 2009. Brain injury in premature infants: a complex amalgam of destructive and developmental disturbances. Lancet Neurol. 8, 110–124. https://doi.org/10.1016/S1474-4422(08)70294-1

Volpe, J.J., 2019. Pediatric Neurology Dysmaturation of Premature Brain: Importance Cellular Mechanisms, and Potential Interventions. Pediatr. Neurol. 95, 42–66. https://doi.org/10.1016/j.pediatrneurol.2019.02.016

Vukojevic, V., Kolassa, I., Fastenrath, M., Gschwind, L., Spalek, K., Milnik, A., Heck, A., Vogler, C., Wilker, X.S., Demougin, P., Peter, F., Atucha, E., Stetak, A., Roozendaal, B., Elbert, X.T., Papassotiropoulos, A., Quervain, D.J. De, 2014. Epigenetic Modification of the Glucocorticoid Receptor Gene Is Linked to

Traumatic Memory and Post-Traumatic Stress Disorder Risk in Genocide Survivors. J. Neurosci. 34, 10274–10284. https://doi.org/10.1523/JNEUROSCI.1526-14.2014

Wade, M., Browne, D.T., Madigan, S., Plamondon, A., Jenkins, J.M., 2014. Normal birth weight variation and children's neuropsychological functioning: Links between language, executive functioning, and theory of mind. J. Int. Neuropsychol. Soc. 20, 909–919. https://doi.org/10.1017/S1355617714000745

Wahl, S., Drong, A., Lehne, B., Loh, M., Scott, W.R., Kunze, S., Tsai, P.C., Ried, J.S., Zhang, W., Yang, Y., Tan, S., Fiorito, G., Franke, L., Guarrera, S., Kasela, S., Kriebel, J., Richmond, R.C., Adamo, M., Afzal, U., Ala-Korpela, M., Albetti, B., Ammerpohl, O., Apperley, J.F., Beekman, M., Bertazzi, P.A., Black, S.L., Blancher, C., Bonder, M.J., Brosch, M., Carstensen-Kirberg, M., De Craen, A.J.M., De Lusignan, S., Dehghan, A., Elkalaawy, M., Fischer, K., Franco, O.H., Gaunt, T.R., Hampe, J., Hashemi, M., Isaacs, A., Jenkinson, A., Jha, S., Kato, N., Krogh, V., Laffan, M., Meisinger, C., Meitinger, T., Mok, Z.Y., Motta, V., Ng, H.K., Nikolakopoulou, Z., Nteliopoulos, G., Panico, S., Pervjakova, N., Prokisch, H., Rathmann, W., Roden, M., Rota, F., Rozario, M.A., Sandling, J.K., Schafmayer, C., Schramm, K., Siebert, R., Slagboom, P.E., Soininen, P., Stolk, L., Strauch, K., Tai, E.S., Tarantini, L., Thorand, B., Tigchelaar, E.F., Tumino, R., Uitterlinden, A.G., Van Duijn, C., Van Meurs, J.B.J., Vineis, P., Wickremasinghe, A.R., Wijmenga, C., Yang, T.P., Yuan, W., Zhernakova, A., Batterham, R.L., Smith, G.D., Deloukas, P., Heijmans, B.T., Herder, C., Hofman, A., Lindgren, C.M., Milani, L., Van Der Harst, P., Peters, A., Illig, T., Relton, C.L., Waldenberger, M., Järvelin, M.R., Bollati, V., Soong, R., Spector, T.D., Scott, J., McCarthy, M.I., Elliott, P., Bell, J.T., Matullo, G., Gieger, C., Kooner, J.S., Grallert, H., Chambers, J.C., 2017. Epigenome-wide association study of body mass index, and the adverse outcomes of adiposity. Nature 541, 81–86. https://doi.org/10.1038/nature20784

Walhovd, K.B., Fjell, A.M., Brown, T.T., Kuperman, J.M., Chung, Y., Hagler, D.J., Roddey, J.C., Erhart, M., McCabe, C., Akshoomoff, N., Amaral, D.G., Bloss, C.S., Libiger, O., Schork, N.J., Darst, B.F., Casey, B.J., Chang, L., Ernst, T.M., Frazier, J., Gruen, J.R., Kaufmann, W.E., Murray, S.S., Van Zijl, P., Mostofsky, S., Dale, A.M., 2012. Long-term influence of normal variation in neonatal characteristics on human brain development. Proc. Natl. Acad. Sci. U. S. A. 109, 20089–20094. https://doi.org/10.1073/pnas.1208180109

Walhovd, K.B., Krogsrud, S.K., Amlien, I.K., Bartsch, H., Bjørnerud, A., Due-Tønnessen, P., Grydeland, H., Hagler, D.J., Håberg, A.K., Kremen, W.S., Ferschmann, L., Nyberg, L., Panizzon, M.S., Rohani, D.A., Skranes, J., Storsve, A.B., Sølsnes, A.E., Tamnes, C.K., Thompson, W.K., Reuter, C., Dale, A.M., Fjell, A.M., 2016. Neurodevelopmental origins of lifespan changes in brain and cognition. Proc. Natl. Acad. Sci. U. S. A. 113, 9357–9362. https://doi.org/10.1073/pnas.1524259113

Walton, E., Liu, J., Hass, J., White, T., Scholz, M., Roessner, V., Gollub, R., Calhoun, V.D., Ehrlich, S., 2014. MB-COMT promoter DNA methylation is

associated with working-memory processing in schizophrenia patients and healthy controls. Epigenetics 9, 1101–1107. https://doi.org/10.4161/epi.29223

Wang, M., Huang, T., Calhoun, V.D., Fang, J., Wang, Y., 2017. Integration of multiple genomic imaging data for the study of Schizophrenia using joint nonnegative matrix factorization. IEEE Trans Biomed Eng 1083–1087.

Wardlaw, J.M., Bastin, M.E., Valdés Hernández, M.C., Maniega, S.M., Royle, N.A., Morris, Z., Clayden, J.D., Sandeman, E.M., Eadie, E., Murray, C., Starr, J.M., Deary, I.J., 2011. Brain aging, cognition in youth and old age and vascular disease in the Lothian Birth Cohort 1936: Rationale, design and methodology of the imaging protocol. Int. J. Stroke 6, 547–559. https://doi.org/10.1111/j.1747-4949.2011.00683.x

Wardlaw, J.M., Valdés Hernández, M.C., Munõz-Maniega, S., 2015. What are White Matter Hyperintensities Made of? Relevance to Vascular Cognitive Impairment. J. Am. Heart Assoc. 4. https://doi.org/10.1161/JAHA.114.001140

Weemaes, C., Tol, M.J.D. Van, Wang, J., Dam, M.M.V.O., Eggermond, M.C.J.A. Van, Thijssen, P.E., Aytekin, C., Brunetti-pierri, N., Burg, M. Van Der, Davies, E.G., Ferster, A., Furthner, D., Gimelli, G., Gennery, A., 2013. Heterogeneous clinical presentation in ICF syndrome: correlation with underlying gene defects 1219–1225. https://doi.org/10.1038/ejhg.2013.40

Wei, N., Deng, Y., Yao, L., Jia, W., Wang, J., Shi, Q., 2019. A Neuroimaging Marker Based on Diffusion Tensor Imaging and Cognitive Impairment Due to Cerebral White Matter Lesions 10, 1–7. https://doi.org/10.3389/fneur.2019.00081

Whalley, L.J., Dick, F.D., McNeill, G., 2006. A life-course approach to the aetiology of late-onset dementias. Lancet Neurol. 5, 87–96. https://doi.org/10.1016/S1474-4422(05)70286-6

Wheater, E.N.W., Stoye, D.Q., Cox, S.R., Wardlaw, J.M., Drake, A.J., Bastin, M.E., Boardman, J.P., 2020. DNA methylation and brain structure and function across the life course: A systematic review. Neurosci. Biobehav. Rev. 113, 133–156. https://doi.org/10.1016/j.neubiorev.2020.03.007

Wiemerslage, L., Islam, R., Van Der Kamp, C., Cao, H., Olivo, G., Ence-Eriksson, F., Castillo, S., Larsen, A.L., Bandstein, M., Dahlberg, L.S., Perland, E., Gustavsson, V., Nilsson, J., Vogel, H., Schürmann, A., Larsson, E.M., Rask-Andersen, M., Benedict, C., Schiöth, H.B., 2017. A DNA methylation site within the KLF13 gene is associated with orexigenic processes based on neural responses and ghrelin levels. Int. J. Obes. 41, 990–994. https://doi.org/10.1038/ijo.2017.43

Wiers, C.E., Shumay, E., Volkow, N.D., Frieling, H., Kotsiari, A., Lindenmeyer, J., Walter, H., Bermpohl, F., 2015. Effects of depressive symptoms and peripheral DAT methylation on neural reactivity to alcohol cues in alcoholism. Transl. Psychiatry 5, e648-8. https://doi.org/10.1038/tp.2015.141

Wijetunge, L.S., Chattarji, S., Wyllie, D.J.A., Kind, P.C., 2013. Fragile X syndrome: From targets to treatments. Neuropharmacology 68, 83–96. https://doi.org/10.1016/j.neuropharm.2012.11.028

Williams, K., Christensen, J., Pedersen, M.T., Johansen, J. V., Cloos, P.A.C., Rappsilber, J., Helin, K., 2011. TET1 and hydroxymethylcytosine in transcription and DNA methylation fidelity. Nature 473, 343–349. https://doi.org/10.1038/nature10066

Wiseman, S.J., Booth, T., Ritchie, S.J., Cox, S.R., Muñoz Maniega, S., Valdés Hernández, M. del C., Dickie, D.A., Royle, N.A., Starr, J.M., Deary, I.J., Wardlaw, J.M., Bastin, M.E., 2018. Cognitive abilities, brain white matter hyperintensity volume, and structural network connectivity in older age. Hum. Brain Mapp. 39, 622–632. https://doi.org/10.1002/hbm.23857

Wolf, E.J., Logue, M.W., Hayes, J.P., Sadeh, N., Schichman, S.A., Stone, A., Salat, D.H., Milberg, W., McGlinchey, R., Miller, M.W., 2016. Accelerated DNA methylation age: Associations with PTSD and neural integrity. Psychoneuroendocrinology 63, 155–162. https://doi.org/10.1016/j.psyneuen.2015.09.020

Wolf, H., Julin, P., Gertz, H.J., Winblad, B., Wahlund, L.O., 2004. Intracranial volume in mild cognitive impairment, Alzheimer's disease and vascular dementia: Evidence for brain reserve? Int. J. Geriatr. Psychiatry 19, 995–1007. https://doi.org/10.1002/gps.1205

Won, E., Choi, S., Kang, J., Kim, A., Han, K.-M., Chang, H.S., Tae, W.S., Son, K.R., Joe, S.-H., Lee, M.-S., Ham, B.-J., 2016. Association between reduced white matter integrity in the corpus callosum and serotonin transporter gene DNA methylation in medication-naive patients with major depressive disorder. Transl. Psychiatry 6, e866-9. https://doi.org/10.1038/tp.2016.137

Ye, J., Wu, C., Chu, X., Wen, Y., Li, P., Cheng, B., Cheng, S., Liu, L., Zhang, L., Ma, M., Qi, X., Liang, C., Kafle, O.P., Jia, Y., Wang, S., Wang, X., Ning, Y., Zhang, F., 2020. Evaluating the effect of birth weight on brain volumes and depression: An observational and genetic study using UK Biobank cohort. Eur. Psychiatry 63. https://doi.org/10.1192/j.eurpsy.2020.74

Ylihärsilä, H., Kajantie, E., Osmond, C., Forsén, T., Barker, D.J.P., Eriksson, J.G., 2007. Birth size, adult body composition and muscle strength in later life. Int. J. Obes. 31, 1392–1399. https://doi.org/10.1038/sj.ijo.0803612

Zhang, H., Schneider, T., Wheeler-Kingshott, C.A., Alexander, D.C., 2012. NODDI: Practical in vivo neurite orientation dispersion and density imaging of the human brain. Neuroimage 61, 1000–1016. https://doi.org/10.1016/j.neuroimage.2012.03.072

Zhang, G., Feenstra, B., Bacelis, J., Liu, X., Muglia, L.M., Juodakis, J., Miller, D.E., Litterman, N., Jiang, P.-P., Russell, L., Hinds, D.A., Hu, Y., Weirauch, M.T., Chen, X., Chavan, A.R., Wagner, G.P., Pavličev, M., Nnamani, M.C., Maziarz, J., Karjalainen, M.K., Rämet, M., Sengpiel, V., Geller, F., Boyd, H.A., Palotie, A., Momany, A., Bedell, B., Ryckman, K.K., Huusko, J.M., Forney, C.R., Kottyan, L.C., Hallman, M., Teramo, K., Nohr, E.A., Davey Smith, G., Melbye, M., Jacobsson, B., Muglia, L.J., 2017. Genetic Associations with Gestational Duration and Spontaneous Preterm Birth. N. Engl. J. Med. 377, 1156–1167. https://doi.org/10.1056/nejmoa1612665

Zhang, Q., Vallerga, C.L., Walker, R.M., Lin, T., Henders, A.K., Montgomery, G.W., He, J., Fan, D., Fowdar, J., Kennedy, M., Pitcher, T., Pearson, J., Halliday, G., Kwok, J.B., Hickie, I., Lewis, S., Anderson, T., Silburn, P.A., Mellick, G.D., Harris, S.E., Redmond, P., Murray, A.D., Porteous, D.J., Haley, C.S., Evans, K.L., McIntosh, A.M., Yang, J., Gratten, J., Marioni, R.E., Wray, N.R., Deary, I.J., McRae, A.F., Visscher, P.M., 2019. Improved precision of epigenetic clock estimates across tissues and its implication for biological ageing. Genome Med. 11, 1–11. https://doi.org/10.1186/s13073-019-0667-1

Zhang, X., Wang, Y., Yang, F., Tang, J., Xu, X., Yang, L., Yang, X.A., Wu, D., 2020. Biallelic INTS1 Mutations Cause a Rare Neurodevelopmental Disorder in Two Chinese Siblings. J. Mol. Neurosci. 70, 1–8. https://doi.org/10.1007/s12031-019-01393-x

Zheng, S.C., Webster, A.P., Dong, D., Feber, A., Graham, D.G., Sullivan, R., Jevons, S., Lovat, L.B., Beck, S., Widschwendter, M., Teschendorff, A.E., 2018. A novel cell-type deconvolution algorithm reveals substantial contamination by immune cells in saliva, buccal and cervix. Epigenomics 10, 925–940. https://doi.org/10.2217/epi-2018-0037

Zhou, X., Xu, Y., Xie, Z., Xu, S., Bi, J., 2016. Association of extracellular superoxide dismutase gene methylation with cerebral infarction. Chinese J. Med. Genet. 33, 378–382. https://doi.org/10.3760/cma.j.issn.1003-9406.2016.03.023

Ziegler, C., Dannlowski, U., Brauer, D., Stevens, S., Laeger, I., Wittmann, H., Kugel, H., Dobel, C., Hurleman, R., Reif, A., Lesch, K.-P., Heindel, W., Kirschbaum, C., Arolt, V., Gwerlach, A.L., Hoyer, J., Deckert, J., Zwanzger, P., Domschke, K., 2015. Oxytocin Receptor Gene Methylation : Converging Multilevel Evidence for a Role in Social Anxiety. Neuropsychopharmacology 40, 1528–1538. https://doi.org/10.1038/npp.2015.2